Impact of Gravity Loads on the Lateral Performance of Cold-Formed Steel Frame/
Steel Sheathed Shear Walls

By

Jamin DaBreo

Research Project Director

Colin A. Rogers

Department of Civil Engineering and Applied Mechanics

McGill University, Montréal, Canada

September 2012

A thesis submitted to McGill University in partial fulfillment of the requirements of the degree of Masters of Engineering

ABSTRACT

Canadian seismic design provisions for cold-formed steel framed/ steel sheathed shear walls have been developed from previous research at McGill University with the intent of being incorporated into the Canadian section of the North American Lateral Design Standard for Cold-Formed Steel Framing (AISI S213), and ultimately to provide guidelines for design of these systems in the National Building Code of Canada and CSA-S136 Specification.

In this previous research, a limited number of shear walls displayed unfavourable damage due to twisting deformations of the chord-studs and by local buckling. Also, the shear walls tested in previous research were only laterally loaded. The objective of the current research program was to address this unfavourable failure mode by evaluating the performance of cold-formed steel framed/ steel sheathed shear walls, constructed with blocked stud members, which were tested under combined gravity and lateral loading. In total, fourteen single-storey shear walls (8 configurations) were subjected to monotonic and CUREE reversed cyclic lateral loading protocols.

The Equivalent Energy Elastic-Plastic (EEEP) approach was used to analyse the test data and determine nominal shear resistance values. Relevant design parameters were determined: a resistance factor, ϕ, of 0.7, an overstrength value of 1.4, and ductility and overstrength seismic force modification factors (R_d = 2.0 and R_o = 1.3).

Dynamic analysis of a two storey representative building model was carried out to validate the 'test-based' *R*-values following a methodology adopted from FEMA P695 to evaluate the seismic performance of a building system.

The research program indicated that the blocking reinforcement detail had adequately resolved chord-stud twisting deformations and that the chord-studs, once designed to carry the combined gravity and lateral forces following a

capacity based approach, would not fail thereby preventing any detrimental collapse of the framing system.

RÉSUMÉ

Les dispositions de conception sismique pour les murs de refend (dotés de cadres ou de revêtements en acier laminé à froid) mises au point précédemment à l'Université McGill avaient pour but d'être ajoutées aux dispositions canadiennes présentées dans le *North American Lateral Design Standard for Cold-Formed Steel Framing (AISI S213)* et de proposer des lignes directrices qui pourraient être intégrées au Code national du bâtiment du Canada et à la norme CSA-S136.

Au cours de ces recherches, un nombre limité de murs de refend ont été endommagés par le voilement local et les déformations des membrures-montants liées à la torsion. Les murs de refend avaient été uniquement testés sous l'effet d'une charge latérale. Ce programme de recherche tente de comprendre ce processus de défaut défavorable en évaluant la performance des murs de refend (dotés de cadres ou de revêtements en acier laminé à froid) construits à l'aide montants munis de cales et testés sous l'effet combiné de la gravité et de la charge latérale. Un total de quatorze murs de refend à un étage (8 configurations) ont été soumis aux protocoles de chargement monotone et de chargement cyclique-réversible de CUREE.

La méthode équivalente de l'énergie élasto-plastique (EEEP) a été appliquée pour analyser les données des essais et déterminer les valeurs nominales de résistance au cisaillement. Les paramètres pertinents de conception ont été déterminés: un facteur de résistance (ϕ= 0.7), une valeur de sur-résistance de 1.4 et des facteurs de modification de force sismique reliés à la ductilité et à la sur-résistance (R_d = 2.0 et R_o = 1.3).

Une analyse dynamique a été menée sur un modèle représentatif d'un bâtiment à deux étages pour valider les valeurs de R obtenues lors des essais. Une méthode adoptée par le FEMA P695 a servi à évaluer la résistance sismique d'un système de construction.

Ce programme de recherche a montré que le dispositif de blocage de l’armature empêche adéquatement les déformations des membrures-montants liées à la torsion. Grâce à une approche de conception par capacité, des membrures-montants peuvent résister à l’action combinée de la gravité et des forces latérales, et ainsi prévenir l’effondrement de l’ossature du bâtiment.

ACKNOWLEDGEMENTS

First and foremost I wish to thank the Sovereign Lord Jehovah God for all his blesses. The God of Comfort; he has sustained me through all the tough times. “I shall make you have insight and instruct you in the way you should go. I will give advice with my eye upon you”, says Jehovah God of armies (Psalms 32:8). To him be the glory, and the honor, and the power and magnificence forever and into eternity.

A special thanks to my supervisor Professor Colin A. Rogers. It was indeed a privilege to work with such an intelligent and understanding individual. His patience with me was particularly noteworthy. His guidance from day one has help me transition into the path I have undertaken of becoming a structural engineer. Much heartfelt thanks and respect goes out Professor Rogers.

I would like to thank my fellow colleagues, Anthony Caruso, Nick Ditommaso, and especially Iman Shamim. It was a truly fun experience working alongside them at Ecole Polytechnique de Montreal and the structures laboratory at McGill University. I would also like to thank the laboratory technicians Marek Przykorski, Ron Sheppard, Damon Kiperchuk and Jon Bartczak.

I would like to acknowledge the financial support provided by: the Natural Sciences and Engineering Research Council of Canada (NSERC), the Canadian Sheet Steel Building Institute (CSSBI), and the American Iron and Steel Institute (AISI). The materials for construction were provided by Simpson Strong-Tie Co. Inc., ITW Buildex and Grabber Construction Production. Bailey Metal Products Ltd. assisted with the procurement of construction materials.

I would also like to thank the AISI sponsored FEMA P695 peer review group for their comments and contributions to the model development and their oversight of the IDA portion of this research.

Finally I would like to thank my family and friends for all their love, encouragement and support throughout this stage of my life’s journey.

Thank you to all and one love.

TABLE OF CONTENTS

List of Figures

List of Tables

CHAPTER 1- INTRODUCTION

1.1 General Overview

Cold-formed steel (CFS) has gained much popularity throughout the North American construction industry, especially in low to medium rise residential and commercial buildings including single family dwellings, apartments, multi-family residential units, senior care centres, office building, box store and much more. An example of its increased popularity can be found in Hawaii, where approximately 40% of residential buildings are built with CFS framing (*Steel Framing Alliance, 2005*).

Its popularity over traditional materials is attributed to its high quality, durability, dimensional stability, strength and ease of handling. It is also non-combustible, light weight, recyclable and a more economical alternative. Cold-formed steel is used for numerous purposes including, roof diaphragm and floor decking, cladding, concrete formwork and more importantly, as structural framing members (Figure 1.1).

Figure 1.1 Example of a steel sheathed shear wall (*Courtesy of RJC Ltd.*)

On the contrary, CFS for load bearing construction, has not gained as much popularity in Canada. This is due in part to the deficiencies of the Canadian standards to provide guidelines for seismic design of CFS structures; namely the 2005 and the more recent 2010 National Building Code of Canada (NBCC) (*NRCC, 2005 & NRCC, 2010*) and the Canadian Standards Association (CSA) S136 Standard (*2007*). US designers utilize seismic design guidelines found in the American Iron and Steel Institute (*AISI*) S213 Standard, North American Standard for Cold-Formed Steel Framing- Lateral Design (*AISI S213, 2007*).

Presently, Canadian seismic guidelines only address wood sheathed and gypsum panel CFS framed shear walls as well as strap braced walls. CFS framed shear walls constructed with steel sheathing is a relatively new concept to Canada and as such must be investigated.

Shear walls provide stability to the framing system and resistance to lateral forces such as those imposed by wind and earthquakes. In-plane forces are transferred from roof and flooring system, through the shear walls, and down to the foundation. The sheathing installed onto the CFS framing provides this in-plane shear resistance and the connection between the sheathing and framing influences the overall shear wall behaviour.

1.2 Problem Statement

At present, in Canada, there are no seismic design provisions within the National Building Code of Canada (NBCC) (*NRCC, 2010*) that address steel sheathed cold-formed steel (CFS) framed shear walls; in contrast, force modification values, R_d and R_o, are provided for wood based panel and wood based and gypsum panels in combination CFS shear walls and diagonal strap concentrically braced CFS walls. The Canadian Standards Association (CSA) S136 Specification (*2007*) has no design and detailing information for steel sheathed CFS shear walls but refers to the AISI S213 North American Standard for Cold-formed Steel Framing- Lateral Design (*2007*). As such, R values for the steel sheathed / CFS framed shear wall seismic force resisting system (SFRS) should be provided in the NBCC and seismic design and detailing provisions for Canada should be included in AISI S213.

To date, seismic design provisions have been proposed for steel sheathed walls with the intent of being included into the Canadian sections of AISI S213 and to be used in conjunction with the NBCC. This was the objective of the research program at McGill University initiated in 2008. Fifty-four steel sheathed/CFS framed single-storey shear walls were tested using displacement based testing (*Balh & Rogers 2010; Ong-Tone & Rogers 2009*) and test data from the US was used to complement the research program (*El-Saloussy & Rogers 2010*).

A limited number of previous shear wall tests displayed unfavourable damage due to twisting failure and also by local buckling of chord studs (Figure 1.2). Additionally, the steel sheathed/ CFS framed shear walls tested by Ong-Tone & Rogers (*2009*) and Balh & Rogers (*2010*) were only subjected to lateral loading. As such, it was deemed necessary to address combined gravity and lateral loading and to improve detailing and design to prevent chord stud damage/failure.

Figure 1.2 Twisting and local buckling of chord stud (*Balh, 2010*)

1.3 Objectives

The objectives of this research project are as follows:

i) Perform tests on single-storey steel sheathed/cold-formed steel framed shear walls constructed with special blockings detailing and subjected to combined lateral and gravity loading.

ii) Use the Equivalent Energy Elastic Plastic (EEEP) concept (*Park, 1989 and Foliente, 1996*), deemed appropriate by Branston (*Branston & Rogers, 2004*), to determine relevant design parameters and nominal shear resistance values for the tested shear walls.

iii) Determine the resistance factor, ϕ, for ultimate limit states design, the corresponding factor of safety, and the 'test-based' seismic force modification factors for ductility and over-strength, R_d and R_o respectively.

iv) Compare blocked/reinforced walls to previous test results of walls without special detailing and combined gravity loading.

v) Use the OpenSees software (*McKenna et al. 2006*) to perform dynamic analysis on the CFS-NEES (*Madsen et al. 2011*) two storey representative building following the FEMA P695 (*2009*) methodology to evaluate building system seismic performance.

1.4 Scope and Limitations of Study

During the summer of 2010, 14 single-storey steel sheathed/CFS frame blocked shear walls (8 configurations) were tested under combined gravity and lateral loading. Specimens were subjected to monotonic and CUREE (*ASTM E2126 2007; Krawinkler et al. 2000*) reversed cyclic lateral loading protocols (displacement based testing).

Shear walls were limited to 2440x1220mm (8’x4’) in dimension, and varied in configuration in terms of framing and sheathing thickness and fastener spacing. Materials used were 0.46mm (0.018”) and 0.76mm (0.030”) thick steel sheathing, 1.09mm (0.043”) and 1.37mm (0.054”) thick framing elements and 50, 75, 100, 150mm (2”, 3”, 4”, 5”) sheathing fastener spacing.

Ancillary testing was run on sheathing and framing materials. This included coupon testing to confirm thickness and mechanical properties and screw connection testing to evaluate shear and bearing/tilting resistances of the sheathing fasteners.

Analysis of test data was performed using the EEEP analysis technique. Seismic force modification factors were determined based on the interpreted test data. The OpenSees software was used to perform non-linear dynamic time history analysis on the 2 storey representative building. Dynamic analyses along with the

FEMA P695 methodology were used in the validation of the ‘test-based’ R-values.

1.5 Thesis Outline

The content of this thesis is as follows:

Chapter 2 contains a description of the shear wall test program. This includes specifications of materials and members, the construction method, test set-up and instrumentation, testing protocols, test results, observed failure modes, ancillary testing of materials, and a comparison of the shear wall configurations.

Chapter 3 contains the interpretation of test data and prescriptive design recommendations. Test data are extracted using the EEEP analysis made possible by an automated spreadsheet produced by Balh (*2010*) and edited by the author. Nominal shear resistance values are calculated for each wall configuration and relevant design parameters are established.

Chapter 4 outlines the design procedure used for the blocked steel sheathed/CFS framed shear walls using the design parameters and factors established in the preceding chapter. Also, described is the verification phase through dynamic analysis following the FEMA P695 methodology. The OpenSees software is used for the dynamic analyses whereby a suitable representative building model is subjected to a suite of 38 ground motion representing the seismic hazard of Vancouver BC. The representation building model used in the dynamic analysis is further described in this chapter.

Chapter 5 provides conclusions for this research project and recommendations for future research on steel sheathed/CFS frame shear walls are presented.

1.6 Literature Review

This section presents a summary of information of past research that is especially relevant to this report. These are namely: combined gravity and lateral loading of CFS framed shear walls and usage and effects of blockings. Also mentioned is the dynamic software, OpenSees (*McKenna et al.2006*), used to perform the dynamic analysis.

1.6.1 Combined Gravity and Reversed Cyclic Loading of Shear Walls

Detailed information regarding previous research on combined gravity and reversed cyclic loading of shear walls is presented in the literature review by Hikita (*Hikita & Rogers, 2006*). Earlier shear wall tests at McGill University by Branston (*Branston & Rogers*, *2004*) revealed a detrimental and undesirable failure mode of the framing members. Chord stud failure due to permanent deformation by buckling and distortion of the framing studs was caused by the compression forces associated with lateral loading and gravity loading if included (Figure 1.3). This failure mode must be avoided to prevent the collapse of the framing system and to maintain gravity loading capacity post earthquake (serviceability). Thus it is important that gravity loading be considered in the capacity based design of the chord studs.

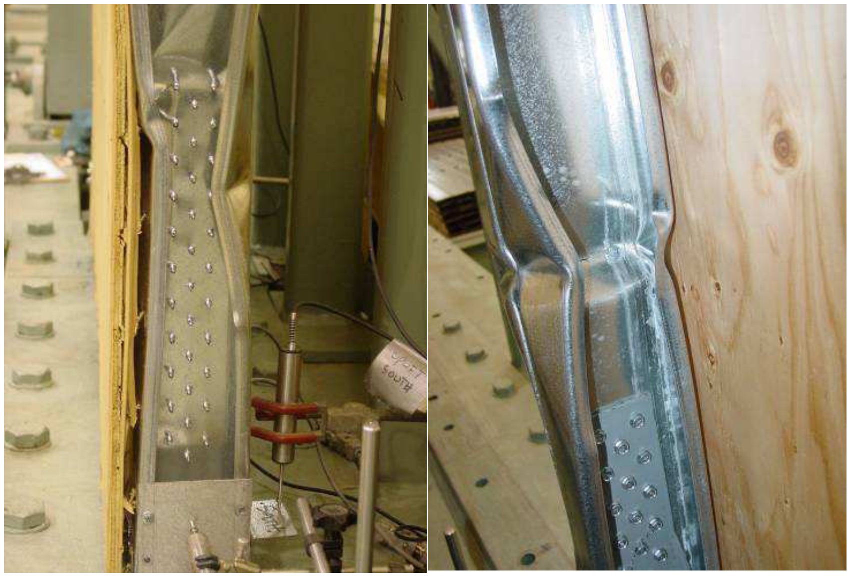

Figure 1.3 Compression chord local buckling in test 13B (*Branston, 2004*)

Hikita (*2006*) investigated the influence of combined loading, gravity and lateral loading, on wood panel/CFS framed shear walls. Thirty-two 1220 mm x 2440 mm (4' x 8') CFS frame/ wood panel shear walls were tested. Wood sheathing types used were 12.5 mm Douglas fir Plywood (DFP), 11 mm Oriented Strand Board (OSB) and 12.5 mm Canadian Softwood Plywood (CSP). Framing thicknesses were 1.09 mm (0.043") and 1.37 mm (0.054") and were selected based on capacity based design principles accounting for combined lateral and gravity loads. The sheathing fastener spacing/ screw schedules were 75 mm (3") and 152 mm (6") along the panel edges and the standard 305 mm (12") spacing along the interior field stud.

The shear wall test frame in the Jamieson Structures Laboratory of McGill University was specially modified so as to incorporate a gravity loading system (Figure 1.4). Enerpac loading jacks were installed below the main beams of the test frame at each end of the shear wall. Threaded rods were used to connect the jacks to the lateral loading beam at the top of the wall. Half-rounds were used as the reaction surface to allow the gravity system to follow the shear wall's lateral displacement. Load cells integrated into the threaded rod and half-round setup were relied on to ensure that a constant force from each jack was maintained.

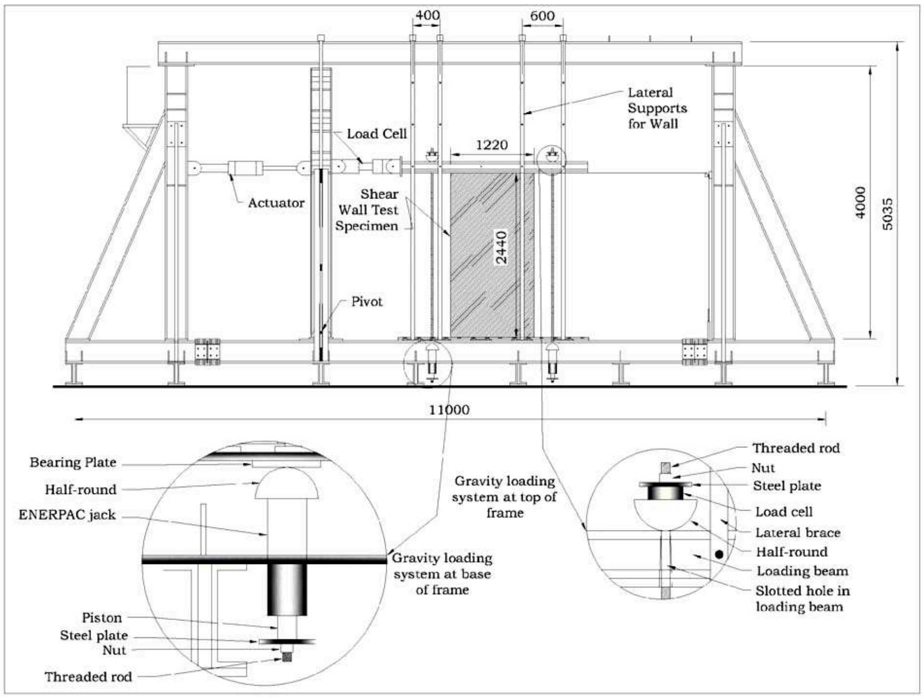

Figure 1.4 Modified test frame with 1220 mm x 2440 mm (4' x 8') wall specimen (*Hikita & Rogers, 2006*)

The gravity loading system had two drawbacks: the first was the need for an independent hydraulic system for the two jacks used to apply the gravity loads and secondly, there was an additional lateral load imposed on the wall due to the horizontal component of the tension force in the threaded rods as the wall displaced laterally.

From Hikita's (*2006*) experimental program, it was concluded that the presence of gravity loads did not influence the behaviour of the shear wall given that an appropriate selection of the chord-studs was made, i.e. the chord-studs were designed to resist the compression forces due to the combination of gravity loads and forces associated with the probable ultimate shear capacity of the wall as controlled by the screw connections failure.

1.6.2 Blocking and Bridging (for Reduced Buckling and Distortion of Framing Studs)

Aforementioned, permanent local buckling and distortion of the framing studs were noticed in previous test programs. As such, certain configurations were introduced in previous research programs to address this problem.

Yu et al. (*2007, 2009*) of the University of North Texas conducted an AISI sponsored research project on the “Steel Sheet Sheathing Options for Cold-Formed Steel Framed Shear Wall Assemblies Providing Shear Resistance”. Phase 2 of this project (*Yu et al., 2009*) focused on seismic detailing requirements for 6 ft.×8 ft., 4 ft.×8 ft., and 2 ft.×8 ft. CFS shear walls. The 6 ft.×8 ft. walls had a steel sheathing combination of 4 ft and 2 ft width. A wall configuration C (Figure 1.5), with additional special detailing, was developed to improve seismic performance. This detailing included: replacing No. 8x1/2” screws with No. 10x3/4” screws, using a staggered screw pattern at end and joint studs, and of major importance, the use of blocking and strapping installed at the wall’s mid-height. The strapping and blocking was of the same material as the framing members and the detail was in accordance with AISI S230 Standard for Cold-Formed Steel Framing- Prescriptive Method for One and Two Family Dwellings (*AISI S230,2007*) Section E. (Figure 1.6)

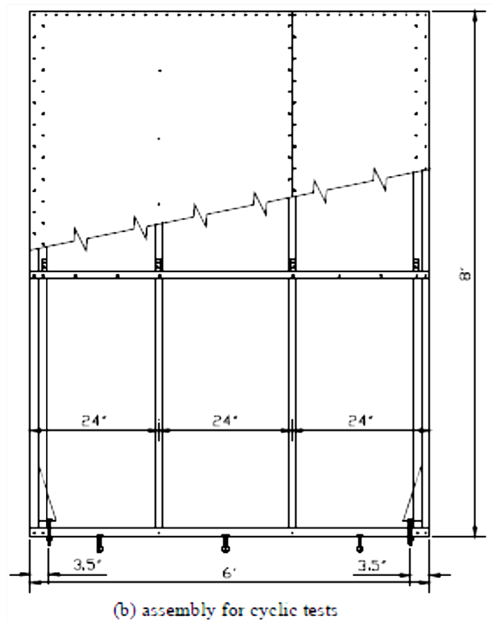

Figure 1.5 Configuration C- Dimensions of 8 ft. x 6 ft. wall assembly (*Yu et al., 2009*)

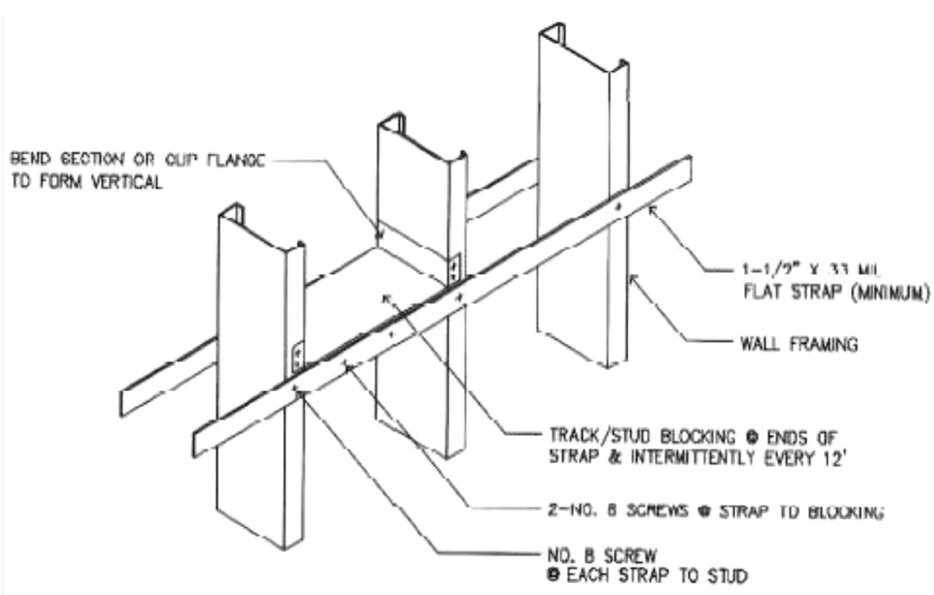

Figure 1.6 Strapping and blocking details for wall configuration C (*Excerpt from AISI S230-07*)

The following improvements due to the special detailing (configuration C) were obtained for the 6 ft.×8 ft. walls: a 9% increase in max shear capacity for the 43 mil framed shear walls with 30 mil steel sheathing; an average increase of 11.4% in max shear capacity and a 21.7% increase in the ductility factor for 54 mil framed shear walls with 33 mil sheathing under cyclic loading. The special detailing successfully restricted the flexural buckling of the interior studs (Figure 1.7), though damage to the flange of the interior field stud was observed due to sheathing screw pull-out.

Figure 1.7 Failure mode of 6 ft.×8 ft. wall with (*right*) and without special detailing (*left*) (*Yu et al., 2009*)

Similar to the 6 ft.×8 ft. walls, the 4 ft.×8 ft. walls also experienced improved performance. Figure 1.8 illustrates a comparison of the hysteresis curves of two 43 mil framed shear walls with 33 mil steel sheathing with and without the special detailing. The figure clearly depicts increases in initial elastic stiffness and shear capacity. There was an average increase of 16.7% in nominal shear strength. Again, the special detailing successfully restricted the flexural buckling of the interior stud and the walls failed by screw pull-out at the centre of the interior stud and at the corners of the sheathing. For the test walls with the special detailing (Configuration C) listed above, none had chord stud failure due to twisting, although localised flange distortion due to screw pull-out was observed.

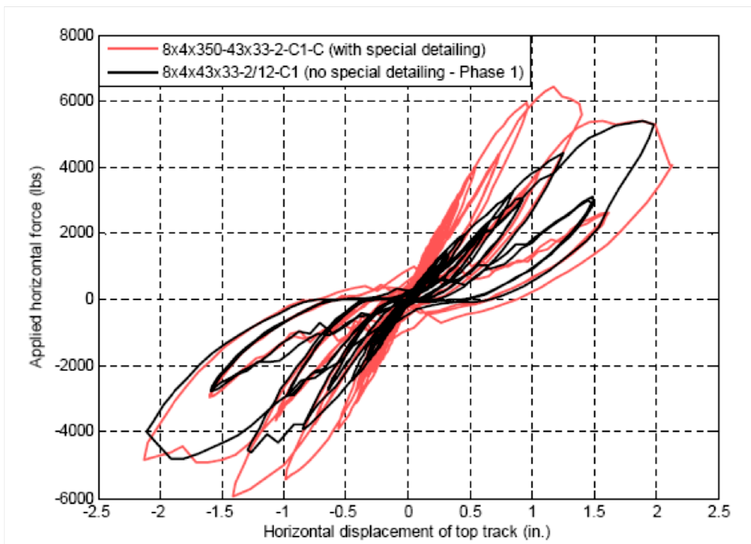

Figure 1.8 Test hysteresis curves for 4 ft.×8 ft. walls (*Yu et al., 2009*)

El-Saloussy (*2010*) analyzed test data obtained from Yu *et al*. (*2007, 2009*) using the EEEP analysis approach to aid in the development of Canadian design parameters and to supplement previous research data from tests conducted at McGill University. The effect of the mid-height blocking was addressed whereby a comparison of nominal shear values of ordinary walls to blocked walls was made (Table 1.1). Again, blockings were effective in increasing the nominal shear resistance of walls.

Table 1.1 Nominal shear values comparing the values between ordinary and blocked walls (*El-Saloussy, 2010*)

Sheathing	Max Aspect Ratio (h/w)	Fastener Spacing at Panel Edges mm (in.)	Mid-Height Blocking
		50 (2)	
0.84mm (0.033 in.)	2:1	13.95 (956)	No
		14.67 (1005)	Yes
	4:3	18.15 (1244)	No
		20.85 (1429)	Yes

Ong-Tone and Rogers (*2009*) and Balh and Rogers (*2010*) examined the effects of bridging with the main intention of reducing the chord-stud tendency to twist. Three rows of bridging were installed through the web cut-out/hole locations along the studs at the back of the wall (Figure 1.9).

Figure 1.9 Location of bridging elements (*Ong-Tone & Rogers, 2009*)

Tests 9M-c, 5M-c and 6M-c, variations of configurations 9, 5 and 6 respectively, were constructed with installed bridging members. Balh and Rogers (*2010*) examined the impact of bridging on the behaviour of shear wall Test 9M-c, a 610x2440 mm (2' x 8') wall constructed using 1.09 mm (0.043") framing, 0.76 mm (0.030") sheathing and a 50mm (2") fastener spacing. The latter two tests, 1220x2440 mm (4' x 8') walls, were examined by Ong-Tone and Rogers (*2009*). Configuration 5 was constructed using 1.09 mm (0.043") framing, 0.76 mm (0.030") sheathing using a 100 mm (4") fastener spacing, and Configuration 6 comprised 1.09 mm (0.043") framing, 0.76 mm (0.030") sheathing and a 50 mm (2") fastener spacing.

As intended, chord-stud twisting/damage was reduced and walls were able to reach higher ultimate shear resistances (Figure 1.10 & 1.11). Also, the corner fasteners where able to better participate in tension field development of the sheathing. As such, walls with bridging were more effective at resisting the applied loads.

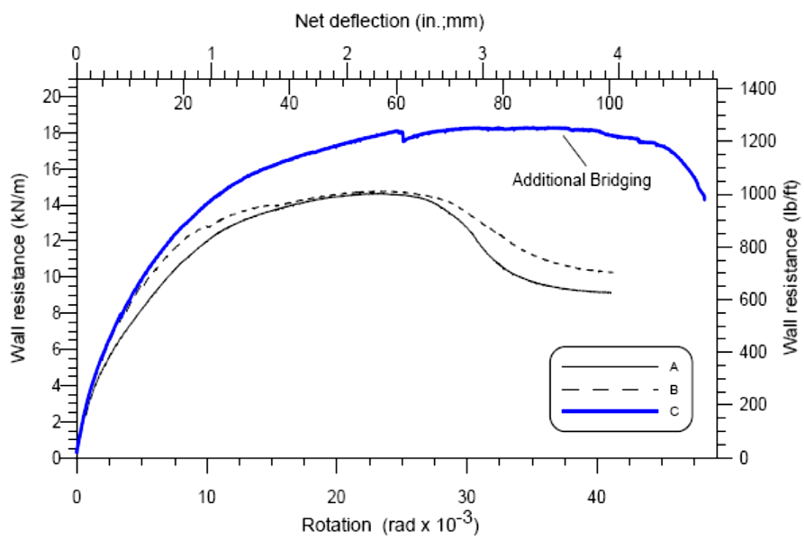

Figure 1.10 Comparison of bridging: Wall resistance vs. displacement of tests 9M-a,b,c (*Balh & Rogers, 2010*)

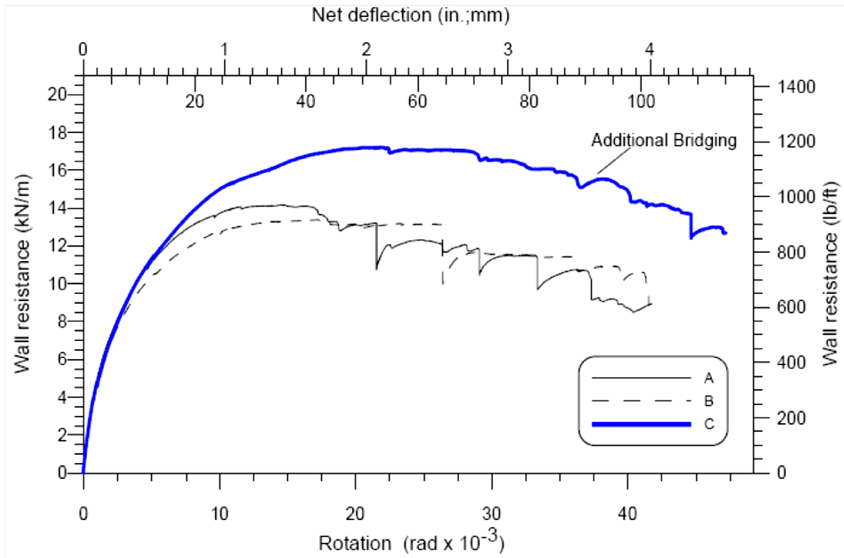

Figure 1.11 Comparison of bridging: Wall resistance vs. displacement of tests 5M-a,b,c (*Balh & Rogers, 2010*)

Though bridging did provide some degree of restraint to chord-stud twisting it was not totally effective. The bridging channel itself exhibited lateral-torsional buckling which made it ineffective in resisting chord-stud twisting at the later stage of wall loading (Figure 1.12). It was recommended that a more rigid blocking to provide better torsional restraint be investigated.

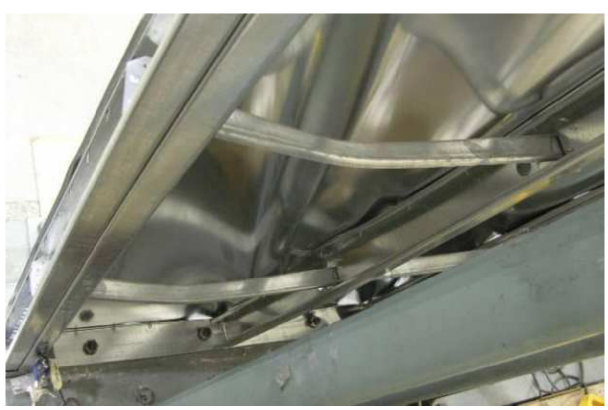

Figure 1.12 Lateral torsional buckling of bridging channel in Test 5M-c (*Ong-Tone & Rogers, 2009*)

1.6.3 Dynamic Analysis

In order to verify the 'test based' seismic force modification factors, R_d and R_o, non-linear time history dynamic analyses must be carried out to predict the performance of multi-storey CFS framed representative buildings during seismic events.

Morello (*2009*), Comeau (*2010*) and Velchev (*2010*) have examined and used a modified procedure of the US Federal Emergency Management Agency (FEMA) P695 methodology (*2009*) on the 'quantification of building seismic performance factors' to verify the Canadian seismic deign provisions developed of wood sheathed and strap braced CFS framed lateral systems. Modifications were made to account for the seismic hazard specific to Canada and to consider the seismic design procedures existing in the 2005 NBCC (*NRCC, 2005*).

Synthetic earthquake records specific to Canadian seismic hazard which were produced by Atkinson (*2009*) and the far-field record set of ground motions provided by FEMA were used for Incremental Dynamic Analysis (IDA). The ground motion records were scaled to match the uniform hazard spectrum (UHS) of the location required and applied at different intensities (scaling factors) to model buildings which represented different performance archetypes. The probability of failure/collapse probabilities were identified as the fraction of ground motions that caused structural collapse based on the maximum inelastic inter-storey drift. Finally, collapse fragility curves were produced and the building performance was evaluated based on acceptable values outlined in the FEMA document.

Balh (*2010*) used this same approach mentioned above to evaluate the seismic performance of the representative buildings used in the development of Canadian seismic design provisions for ordinary steel sheathed / CFS framed shear walls. From this study she was able to justify the use of R_d = 2.0 and R_o = 1.3 for the seismic design of steel sheathed / CFS framed shear walls.

In previous research, Boudreault (*2007*), Morello (*2009*), Comeau (*2010*), Velchev (*2010*) and Balh (*2010*) used the software Ruaumoko (*Carr, 2008*) to carry out non-linear dynamic analysis of CFS framed structures. This software incorporated the Stewart Model (Stewart, 1987) to simulate the hysteretic behaviour of the CFS systems based on stiffness and strength parameters including pinching effects. A key disadvantage of using Ruaumoko was it inability to model post peak strength degradation.

Shamim (*Shamim & Rogers, 2011*) have performed dynamic shake table tests on single-storey and double-storey steel sheathed shear walls. The non-linear dynamic analysis software, OpenSees (*McKenna et al. 2006*) has the ability to model strength degradation and was used for the purpose of producing more accurate dynamic models which were calibrated from the test results obtained from shake table tests.

CHAPTER 2- SHEAR WALL TEST PROGRAM

2.1 Steel Frame/Steel Panel Shear Walls Testing Program

During the summer of 2010, a total of 14 steel sheathed/ cold-formed steel framed shear walls were tested using the shear wall testing frame in the Jamieson Structures Laboratory of McGill University. The major difference of these walls compared to those tested in 2008 by Ong-Tone *(Ong-Tone and Rogers, 2009)* and Balh *(Balh and Rogers, 2010)* was the use of blocking re-enforcement in the framing and the addition of a constant applied gravity load. The intent of this test program was to investigate a means to minimize the effect of the chord-stud twisting failures encountered in previous test programs an to evaluate the wall behaviour under combined lateral and gravity loading.

The testing frame incorporated a MTS ±125 mm (±5") stroke dynamic actuator with a 250kN (55 kips) load cell to move the loading beam attached to the top of the shear wall in the in-plane longitudinal direction. Lateral movement of the wall specimen was restricted by HSS lateral supports. A plywood box into which metal bars were closely packed served as a gravity load which was applied onto the loading beam. This had a total weight of 12.25kN (10kN/m) and was considered appropriate as it fell into the range of gravity loads used in past research on combined gravity and lateral loading of shear walls. A detailed review of the past research can be found in the report by Hikita (*2006*). The shear wall specimens were constructed by platform framing techniques whereby the walls were *constructed* horizontally on the ground and then were installed vertically into the testing frame (Figure 2.1 and Figure 2.2).

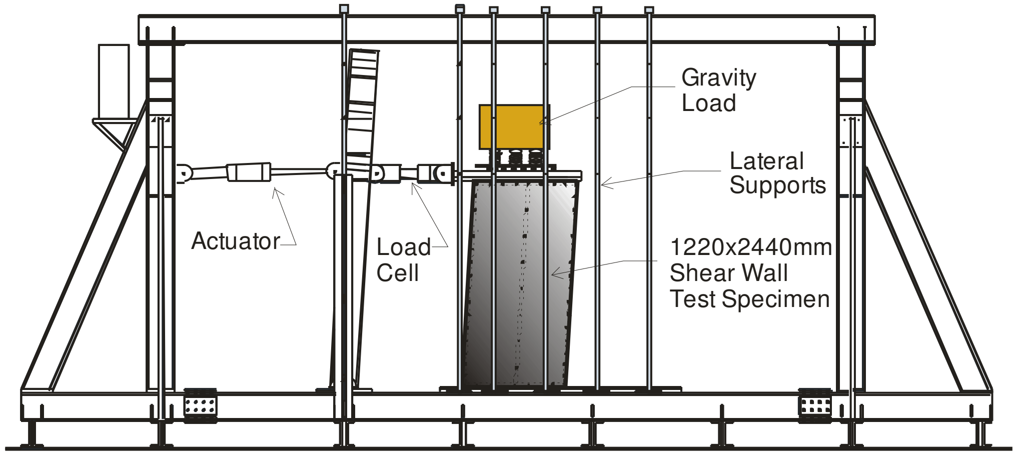

Figure 2.1 Schematic drawing of the test frame with a 1220 x 2440 mm shear wall

Figure 2.2 Shear wall in test frame

2.2 Description of Design of the Shear Wall Test Specimens

This section describes how the eight shear wall configurations, test labelled B1 to B8 were designed (Table 2.1). These configurations varied in framing thickness (studs, tracks and blockings), sheathing thickness and sheathing fastener.

Table 2.1 Configurations of shear wall test labels

Test Label	Fastener Spacing (mm)	Sheathing Thickness (mm)	Framing Thickness (mm)
B1	50/300	0.76	1.37
B2	50/300	0.46	1.09
B3	100/300	0.76	1.09
B4	150/300	0.76	1.09
B5	100/300	0.46	1.09
B6	150/300	0.46	1.09
B7	75/300	0.76	1.37
B8	75/300	0.46	1.37

Capacity based design principles were implemented to ensure that the failure mode was of the sheathing screw connections; other structural components of the Seismic Force Resisting System (SFRS) were required to remain elastic and undamaged, keeping their structural integrity and thus vertical load carrying capacity. The blocked shear walls tested by the author were expected to be stronger than previous test programs of steel sheathed shear walls without blocking reinforcement and the double chord-studs (DCSs) were not expected to fail due to twisting as they were restrained.

Since the steel sheathing was only attached to one face of the test walls, the forces imposed were eccentric. The DCSs were treated as beam-column elements with combined compressive axial loads and flexural bending. As such, the two interaction equations specified in Clause C5.2.2 of the CSA-S136 Standard (*2007*) for stability (Equation 2-1) and strength considerations (Equation 2-2) were used for design.

$$\frac{\bar{P}}{\emptyset_c P_n} + \frac{C_{mx}\overline{M_x}}{\emptyset_b M_{nx}\alpha_x} + \frac{C_{my}\overline{M_y}}{\emptyset_b M_{ny}\alpha_y} \quad (2\text{-}1)$$

$$\frac{\bar{P}}{\emptyset_c P_{no}} + \frac{\overline{M_x}}{\emptyset_b M_{nx}} + \frac{\overline{M_y}}{\emptyset_b M_{ny}} \quad (2\text{-}2)$$

where,

$\overline{\mathrm{P}}$ = Probable/Expected compression force

$\overline{\mathrm{M_x}}$, $\overline{\mathrm{M_y}}$ = Moments due to eccentric loading

$\emptyset_c$ = Compressive resistance factor, 1.00 (for capacity based design)

$\emptyset_b$ = Flexural resistance factor, 1.00 (for capacity based design)

C_{mx}, C_{my} = Coefficients of equivalent uniform bending moments, 0.85

P_{no} = Nominal compressive resistance with F_n = F_y (local buckling capacity)

P_n = Nominal compressive resistance (accounting for overall buckling modes)

M_{nx}, M_{ny} = Effective moment resistance (calculated with F_y for strength & F_c for stability interaction)

α_x, α_y = Second order amplification factors

The compression force imposed on the DCSs comprised of two components: the compression force due to the vertical component of the tension field developed in the steel sheathing and due to the direct gravity load. For the former, the nominal yield resistance values and an overstrength factor of 1.40 proposed by Balh *(2010)* were used to determine the probable/expected compression force due to shear (Equation 2-3). This compression force due to the tension field action was assumed to be constant throughout the wall height which is a conservative approach (Figure 2.3). The compression force applied to a DCS due to the gravity loading system was calculated as 4.90kN assuming a rigid top beam and the contribution of the field stud. The load was taken as constant along the DCS height. Therefore, the probable compression force applied to the DCS was the summation of these two components (Equation 2-4).

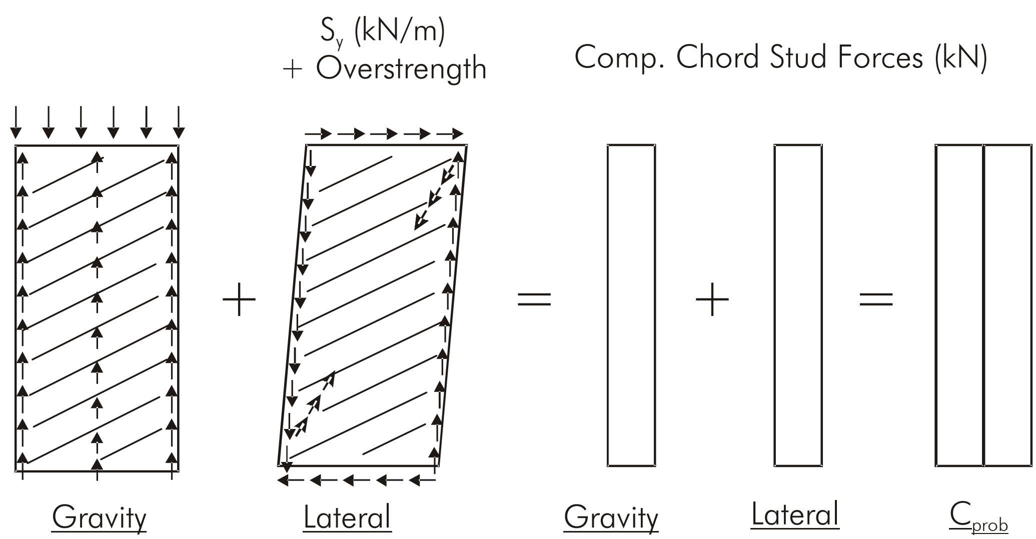

Figure 2.3 Determination of the probable compression force on the DCS

$$C_s = {}^{S_y h}/_{b} \times b \times \text{overstrength} \qquad (2\text{-}3)$$

where,

C_s = Compression force due to shear

S_y= Nominal yield resistance of specified wall (Balh *(2010)*)

h = height of test wall (m)

b = width of specified shear wall (m)

overstrength = overstrength factor, 1.40 (Balh *(2010)*)

C_g= Compression force due to gravity, 4.90 kN

$$\bar{P} = C_s + C_g \tag{2-4}$$

The moments imposed on the DCSs, $\overline{M_x}$ and $\overline{M_y}$, due to the assumed eccentricities of the applied gravity load and the mono-sided steel sheathing were conservatively determined as follows: $\overline{M_x}$ was the summation of the gravity load (6.13kN) applied at 5% the distance of 92.1mm from the neutral axis, and the compressive force due to shear, C_s, applied at the flange edge or half of the nominal web dimension which represented the moment caused by the horizontal component of the sheathing tension field exerted at the flange edge (Equation 2-5). $\overline{M_y}$ was taken as the gravity load applied at 5% the distance of twice the nominal flange dimension since the chords were constructed two studs (Equation 2-6).

$$\overline{M_x} = \left(C_g \times 5\% \times {}^{92.1}/_{1000}\right) + \left(C_s \times {}^{92.1}/_{2 \times 1000}\right) \tag{2-5}$$

$$\overline{M_y} = C_g \times 5\% \times \left({}^{2 \times 41.3}/_{1000}\right) \tag{2-6}$$

The nominal values for both compressive and flexure resistances were determined as prescribed by CSA S136-07. The cold-formed steel design software, CFS Version 6.0.4 software *(Glauz, 2011)* was used which has the inbuilt ability to automatically perform the stability and strength interactions (CSA S136-07) based on the inputted probable compressive forces, $\bar{P}$, and moments due to eccentric loading, $\overline{M_x}$ and $\overline{M_y}$. The buckling lengths of L_x = 2440 mm (wall height) and L_y & L_z = 610 mm (quarter point bracing) and effective length factor of $K_x = K_y = K_z$ =1.0 were used to calculate the resistances for respective axes. The results provided by the software are summarized in Table 2.2 and a detailed example of wall configuration B1 can be seen in Appendix A. It is important to note that the software output shown in Appendix A uses the factored resistances, i.e. with the resistance factors ϕ_c = 0.8 and ϕ_b = 0.9. Thus these values were modified to represent the un-factored values shown in Table 2.2 with ϕ_c & ϕ_b = 1.0 used for capacity based design.

Although a few of the resulting ratios exceeded 1.0, particularly the stability interactions, they were deemed acceptable when considering past research. Hikita (*2006*) used the capacity based design approach in the design of the double chord studs of wood sheathed shear walls for which no test wall failed by local buckling or twisting of the DCSs. More importantly, only the axial capacities were considered by Hikita (*2006*) and the moments due to the eccentric loading, $\overline{M_x}$ and $\overline{M_y}$, were not accounted for. The contribution of the applied moments in the interaction Equations 2-1 and 2-2 were significant, particularly $\overline{M_x}$, which had the effect of almost doubling the ratios when compared to the contribution of the axial component alone. As such, it was necessary to revise the method used to calculate $\overline{M_x}$. A reduction of $\overline{M_x}$ was made whereby quarter of the nominal web dimension was used instead of half. The resulting ratios using the revised equation were below 1.0 as required (Table 2.3).

The author's test walls were expected to produce higher shear resistance compared with similar, but unblocked, walls tested by Balh (*Balh & Rogers, 2010*) and Ong-Tone (*Ong-Tone & Rogers, 2009*) with no failure of the DCSs. After the testing and evaluation of test results were complete and the new shear wall nominal resistances, S_y, were obtained (See Chapter 3), the DCSs were rechecked with the measured material properties (Table 2.7) and can be seen in Table B.1 of Appendix B. None of the test walls suffered from the twisting failure of the DCS but other failure modes were noted (Section 2.7.2). Again, a reduction of $\overline{M_x}$ as above was deemed necessary since most of the resulting ratios exceeded 1.0 although the vertical load carrying ability of the test walls were maintained. The updated table (Table B.2) can be seen in Appendix B.

Table 2.2 Design of double chord ctuds[1] for shear wall test specimens

Test Label	B1	B2	B3	B4	B5	B6	B7	B8
Nominal Stud Thickness (mm)	1.37	1.09	1.09	1.09	1.09	1.09	1.37	1.37
Nominal Yield Stress (MPa)	340	230	230	230	230	230	340	340
Sheathing Thickness (mm)	0.76	0.46	0.76	0.76	0.46	0.46	0.76	0.46
Fastener Spacing (mm)	50	50	100	150	100	150	75	75
S_y, Nominal Yield Resistance[2] (kN/m)	13.93	7.53	10.58	8.89	6.03	4.53	12.97	6.78
Overstrength[2]	1.40	1.40	1.40	1.40	1.40	1.40	1.40	1.40
Gravity Load/per DCS (kN)	4.90	4.90	4.90	4.90	4.90	4.90	4.90	4.90
$\overline{\mathbf{P}}$, Probable Compression Force (kN)	52.45	30.60	41.01	35.24	25.48	20.36	49.17	28.04
$\overline{M_x}$ (kNm)	2.21	1.21	1.69	1.42	0.97	0.73	2.06	1.09
$\overline{M_y}$ (kNm)	0.02	0.02	0.02	0.02	0.02	0.02	0.02	0.02
Stability Interaction[3]								
$\emptyset_c P_n$ (kN)	112.10	65.86	65.86	65.86	65.86	65.86	112.10	112.10
$\emptyset_b M_{nx}$ (kNm)	4.76	2.72	2.72	2.72	2.72	2.72	4.76	4.76
$\emptyset_b M_{ny}$ (kNm)	1.71	0.99	0.99	0.99	0.99	0.99	1.71	1.71
Stability Interaction Eq. (C5.2.2-1)	**0.94**	**0.93**	**1.26**	**1.08**	**0.76**	**0.60**	**0.88**	**0.49**
Strength Interaction[3]								
$\emptyset_c P_{no}$ (kN)	140.81	79.10	79.10	79.10	79.10	79.10	140.81	140.81
$\emptyset_b M_{nx}$ (kNm)	4.94	2.81	2.81	2.81	2.81	2.81	4.94	4.94
$\emptyset_b M_{ny}$ (kNm)	1.71	0.99	0.99	0.99	0.99	0.99	1.71	1.71
Strength Interaction Eq. (C5.2.2-2)	**0.83**	**0.84**	**1.14**	**0.97**	**0.69**	**0.54**	**0.78**	**0.43**
Axial Ratio[3]								
$\overline{\mathbf{P}}/\emptyset_c P_n$	**0.47**	**0.46**	**0.62**	**0.54**	**0.39**	**0.31**	**0.44**	**0.25**

[1] Nominal dimensions of stud: 92.1mm (3-5/8”) web, 41.3mm (1-5/8”) flange, and 12.7mm (1/2”) lip

[2] From Balh *(2010)*

[3] Calculations were according to CSA-S136 Standard (2007): resistance factors ϕ_c= ϕ_b=1.0 end conditions K_x=K_y=K_t=1.0 and buckling lengths L_x= 2440mm, L_y=L_z=610mm

Table 2.3 Design of double chord studs[1] with reduced M_x

Test Label	B1	B2	B3	B4	B5	B6	B7	B8
Nominal Stud Thickness (mm)	1.37	1.09	1.09	1.09	1.09	1.09	1.37	1.37
Nominal Yield Stress (MPa)	340	230	230	230	230	230	340	340
Sheathing Thickness (mm)	0.76	0.46	0.76	0.76	0.46	0.46	0.76	0.46
Fastener Spacing (mm)	50	50	100	150	100	150	75	75
S_y, Nominal Yield Resistance[2] (kN/m)	13.93	7.53	10.58	8.89	6.03	4.53	12.97	6.78
Overstrength[2]	1.40	1.40	1.40	1.40	1.40	1.40	1.40	1.40
Gravity Load/per DCS (kN)	4.90	4.90	4.90	4.90	4.90	4.90	4.90	4.90
$\overline{\mathbf{P}}$, Probable Compression Force (kN)	52.45	30.60	41.01	35.24	25.48	20.36	49.17	28.04
$\overline{M_x}$ (kNm)	1.12	0.61	0.85	0.72	0.50	0.38	1.04	0.56
$\overline{M_y}$ (kNm)	0.02	0.02	0.02	0.02	0.02	0.02	0.02	0.02
Stability Interaction[3]								
$\emptyset_c P_n$ (kN)	112.10	65.86	65.86	65.86	65.86	65.86	112.10	112.10
$\emptyset_b M_{nx}$ (kNm)	4.76	2.72	2.72	2.72	2.72	2.72	4.76	4.76
$\emptyset_b M_{ny}$ (kNm)	1.71	0.99	0.99	0.99	0.99	0.99	1.71	1.71
Stability Interaction Eq. (C5.2.2-1)	**0.71**	**0.71**	**0.95**	**0.82**	**0.59**	**0.47**	**0.67**	**0.38**
Strength Interaction[3]								
$\emptyset_c P_{no}$ (kN)	140.81	79.10	79.10	79.10	79.10	79.10	140.81	140.81
$\emptyset_b M_{nx}$ (kNm)	4.94	2.81	2.81	2.81	2.81	2.81	4.94	4.94
$\emptyset_b M_{ny}$ (kNm)	1.71	0.99	0.99	0.99	0.99	0.99	1.71	1.71
Strength Interaction Eq. (C5.2.2-2)	**0.61**	**0.62**	**0.84**	**0.72**	**0.52**	**0.41**	**0.57**	**0.32**
Axial Ratio[3]								
$\overline{\mathbf{P}}/\emptyset_c P_n$	**0.47**	**0.46**	**0.62**	**0.54**	**0.39**	**0.31**	**0.44**	**0.25**

[1] Nominal dimensions of stud: 92.1mm (3-5/8”) web, 41.3mm (1-5/8”) flange, and 12.7mm (1/2”) lip

[2] From Balh *(2010)*

[3] Calculations were according to CSA-S136 Standard (2007): resistance factors ϕ_c= ϕ_b=1.0 end conditions K_x=K_y=K_t=1.0 and buckling lengths L_x= 2440mm, L_y=L_z=610mm

2.3 Test Matrix

In all, fourteen shear walls of eight different configurations were tested (Table 2.4). Six configurations, test label B1 to B6, were tested under monotonic and reversed cyclic protocols (B1-M, B1-R, B2-M, B2-R,… etc.). The remaining two configurations, B7-M and B8-M, were only tested by monotonic protocol. The reason for testing these last two configurations was to obtain data for a 75 mm (3”) fastener spacing walls instead of relying on linear interpolation of data between 50 mm (2”) and 100 mm (4”) fastener spaced walls. Details of each specimen are found in the Test Data Sheets in Appendix C.

Table 2.4 Shear wall test matrix

Test Label	Protocol	Test Specimen	Wall Size (mm)	Fastener Spacing (mm)	Sheathing Thickness (mm)	Framing Thickness (mm)
B1	Monotonic	B1-M	1220 x 2440	50/300	0.76	1.37
	Cyclic	B1-R	1220 x 2440	50/300	0.76	1.37
B2	Monotonic	B2-M	1220 x 2440	50/300	0.46	1.09
	Cyclic	B2-R	1220 x 2440	50/300	0.46	1.09
B3	Monotonic	B3-M	1220 x 2440	100/300	0.76	1.09
	Cyclic	B3-R	1220 x 2440	100/300	0.76	1.09
B4	Monotonic	B4-M	1220 x 2440	150/300	0.76	1.09
	Cyclic	B4-R	1220 x 2440	150/300	0.76	1.09
B5	Monotonic	B5-M	1220 x 2440	100/300	0.46	1.09
	Cyclic	B5-R	1220 x 2440	100/300	0.46	1.09
B6	Monotonic	B6-M	1220 x 2440	150/300	0.46	1.09
	Cyclic	B6-R	1220 x 2440	150/300	0.46	1.09
B7	Monotonic	B7-M	1220 x 2440	75/300	0.76	1.37
B8	Monotonic	B8-M	1220 x 2440	75/300	0.46	1.37

2.4 Specimen Fabrication, Test Setup and Instrumentation

A description of the materials used in the construction, specimen fabrication, the test setup and instrumentation is provided in this section.

2.4.1 Materials

The materials used in the construction of the shear wall specimens were as follows:

i) 0.46 mm (0.018”) nominal thickness cold-formed sheet steel of 230 MPa (33 ksi) nominal grade *(ASTM A653 (2008))*.

ii) 0.76 mm (0.030”) nominal thickness cold-formed sheet steel of 230 MPa (33 ksi) nominal grade *(ASTM A653 (2008))*.

iii) 1.09 mm (0.043”) nominal thickness cold-formed ‘C’ section steel stud of 230 MPa (33 ksi) nominal grade (*ASTM A653 (2008))*. The nominal dimensions were 92.1 mm x 41.3 mm x 12.7 mm (3-5/8” x 1-5/8” x 1/2”) of the web, flange and lip respectively.

iv) 1.37 mm (0.054”) nominal thickness cold-formed ‘C’ section steel stud of 340 MPa (50 ksi) nominal grade (*ASTM A653 (2008))*. The nominal dimensions were 92.1 mm x 41.3 mm x 12.7 mm (3-5/8” x 1-5/8” x 1/2”) of the web, flange and lip respectively.

v) 1.09 mm (0.043”) nominal thickness cold-formed channel section steel tracks of 230 MPa (33 ksi) nominal grade (*ASTM A653 (2008))*. The nominal dimensions were 92.1 mm x 31.8 mm (3-5/8” x 1-1/4”) of the web and flange respectively.

vi) 1.37 mm (0.054”) nominal thickness cold-formed channel section steel tracks of 340 MPa (50 ksi) nominal grade (*ASTM A653 (2008))*. The nominal dimensions were 92.1 mm x 31.8 mm (3-5/8” x 1-1/4”) of the web and flange respectively.

vii) The blockings were cut from the channel section tracks listed above.

viii) Simpson Strong-Tie S/HD 10S hold-down connectors were fastened to the test frame by 22 mm (7/8”) diameter anchor rods Grade B7 *(ASTM A193 (2008)).* The hold-downs were attached to the web at both ends of the chord studs with 33 No. 10 gauge 25.4 mm (1”) self-drilling hex washer head screws.

ix) No. 10 gauge 19 mm (3/4”) self-drilling wafer head screws, spaced at 300 mm (12”) along the stud length were used to make back-to-back/double chord studs.

x) No. 8 gauge 12.7 mm (1/2”) self-drilling wafer head screws were used to connect the tracks, studs and blockings to make the CFS frame.

xi) No. 8 gauge 19 mm (3/4”) self-drilling pan head screws were used to connect the steel sheathing to the CFS frame.

2.4.2 Specimen Fabrication

All components were made in an assembly type manner prior to the shear wall fabrication. All back-to-back chord studs were made with a hold-down installed at each end. The base of each hold-down was placed flush with the end of the chord studs. The top and bottom tracks were pre-drilled with holes to facilitate 19.1 mm (3/4”) A325 shear bolts along the track’s length and 22 mm (7/8”) threaded anchor rods at the hold-down locations (Figure 2.4).

Figure 2.4 Pre-drilling of tracks

The blockings were cut from the channel section tracks and were detailed such that the flanges overlapped the back-to-back chord stud when the frame was assembled. The blocking detail was similar to the strapping and blocking detail recommended by the AISI S230 Standard for Cold-Formed Steel Framing-Prescriptive Method for One and Two Family Dwellings (*AISI S230,2007*) Section E (Figure 1.6). Bridging clips and 127 mm (5”) long track sections were also used to accommodate the attachment of the blocking to the chord studs (Figure 2.5).

Figure 2.5 Blocking reinforcment detail at field stud (*left*) and double chord stud (*right*)

Platform framing techiques were used to assemble the steel frame and the framing components were connected using No. 8 gauge 12.7 mm (1/2”) wafer head screws. The frame consisted of two back-to-back chord studs at the frame ends, a single field stud 610 mm (2’) on-centre along the 1220 mm (4’) wall length, top and bottom tracks and three rows of full blocking at quarter points along the wall’s height. A diagonal channel was used during the assembly to ensure the frame remained square (Figure 2.6).

Figure 2.6 Frame assembly

The steel sheathing was mounted vertically on one side of the steel frame using No. 8 gauge 19 mm (3/4”) self-drilling pan head screws. The sheathing was attached along the frame perimeter 9.5 mm (3/8”) from the sheathing panel edge at 50, 75, 100 or 150 mm (2”, 3”, 4” or 6”) fastener spacing according to the wall’s configuration (Table 2.4). The sheathing was attached to the interior field stud with screws spaced at 305 mm (12”) o/c.

2.4.3 Test Setup

To facilitate the gravity loading system, a new loading beam had to be built. After the wall specimens were fabricated each one was mounted vertically into the test frame (Figure 2.7). Once positioned, the shear bolts and hold-down anchor rods were installed to attach the wall to the reaction base and loading beam. Washers were used to minimize possible deformation and bearing damage to the tracks. Square plate washers were used for shear bolts between the top track and aluminum spacer plate and cut washers between the bottom track and aluminum spacer plate. The cut washers were also used for installing the hold-down anchor rods.

Figure 2.7 Shear wall specimen B4-R installed into test frame

Additional chain blocks were installed onto the test frame to facilitate the new gravity loading system. Once the loading beam was fastened to the wall specimen, an aluminum plate was placed above the loading beam, followed by an assembly of rollers, then another aluminum plate. These plates provided a smooth surface for the roller assembly. A channel section which also served as a guide was placed above the top aluminum plate, followed by three springs, and finally the gravity load box was dropped onto the springs. The roller assembly and springs allowed the gravity box to move vertically with the test wall, but not longitudinally in the plane of the wall. Stoppers were installed onto the sides of the load box to provide longitudinal restraint as the loading beam moved according to the monotonic or reversed cyclic protocols (Figure 2.8). Once the wall was secured and the gravity load system was in place, instrumentation devices were installed.

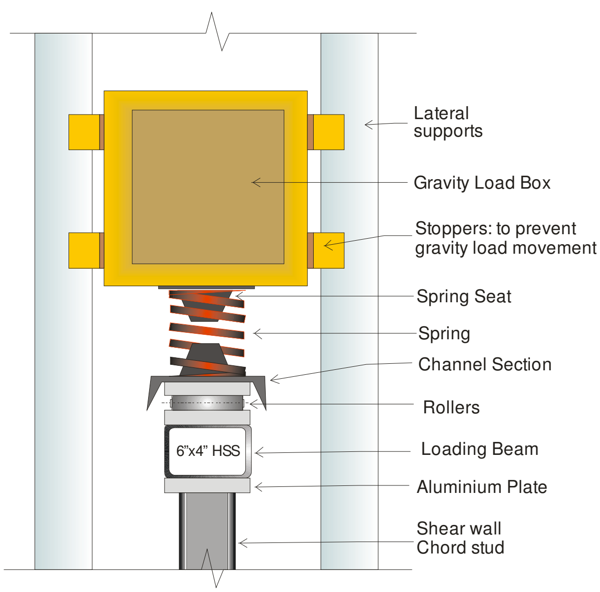

Figure 2.8 Front section of gravity load system

2.4.4 Instrumentation and Data Acquisition

After the shear wall specimen had been secured to the test frame, load cells were attached to both bottom hold-down anchor rods to monitor the uplift forces through the chord studs. Four linear variable differential transformers (LVDTs) were positioned at the base of the wall to capture the uplift movement and longitudinal slip. A string potentiometer was used to measure the in-plane lateral displacement at the wall top. Lastly, the internal load cell and LVDT within the MTS actuator measured the lateral resistance of the wall and the in-plane lateral displacement of the wall top respectively (Figure 2.9).

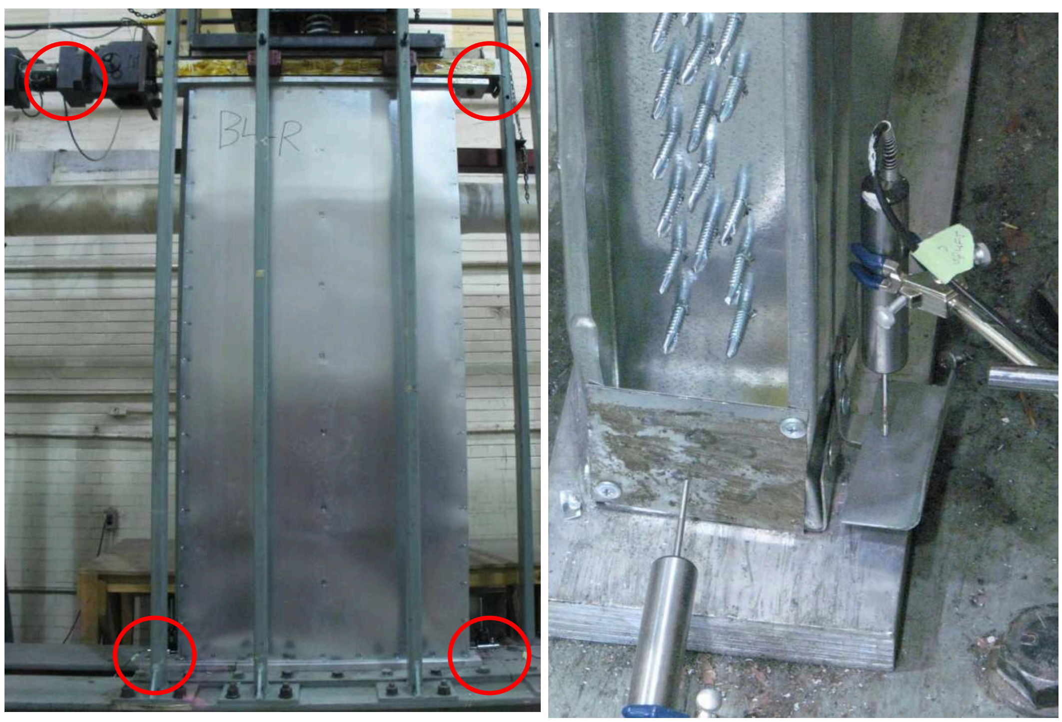

Figure 2.9 Locations of instrumentation (*left*) and orientation of LVDTs (*right*)

2.5 Testing Protocols

Two displacement based loading protocols were used for testing the shear wall specimens: monotonic and reversed cyclic protocols. A detailed description of each is provided in this section.

2.5.1 Monotonic Tests

The monotonic testing was performed on each shear wall configuration whereby the lateral displacement was applied at a constant rate of 2.5 mm/min. Strain rate effects were avoided using this slow loading and static/wind loading conditions were simulated. This protocol was identical to that used by Ong-Tone *(2009)* and Balh *(2010)* for the steel sheathed shear wall tests previously performed at McGill University. The load was applied to the wall from the zero displacement position, which is the stable position whereby the wall carried zero lateral load, and continued until the displacement reached 100 mm. This limit is well past the allowable drift limit of 2.5% of the wall height (61 mm for a 2440 mm high wall) prescribed by the 2005 NBCC *(NRCC, 2005)*. A typical graph of the wall resistance verses displacement is shown in Figure 2.10.

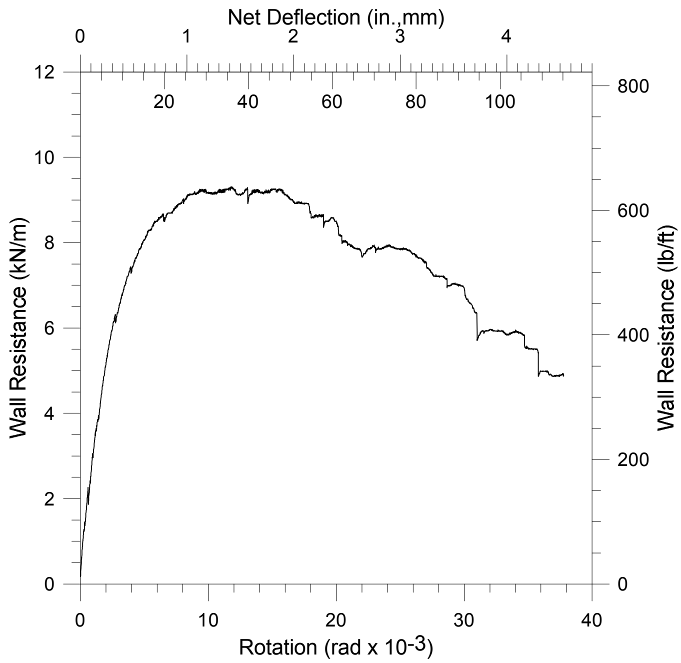

Figure 2.10 Example of monotonic curve (Test B6-M)

2.5.2 Reversed Cyclic Tests

Once the monotonic testing of each configuration was completed, reversed cyclic testing based on the CUREE (Consortium of Universities of Research in Earthquake Engineering) ordinary ground motions protocol was performed. This protocol represents the demand expected during a design level earthquake and is further described by Krawinkler *et al. (2000)* and ASTM E2126 *(2007)*. This protocol was also used by Ong-Tone *(2009)*, Balh *(2010)* and past research on wood sheathing and strap braced CFS framing shear walls performed at McGill University (*Branston et al. (2006), Hikita (2006), Comeau (2008), Velchev (2008) and Morello (2009)*).

From the monotonic test data the post-peak displacement, Δ_m, corresponding to 80% of the ultimate shear resistance (S_u) was obtained. Sixty percent of this post-peak displacement was used as the reference displacement, Δ, for the CUREE protocol. All reversed cyclic tests were run at a rate of 0.1Hz which ensured the smooth operation of the gravity rolling system and eliminated any inertia effects since any acceleration taking place was minute. The protocol consisted of three cycles: the initiation, primary and trailing cycles, all of which were multiples of Δ. A full cycle started from the zero displacement position, went through positive and negative displacements of equal magnitude and returned to the origin. The initiation cycles were used to confirm the proper operation of the instrumentation and data acquisition devices and were within the elastic range of the wall specimen. These were 0.05Δ and occurred for six cycles. The primary cycles allowed the wall to enter into the inelastic range with progressively increasing displacements. The first primary cycle was 0.75Δ and increased to 0.1Δ, 0.2Δ, 0.3Δ, 0.4Δ, 0.7Δ, 1.0Δ and lastly to 0.5Δ increases in displacements. Finally, the trailing cycles in-between the primary cycles were 75% of the preceding primary cycle. Table 2.5 shows an example of a typical loading protocol and the corresponding displacement time histories and the wall resistance vs. displacement hysteresis curves are shown in Figure 2.11 and Figure 2.12 respectively.

Table 2.5 CUREE protocol input displacements for Test B3-R

$\Delta = 0.6 \times \Delta_m =$	30.732 mm		
Displ.	Actuator Input(mm)	No. of Cycles	Cycle Type
0.050 Δ	1.537	6	Initiation
0.075 Δ	2.305	1	Primary
0.056 Δ	1.721	6	Trailing
0.100 Δ	3.073	1	Primary
0.075 Δ	2.305	6	Trailing
0.200 Δ	6.146	1	Primary
0.150 Δ	4.610	3	Trailing
0.300 Δ	9.220	1	Primary
0.225 Δ	6.915	3	Trailing
0.400 Δ	12.293	1	Primary
0.300 Δ	9.220	2	Trailing
0.700 Δ	21.512	1	Primary
0.525 Δ	16.134	2	Trailing
1.000 Δ	30.732	1	Primary
0.750 Δ	23.049	2	Trailing
1.500 Δ	46.098	1	Primary
1.125 Δ	34.574	2	Trailing
2.000 Δ	61.464	1	Primary
1.500 Δ	46.098	2	Trailing
2.500 Δ	76.830	1	Primary
1.875 Δ	57.623	2	Trailing
3.000 Δ	92.196	1	Primary
2.250 Δ	69.147	2	Trailing
3.500 Δ	107.562	1	Primary
2.625 Δ	80.672	2	Trailing

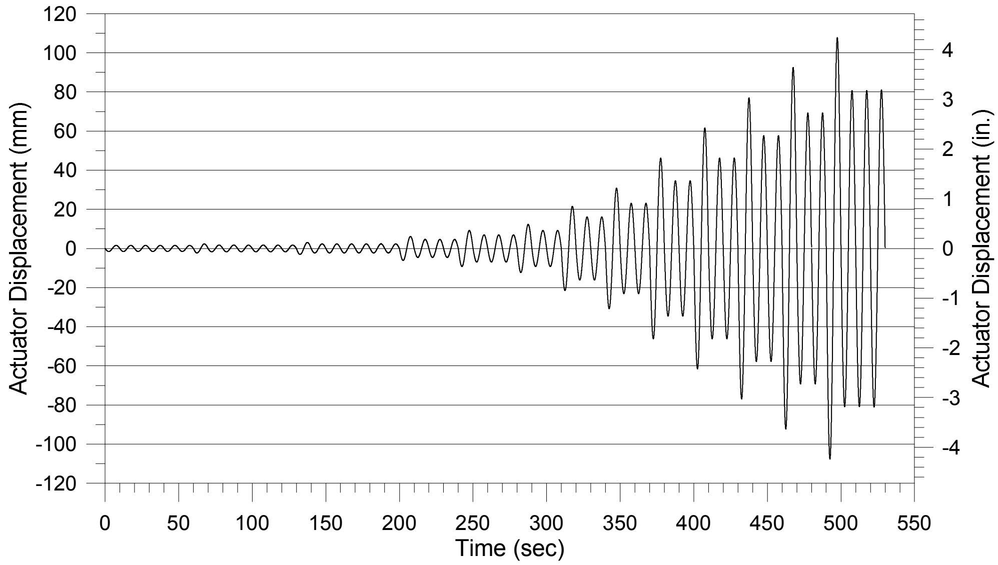

Figure 2.11 Displacement time history for Test B3-R

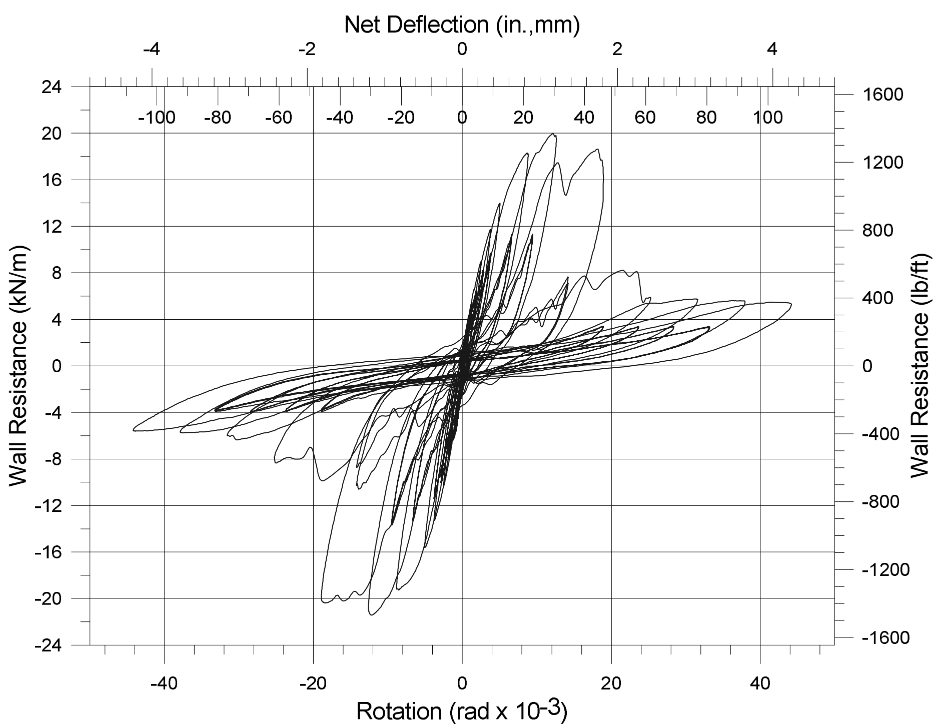

Figure 2.12 CUREE reserved-cyclic curve (Test B3-R)

2.6 Test Results

The raw test data recorded by the data acquisition system from the monotonic and reversed cyclic tests were inputted into the modified automated spreadsheet created by Balh *(2010)* and the following parameters of the analysed data were obtained. For the monotonic tests, the maximum wall resistance, S_u, wall resistance at $0.4S_u$, wall resistance at $0.8S_u$ post peak, and their corresponding displacements, $\Delta_{net,u}$, $\Delta_{net,0.4u}$ and $\Delta_{net,0.8u}$ respectively. The rotations at S_u, θ_u, rotation at $0.4S_u$, $\theta_{0.4u}$, rotation at $0.8S_u$, $\theta_{0.8u}$, and energy dissipation, *E*, were also listed. For the reversed cyclic tests, the positive and negative maximum wall resistance, $S_u'_+$ and $S_u'_-$, wall resistance at 0.4 $S_u'_+$ and 0.4 $S_u'_-$, wall resistance at $0.8S_u'_+$ and 0.8 $S_u'_-$, and their corresponding displacements and rotations, $\Delta_{net,u+}$, $\Delta_{net,u-}$, $\Delta_{net,0.4u+}$, $\Delta_{net,0.4u-}$, $\Delta_{net,0.8u+}$, $\Delta_{net,0.8u-}$, and θ_{u+}, θ_{u-}, $\theta_{0.4u+}$, $\theta_{0.4u-}$, $\theta_{0.8u+}$, $\theta_{0.8u-}$ respectively. The total energy dissipated, ***E*****,** was also included. A graphically presentation of the parameters are shown in Figures 2.13 and 2.14 for a monotonic and reversed cyclic tests respectively. The test results are listed in Tables 2.6, 2.7 and 2.8 and an example figure of the output parameters from the automated spreadsheet of both monotonic and reversed cyclic tests are shown in Figure 2.15.

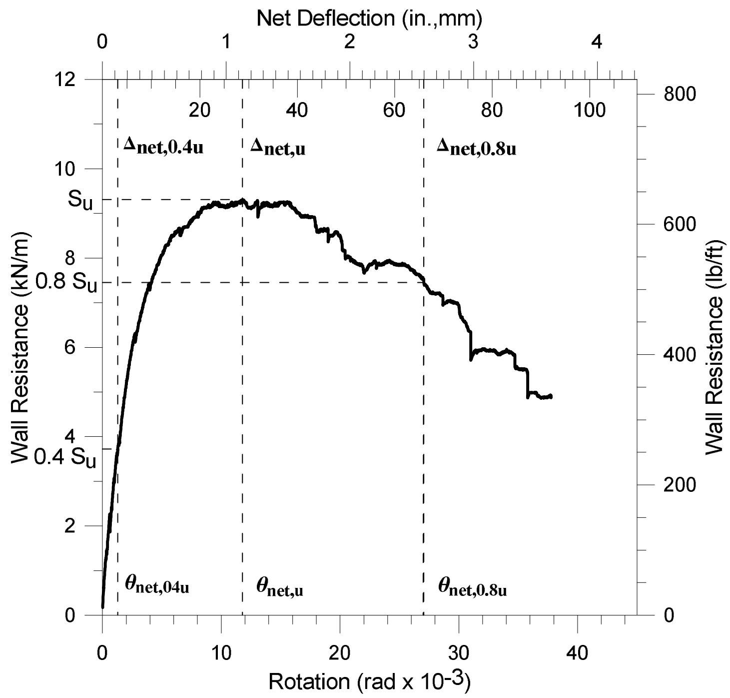

Figure 2.13 Parameters of monotonic tests (test B6-M)

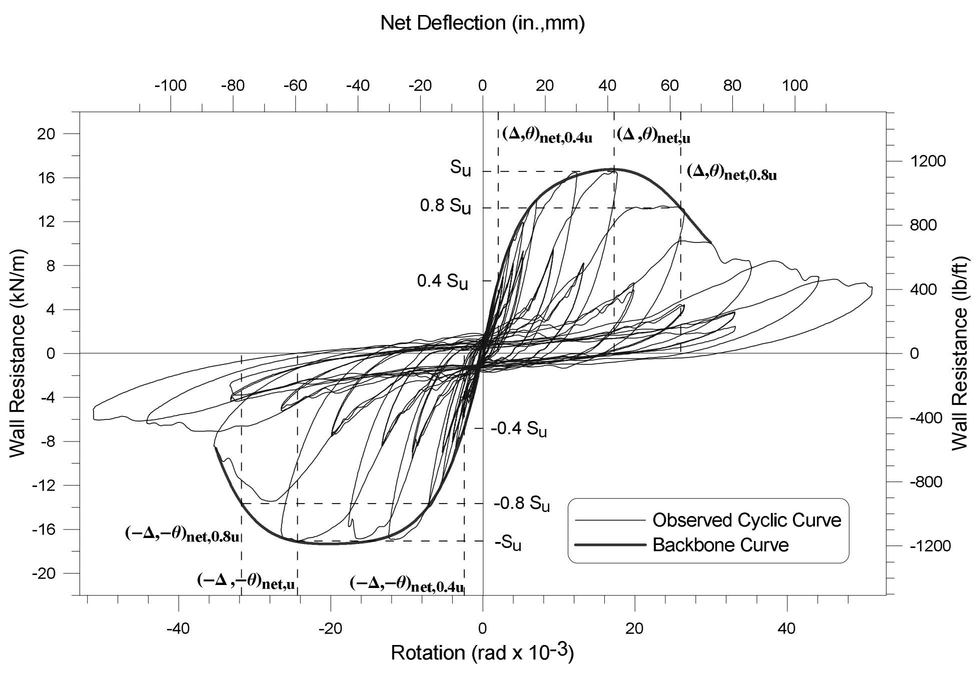

Figure 2.14 Parameters of reversed cyclic tests (test B2-R)

Parameters		Units
F_u	20.62	kN
$F_{0.8u}$	16.49	kN
$F_{0.4u}$	8.25	kN
F_y	18.96	kN
K_e	1.35	kN/mm
Ductility (μ)	4.85	-
$\Delta_{net,y}$	14.09	mm
$\Delta_{net,u}$	47.57	mm
$\Delta_{net,0.8u}$	68.26	mm
$\Delta_{net,0.4u}$	6.13	mm
$Area_{Backbone}$	1160.66	J
$Area_{EEEP}$	1160.66	J
Check	OK	
R_d	2.95	-
S_y	15.55	kN/m

Parameters			Units
	Positive	Negative	
F_u	20.20	-20.80	kN
$F_{0.8u}$	16.16	-16.64	kN
$F_{0.4u}$	8.08	-8.32	kN
F_y	18.61	-19.63	kN
K_e	1.65	1.39	kN/mm
Ductility (μ)	5.62	5.47	-
$\Delta_{net,y}$	11.28	-14.16	mm
$\Delta_{net,u}$	42.08	-59.47	mm
$\Delta_{net,0.8u}$	63.40	-77.40	mm
$\Delta_{net,0.4u}$	4.90	-6.00	mm
$Area_{Backbone}$	1074.60	1380.64	J
$Area_{EEEP}$	1074.60	1380.64	J
Check	OK	OK	-
R_d	3.20	3.15	-
S_y	15.26	-16.10	kN/m

Figure 2.15 Parameters obtained from monotonic (*left*) and reversed cyclic (*right*) spreadsheets for Tests B2-M and B2-R respectively

Table 2.6 Monotonic test data

Test Specimen	Maximum Wall Resistance F_u (kN)	Maximum Wall Resistance S_u (kN/m)	Displacement at S_u $\Delta_{net,u}$ (mm)	Displacement at $0.4S_u$ $\Delta_{net,0.4u}$ (mm)	Displacement at $0.8S_u$ $\Delta_{net,0.8u}$ (mm)	Rotation at S_u $\theta_{net,u}$ (rad)	Rotation at $0.4S_u$ $\theta_{net,0.4u}$ (rad)	Rotation at $0.8S_u$ $\theta_{net,0.8u}$ (rad)	Energy Dissipation, E (Joules)
B1-M	41.40	33.96	40.71	7.03	74.31	0.01670	0.00288	0.03048	3188
B2-M	20.62	16.91	47.57	6.13	68.26	0.01951	0.00251	0.02799	1624
B3-M	23.65	19.40	35.79	6.98	51.22	0.01468	0.00286	0.02101	1136
B4-M	20.52	16.83	43.17	4.02	53.95	0.01771	0.00165	0.02212	1299
B5-M	14.64	12.00	35.45	5.62	55.93	0.01454	0.00230	0.02294	928
B6-M	11.35	9.31	28.71	3.13	65.98	0.01177	0.00128	0.02706	836
B7-M	34.15	28.01	39.69	6.79	63.81	0.01628	0.00278	0.02617	2089
B8-M	17.68	14.50	26.61	3.56	38.58	0.01091	0.00146	0.01582	851

Table 2.7 Positive cycles reversed cyclic test results

Test Specimen	Maximum Wall Resistance $F_u'_+$ (kN)	Maximum Wall Resistance $S_u'_+$ (kN/m)	Displacement at $S_u'_+$, $\Delta_{net,u+}$ (mm)	Displacement at $0.4S_u'_+$, $\Delta_{net,0.4u+}$ (mm)	Displacement at $0.8S_u'_+$, $\Delta_{net,0.8u+}$ (mm)	Rotation at $S_u'_+$, $\theta_{net,u+}$ (rad)	Rotation at $0.4S_u'_+$, $\theta_{net,0.4u+}$ (rad)	Rotation at $0.8S_u'_+$, $\theta_{net,0.8u+}$ (rad)	Energy Dissipation, E (Joules)
B1-R	38.01	31.17	30.72	7.20	61.40	0.01260	0.00295	0.02518	13282
B2-R	20.20	16.57	42.08	4.90	63.40	0.01726	0.00201	0.02600	8688
B3-R	24.37	19.99	29.76	5.00	48.30	0.01221	0.00205	0.01981	7285
B4-R	19.52	16.01	29.64	3.60	40.50	0.01216	0.00148	0.01661	5514
B5-R	14.73	12.08	23.00	4.10	34.50	0.00943	0.00168	0.01415	5595
B6-R	11.39	9.34	27.08	3.20	42.30	0.01110	0.00131	0.01735	4034

Table 2.8 Negative cycles reversed cyclic test results

Test Specimen	Maximum Wall Resistance $F_u'_-$ (kN)	Maximum Wall Resistance $S_u'_-$ (kN/m)	Displacement at $S_u'_-$, $\Delta_{net,u-}$ (mm)	Displacement at $0.4S_u'_-$, $\Delta_{net,0.4u-}$ (mm)	Displacement at $0.8S_u'_-$, $\Delta_{net,0.8u-}$ (mm)	Rotation at $S_u'_-$, $\theta_{net,u-}$ (rad)	Rotation at $0.4S_u'_-$, $\theta_{net,0.4u-}$ (rad)	Rotation at $0.8S_u'_-$, $\theta_{net,0.8u-}$ (rad)	Energy Dissipation, E (Joules)
B1-R	-38.85	-31.87	-58.81	-9.60	-78.80	-0.02412	-0.00394	-0.03232	13282
B2-R	-20.80	-17.06	-59.47	-6.00	-77.40	-0.02439	-0.00246	-0.03174	8688
B3-R	-26.13	-21.43	-29.77	-5.40	-41.60	-0.01221	-0.00221	-0.01706	7285
B4-R	-20.74	-17.01	-31.92	-4.00	-44.70	-0.01309	-0.00164	-0.01833	5514
B5-R	-15.51	-12.72	-30.65	-4.40	-47.80	-0.01257	-0.00180	-0.01960	5595
B6-R	-11.74	-9.63	-26.75	-4.70	-43.80	-0.01097	-0.00193	-0.01796	4034

2.7 Observed Failure Modes

This section describes the different failure modes observed and recorded after testing. Figure 2.16 illustrates a damaged shear wall after monotonic testing. The shear buckling of the steel sheathing was the first to be observed by the diagonal pattern visible during testing. This diagonal pattern was due to the development of tension field action in the direction of loading which caused large tension forces concentrated at the bottom corners of the shear wall. In reversed cyclic loading the diagonal pattern caused by shear buckling was visible in both directions. In most cases the dominant failure mode was that of the connection failure between the sheathing and framing. Minor damage to the framing was also observed in some cases. The failure modes of each shear wall specimen were recorded in detail on the test observation sheets located in Appendix C.

Figure 2.16 Damaged shear wall showing tension field action

2.7.1 Connection Failure

Connection failure was the desired mode of failure of the shear walls since energy dissipation was isolated through damage of the sheathing-to-frame connections. The failure consisted of various types of connection failure modes occurring in combinations but some more predominant than others. Failure occurred in a progressive manner and often led to the unzipping/removal of the sheathing from the frame.

2.7.1.1 Shear Failure of Screw (SF)

The shear failure/fracture of the screw was not a common failure mode and was only recorded in one case. This failure mode took place in shear walls with thicker sheathing and framing member and also where screws were installed through three layers of steel (sheathing, stud and track or blocking). In both cases the tilting of the screw was restricted which led to a sudden shear fracture close to the screw head region (Figure 2.17).

Figure 2.17 Shear failure of screw

2.7.1.2 Tilting of Screw (TS)

The tilting of the sheathing screws was the first mechanism to occur during the connection failure process. The eccentric shear force imposed by the sheathing tension field action caused the screws to tilt and become loose. This led to localized bearing of the sheathing and frame (Figure 2.18).

Figure 2.18 Tilting of screw (Test B4-M)

2.7.1.3 Bearing Sheathing Failure (SB)

The bearing sheathing failure was caused due to the failure of the sheathing material which was typically thinner than the framing underneath. Bearing failure occurred during testing as the sheathing moved independently to the frame. Slotted holes at the screw connection locations along the sheathing were gradually produced (Figure 2.19).

Figure 2.19 Bearing sheathing failure (Test B6-R)

2.7.1.4 Pull-out Failure (PO)

Screw tilting caused bearing damage to the hole of the framing which gradually increased the hole diameter. Eventually, the screw was partially pulled-out (PPO) or fully pulled-out of the framing. In some instances the screw remained intact within the sheathing. The pull-out failure mode was found more common with shear walls with thicker sheathing (Figure 2.20).

Figure 2.20 Pull-out failure (Test B4-M)

2.7.1.5 Pull-through Sheathing Failure (PT)

The pull-through sheathing failure mode occurred when the fastener screw remained intact within the framing but the sheathing was pulled-though the screw head above. This failure mode was more common in specimens with thicker framing and also at the field connections locations along the intermediate stud. Pull-through failure was also associated with the tear-out sheathing failure mode (Figure 2.21).

Figure 2.21 Pull-through sheathing failure (Test B7-M)

2.7.1.6 Tear-out Sheathing Failure

Tear-out sheathing failure occurred as a result of bearing sheathing failure. Since the perimeter screws were placed at a particular panel edge distance, 9.5 mm (3/8”), slotting due to bearing sheathing failure became so large the sheathing eventually tore out (Figure 2.22).

Figure 2.22 Tear-out sheathing failure (Test B2-M)

2.7.2 Framing Damage

Other than connection failures, damage to the framing members, which is an unfavourable mode of failure, was observed in some specimens. These damages were caused either by the horizontal or vertical components of the tension field force.

2.7.2.1 Flange and Lip Distortion (FLD)

Flange and lip distortion was caused by the tension field action developed in the sheathing and were of two forms. The first form was caused by the horizontal force component of the tension field which exerted a lateral force on the chord stud. This distortion was prevalent in specimens with closely spaced sheathing fasteners and thicker sheathing. Since the closely spaced connections were able to withstand higher lateral loads coupled with the three rows of blocking which restrained the chord stud from twisting, the flange and lip eventually unwrapped due to the high horizontal force. This mostly occurred at the bottom corner of the tension chord stud (Figure 2.23).

Figure 2.23 Flange and lip distorted/unwrapped after testing (Test B1-M) (*left*) and (Test B1-R) (*right*)

The new blocking reinforcement was also effective at eliminating the bending and twisting failure of the field stud encountered in past research by Ong-Tone (*2009*) and Balh (*2010*). Figure 2.24 shows a comparison of the field studs of test walls of similar configuration with and without the blocking detail. None of the author's test walls experienced failure of the field stud.

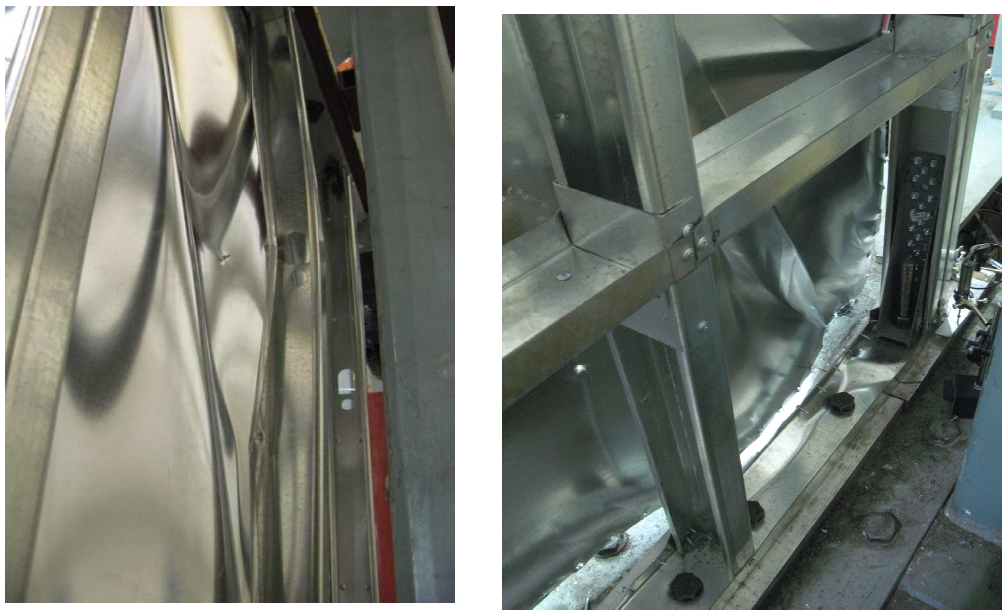

Figure 2.24 Use of blocking reinforcement to eliminate field stud failure. Test 6C-a (Ong-Tone (*2009*)) (*left*) and Test B1-R (*right*)

The second form of flange and lip distortion was caused by the strong axis bending of the chord stud which resulted in the local buckling of these elements. This occurred at the later stages of loading when the lateral displacements are higher and after sheathing had become detached from the frame. Essentially, the wall top to mid-height where the sheathing was attached remained a shear wall and the lower region of chord studs, where the sheathing was no longer attached, were cantilever beams. The beams (studs) bent under lateral loading which eventually resulted in the local buckling of the lip and flange (compression edge) at high lateral displacements (Figure 2.25).

Figure 2.25 Local buckling of the chord stud flange and lip (Test B3-R)

2.7.2.2 Track Uplift and Deformation

This type of failure was also due to the ability of the closely spaced sheathing fasteners and thicker sheathing to resist higher lateral loads. The vertical and horizontal component of the tension field within the sheathing and the tension/uplift force transmitted through the tension chord stud led to the deformation of the bottom and in some cases, the top track (Figure 2.26).

Figure 2.26 Deformation of bottom track (Test B1-M)

2.8 Ancillary Testing of Materials

To verify thickness and mechanical properties of the framing and sheathing materials used for the construction of the shear wall specimens, coupons of each material type were tested according to ASTM A370 *(2009)* requirements. The studs and tracks of same thickness were rolled from the same coil. Coupons of each particular thickness included: two samples of each sheathing thickness of 0.46 mm (0.018") and 0.76 mm (0.030") and four samples of each stud thickness of 1.09 mm (0.043") and 1.37 mm (0.054"). All steels were Grade 230MPa (33ksi) with the exception of studs of thickness 1.37 mm (0.054") which were 340 MPa (50ksi) as specified by ASTM A653 *(2008)*. A 50 mm (2") gauge length extensometer was used to measure the elongation and strain and the tensile tests were performed at a cross-head rate of 0.02mm/sec in the elastic range and increased to 0.05mm/sec beyond the yield point into the plastic range. To determine the true thickness or base metal thickness, the galvanized (zinc) coating was removed with 25% hydrochloric acid solution post coupon testing. F_y and F_u values were determined using the area of the base metal. A summary of the measured material properties is shown in Table 2.9.

Table 2.9 Summary of measured material properties

Specimen (mm)	Member	Base Metal Thickness (mm)	Yield Stress, F_y (MPa)	Tensile Stress, F_u (MPa)	F_u / F_y	Elongation %
1.09	Stud/track	1.12	301	347	1.16	45.3
1.37	Stud/track	1.37	388	529	1.36	34.6
0.76	Sheathing	0.79	337	377	1.12	31.9
0.46	Sheathing	0.45	266	358	1.35	24.8

As specified by the CSA-S136 Standard *(2007)* all coupons satisfied the minimum requirement that $F_u/F_y \geq 1.08$ and the elongation over a 50 mm (2") gauge length is 10% at minimum. The AISI S213 *(2007)* lists values for the ratio of the measured yield stress to minimum specified yield stress, R_y, and measured tensile stress to minimum specified tensile stress, R_t. For 230 MPa (33ksi) yield stress material with a 310 MPa (45ksi) minimum specified tensile stress, a value of 1.5 for R_y and 1.2 for R_t are listed. For 340 MPa (50ksi) yield stress material with a 450 MPa (65ksi) minimum specified tensile stress, a value of 1.1 for both R_y and R_t are listed. The values determined from the ancillary tests are shown in Table 2.10. All values are lower than that recommended by AISI S213 except for the R_y and R_t values of the 1.37 mm (0.054") thick stud which are higher than 1.1 and the R_t value of the 0.76 mm (0.03") sheathing which is higher than 1.2.

Table 2.10 R_y and R_t values of studs/tracks and sheathing

Member	Thickness (mm)	R_y	R_t
Stud	1.09	1.31	1.12
Stud	1.37	1.14	1.18
Sheathing	0.76	1.47	1.22
Sheathing	0.46	1.16	1.16

2.9 Screw Connection Testing

Screw connection tests were performed since a new type of screw, No.8 x 19.1 mm (3/4”) pan head self-drilling (Robertson square drive) screw was used in comparison to that used for the walls tested by Ong-Tone (*Ong-Tone & Roger, 2009*) and Balh (*Balh & Rogers, 2010*). The bearing/tilting capacities of the screw connections for different sheathing-to-framing combinations were determined following the procedure contained in Clause E4.3.1 of the CSA S136 Standard *(2007)*. A comparison of the shear and bearing/tilting capacities were made of the new screws to the previously used No.8 x 19.1 mm (3/4”) pan head (LOX drive) screws from the test program by Ong-Tone *(Ong-Tone & Roger, 2009)* and Balh *(Balh & Rogers, 2010).* The comparison of the bear/tilting resistances showed that the average resistances of connection test results from Balh (2010) were approximately 5% higher whereas the nominal resistances were lower (Table 2.11). The shear capacity of the new screws were determined by using thick metal plates (2.46 mm (0.097”)) in the testing setup which caused the shear fracture failure of the screws. The new screws were approximately 14% stronger in shear resistance than the old (Table 2.12). The results above had little to no impact when comparing the shear wall resistances of the past research program by Balh (*Balh & Rogers, 2010*) to the author’s since the use of blocking reinforcement resulted in significantly higher shear wall resistances. The 14% higher shear fracture resistance would have a notable affect but this fracture mode was uncommon as noted in Section 2.6.1.1.

Table 2.11 Bearing/tilting resistance

Test	Nominal Sheathing Thickness	Nominal Framing Thickness	Maximum Resistance (kN)	Average Resistance (kN)	Nominal Resistance (kN)	Balh *(2010)* Average Resistance (kN)	Balh *(2010)* Nominal Resistance (kN)
11	0.46mm (0.018")	1.09mm (0.043")	2.07	2.01	1.62	2.11	1.56
12			1.72				
11α			1.86				
12α			2.38				
6	0.76mm (0.03")		4.21	3.80	2.67	4.01	2.43
9			3.67				
10			3.71				
9α			3.58				
10α			3.83				
5		1.37mm (0.054")	5.47	5.15	2.67	-	-
7			5.75				
8			4.19				
8α			5.18				

Table 2.12 Shear capacity comparison

Test	Sheet Metal Thickness	Screw type	Maximum Resistance (kN)	Average Resistance (kN)
3	2.46mm (0.097")	No.8 19.1mm (3/4") Flat Pan Head Screw (LOX Drive)(*old*)[1]	6.3	5.89
4			6.25	
4c2α			5.13	
1		No.8 19.1mm (3/4") Pan Head Screw (Square Drive) (*new*)	6.81	6.71
2			7.11	
4b2α			6.21	

[1] Used by Ong-Tone (*2009*) and Balh (*2010*)

Chapter 3- Interpretation of Test Results and Prescriptive Design

3.1 Introduction/EEEP Concept

The Equivalent Energy Elastic Plastic (EEEP) (*Park, 1989 and Foliente, 1996*) was used to analyse the shear wall test data. This method was recommended by Branston *et al. (2004)* and was the preferred method of analysis of past research on wood sheathed shear walls used to establish the Canadian design provisions in the AISI S213 Standard. It was also used by Balh (*Balh & Roger, 2010*) and Ong-Tone (*Ong-Tone & Roger, 2009*) for the development of design shear resistance values for steel sheathed shear walls. The EEEP method is based on the assumption that the energy dissipated up to ultimate failure (also known as the functional capacity (*ASTM E2126, 2007*)) taken as 80% post-peak load, during the nonlinear response of the test specimen can be represented by a simplified bilinear elastic-plastic curve with the same energy dissipation i.e. areas A1 and A2 are equal (Figure 3.1).

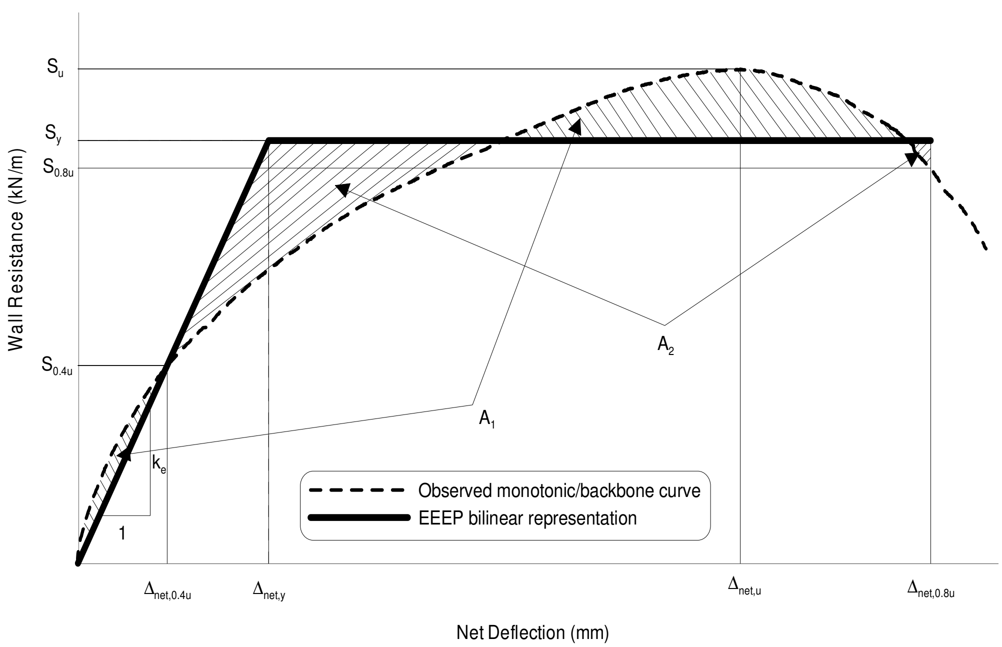

Figure 3.1 EEEP model (*Branston & Rogers, 2004*)

The nonlinear monotonic curves and the positive and negative backbone curves of the reversed cyclic tests were analyzed by an automated spreadsheet using the EEEP method. Three main parameters from each observed backbone curve were used to derive the EEEP bi-linear curve. These were: the ultimate wall resistance, S_u, 40% of the ultimate wall resistance, $0.4S_u$, 80% of the ultimate wall resistance, $0.8S_u$, and their corresponding displacements, $\Delta_{net,u}$, $\Delta_{net,0.4u}$ and $\Delta_{net,0.8u}$ respectively. From these primary parameters, other important parameters were derived. These include: the unit elastic stiffness, k_e, (Equation 3-1), the yield wall resistance, S_y, (Equation 3-2) and its corresponding yield displacement, $\Delta_{net,y}$, (Equation 3-3), and the ductility, μ, (Equation 3-4). The total energy dissipated, E, represented by the area below the observed curve up to the ultimate failure displacement, $\Delta_{net,0.8u}$, was determined using an incremental approach to calculate the energy between two consecutive points (Equation 3-5). The total/cumulative energy dissipated is the summation of all incremental energies (Equation 3-6).

$$k_e = \frac{0.4S_u}{\Delta_{net,0.4u}} \tag{3-1}$$

$$S_y = \frac{-\Delta_{net,0.8u} \pm \sqrt{\Delta^2_{net,0.8u} - \frac{2A}{k_e}}}{-\frac{1}{k_e}} \tag{3-2}$$

$$\Delta_{net,y} = \frac{S_y}{k_e} \tag{3-3}$$

$$\mu = \frac{\Delta_{net,0.8u}}{\Delta_{net,y}} \tag{3-4}$$

where,

S_y = Yield wall resistance (kN/m)

S_u = Ultimate wall resistance (kN/m)

A = Area under observed curve up to 80% load ($\Delta_{net,0.8u}$)

The Energy was calculated using an incremental approach as follows:

$$E_i = \frac{F_i + F_{i-1}}{2} \times (\Delta_{top,i} - \Delta_{top,i-1}) \tag{3-5}$$

where,

E_i = Energy between two consecutive points

F_i = Corrected shear force between two consecutive data points

$\Delta_{top,i}$ = Measured wall top displacement

$$E_{total} = \sum E_i \tag{3-6}$$

A summary of the design values obtained from the EEEP analysis is provided in Tables 3.1, 3.2, and 3.3. Graphical examples displaying the resulting EEEP bi-linear curves are shown in Figure 3.2 of a monotonic test and Figure 3.3 of a reversed cyclic test. All graphical results can be found in Appendix D For the reversed cyclic tests, backbones curves which embody the hysteretic loops of the positive and negative regions of the force vs. displacement cycles were created but treated separately. The backbones curves were then analysed in the same manner as the nonlinear monotonic curve.

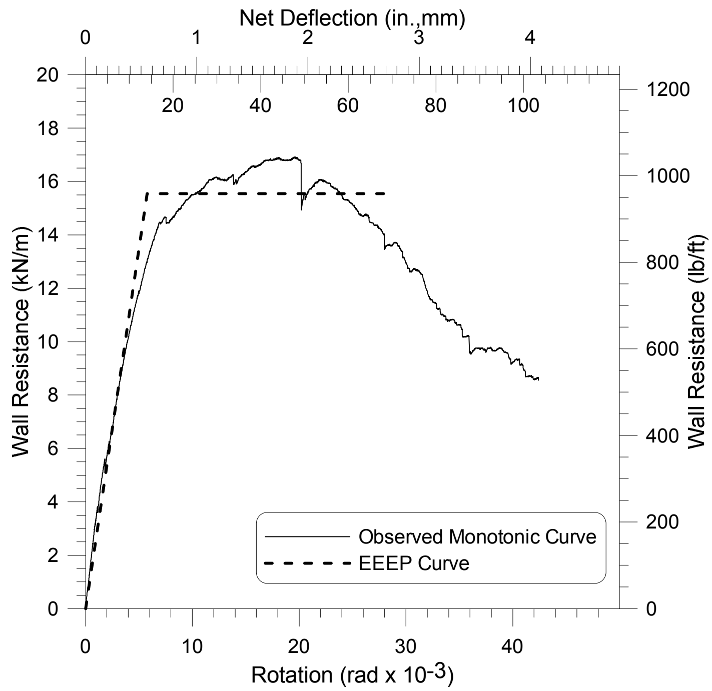

Figure 3.2 Resulting EEEP curve for the observed monotonic curve (test B2-M)

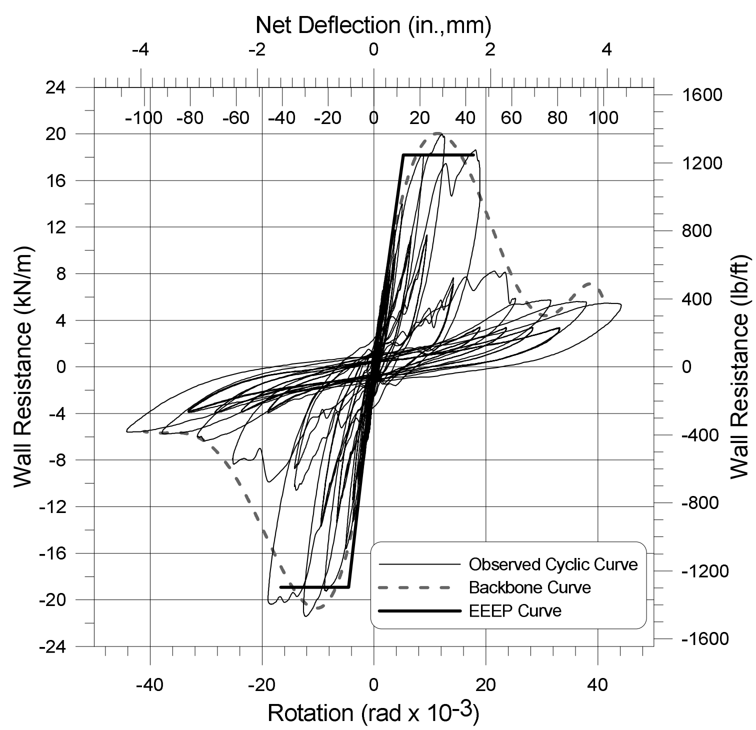

Figure 3.3 Resulting EEEP curve for the observed reversed cyclic hysteretic curves (test B3-R)

Table 3.1 Design values for monotonic tests

Test Specimen	Yield Wall Resistance, S_y (kN/m)	Displacement at $0.4S_u$, $\Delta_{net,0.4u}$ (mm)	Displacement at S_y, $\Delta_{net,y}$ (mm)	Unit Elastic Stiffness, k_e ((kN/m)/mm)	Rotation at $0.4S_u$, $\theta_{net,0.4u}$ (rad)	Rotation at S_y, $\theta_{net,y}$ (rad)	Ductility, μ	Energy Dissipation, E (Joules)
B1-M	30.26	7.03	15.67	1.93	0.00288	0.00642	4.74	2453
B2-M	15.55	6.13	14.09	1.10	0.00251	0.00578	4.85	1161
B3-M	17.43	6.98	15.69	1.11	0.00286	0.00643	3.27	922
B4-M	14.85	4.02	8.87	1.67	0.00165	0.00364	6.08	896
B5-M	10.97	5.62	12.84	0.85	0.00230	0.00526	4.36	662
B6-M	8.44	3.13	7.09	1.19	0.00128	0.00291	9.30	643
B7-M	25.17	6.79	15.24	1.65	0.00278	0.00625	4.19	1725
B8-M	12.98	3.56	7.97	1.63	0.00146	0.00327	4.84	548

Table 3.2 Design values for reversed cyclic tests- positive cycles

Test Specimen	Yield Wall Resistance, S_{y+} (kN/m)	Displacement at $0.4S_{u+}$, $\Delta_{net,0.4u+}$ (mm)	Displacement at S_{y+}, $\Delta_{net,y+}$ (mm)	Unit Elastic Stiffness, k_e ((kN/m)/mm)	Rotation at $0.4S_{u+}$, $\theta_{net,0.4u+}$ (rad)	Rotation at S_{y+}, $\theta_{net,y+}$ (rad)	Ductility, μ	Energy Dissipation, E (Joules)
B1-R	28.39	7.20	16.39	1.73	0.00295	0.00672	3.75	1842
B2-R	15.26	4.90	11.28	1.35	0.00201	0.00463	5.62	1075
B3-R	18.08	5.00	11.31	1.60	0.00205	0.00464	4.27	940
B4-R	14.24	3.60	8.01	1.78	0.00148	0.00328	5.06	634
B5-R	11.06	4.10	9.38	1.18	0.00168	0.00385	3.68	402
B6-R	8.50	3.20	7.28	1.17	0.00131	0.00298	5.81	401

Table 3.3 Design values for reversed cyclic tests- negative cycles

Test Specimen	Yield Wall Resistance, S_{y-} (kN/m)	Displacement at $0.4S_{u-}$, $\Delta_{net,0.4u-}$ (mm)	Displacement at S_{y-}, $\Delta_{net,y-}$ (mm)	Unit Elastic Stiffness, k_e ((kN/m)/mm)	Rotation at $0.4S_{u-}$, $\theta_{net,0.4u-}$ (rad)	Rotation at S_{y-}, $\theta_{net,y-}$ (rad)	Ductility, μ	Energy Dissipation, E (Joules)
B1-R	-29.10	-9.60	-21.92	1.33	-0.00394	-0.00899	3.60	2407
B2-R	-16.10	-6.00	-14.16	1.14	-0.00246	-0.00581	5.47	1381
B3-R	-19.58	-5.40	-12.33	1.59	-0.00221	-0.00506	3.37	846
B4-R	-15.24	-4.00	-8.96	1.70	-0.00164	-0.00367	4.99	747
B5-R	-11.71	-4.40	-10.13	1.16	-0.00180	-0.00415	4.72	610
B6-R	-8.68	-4.70	-10.59	0.82	-0.00193	-0.00434	4.13	408

3.2 Comparison of Shear Wall Configurations

The shear wall configurations were chosen to be comparable with the walls of the past research program by Ong-Tone (*2009*) and Balh (*2010*). The configurations differ in framing thickness, sheathing thickness, fastener spacing, and most importantly, the use of blocking reinforcement. The test results and tabulated design values were used to evaluate the effects of the blocking detail on the shear wall system. Both monotonic and reversed cyclic tests of the same configuration obtained similar results (Table 3.1, 3.2 & 3.3). For the reversed cyclic tests, the negative cycles obtained higher shear resistances since the loading protocol began with the walls being displaced in the negative direction (north direction). Hence, once in the inelastic range, the wall's performance in terms of shear resistance during the positive cycle is reduced since it had been damaged in the previous negative cycle. Often, the curves of wall resistance vs. displacement for both monotonic and reversed cyclic tests were not smooth. Sharp depressions/dips were present which indicate a sudden loss of shear resistance; smaller dips until the peak at ultimate wall resistance and larger dips post peak during strength degradation. The sudden shear buckling of the sheathing caused by the tension field action attributed to the smaller dips, and screw connection failure which was at times accompany by shear buckling of the sheathing attributed to the larger dips (Figure 3.4).

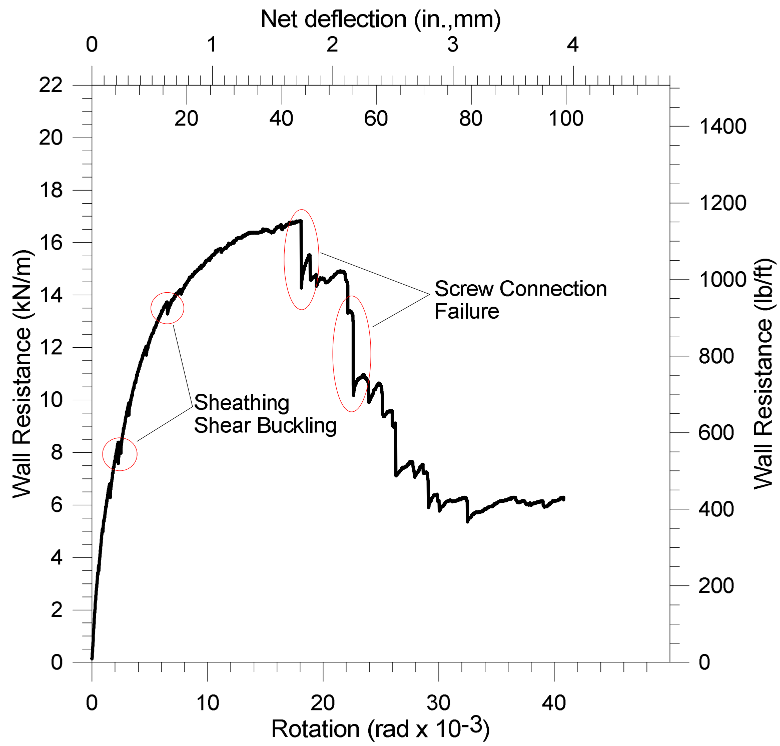

Figure 3.4 Loss of shear resistance due to sheathing shear buckling and screw connection failure (test B4-M)

3.2.1 Effect of Fastener Spacing

Shear walls of similar configuration with differing fastener spacing were grouped together by colour and compared (Figure 3.5). All groups performed similarly i.e. as the fastener spacing decreased, the wall resistance verses the displacement increased. This behaviour was expected because screw connections with a denser/smaller fastener spacing act as a group in resisting the forces caused by the tension field action. The more screws connections available, the less force each individual connection has to resist. With a larger fastener spacing, less screw connections are available along the wall perimeter. Hence, each connection has to resist greater forces and the failure is more localised.

Figure 3.6 illustrates the difference in behaviour of two shear walls with the same configuration with differing fastener spacing. Test B2-M had a 50 mm fastener spacing whereas test B6-M had a 150 mm fastener spacing. Note the localised screw connection failure due to screw pull-through of test B6-M, whilst the screw connections of test B2-M have not failed but caused framing damage in the form of track uplift and flange and lip distortion of the DCS outer stud.

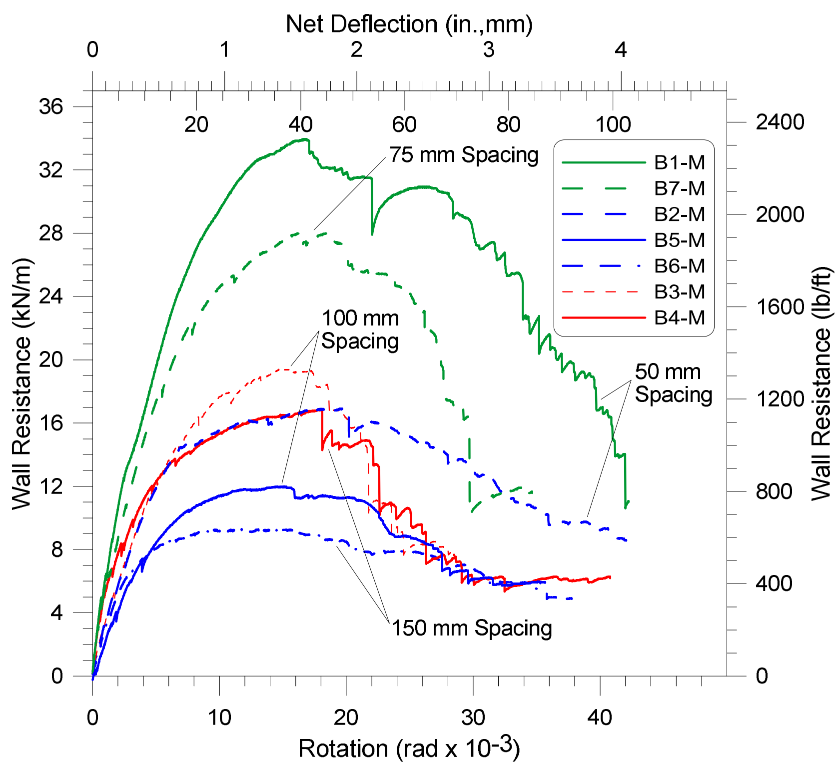

Figure 3.5 Comparison of fastener spacing: Wall resistance vs. displacement

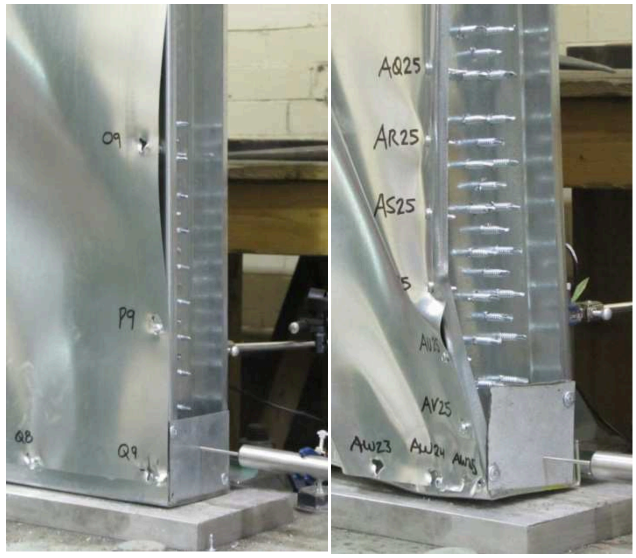

Figure 3.6 Effect of different fastener spacing on the failure mode of test B6-M (*left*) and test B2-M (*right*)

3.2.2 Effect of Sheathing Thickness

Wall specimens with thicker steel sheathings were able to attain higher shear resistances. The thicker sheathing has higher mechanical properties; hence, the bearing and tilting resistance with a constant framing thickness, would be larger as shown in Table 2.9 of Section 2.9. Figure 3.7 illustrates this relationship. Wall specimens B3-M and B5-M differ in sheathing thickness with the former having the thicker sheathing of 0.76 mm (0.030”) and the later of thickness of 0.46mm (0.018”). Curves B4-M and B6-M demonstrated similar behaviour but had lower wall resistances, thus ultimate shear resistances due to a larger fastener spacing of 150 mm (6”). All test walls shown were constructed with 1.09 mm (0.043”) framing.

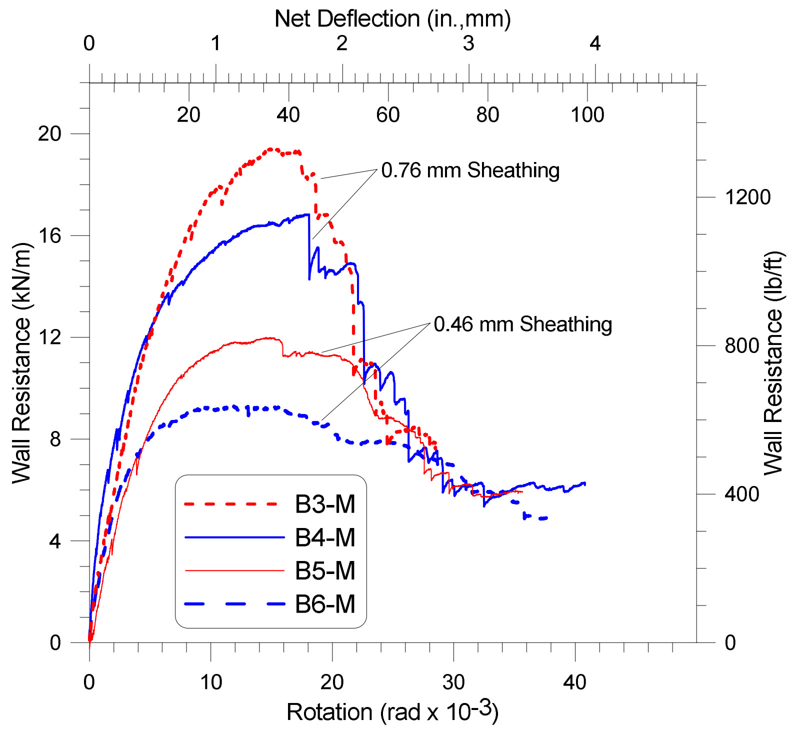

Figure 3.7 Comparison of sheathing thickness: Wall resistance vs. displacement (test walls of 1.09mm framing)

3.2.3 Effect of Blockings

A comparison of the relevant test data and design values of the blocked shear walls verses the conventional (unblocked) shear walls tested by Balh (*2010*) and Ong-Tone (*2009*) was made. Comparison groups were created which consisted of nominally identical walls which had same configurations in terms of framing and sheathing thickness, and fastener spacing (Table 3.4). It is important to note that the shear walls tested by Balh (*2010*) and Ong-Tone (*2009*) were only laterally loaded. As concluded by Hikita (*2006*), once a shear wall under combined vertical and lateral loading was properly designed following capacity based principles, the wall maintained a similar lateral performance to one tested under lateral loading alone. Thus, a direct comparison between the shear walls tested by the authors above was acceptable.

The test data used includes the ultimate shear resistance and displacement at $0.8S_u$. The design values used includes the yield shear resistance, unit elastic stiffness, ductility, and energy dissipation. Normalized ratios for the comparison of the parameters listed above were determined by dividing the values of the blocked shear walls by the average of the values of their conventional counterparts within the same comparison group. Both monotonic tests and combined positive and negative cycles of the reversed cyclic tests are listed in Tables 3.5 and 3.6. Bar charts were also created for ease of visual comparison and to illustrate the deviation of the conventional walls' normalized ratios from their average (1.00) (Appendix E).

Table 3.4 Comparison groups and shear wall configurations

Comparison Group	Monotonic Test Specimen	Reversed Cyclic Test Specimen	Fastener Spacing (mm)	Sheathing Thickness (mm)	Framing Thickness (mm)
1	B2-M	B2-R	50/300	0.46	1.09
	2M-a†	2C-a†			
	2M-b†	2C-b†			
2	B6-M	B6-R	150/300	0.46	1.09
	1M-a†	1C-a†			
	1M-b†	1C-b†			
	1M-c†	-			
3	B3-M	B3-R	100/300	0.76	1.09
	5M-a*	5C-a*			
	5M-b*	5C-b*			
4	B4-M*	B4-R	150/300	0.76	1.09
	4M-a*	4C-a*			
	4M-b*	4C-b*			

† Balh (*2010*)
* Ong-Tone *(2009)*

Table 3.5 Normalized parameters for comparison of blocked to conventional shear wall- Monotonic Test

Comparison Group	Test Specimen	Ultimate Resistance, S_u (kN/m)	Displacement at $0.8S_u$, $\Delta_{net,0.8u}$ (mm)	Yield Resistance, S_y (kN/m)	Unit Elastic Stiffness, k_e ((kN/m)/mm)	Ductility.μ	Energy Dissipation E (Joules)	Normalized Properties					
								S_u	$\Delta_{net,0.8u}$	S_y	k_e	μ	E
1	B2-M	16.91	68.26	15.55	1.10	4.85	1161	**1.70**	**0.72**	**1.69**	**1.09**	**0.46**	**1.14**
	2M-a†	10.10	90.42	9.00	0.91	9.10	937	**1.00**	**1.00**	**1.00**	**1.00**	**1.00**	**1.00**
	2M-b†	9.81	100	9.36	1.11	11.91	1094						
2	B6-M	9.31	65.98	8.44	1.19	9.30	643	**1.43**	**1.36**	**1.44**	**1.20**	**1.19**	**1.98**
	1M-a†	6.50	72.99	5.87	0.79	9.79	496	**1.00**	**1.00**	**1.00**	**1.00**	**1.00**	**1.00**
	1M-b†	6.63	37.07	5.85	0.94	5.97	242						
	1M-c†	6.41	35.73	5.83	1.26	7.7	238						
3	B3-M	19.40	51.22	17.43	1.11	3.27	922	**1.41**	**0.88**	**1.38**	**0.61**	**0.39**	**1.09**
	5M-a*	14.19	52.6	12.90	1.87	7.61	773	**1.00**	**1.00**	**1.00**	**1.00**	**1.00**	**1.00**
	5M-b*	13.39	64.45	12.41	1.77	9.18	922						
4	B4-M*	16.83	53.95	14.85	1.67	6.08	896	**1.53**	**0.83**	**1.48**	**0.97**	**0.54**	**1.17**
	4M-a*	11.02	67.57	10.08	1.67	11.19	793	**1.00**	**1.00**	**1.00**	**1.00**	**1.00**	**1.00**
	4M-b*	10.98	62.97	10.03	1.78	11.17	735						

† Balh (*2010*)
* Ong-Tone *(2009)*

Table 3.6 Normalized parameters for comparison of blocked to conventional shear wall- Combined positive and negative cycles

Comparison Group	Test Specimen	Ultimate Resistance, S_u (kN/m)	Displacement at $0.8S_u$, $\Delta_{net,0.8u}$ (mm)	Yield Resistance, S_y (kN/m)	Unit Elastic Stiffness, k_e ((kN/m)/mm)	Ductility μ	Energy Dissipation, E (Joules)	Normalized Properties					
								S_u	$\Delta_{net,0.8u}$	S_y	k_e	μ	E
1	B2-R	16.81	70.40	15.68	1.24	5.54	1228	**1.55**	**0.81**	**1.56**	**1.18**	**0.60**	**1.21**
	2C-a†	10.93	83.00	10.07	1.04	8.61	959	**1.00**	**1.00**	**1.00**	**1.00**	**1.00**	**1.00**
	2C-b†	10.70	91.90	10.01	1.07	9.83	1064						
2	B6-R	9.49	43.05	8.59	0.99	4.97	404	**1.51**	**1.03**	**1.50**	**1.16**	**0.80**	**1.52**
	1C-a†	6.32	45.80	5.79	0.87	6.97	299	**1.00**	**1.00**	**1.00**	**1.00**	**1.00**	**1.00**
	1C-b†	6.24	37.40	5.64	0.83	5.51	234						
3	B3-R	20.71	44.95	18.83	1.59	3.82	893	**1.44**	**0.79**	**1.47**	**1.04**	**0.57**	**1.09**
	5C-a*	14.47	53.80	12.88	1.58	6.58	781	**1.00**	**1.00**	**1.00**	**1.00**	**1.00**	**1.00**
	5C-b*	14.22	59.50	12.78	1.48	6.90	858						
4	B4-R	16.51	42.60	14.74	1.74	5.02	691	**1.37**	**0.88**	**1.36**	**1.23**	**0.79**	**1.17**
	4C-a*	11.84	51.10	10.99	1.55	7.25	638	**1.00**	**1.00**	**1.00**	**1.00**	**1.00**	**1.00**
	4C-b*	12.29	45.90	10.71	1.28	5.46	545						

† Balh (*2010*)

* Ong-Tone *(2009)*

3.2.3.1 Comparison of Ultimate Shear Resistance & Yield Shear Resistance

The blocked walls attained higher ultimate shear resistances, S_u, and yield shear resistances, S_y, compared to their conventional (unblocked) counterparts. The increase in shear resistance was attributed to the addition of the quarter point blocking reinforcements which reduced distortion of the chord studs and allowed for higher lateral loads to be carried. Figure 3.8 contains a comparison of the monotonic resistance vs. rotation curves and illustrates the normalized increase in shear resistance of the blocked walls compared to a conventional wall per comparison group. The curves from test walls of the same comparison group are shown with the same colour.

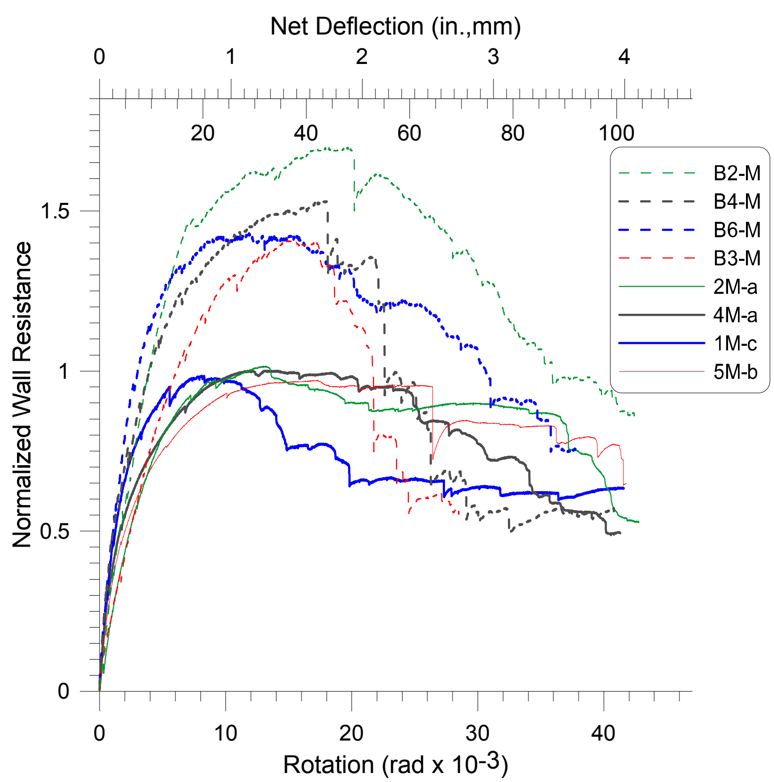

Figure 3.8 Increase of normalized wall resistance of blocked walls compared to conventional walls of comparison group 1 to 4

The normalized S_u results had a range of 1.41 to 1.70 for monotonic tests and 1.37 to 1.55 for reversed cyclic tests (Figures 3.9 & 3.10). The normalized S_y closely followed the S_u and had a range of 1.38 to 1.69 for monotonic tests and 1.36 to 1.56 for reversed cyclic tests. Test wall B2 of comparison group 1 consistently achieved the highest increase of S_u and S_y for both monotonic (B2-M) and reversed cyclic (B2-R) protocols. The remaining groups did not show a consistent pattern for the two protocols.

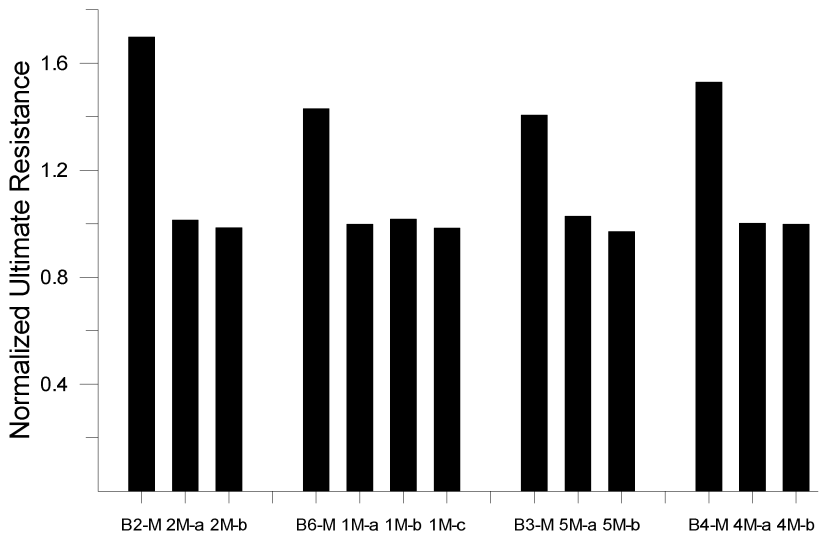

Figure 3.9 Comparison of normalized ultimate resistance for monotonic tests

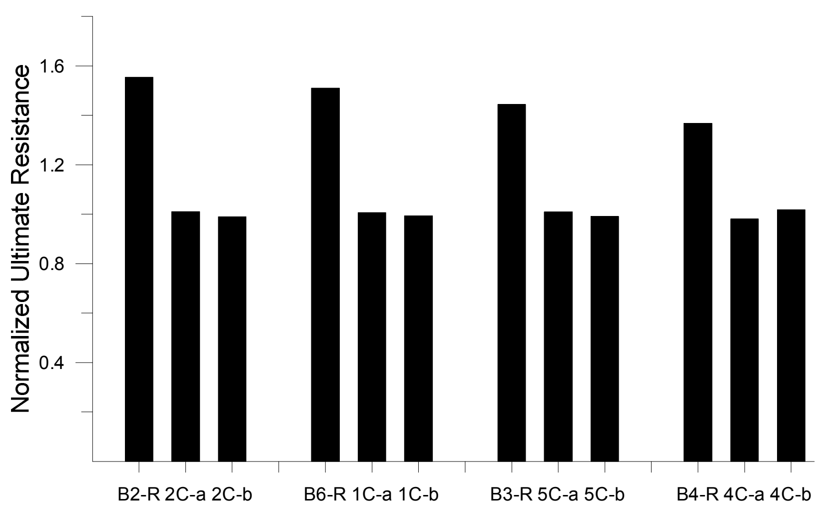

Figure 3.10 Comparison of normalized ultimate resistance for reversed cyclic tests

3.2.3.2 Comparison of Displacement at $0.8S_u$

There was a general decrease in the displacement at $0.8S_u$ post peak, $\Delta_{net,0.8u}$, of the blocked walls compared to the conventional walls. Comparison group 2 was an exception to the trend, which consisted of shear walls constructed with 1.09mm (0.043") framing, 0.46mm (0.018") sheathing, and 150mm (6") fastener spacing (Figures 3.11 & 3.12). The blocked wall (B6) of the group showed normalized increases of 1.36 and 1.03 for the monotonic and reversed cyclic tests respectively.

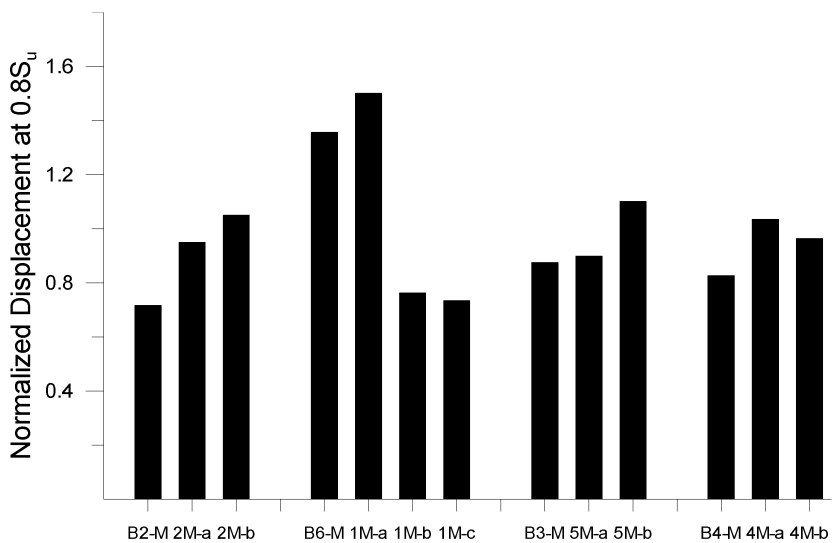

Figure 3.11 Comparison of normalized displacement at $0.8S_u$ for monotonic tests

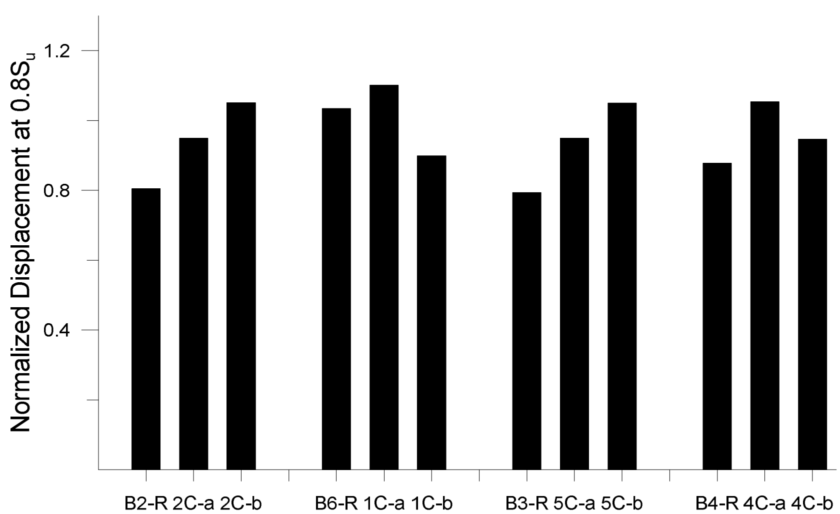

Figure 3.12 Comparison of normalized displacement at $0.8S_u$ for reversed cyclic tests

This can be clearly identified by comparing the end displacements ($\Delta_{net,0.8u}$) of the bi-linear EEEP curves which corresponds to the end of the plastic region (Figure 3.13) . The monotonic curves of the conventional walls (1M-a, 1M-b, 1M-c) illustrate significant variability in the measured performance although the walls were nominally identical. This is especially noticeable in the post peak performance of Tests 1M-a which had a significantly longer plastic region with $\Delta_{net,0.8u}$ of 72.99mm compared to tests 1M-b and 1M-c of $\Delta_{net,0.8u}$ equal to 37.07mm and 35.73mm respectively. These deviations are most likely caused by variations in loading and construction details e.g. inherent variations in the placement of sheathing screws caused by human error.

The blocked wall (B6-R) of comparison group 2 of the reversed cyclic test did not show a marked increase in $\Delta_{net,0.8u}$ (Figure 3.14).

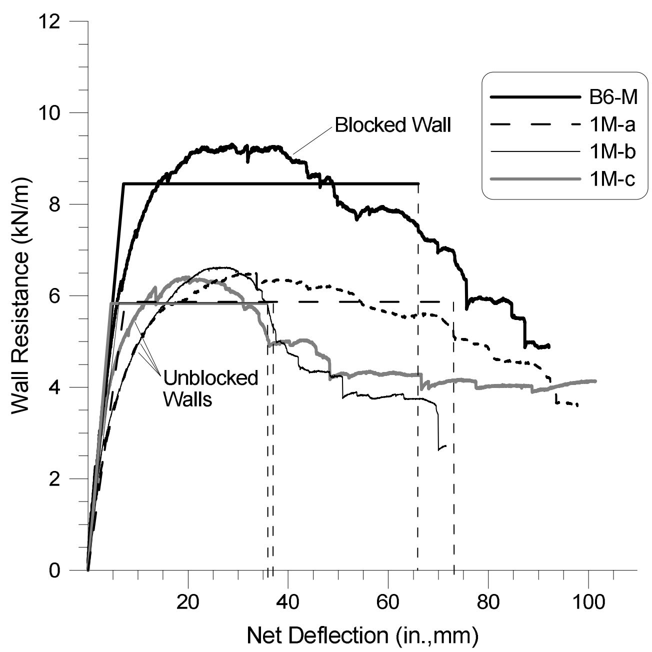

Figure 3.13 Monotonic & EEEP curves of comparison group 2 (test walls of 1.09mm framing, 0.46mm sheathing, 150mm fastener spacing)

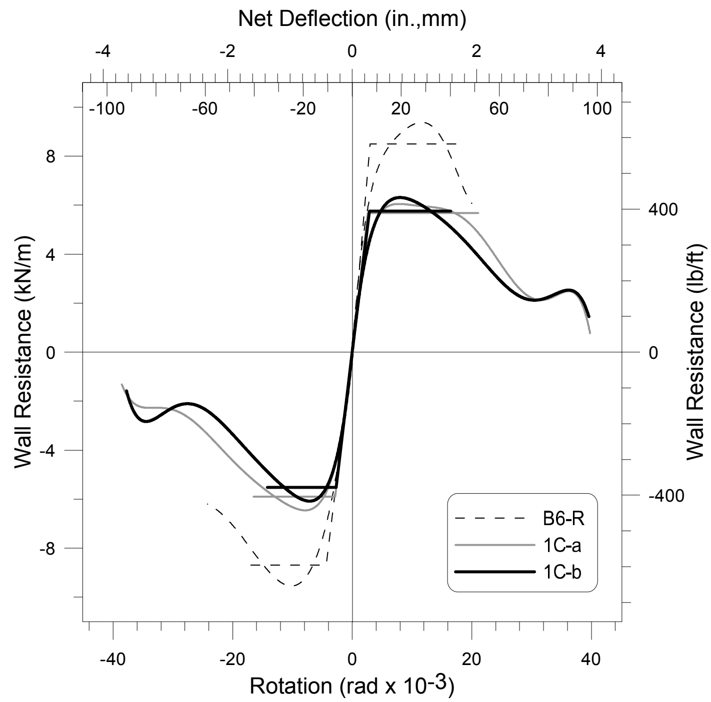

Figure 3.14 Backbone & EEEP curves of comparison group 2 (test walls of 1.09mm framing, 0.46mm sheathing, 150mm fastener spacing)

3.2.3.3 Comparison of Ductility

The ductility, μ, followed an identical trend to $\Delta_{net,0.8u}$, which was expected since both parameters are directly proportional as previously shown in Equation 3-4. The normalized μ results encompassed a wide range of 0.39 to 1.19 and 0.57 to 0.80 for the monotonic and reversed cyclic tests respectively. As with the $\Delta_{net,0.8u}$, test B6-M of comparison group 2 was the exception with a normalized ratio of 1.19 (Figures 3.15 & 3.16).

The normalized μ of the blocked walls of the four comparison groups displayed a consistent pattern for both monotonic and reserved cyclic tests. The blocked test walls, B6 of comparison group 2 exhibited the highest normalized ductility of the comparison groups and represented the upper bound of 1.19 and 0.80 for the monotonic and reversed cyclic respectively. This was followed by comparison group 4 (test wall B4), comparison group 1 (test wall B2), and lastly comparison group 3 (test wall B3).

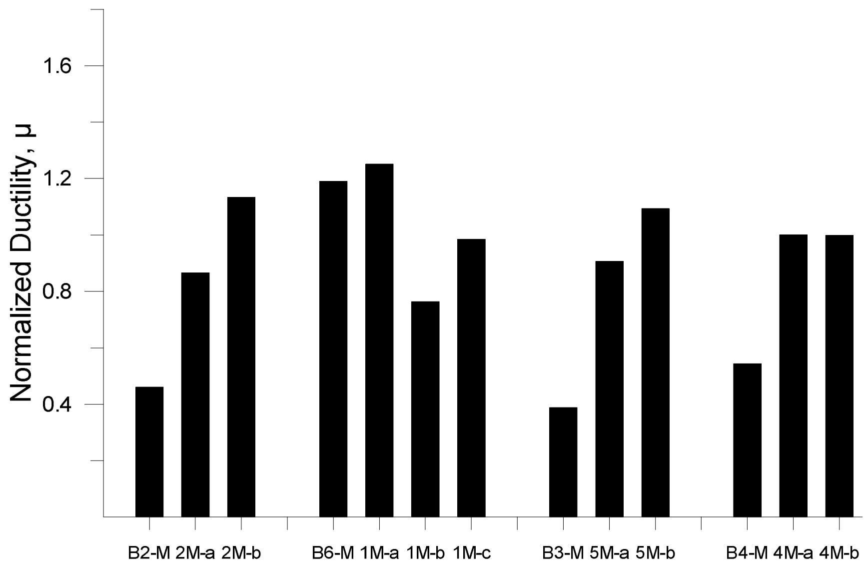

Figure 3.15 Comparison of normalized ductility for monotonic tests

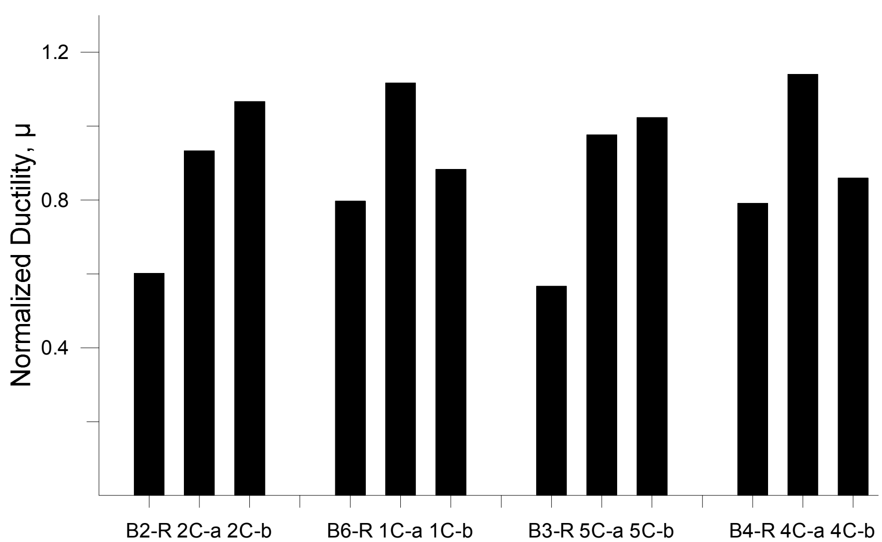

Figure 3.16 Comparison of normalized ductility for reversed cyclic tests

The length of the plastic region of the resulting bi-linear EEEP curve serves as a visual indicator of the shear wall's ductility; a longer plastic region indicates a higher ductility. Another visual indicator of a shear wall's ductility is the rate of strength degradation of the post peak monotonic curve and reversed cyclic backbone curve. A rapidly declining post peak curve represents a high rate of strength degradation and a wall of less ductility. Whereas a slowly declining post peak curve represents a slower rate of strength degradation and a more ductile wall.

A visual comparison of the monotonic and resulting EEEP curves of comparison groups 2 and 3, which represents the highest and lowest normalized ductility, illustrates the relationship between the ductility and strength degradation (Figure 3.17). Only one conventional test wall is shown because the responses of all nominally identical conventional walls were essentially similar e.g. 5M-a & 5M-b. Notice the difference in the lengths of EEEP plastic curves and the rate of strength degradation of the monotonic curves of the blocked walls B6-M and B3-M.

The ductility was observed to have an inverse relationship to the shear resistance (S_u & S_y). Hence, the shear walls constructed with the thinner sheathing and larger fastener spacing were more ductile in behaviour but exhibited the least increase in shear resistance. Figure 3.17 illustrates this relationship; B6-M was constructed with 0.46mm (0.018") sheathing and 150mm (6") fastener spacing whereas B3-M had 0.76mm (0.030") sheathing and 100mm fastener spacing.

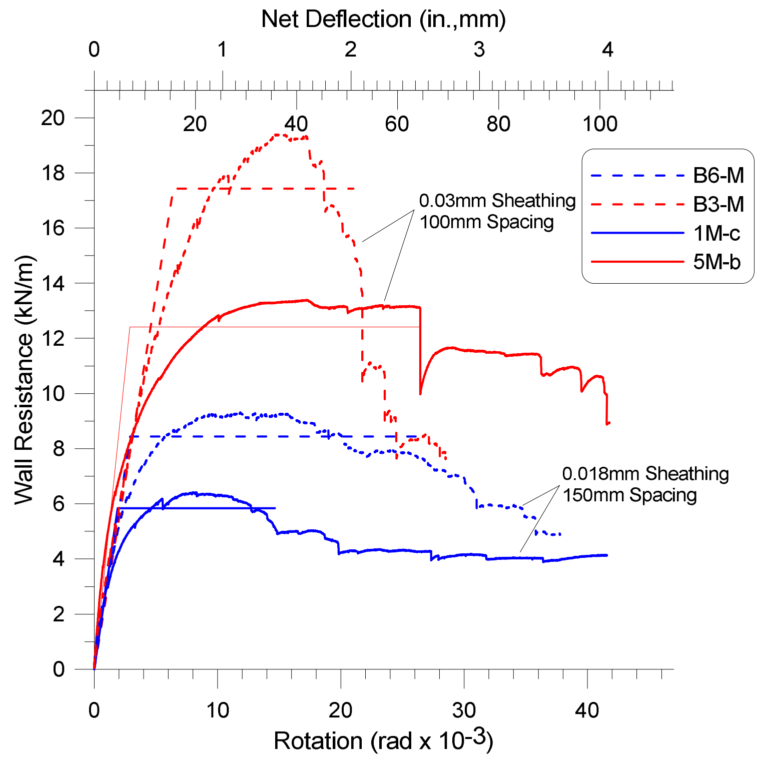

Figure 3.17 Comparison of the change in ductility due to the blocking reinforcement (comparison groups 2 & 3)

3.2.3.4 Comparison of Unit Elastic Stiffness

There was a general increase of unit elastic stiffness, k_e, of the blocked walls with the exception of test B3-M of comparison group 3 which displayed a significant decrease of normalized ratio equal to 0.61 (39% decrease). Test B3-R displayed the lowest normalized increase of 1.04 (4%) of the reserved cyclic tests (Figures 3.18 & 3.19). Test walls B3 were constructed with 1.09 mm (0.043”) framing, 0.76 mm (0.030”) sheathing, and 100 mm (4”) fastener spacing. As previously stated, B3 showed the least ductility and normalized ductility and the highest shear resistance (S_u & S_y) of the comparison groups.

This might seem like an abnormal drop in wall stiffness considering the addition of the blocking reinforcement was expected to increase the stiffness, but k_e is based on the initial stiffness (secant stiffness) at 40% of the ultimate load (S_u). This method reflects an appropriate service level load of a wall subjected to wind loading, thus a visual comparison of the monotonic or reversed cyclic backbone curves would not suffice. The above statement is illustrated in Figure 3.17 and shows the difference in k_e by comparing the slopes of prefect elastic curves of tests B3-M and 5M-b.

Test walls B4 of comparison group 4 had the highest k_e of both monotonic and cyclic test of 1.67 and 1.74 (kN/m)/mm respectively. Test B4-M did not show an increase in k_e but was approximately equal to it conventional counterparts (4M-a & 4M-b) with a normalized ratio of 0.97 (3% decrease). This was inconsistent to test B4-R which showed the highest increase in normalized k_e of 1.23

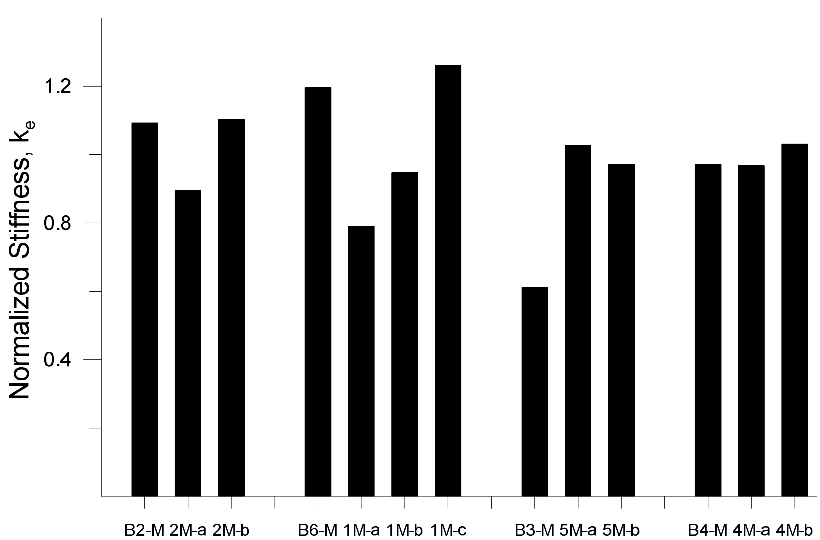

Figure 3.18 Comparison of normalized stiffness for monotonic tests

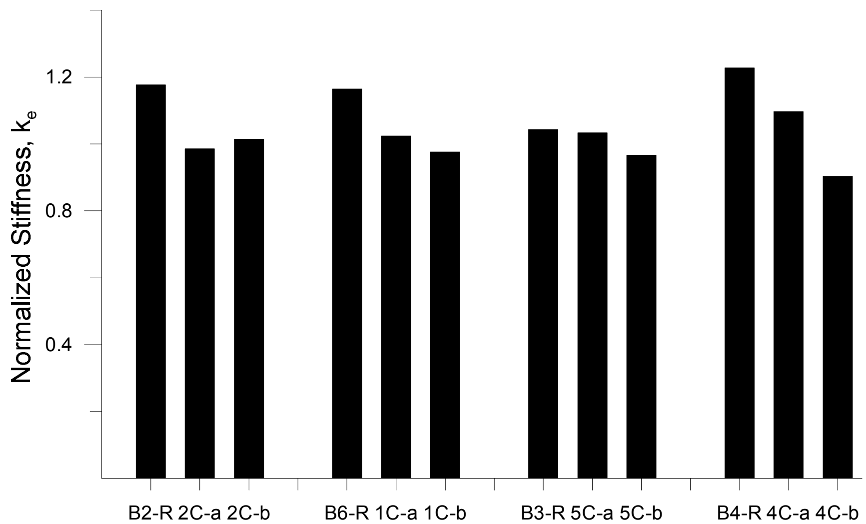

Figure 3.19 Comparison of normalized stiffness for reversed cyclic tests

3.2.3.5 Comparison of Energy Dissipation

There was a consistent increase in energy dissipation, E, of the blocked walls of each comparison group for both monotonic and reserved cyclic tests. The total energy dissipation of a shear wall specimen is the product of the force (wall resistance) by the wall displacement (Equation 3-5). Hence, a combination of higher strength and ductility resulted in higher levels of energy dissipation of a shear wall specimen. As such, test wall B2 which was the second strongest in terms of S_u but had the highest $\Delta_{net,0.8u}$, resulted with the highest E of 1161J and 1228J for the monotonic and reversed cyclic tests respectively. Test walls B6 produced the least E and were the weakest blocked wall for both monotonic and reversed cyclic tests.

The increase in normalized E had a range of 1.09 to 1.98 and 1.09 to 1.52 for the monotonic test and reversed cyclic tests respectively. Both monotonic and reserved cyclic tests results showed a consistent pattern; test walls B6 had the highest increase in normalized E and test walls B3 had the lowest increase of the comparison groups. Also, the normalized E followed a similar trend to the normalized ductility; with test walls B6 as the highest and test walls B3 as the lowest.

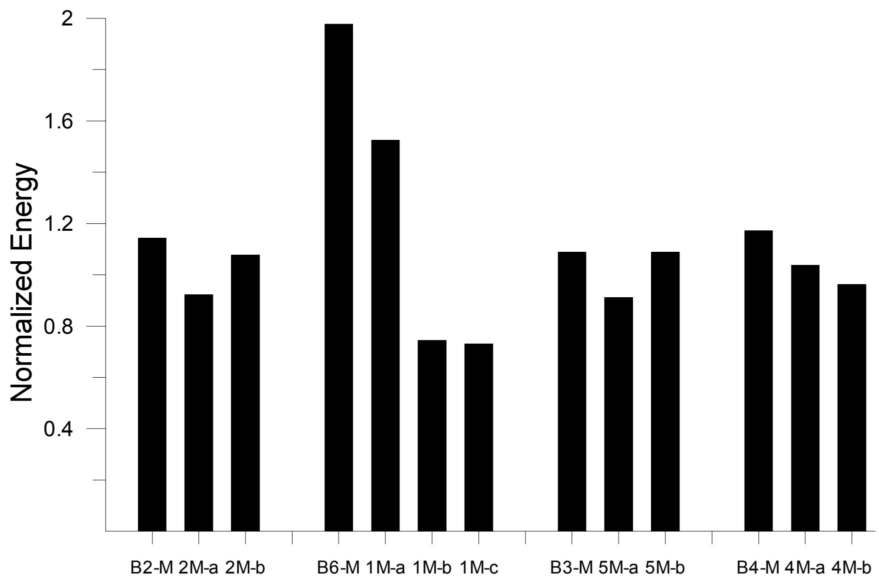

Figure 3.20 Comparison of normalized energy dissipation for monotonic tests

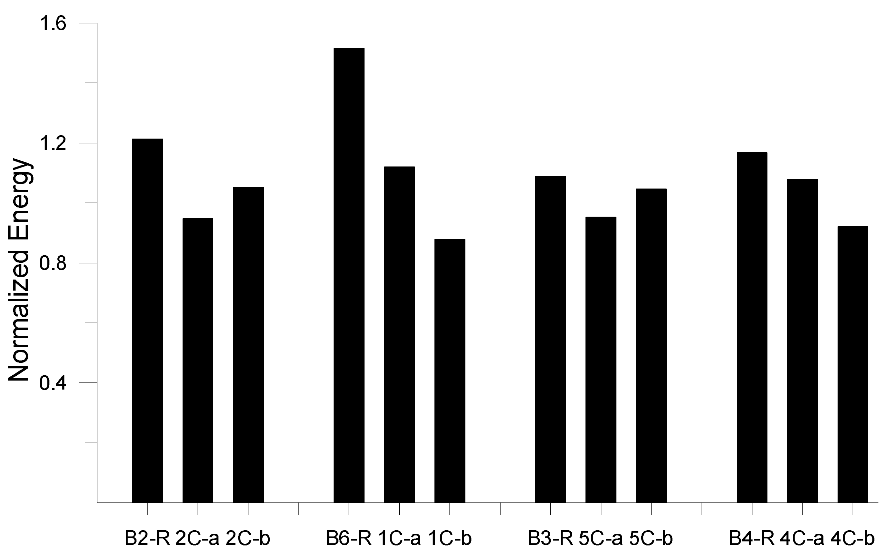

Figure 3.21 Comparison of normalized energy dissipation for reversed cyclic tests

3.2.4 Comparison of Blocking and Bridging

Wall 5M-c, tested by Ong-Tone (*2009*), was constructed with three rows of bridging channels with the intent of minimizing chord stud twisting. The effects of the installed bridging showed promising results compared to the nominally identical conventional walls (5M-a & 5M-b) with the exception of the unit elastic stiffness, k_e, which showed a decrease of normalized ratio equal to 0.80 (Table 3.7). A comparison of design parameters of the two groups i.e. blocked vs. conventional and bridging vs. conventional, showed that the wall with bridging performed better overall especially in terms of ductility and energy dissipation. The blocked wall attained higher shear resistances in terms of yield resistance (S_y) and ultimate wall resistance (S_u) as shown in Figure 3.22.

Most importantly, the blockings remained effective at large displacements compared to the bridging channels which eventually suffered from lateral-torsional buckling failure at increased displacements rendering them ineffective. Hence, the blocked wall (B3-M) did not suffer from twisting of the chord-stud, contrary to the bridged wall (5M-c) which suffered from twisting and local buckling of the chord-stud (Figure 3.23).

Table 3.7 Comparison of blocked and bridged shear walls

Test Specimen	Ultimate Resistance, S_u (kN/m)	Displacement at $0.8S_u$, $\Delta_{net,0.8u}$ (mm)	Yield Resistance, S_y (kN/m)	Unit Elastic Stiffness, k_e ((kN/m)/mm)	Ductility.μ	Energy Dissipation E (Joules)	Normalized Properties					
							S_u	**$\Delta_{net,0.8u}$**	**S_y**	**k_e**	**μ**	**E**
B3-M (blocked)	19.40	51.22	17.43	1.11	3.27	922	**1.41**	**0.88**	**1.38**	**0.61**	**0.39**	**1.09**
5M-c* (bridging)	17.21	100.00	15.72	1.45	9.20	1813	**1.25**	**1.71**	**1.24**	**0.80**	**1.10**	**2.14**
5M-a*	14.19	52.60	12.90	1.87	7.61	773	**1.00**	**1.00**	**1.00**	**1.00**	**1.00**	**1.00**
5M-b*	13.39	64.45	12.41	1.77	9.18	922						

* Ong-Tone *(2009)*

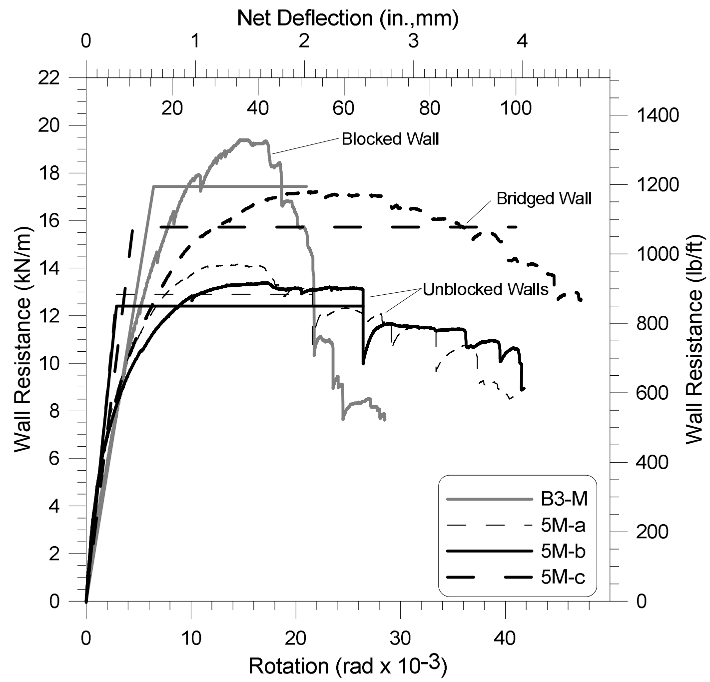

Figure 3.22Comparison of wall reinforcement: Wall resistance vs. displacement (test walls of 1.09mm framing, 0.76mm sheathing, 100mm fastener spacing)

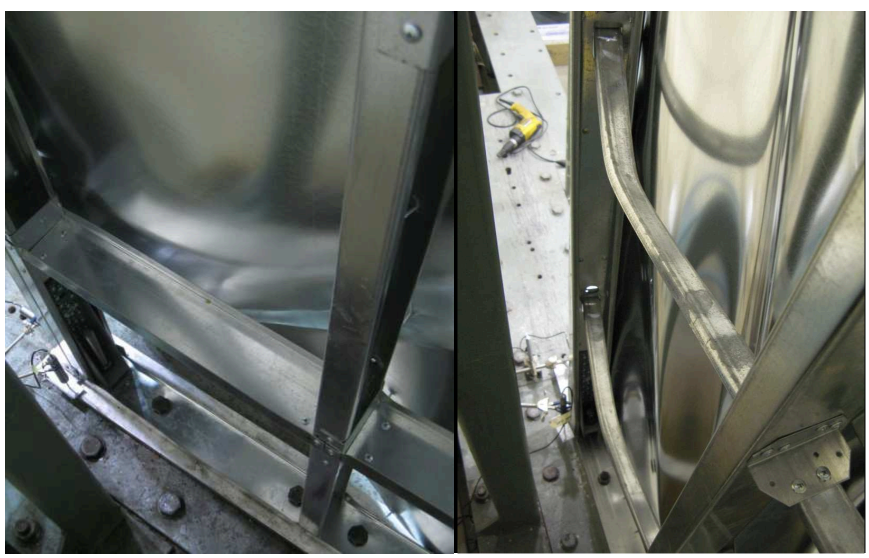

Figure 3.23 Post test observations: Blocking reinforcement remains effective (left); bridging failure by lateral-torsional buckling (right)

3.3 Limit States Design Procedure

A limit states design procedure for cold-formed steel frame/ steel sheathed shear walls have been recommended by Balh (*2010*) and Ong-Tone (*2009*) for use with the 2005 NBCC. The design procedure has been adopted by the author; included herein are the resulting resistance factor, factor of safety, over-strength for capacity based design and 'test-based' seismic force modification factors for the blocked shear walls. The test specimens were separated into 8 groups based on nominal values of framing thickness (studs, tracks, & blockings), sheathing thickness, and fastener spacing (Table 3.8).

Table 3.8 Description of test specimens group configurations

<table>
<tr><th rowspan="2">Configuration</th><th colspan="2">Stud Thickness</th><th colspan="2">Sheathing Thickness</th><th colspan="2">Fastener Spacing</th><th rowspan="2">Protocol</th><th rowspan="2">Test Name</th></tr>
<tr><th>(in.)</th><th>(mm)</th><th>(in.)</th><th>(mm)</th><th>(in.)</th><th>(mm)</th></tr>
<tr><td rowspan="2">1</td><td rowspan="10">0.043</td><td rowspan="10">1.09</td><td rowspan="6">0.018</td><td rowspan="6">0.46</td><td rowspan="2">2</td><td rowspan="2">50</td><td>monotonic</td><td>B2-M</td></tr>
<tr><td>cyclic</td><td>B2-R</td></tr>
<tr><td rowspan="2">2</td><td rowspan="2">4</td><td rowspan="2">100</td><td>monotonic</td><td>B5-M</td></tr>
<tr><td>cyclic</td><td>B5-R</td></tr>
<tr><td rowspan="2">3</td><td rowspan="2">6</td><td rowspan="2">150</td><td>monotonic</td><td>B6-M</td></tr>
<tr><td>cyclic</td><td>B6-R</td></tr>
<tr><td rowspan="2">4</td><td rowspan="6">0.03</td><td rowspan="6">0.76</td><td rowspan="2">4</td><td rowspan="2">100</td><td>monotonic</td><td>B3-M</td></tr>
<tr><td>cyclic</td><td>B3-R</td></tr>
<tr><td rowspan="2">5</td><td rowspan="2">6</td><td rowspan="2">150</td><td>monotonic</td><td>B4-M</td></tr>
<tr><td>cyclic</td><td>B4-R</td></tr>
<tr><td rowspan="2">6</td><td rowspan="2">0.054</td><td rowspan="2">1.37</td><td rowspan="2">2</td><td rowspan="2">50</td><td>monotonic</td><td>B1-M</td></tr>
<tr><td>cyclic</td><td>B1-R</td></tr>
<tr><td>7</td><td>0.054</td><td>1.37</td><td>0.03</td><td>0.76</td><td>3</td><td>75</td><td>monotonic</td><td>B7-M</td></tr>
<tr><td>8</td><td>0.054</td><td>1.37</td><td>0.018</td><td>0.46</td><td>3</td><td>75</td><td>monotonic</td><td>B8-M</td></tr>
</table>

3.3.1 Calibration of Resistance Factor

In limit states design, it is required that the factored resistances of the structural elements be greater than combined effects of the factored loads applied (Equation 3-7) as prescribed in Clause 4.1.3.2 of the 2010 National Building Code of Canada (NRCC, 2010).

$$\emptyset R \geq \sum \alpha S \tag{3-7}$$

where,

$\emptyset$ = Resistance factor of structural element

R = Nominal resistance of structural member

α = Load factor

S = Effect of particular specified load combinations

A method for determining the resistance factor for ultimate limit states design is defined in the North American Specification for Design of Cold-Formed Steel Structural Members (CSA S136 (2007)) (Equation 3-8).

$$\emptyset = C_{\emptyset}(M_m F_m P_m) e^{-\beta_o \sqrt{V_M^2 + V_F^2 + C_P V_P^2 + V_S^2}} \tag{3-8}$$

where,

$C_{\emptyset}$ = Calibration coefficient

M_m= Mean value of material factor

F_m = Mean value of fabrication factor

P_m= Mean value of professional factor

e = Natural logarithmic base

β_o= Target reliability index, 2.5 for structural members (*Branston, 2004*)

V_M= Coefficient of variation of material factor

V_F= Coefficient of variation of fabrication factor

V_P= Coefficient of variation of professional factor

V_S= Coefficient of variation of load effect, 0.37 (*Branston, 2004*)

C_P= Correction factor for sample size

$= {(1 + {}^{1}/_{n})m}/_{(m-2)}$ for n ≥ 4

= 5.7 for n=3

where,

n = Number of tests (sample size)

m = Degrees of freedom = n-1

Table F1 of the CSA-S136 Standard (*2007*) lists the mean values and their corresponding coefficients of variation of the material factor, M_m and V_m, respectively and the fabrication factor, F_m and V_f respectively. These values are based on the failure modes of the components used in the construction of the shear wall specimens. Two failure modes were considered: screw connection failure consisting of (1) shear failure of the screw and (2) tilting and bearing failure (Table 3.9).

Table 3.9 Statistical data for the determination of resistance factor
(CSA-S136, 2007)

Type of Component and Failure Mode	M_m	V_M	F_m	V_F
Type 1: Connection- Shear Strength of Screw	1.10	0.10	1.00	0.10
Type 2: Connection- Bearing and Tilting Strength of Screw	1.10	0.08	1.00	0.05

The target reliability index for structural members, β_o, is a factor describing the probability of failure and has a value of 2.5 listed by CSA-S136 (*2007*). The calibration coefficient, $C_\emptyset$, was determined by Branston (2004) based on wind load statistics. A load factor, α, of 1.4 and a ratio of mean to nominal value, $\bar{S}/S$, of 0.76 for wind load effects and a corresponding coefficient of variation, V_S, of 0.37 were used. The resulting calibration coefficient, $C_\emptyset$, of 1.842 was determined following Equation (3-9).

$$C_\emptyset = \frac{\alpha}{\bar{S}/S} \quad (3\text{-}9)$$

The mean value of the professional factor, P_m, was calculated from Equation (3-10) and is a function of the yield wall resistance, S_y, the average yield wall resistance of both monotonic and reversed cyclic tests, $S_{y,avg}$,(Equation 3-11) and the sample size of each configuration, *n.*

$$P_m = \frac{\sum_{i=1}^{n}\left(S_y / S_{y,avg}\right)_i}{n} \quad (3\text{-}10)$$

$$S_{y,avg} = \frac{S_{y,mono,avg} + \frac{S_{y+,avg} + S_{y-,avg}}{2}}{2} \quad (3\text{-}11)$$

where,

$S_{y,mono,avg}$ = Average yield wall resistance of the monotonic tests of a specific configuration

$S_{y+,avg}$ =Average positive yield wall resistance of the reversed cyclic test of a specific configuration

$S_{y-,avg}$= Average negative yield wall resistance of the reversed cyclic test of a specific configuration

The coefficient of variation of the professional factor, V_P, was calculated using Equation (3-12).

$$V_P = \sigma / P_m \tag{3-12}$$

where,

$$\sigma^2 = \frac{1}{n-1} \sum_{i=1}^{n} \left[\left(S_y / S_{y,avg} \right)_i - P_m \right]^2 \tag{3-13}$$

Table 3.10 summarizes the resistance factors, ϕ, determined for each of the two failure modes. The two resistance factors gave an average resistance factor of 0.77 but a resistance factor of 0.7 is recommended. This value is quite conservative and is consistent with the previous findings from Balh (*2010*), El-Saloussy (*2010*), and Ong-Tone (*2009*). Due to the limited number of tests that were performed, the sample size of each configuration group, *n*, was less than or equal to 3. As such, each of the two resistance factors was determined with a total sample size of *n* equal to 14 (number of shear wall specimens tested). A higher resistance factor would be warranted if the research program could be expanded to test a larger sample size of each configuration group.

Table 3.10 Summary of resistance factor calibration for different types of components and failure modes

Type of Component and Failure Mode	α	$\bar{S}/S$	C_Φ	M_m	F_m	P_m	β_o	V_M	V_F	V_S	*n*	C_p	V_p	ϕ
Type 1: Shear Strength of Screw Connection	1.4	0.76	1.842	1.10	1.00	1.00	2.50	0.10	0.10	0.37	14	1.27	0.0200	0.75
Type 2: Tilting and Bearing of Screw	1.4	0.76	1.842	1.10	1.00	1.00	2.50	0.08	0.05	0.37	14	1.27	0.0200	0.78

3.3.2 Nominal Shear Wall Resistance

The yield wall resistances, S_y, obtained from the EEEP analysis were dependant on the sheathing screw connection resistances which in turn was based on the material thickness and tensile stress. The ancillary tests of the steel sheathing resulted in measured material properties that were higher than the minimum specified values listed in the ASTM A653 Specification (*2008*). As such, the EEEP S_y values must be reduced so as to reflect the minimum specified properties. The calculated modification factors for sheathing thickness and tensile stress are provided in Table 3.11. The modification factors were applied to the EEEP S_y values to obtain nominal shear resistance values of the CFS frame/steel sheathed blocked shear walls (Table 3.13).

This was the same approach used in past research by Balh (*Balh & Rogers, 2010*), El-Saloussy (*El-Saloussy & Rogers, 2010*), and Ong-Tone (*Ong-Tone & Rogers, 2009*) for the development of the design values of all other steel sheathed CFS shear walls. The modifications factors used by the author were similar to those used in past research (Table 3.12). The overall modification factor shown is the total reduction factor used to derive the nominal S_y values and the product of the thickness and tensile stress modification factors.

Table 3.11 Sheathing thickness and tensile stress modification factors

Member	Nominal Thickness (mm)	Measured Thickness (mm)	**Thickness Modification Factor**	Minimum Specified Tensile Stress, F_u (MPa)	Measured Tensile Stress, F_u (MPa)	**Tensile Stress Modification Factor**
Sheathing	0.760	0.794	0.96	310	377	0.823
	0.460	0.448	1.00	310	358	0.866

Table 3.12 Modification factors of past research

Research by:	Nominal Sheathing Thickness	Thickness Modification Factor	Tensile Stress Modification Factor	Overall Modification Factor
DaBreo (*2012*)	0.46mm (0.018")	1.000	0.866	0.866
Balh (*2010*)		1.000	0.784	0.784
El-Saloussy (*2010*)		0.950	0.880	0.836
DaBreo (*2012*)	0.76 (0.030")	0.960	0.823	0.790
Balh *(2010)*		1.000	0.831	0.831
Ong-Tone (*2009*)		1.000	0.831	0.831
El-Saloussy (*2010*)[1]		1.000	0.810	0.810
El-Saloussy (*2010*)[2]		1.000	0.920	0.920

[1] obtained from Phase 1, Yu *et al* (*2007*)

[2] obtained from Phase 2, Yu *et al* (*2009*)

Table 3.13 Proposed nominal shear resistance, S_y, for CFS frame/steel sheathed blocked shear walls[1,2,3] (kN/m (lb/ft))

Assembly Description	Max Aspect Ratio (h/w)	Fastener Spacing[4] at Panel Edges (mm(in))				Designation Thickness[5,6] of Stud, Track, and Blocking ((mm) (mils))	Required Sheathing Screw Size[7]
		150 (6)	100 (4)	75 (3)	50 (2)		
0.46 mm (0.018") steel sheet, one side	2:1	7.37	9.68	11.60	13.52	1.09 (43)	8
0.76 mm (0.030") steel sheet, one side	2:1	11.69	14.33	-	-	1.09 (43)	8
		-	-	19.88	23.31	1.37 (54)	8

1) Nominal resistance, S_y, to be multiplied by the resistance factor, $\phi = 0.7$, to obtain factored resistance
2) Sheathing must be connected vertically to steel frame
3) Nominal shear resistance values are applicable for combined lateral and gravity loading
4) Edge fasteners are to be placed at least 9.5mm (3/8”) from the sheathing edge and field screws to be spaced 305mm (12”) o/c
5) Wall stud and tracks shall be ASTM A653 grade 230MPa (33ksi) for 1.09mm (0.043”) minimum uncoated base metal thickness and grade 340MPa (50ksi) for 1.37mm (0.054”) minimum uncoated base metal thickness
6) Stud dimension: 92.1 mm (3-5/8”) web, 41.3 mm (1-5/8”) flange, 12.7 mm (1/2”) lip
   Track dimension: 92.1 mm (3-5/8”) web, 31.8 mm (1-1/4”) flange
   Blockings are to be made from tracks of same designation thickness
7) Minimum No.8 x 12.7 (1/2”) sheathing screws shall be used

3.3.3 Factor of Safety

The factor of safety is solely applicable for the case of wind loading and includes the effect of the combined gravity loading as was tested by the author. In limit states design (LSD), the factored resistances are compared to factored loads. As such, the factor of safety is defined as the ratio of the ultimate wall resistance, S_u, to the factored wall resistance, S_r, as shown in Equation (3-14) and the relationship is illustrated by Branston *(2004)* in Figure 3.24.

$$Factor\ of\ Safety = \frac{S_u}{S_r} \tag{3-14}$$

where,

S_u = Ultimate shear resistance of test specimen

S_r = $\emptyset S_y$ Factored wall shear resistance ($\emptyset$ = 0.7)

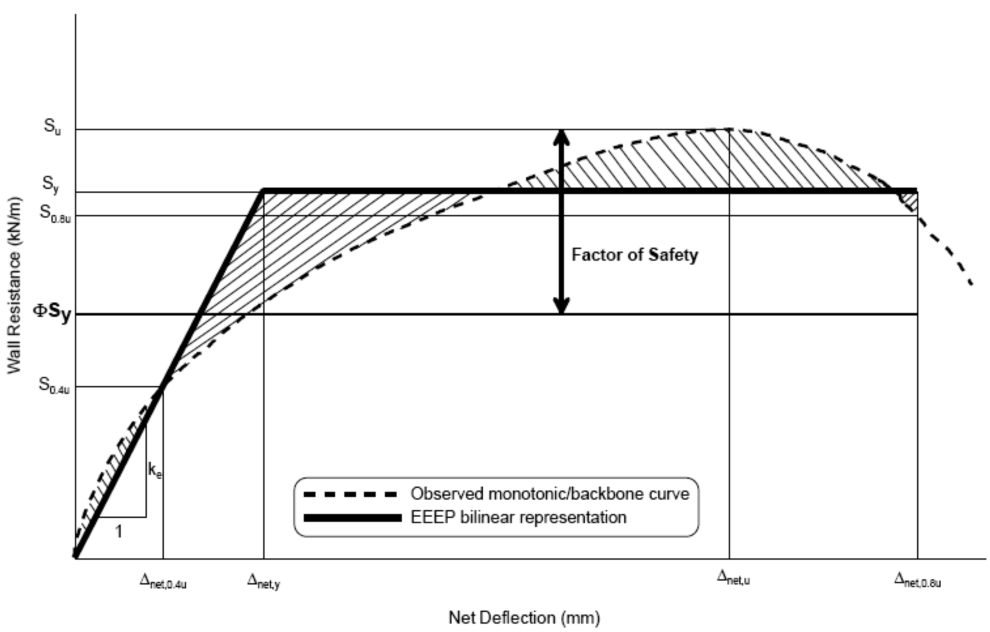

Figure 3.24 Factor of safety relationship with ultimate and factored resistances *(Branston, 2004)*

For allowable stress design (ASD), the factor of safety is multiplied by the load factor for wind loads of 1.4 as defined by the 2010 NBCC (Equation 3-15).

$$Factor\ of\ Safety\ (ASD) = 1.4 \times \frac{S_u}{S_r} \tag{3-15}$$

The factors of safety were calculated for both monotonic and reserved cyclic tests and are provided in Tables 3.14 and 3.15 respectively. For the reversed cyclic tests, the test values from the positive and negative regions were combined since the differences between the two values were small with the positive values always being slightly smaller due to the strength degradation incurred from the previously loaded negative cycle. Average factors of safety of 1.91 and 2.68 were determined for LSD and ASD respectively. Also included in Tables 3.14 and 3.15 are the respective standard deviations (STD.DEV.) and coefficients of variation (CoV).

Table 3.14 Factor of safety for the monotonic test specimens

Configuration	**Test Name**	**Ultimate Resistance, S_u (kN/m)**	**Nominal Resistance, S_y (kN/m)**	**Factored Resistance, S_r (ϕ=0.7) (kN/m)**	**Factor of Safety (LSD) S_u/S_r**	**Factor of Safety (ASD) $1.4xS_u/S_r$**
1	B2-M	16.91	13.52	9.46	1.79	2.50
2	B5-M	12.00	9.68	6.77	1.77	2.48
3	B6-M	9.31	7.37	5.16	1.80	2.53
4	B3-M	19.40	14.33	10.03	1.93	2.71
5	B4-M	16.83	11.69	8.18	2.06	2.88
6	B1-M	33.96	23.31	16.32	2.08	2.91
7	B7-M	28.01	19.88	13.92	2.01	2.82
8	B8-M	14.50	11.24	7.87	1.84	2.58
				Average	**1.91**	**2.68**
				STD. DEV.	**0.1263**	**0.1768**
				CoV.	**0.0160**	**0.0313**

Table 3.15 Factor of safety for the reversed cyclic test specimens

Configuration	Test Name	Ultimate Resistance, S_u (kN/m)	Nominal Resistance, S_y (kN/m)	Factored Resistance, S_r (ϕ=0.7) (kN/m)	Factor of Safety (LSD) S_u/S_r	Factor of Safety (ASD) $1.4xS_u/S_r$
1	B2-R	16.81	13.52	9.46	1.78	2.49
2	B5-R	12.40	9.68	6.77	1.83	2.56
3	B6-R	9.49	7.37	5.16	1.84	2.57
4	B3-R	20.71	14.33	10.03	2.07	2.89
5	B4-R	16.51	11.69	8.18	2.02	2.83
6	B1-R	31.52	23.31	16.32	1.93	2.70
				Average	**1.91**	**2.67**
				STD. DEV.	**0.1143**	**0.1600**
				CoV.	**0.0131**	**0.0256**

3.3.4 Capacity Based Design

Capacity based design of the shear wall structure as part of the seismic force resisting system (SFRS) is required by the AISI S213 Standard. A “fuse” element within the SFRS is chosen as the ductile energy dissipating device during inelastic deformations. The remaining elements of the SFRS such as field and chord studs, hold-downs, anchors, tracks and blockings are designed to remain elastic and resist the probable capacity of the “fuse” element and the corresponding principal and companion loads as defined by the 2010 NBCC. Thus the structural integrity of the building system is maintained. In CFS framed/steel sheathed shear walls the screw connections between the sheathing and framing act as the “fuse” element and provides this ductile energy dissipation through bearing deformations of the sheathing and frame.

During a design level seismic event, the shear wall is expected to reach its ultimate capacity when pushed to the inelastic range. An overstrength factor is used to estimate the probable capacity of the shear wall and is applied in the design of the other structural elements in the SFRS to ensure they remain elastic. The overstrength factor is determined as the ratio of ultimate to nominal shear resistance (Equation (3-16)) and the relationship is illustrated in Figure 3.25.

$$overstrength = \frac{S_u}{S_y} \tag{3-16}$$

where,

S_u = Ultimate shear resistance of test specimen

S_y = Nominal yield wall resistance

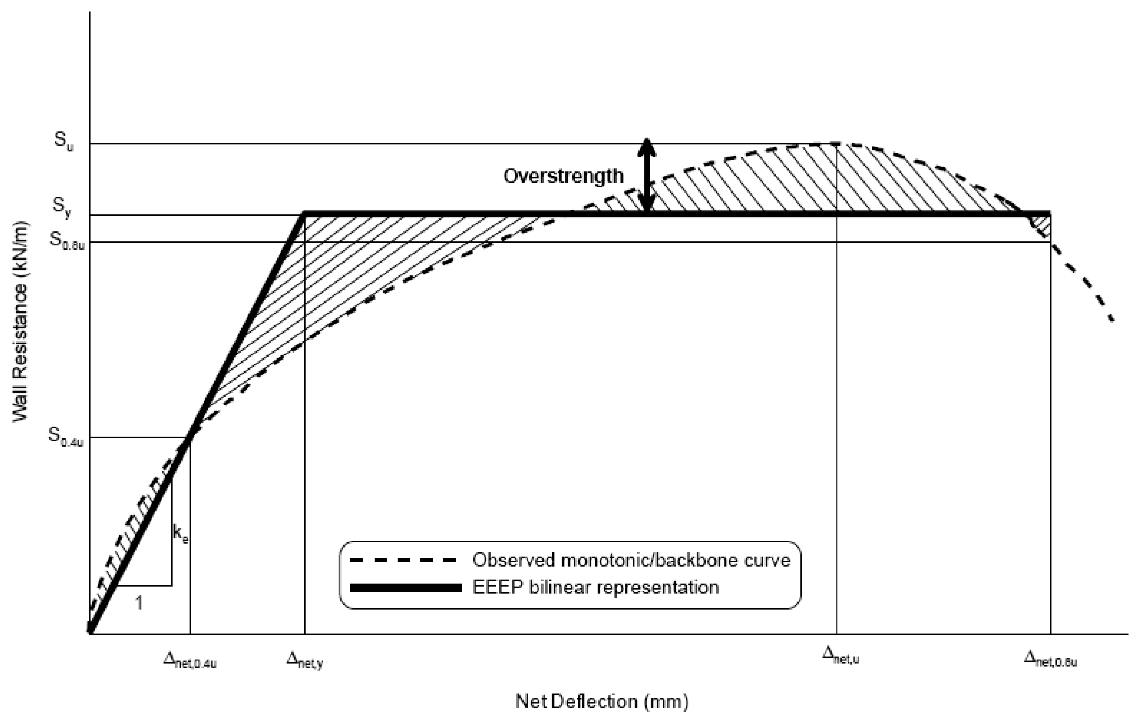

Figure 3.25 Overstrength relationship with ultimate and nominal shear resistance *(Branston, 2004)*

The overstrength factors and their corresponding standard deviations and coefficients of variation are presented in Tables 3.16 and 3.17 for the monotonic and reversed cyclic tests respectively. An average overstrength factor of 1.34 was found for both the monotonic and reversed cyclic tests. Hence, a value of 1.34 is recommended for the design of structural elements within the steel sheathed blocked shear walls. The reduction in overstrength when compared to the value of 1.4 recommended by Balh *(Balh & Rogers, 2010)* was attributed to the higher tensile stress modification factor, particularly for the 0.46mm (0.018") sheathing, which in-turn increased the derived nominal wall resistance (S_y). Table 3.12 lists the tensile stress modification factors of both the author and Balh *(Balh & Rogers, 2010)* which equaled 0.866 and 0.784 respectively. Another contributor to the smaller overstrength value was the decrease in ductility of the blocked shear walls. These walls had shorter plastic regions, thus, smaller displacements at $0.8S_u$ ($\Delta_{net,0.8u}$) which is a factor used for determining S_y as shown in Equation 3.2. Hence the ratios of the ultimate to nominal wall resistance are smaller compared to the conventional (unblocked) walls for the same configuration.

Table 3.16 Overstrength design values for monotonic tests

Configuration	Test Name	Ultimate Resistance, S_u (kN/m)	Nominal Resistance, S_y (kN/m)	Overstrength S_u/S_y
1	B2-M	16.91	13.52	1.25
2	B5-M	12.00	9.68	1.24
3	B6-M	9.31	7.37	1.26
4	B3-M	19.40	14.33	1.35
5	B4-M	16.83	11.69	1.44
6	B1-M	33.96	23.31	1.46
7	B7-M	28.01	19.88	1.41
8	B8-M	14.50	11.24	1.29
			Average	**1.34**
			STD. DEV.	**0.0884**
			CoV.	**0.0078**

Table 3.17 Overstrength design values for reversed cyclic tests

Configuration	Test Name	Ultimate Resistance, S_u (kN/m)	Nominal Resistance, S_y (kN/m)	Overstrength S_u/S_y
1	B2-R	16.81	13.52	1.24
2	B5-R	12.40	9.68	1.28
3	B6-R	9.49	7.37	1.29
4	B3-R	20.71	14.33	1.45
5	B4-R	16.51	11.69	1.41
6	B1-R	31.52	23.31	1.35
			Average	**1.34**
			STD. DEV.	**0.0800**
			CoV.	**0.0064**

3.3.5 Calibration of Seismic Force Modification Factors

The equivalent static force method, as defined in Clause 4.1.8.11 of the 2010 NBCC, is used to calculate the seismic base shear force, V, as shown in Equation (3-17).

$$V = \frac{S(T_a)M_v I_e W}{R_d R_o} \tag{3-17}$$

where,

$S(T_a)$ = Design spectral acceleration

T_a= Fundamental lateral period of vibration of the building

M_v= Factor accounting for higher mode effects

I_e = Earthquake importance factor of the structure

W = Weight of the structure (dead load plus 25% snow load)

R_d = Ductility-related force modification factor

R_o = Overstrength-related force modification factor

The approach used for determining the 'test-based' force modification factors for ductility, R_d, and for overstrength, R_o, used in calculating the base shear force will be described in this section. These R-values will then undergo a verification process following an approach adopted from the FEMA P695 (*2009*) methodology which is discussed in the following chapter.

3.3.5.1 Ductility-Related Force Modification Factor, R_d

The ability of the "fuse" element to dissipate energy during inelastic deformations is measured by the R_d factor. Newmark and Hall *(1982)* derived relationships between the R_d factor and the ductility ratio, μ, based on the structure's natural period as listed in Equations (3-18), (3-19) and (3-20).

$$R_d = \mu \qquad \text{for } T > 0.5\text{s} \qquad (3\text{-}18)$$

$$R_d = \sqrt{2\mu - 1} \qquad \text{for } 0.1\text{s} < T < 0.5\text{s} \qquad (3\text{-}19)$$

$$R_d = 1 \qquad \text{for } T < 0.03\text{s} \qquad (3\text{-}20)$$

where,

R_d = Ductility-related force modification factor

μ = Ductility of shear wall

T = Natural period of structure

Boudreault *(2005)* suggested that the natural period of most light-framed structures should be between 0.03 to 0.5 seconds. Thus, Equation (3-19) was chosen for the calculation of the R_d values. The R_d values of the monotonic and reversed cyclic tests are listed in Tables 3.18 and 3.19 respectively. The monotonic tests produced an average R_d factor of 3.02, whilst the reversed cyclic tests produced an average R_d factor of 2.83. The average R_d factor of 2.93 was found for both monotonic and reversed cyclic tests combined. A conservative value of 2.5 is suggested which is consistent with that recommended by Balh (2010) for sheet sheathed shears walls and also listed in the AISI S213 (*2007*) for CFS framed/wood sheathed shear walls.

Table 3.18 Ductility and R_d values for monotonic tests

Configuration	Test Name	Ductility (μ)	Ductility-Related Force Modification Factor (R_d)
1	B2-M	4.85	2.95
2	B5-M	4.36	2.78
3	B6-M	9.30	4.20
4	B3-M	3.27	2.35
5	B4-M	6.08	3.34
6	B1-M	4.74	2.91
7	B7-M	4.19	2.71
8	B8-M	4.84	2.95
		Average	**3.02**
		STD. DEV.	**0.5487**
		CoV.	**0.3010**

Table 3.19 Ductility and R_d values for reversed cyclic tests

Configuration	Test Name	Ductility (μ)	Ductility-Related Force Modification Factor (R_d)
1	B2-R	5.54	3.18
2	B5-R	4.20	2.71
3	B6-R	4.97	2.98
4	B3-R	3.82	2.57
5	B4-R	5.02	3.01
6	B1-R	3.67	2.52
		Average	**2.83**
		STD. DEV.	**0.2648**
		CoV.	**0.0701**

3.3.5.2 Overstrength-Related Force Modification Factor, R_o

The overstrength-related force modification factor, R_o, is used in seismic design to account for the overstrength within the “fuse” element. For capacity based design, energy is dissipated through the inelastic deformation of the “fuse” element. Hence, the R_o factor is used to cancel the often overestimated factored loads so that energy dissipation can be achieved. Mitchell *et al. (2003)* proposed the following formula shown in Equation (3-21) for calculating the R_o factor.

$$R_o = R_{size} R_{\emptyset} R_{yield} R_{sh} R_{mech} \tag{3-21}$$

where,

R_{size} = overstrength due to restricted choices for sizes of components

$R_{\emptyset} = 1/\emptyset, \ (\emptyset = 0.7)$

R_{yield} = ratio of test yield strength to minimum specified yield strength

R_{sh} = overstrength due to development of strain hardening

R_{mech} = overstrength due to collapse mechanism

The R_o factor is a function of the five overstrength factors listed above. The R_{size} factor is used to account for the limitations to the choice of component/member sizes available to the designer. The $R_{\emptyset}$ factor is the inverse of the resistance factor, ϕ, and accounts for nominal load values and not factored loads. The R_{yield} factor is the average overstrength value that was previously determined in Section 3.3.4. The R_{sh} and R_{mech} factors are taken as unity since the shear walls are not affected by strain hardening and the collapse mechanism has not yet been established. The overstrength factors are presented in Table 3.20 and a R_o value of 2.01 was determined. At this time, a R_o value of 1.7 is suggested which is consistent with the recommendation by Balh (*2010*) and the value listed in the AISI S213 (*2007*) for CFS framed/wood sheathed shear walls.

Table 3.20 Overstrength factors for calculating the overstrength-related force modification factor, R_o

	R_{size}	R_{ϕ}	R_{yield}	R_{sh}	R_{mech}	R_o
All Groups	1.05	1.43	1.34	1.00	1.00	2.01

3.3.6 Inelastic Drift Limit

The inelastic drift of the shear wall specimen is the ratio of the displacement at 80% post-peak load, $\Delta_{0.8u}$, to the wall height. The 2010 NBCC specifies an inelastic drift limit of 2.5% of the storey height which gives a limit of 61 mm to the 2440 mm high shear walls. The percentage drifts measured from the monotonic and reversed cyclic tests are presented in Table 3.21 and 3.22 respectively. The monotonic tests resulted in higher drifts compared to the reversed cyclic tests with the exception of test B2-M. The monotonic and reversed cyclic tests had average $0.8S_u$ post peak drift limits of 2.42% and 2.13% respectively, and an average drift limit of 2.28% for both tests combined. These average drift values are all lower than the 2.5% limit specified by the 2010 NBCC. The stronger wall specimens, particularly tests B2-(M&R) and B1-(M&R), produced drifts higher than 2.5%. Though these higher drifts may seem promising and warrant an increase in the inelastic drift limit, Section 3.2.3 showed that the blocked walls reached lower displacements ($\Delta_{0.8u}$) compared to the nominally identical unblocked walls. Also, the blocked walls showed less ductility and higher rates of strength degradation. Thus a conservative drift limit of 2% is proposed which is consistent with that recommended by Balh (*2010*) for ordinary steel sheathed shear walls.

Table 3.21 Drifts of monotonic tests

Configuration	Test Name	$\Delta_{0.8u}$ (mm)	% Drift
1	B2-M	68.26	2.80
2	B5-M	55.93	2.29
3	B6-M	65.98	2.70
4	B3-M	51.22	2.10
5	B4-M	53.95	2.21
6	B1-M	74.31	3.05
7	B7-M	63.81	2.61
8	B8-M	38.58	1.58
		Average	**2.42**
		STD. DEV.	**0.4658**
		CoV.	**0.2170**

Table 3.22 Drifts of reversed cyclic tests

Configuration	Test Name	$\Delta_{0.8u}$ (mm)	% Drift
1	B2-R	70.40	2.89
2	B5-R	41.15	1.69
3	B6-R	43.05	1.76
4	B3-R	44.95	1.84
5	B4-R	42.60	1.75
6	B1-R	70.10	2.87
		Average	**2.13**
		STD. DEV.	**0.5802**
		CoV.	**0.3366**

CHAPTER 4- EVALUATION OF STEEL SHEATHED CFS SHEAR WALL SYSTEMS BY DYNAMIC ANALYSIS

In order to verify the parameters and factors used in the seismic design method, non-linear time history dynamic analysis had to be carried out to predict the performance of multi-storey CFS framed buildings during seismic events. An approach from the US Federal Emergency Management Agency (FEMA) P695 (*2009*) document on the "Quantification of Building Seismic Performance Factors" was adopted for this verification. A representative building was selected and its seismic force resisting system (SFRS) was designed to resist the expected seismic force for a specific region. The OpenSees software (*McKenna et al. 2006*) was used to model the building and perform the non-linear time history dynamic analysis. With the use of Incremental Dynamic Analysis (IDA) (*Vamvatsikos & Cornell, 2002*), input ground motion records were scaled and subjected to the building at incrementally increasing scaling factors. Finally, the IDA results were used to evaluate the building design based on the failure criterion of 2% inter-storey drift

4.1 Building Selection

The CFS-NEES project (*Schafer et al. 2011*), "Enabling Performance-Based Seismic Design of Multi-Story Cold-Formed Steel Structures", conducted at the Johns Hopkins University aims to study the seismic behaviour of light-framed structures using CFS C-sections as the primary gravity load carrying elements and wood structural panel shear walls as the Lateral Force Resisting System (LFRS). The building plan used in the aforesaid project was adopted as an appropriate representative building model to evaluate seismic performance of the steel sheathed CFS framed shear wall system (Figure 4.1). The structure represents a typical office building in Canada and has a floor plan of dimensions 15.61 m x

7.01 m (49’9” x 23’0”) resulting in a floor area of 106.27 m^2. Both the first and second storeys are 2.74 m (9’-0”) excluding the 0.38 m (1’-3”) roof parapet.

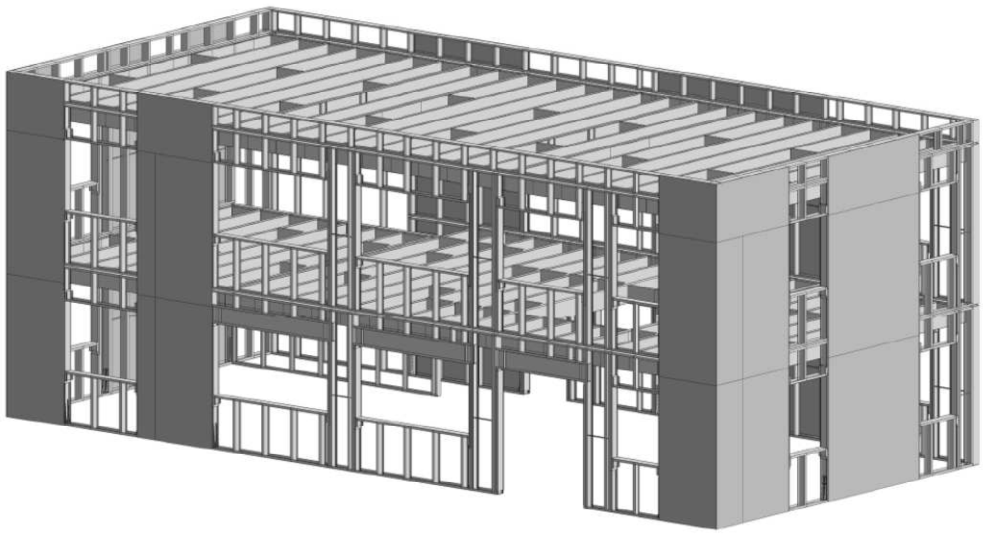

Figure 4.1 CFS-NEES Building (*Schafer et al. 2011*)

4.2 Description of Design Procedure

It was decided that the shear wall system be designed for the representative building located in Vancouver, BC, on Soil Class C; a high seismicity zone and on very dense soil to soft rock. The design was carried out using the shear wall design values obtained in the previous Chapter 3 to resist the Case 5 load combination found in Table 4.1.3.2.A from the 2010 National Building Code of Canada (*NRCC, 2010*) (Equation 4-1).

$$w_f = 1.0D + 1.0E + 0.5L + 0.25S \quad (4\text{-}1)$$

where,

D = Specified dead load

E = Specified earthquake load

L = Specified live load

S = Specified snow load

The specified snow load on the roof was determined according to Clause 4.1.6.2 of the 2010 NBCC (Equation 4-2). The location specific parameters: ground snow load, S_s, and rain load, S_r, were obtained from Appendix C (Climatic and Seismic Information for Building Design in Canada) of the 2010 NBCC for Vancouver. Table 4.1 lists the calculated specified snow load, specified live load (office area occupancy), and specified dead loads for both the roof and floor area. A description of the typical construction components of the roof, walls, and flooring were obtained from the Handbook of Steel Construction, 9th Edition (*CISC,2007*) and was used to approximate the specified dead loads.

$$S = I_S\,[S_S(C_b C_w C_S C_a) + S_r] \tag{4-2}$$

where,

I_S = Importance factor for snow load, 1.0

S_S = 1/50 year ground snow load, 1.8kPa

C_b = Basic roof snow load factor, 0.8

C_w = Wind exposure factor, 1.0

C_S = Roof slope factor, 1.0

C_a = Shape factor, 1.0

S_r = 1/50 year associated rain load, 0.2kPa

Table 4.1 Description of specified loads

Dead Loads		
	Description of Typical Roof	Load (kPa)
All walls (1/2)	-	0.39
Sheathing	12.5 mm plywood	0.07
Insulation	rigid glass fibre	0.07
Ceiling	12.5 mm gypsum	0.10
Purlins	cold-formed steel (spacing at 400 mm)	0.19
Roofing	asphalt- 3 ply, no gravel	0.15
Other fixtures	-	0.22
Total Dead Load		**1.19**
	Description of Typical Floor	
All walls	exterior, load bearing, shear and partition	1.33
Flooring	10 mm hardwood	0.08
Floating concrete	38.1 mm thick (1-1/2”)	0.88
Plywood	15.9 mm plywood	0.09
Joists	cold-formed steel (spaced at 600 mm)	0.14
Ceiling	12.5 mm gypsum	0.10
Other fixtures	-	0.25
Total Dead Load		**2.87**
Live Load		
Office area type occupancy		**2.40**
Snow Load		
Roof		**1.64**

4.3 Evaluation of Design Base Shear Force

The building was deemed a regular structure following the outline for structural irregularities listed in Table 4.1.8.6 of the 2010 NBCC. Hence, the Equivalent Static Force Procedure given in Clause 4.1.8.6 of the NBCC was used to calculate the base shear force, V (Equation 4-3).

$$V = \frac{S(T_a) M_v I_E W}{R_d R_o} \tag{4-3}$$

where V must not be less than,

$$V \geq \frac{S(2.0) M_v I_E W}{R_d R_o} \tag{4-4}$$

and must not be greater than,

$$V \leq \frac{2}{3} \frac{S(0.2) M_v I_E W}{R_d R_o} \tag{4-5}$$

where,

$S(T_a)$ = 5% damped spectral response acceleration at the given period

T_a= Fundamental lateral period of vibration of the building, sec

M_v= Factor accounting for higher mode effects

I_E = Earthquake importance factor of the structure, 1.0

W = Seismic weight of the structure (1.0D + 0.25S), kN

R_d = Ductility-related force modification factor

R_o = Overstrength-related force modification factor

The fundamental lateral period of the structure, T_a, was calculated according to the equation given in the NBCC for shear walls (Equation 4-6). The NBCC provides an allowance for the reduction of the seismic force of up to $2T_a$ or by using the fundamental period of the building model found through dynamic analysis, T_{model}; whichever of the two is lowest. T_a was calculated to be 0.18 sec, therefore $2T_a$ was 0.36 sec. T_{model} was by determined by Shamim (*Shamim & Rogers, 2011*) to be 0.26 sec.

$$T_a = 0.05h_n^{3/4} \tag{4-6}$$

where,

h_n = total height of building, 5.48 m

The design spectral response acceleration, $S(T_a)$, was found using the Uniform Hazard Spectrum (UHS) for Vancouver obtained from Appendix C of the 2010 NBCC (Table 4.2 & Figure 4.2). The UHS was representative of Site Class C soil with acceleration and velocity based site coefficients, F_a and F_v, equal to 1.0. The Higher Mode Factor, M_v, was determined from Table 4.1.8.11 of the 2010 NBCC and was equal to 1.0 for fundamental lateral periods less than 1.0sec. The Earthquake Importance Factor, I_E, was equal to 1.0 since the structure was of normal importance. The ductility and overstrength-related force modification factors, R_d and R_o, were 2.0 and 1.3 respectively. These were lower than the values recommended in Chapter 3 but were consistent with the recommendation by Balh & Rogers (2010). In Phase 1 of the design procedure by Balh & Rogers (*2010*), the results did not meet the acceptance criteria of the FEMA P695 with the recommended R_d and R_o values of 2.5 and 1.7. Hence Phase 2 incorporated reduced R_d and R_o values of 2.0 and 1.3 respectively to address the inadequacy of the building performance

The seismic weight, *W*, of the structure was the summation of the dead load plus 25% of the snow load and is summarized in Table 4.3.

Table 4.2 Uniform Hazard Spectrum for Vancouver, BC

Period, T (sec)	$S_a(T)$ %g
0.2	0.94
0.5	0.64
1.0	0.33
2.0	0.17

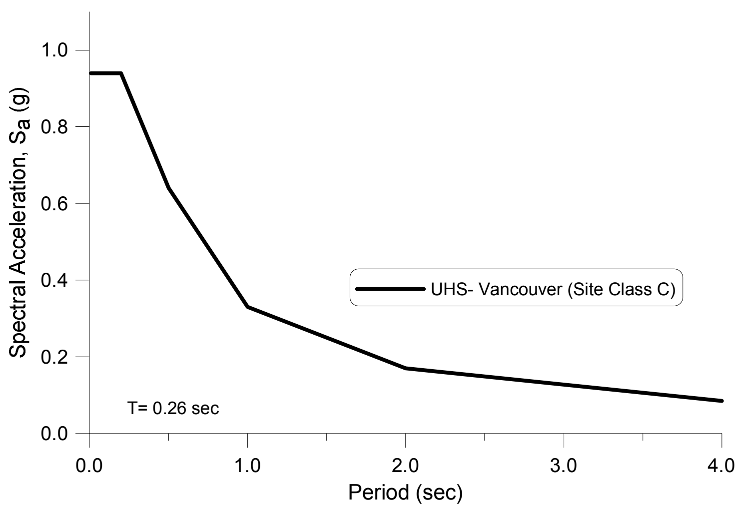

Figure 4.2 Uniform Hazard Spectrum for Vancouver, BC

Table 4.3 Seismic weight distribution

Storey	***Load Combo: 1.0D+0.25S (kPa)***	**Area (m^2)**	**Seismic Weight, W (kN)**	**Cumulative W (kN)**
2^{nd}/Roof	1.60	106.27	170	170
1^{st}	2.87	106.27	305	475
Ground	-	-	-	**475**

The base shear and it limits were calculated using the preceding Equations 4-3 to 4-5 and the resulting design base shear, V_{design}, was determined (Table 4.4).

Table 4.4 Determination of the design base shear

V	V_{min}	V_{max}	V_{design}
160.78	31.1	114.5	114.5

The design base shear was then distributed to each storey in accordance with Clause 4.1.8.11 (6) of the 2010 NBCC (Equation 4-7).

$$F_x = \frac{(V - F_t) W_x h_x}{\left(\sum_{i=1}^{n} W_i h_i\right)} \tag{4-7}$$

where,

F_x = distributed base shear force applied to storey x (kN)

V = design base shear force (kN)

F_t= roof surcharge load = 0 for $T_a < 0.7s$

W_x = seismic weight at storey x, (kN)

h_x = height of storey x, (m)

$W_i h_i$ = seismic weight times storey height for storey i, (kNm)

Torsional effects were considered as prescribed by the NBCC using Equation 4-8. The centre of mass and centre of rigidity were assumed to coincide, thus, the eccentricity, e_x, was equal to 0. The shear force applied to each storey due to torsion, F_{tx}, was taken as 10% of the seismic load of the storey being considered

(Equation 4-9). The total seismic force expected at each level is summarized in Table 4.5.

$$T_x = F_x(e_x \pm 0.10D_{nx}) \tag{4-8}$$

$$F_{tx} = \frac{T_x}{D_{nx}} = 0.1F_x \tag{4-9}$$

where,

T_x = floor torque at storey x (kNm)

F_x = seismic force applied to storey x (kN)

e_x = eccentricity between centre of mass and centre of rigidity (m)

D_{nx} = building dimension perpendicular to applied seismic load (m)

F_{tx} = additional force due to torsional effects at storey x (kN)

Table 4.5 Expected seismic force distribution

Storey	h_i (m)	W_i (kN)	h_iW_i (kNm)	F_x (kN)	F_{tx} (kN)	**Seismic Force** (kN)	**Cumulative. Seismic Force** (kN)
2nd/Roof	5.48	170	932	60.4	6.0	66.4	66.4
1st	2.74	305	836	54.1	5.4	59.6	125.9
Ground	0.00	-	-	-	-	-	-
Total	**5.48**	**475**	**1768**	**114.5**	-	**125.9**	-

4.4 Design and Selection of Shear Walls

Once the expected seismic force at each storey was calculated, the configurations (screw fastener spacing and steel sheathing thickness) of the shear walls required to resist these forces were determined. Figure 4.3 shows the final building floor plan with the respective shear walls outlined in red; the lengths of the shear wall segments at each building side (north, south, east, and west) are listed in Table 4.6.

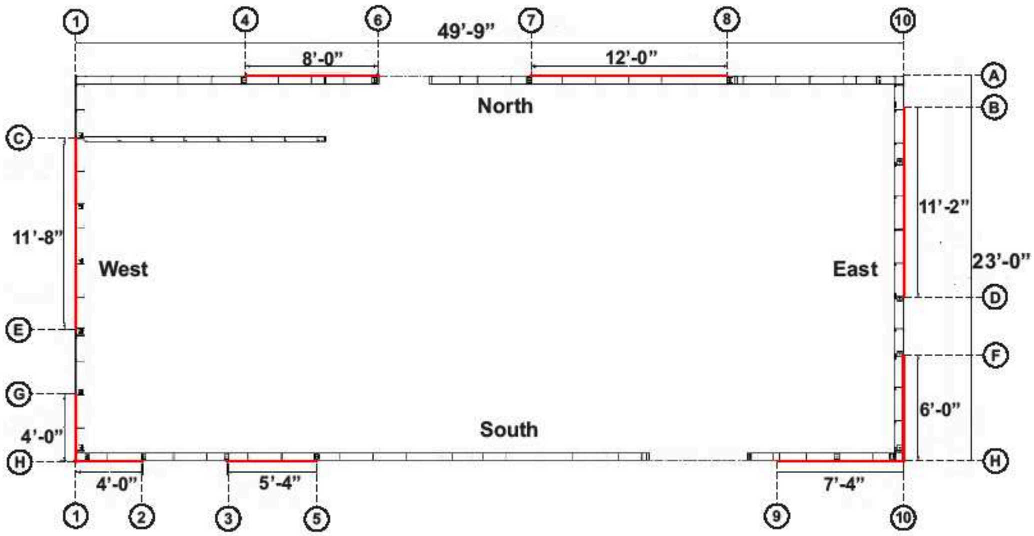

Figure 4.3 Floor plan of two-storey office building

Table 4.6 Length of model building shear walls

Shear Wall Lengths (m)				
Shear Wall Segment	North	South	East	West
1	2.44	1.22	3.40	1.22
2	3.66	1.63	1.83	3.56
3	-	2.24	-	-
Total	**6.10**	**5.08**	**5.23**	**4.78**

The design was carried out with the for the North-South and East-West directions separately. The shear walls on each building side were assumed to resist half of the seismic load imposed in either direction, i.e. the North-South or East-West directions, due to the assumption of a rigid diaphragm The shear flow,

S_f, was then calculated by dividing half the cumulative seismic force of the considered storey by the total shear wall length of the given side (Table 4.7).

Table 4.7 Expected seismic demand on model building

Shear flow, S_f (kN/m)					
Storey	Cumu. Seismic Force (kN)	North	South	East	West
2nd/Roof	66.4	5.45	6.54	6.34	6.95
1st	125.9	10.33	12.40	12.04	13.19

A shear wall configuration was selected based on the factored shear resistance required to resist the shear flow on a given building side. The factored shear resistances, S_r, were calculated from the proposed nominal shear resistances, S_y, found in Table 3.13 of Chapter 3, multiplied by the resistance factor, ϕ, of 0.7 (Equation 4-10). Table 4.8 summarizes the respective design shear resistances for each building side and storey level.

$$S_r = \emptyset S_y \tag{4-10}$$

where,

S_r = Design (factored) shear resistance (kN/m)

$\emptyset$ = resistance factor, 0.7

S_y = Nominal shear resistance (kN/m)

Table 4.8 Preliminary shear wall design

Design Shear Resistance, S_r (kN/m)				
Storey	North	South	East	West
2^{nd}/Roof	6.77	6.77	6.77	10.03
1^{st}	13.92	13.92	13.92	13.92

Although the shear wall selection satisfied the resistance criterion, it did not satisfy all the conditions of structural irregularities outlined in Table 4.1.8.6 of the 2010 NBCC. The preliminary shear wall design had to be re-evaluated to satisfy the Type 1- Vertical Stiffness Irregularity criterion whereby the lateral stiffness of the SFRS at a given storey must not be less than 70% of the stiffness of any adjacent storey. Hence the configurations of the second storey shear walls were altered to increase their lateral stiffness (shear resistance).

The final wall configurations were as follows: all the shear walls had a sheathing thickness of 0.76 mm (0.30") with 75 mm (3") screw fastener spacings at the first storey and 100 mm (4") spacings at the second storey. Table 4.9 lists the final design shear resistances.

Table 4.9 Final shear wall design

Design Shear Resistance, S_r (kN/m)				
Storey	North	South	East	West
2^{nd}/Roof	10.03	10.03	10.03	10.03
1^{st}	13.92	13.92	13.92	13.92

4.5 Capacity-based Design

Having designed the shear walls to resist the expected lateral forces, the remaining elements of the seismic force resisting system (SFRS) had to be designed. Capacity-based design principles were employed to ensure the other elements of the SFRS were able to remain elastic and undamaged during a design level seismic level. This was achieved by applying the overstrength factor to estimate the maximum probable forces that would occur, thereby ensuring that elements were able to resist these expected forces.

The double chord studs (DSC) were designed using the same procedure outlined in Section 2.2. The total compression force in a DCS was the sum of the compressive force transferred from the probable shear capacity of the shear wall plus the gravity load applied to the tributary area of the DCS. The nominal yield resistances and overstrength factor (1.34) determined in Chapter 3 were used to determine the probable shear capacities of the shear walls (Equations 4-11 & 4-12)

$$C_s = {}^{S_y\,h}\!/_{b} \times b \times \text{overstrength} \tag{4-11}$$

$$C_g = (D + 0.5L + 0.25S) \times T.A. \tag{4-12}$$

where,

C_s = Compression force due to shear (kN)

C_g= Compression force due to gravity (kN)

S_y= Nominal yield resistance (kN/m)(Table 3.13, Chapter 3)

h = Height of test wall (m)

b = Width of specified shear wall (m)

Overstrength factor = 1.34 (Section 3.3.4, Chapter 3)

$T.A.$ = Tributary area of DCS (m^2)

The total compression force on the DSCs of shear walls shown in Figure 4.3 are summarized in Table 4.10. Also included in the table are the moments due to eccentric loading, $\overline{M_x}$ and $\overline{M_y}$ which were calculated using Equations 2.5 & 2-6 of Section 2.2. It is important to note that the recommended value of a quarter (25%) of the nominal web dimension was used in the calculation of $\overline{M_x}$.

Table 4.10 Probable compressive forces and moments on double chord studs

Storey	Wall Location[1]	S_y (kN/m)	Compression Shear (kN)	Gravity Load (kN)	Compression Total (kN)	M_x (kNm)	M_y (kNm)
2nd	A4:A6	14.33	46.84	3.42	50.26	1.81	0.01
	A7:A8	14.33	46.84	3.42	50.26	1.81	0.01
	B10:D10	14.33	46.84	0.60	47.43	1.79	0.00
	F10:H10	14.33	46.84	0.60	47.43	1.79	0.00
	H1:H2	14.33	46.84	2.91	49.75	1.81	0.01
	H3:H5	14.33	46.84	2.91	49.75	1.81	0.01
	H9:H10	14.33	46.84	3.42	50.26	1.81	0.01
	C1:E1	14.33	46.84	0.60	47.43	1.79	0.00
	G1:H1	14.33	46.84	0.60	47.43	1.79	0.00
1st	A4:A6	19.88	65.01	8.70	123.97	2.57	0.05
	A7:A8	19.88	65.01	8.70	123.97	2.57	0.05
	B10:D10	19.88	65.01	1.51	113.96	2.49	0.01
	F10:H10	19.88	65.01	1.51	113.96	2.49	0.01
	H1:H2	19.88	65.01	7.40	122.16	2.56	0.04
	H3:H5	19.88	65.01	7.40	122.16	2.56	0.04
	H9:H10	19.88	65.01	8.70	123.97	2.57	0.05
	C1:E1	19.88	65.01	1.51	113.96	2.49	0.01
	G1:H1	19.88	65.01	1.51	113.96	2.49	0.01

[1] Refer to building floor plan (Figure 4.3) for shear wall locations

The same dimension chord studs used in the CFS-NEES project building plan were maintained for the representative building design herein. The nominal dimensions of the 'C' section stud were 152.4 mm x 41.3 mm x 12.7 mm (6" x 1-5/8" x 1/2") of the web, flange and lip respectively. The compressive and flexural resistances were determined as prescribed by CSA S136-07 for typical chord stud thicknesses and are summarized in Table 4.11. The DCS thickness for each storey was selected based on the interaction equations specified in Clause C5.2.2 of the CSA S136 and the procedure is outlined in Section 2.2 of Chapter 2. Only the stability equation was considered since it produced a higher ratio that governed the design (Equation 2-1). The resulting nominal thicknesses selected were 1.37 mm (0.054") and 1.73 mm (0.068") for the second and first storey respectively (Table 4.12). All studs were of 340 MPa (50 ksi) nominal grade (*ASTM A653 (2008)*).

Table 4.11 Factored resistances of double chord studs[1]

Nominal Thickness	**Compressive Resistance**	**Moment Resistance**	
(mm)	$\phi_c P_{no}$ (kN)	$\phi_b M_{nx}$ (kNm)	$\phi_b M_{ny}$ (kNm)
1.09 (0.043")	73.23	4.82	0.87
1.37 (0.054")	125.58	8.44	1.50
1.73 (0.068")	175.96	11.39	2.01
2.46 (0.097")	291.03	16.86	2.89

[1] Calculations were according to CSA-S136 Standard (2007): resistance factors $\phi_c = \phi_b = 1.0$; end conditions $K_x=K_y=K_t=1.0$; buckling lengths L_x= 2440mm, $L_y=L_z$=610mm

$$\frac{\bar{P}}{\emptyset_c P_n} + \frac{C_{mx}\overline{M_x}}{\emptyset_b M_{nx}\alpha_x} + \frac{C_{my}\overline{M_y}}{\emptyset_b M_{ny}\alpha_y} \quad (2\text{-}1)$$

where,

$\overline{\mathrm{P}}$ = Probable/Expected compression force

$\overline{\mathrm{M_x}}$, $\overline{\mathrm{M_y}}$ = Moments due to eccentric loading

$\emptyset_c$ = Compressive resistance factor, 1.00 (for capacity based design)

$\emptyset_b$ = Flexural resistance factor, 1.00 (for capacity based design)

C_{mx}, C_{my} = Coefficients of equivalent uniform bending moments, 0.85

P_n = Nominal compressive resistance (accounting for overall buckling modes)

M_{nx}, M_{ny} = Effective moment resistance (calculated with F_y for strength & F_c for stability interaction)

α_x, α_y = Second order amplification factors

Table 4.12 Selection of DCS thickness based on stability consideration

Storey	Wall Location[1]	DCS thickness (mm)	Axial Ratio	M_x Ratio	M_y Ratio	Overall Ratio (≤1.0)
2nd	A4:A6	1.37	0.40	0.21	0.01	0.62
	A7:A8	1.37	0.40	0.21	0.01	0.62
	C11:F11	1.37	0.38	0.21	0.00	0.59
	H11:J11	1.37	0.38	0.21	0.00	0.59
	J1:J2	1.37	0.40	0.21	0.01	0.62
	J3:J5	1.37	0.40	0.21	0.01	0.62
	J10:J11	1.37	0.40	0.21	0.01	0.62
	B1:D1	1.37	0.38	0.21	0.00	0.59
	E1:G1	1.37	0.38	0.21	0.00	0.59
1st	A4:A6	1.73	0.70	0.23	0.02	0.96
	A7:A8	1.73	0.70	0.23	0.02	0.96
	C11:F11	1.73	0.65	0.22	0.00	0.87
	H11:J11	1.73	0.65	0.22	0.00	0.87
	J1:J2	1.73	0.69	0.22	0.02	0.94
	J3:J5	1.73	0.69	0.22	0.02	0.94
	J10:J11	1.73	0.70	0.23	0.02	0.96
	B1:D1	1.73	0.65	0.22	0.00	0.87
	I1:J1	1.73	0.65	0.22	0.00	0.87

[1] Refer to building floor plan (Figure 4.3) for shear wall locations

4.6 Inelastic Drift and P-Δ Effects

The inelastic drifts of the shear walls were determined to ensure they conformed to the 2% seismic drift limit recommended in Chapter 3 and to verify whether P-delta effects needed to be considered. The AISI S213 Standard provides a method for calculating the elastic deflection, Δ, of steel sheathed CFS framed shear walls (Equation 4-13). The ductility and overstrength force modification factors used to calculate the design base shear were applied to the elastic deflection to estimate the inelastic deflection (Equation 4-14). A value of 3.15 mm (0.124”) was used for the vertical deformation of the hold-down, δ_v,and was obtained from the Simpson Strong-Tie brochure (*2010*) for the S/HD10S hold-downs used for the shear wall test specimens. This value was consistent with that used by Shamim & Rogers (*2010*). The shear wall height of 2440 mm (8') was used to obtain the inelastic drift. The storey height of 2740 mm (9') was not used since the 300 mm (12") floor was assumed as a rigid diaphragm with no out-of-plane flexibility and no perimeter joist shear deformation (Shamim & Rogers *(2011)*). All the resulting inelastic drifts of the shear walls did not exceed the 2% drift limit (Table 4.12).

$$\Delta = \frac{2\upsilon h^3}{3E_sA_cb} + \omega_1\omega_2\frac{\upsilon h}{\rho G t_{sheathing}} + \omega_1^{5/4}\omega_2\omega_3\omega_4\left(\frac{\upsilon}{\beta}\right) + \frac{h}{b}\delta_\upsilon \qquad (4\text{-}13)$$

$$\Delta_{mx} = \Delta R_d R_o \qquad (4\text{-}14)$$

where,

A_c = gross cross-sectional area of double chord stud (mm^2)

b = width of shear wall (mm)

E_s = Modulus of Elasticity of steel, 203000 MPa

G = Shear modulus of sheathing material, 78000 MPa

h = wall height (mm)

s = maximum fastener spacing at sheathing panel edge (mm)

$t_{sheathing}$ = nominal panel thickness (mm)

t_{stud} = framing thickness (mm)

υ = shear demand (shear flow) , *V/b* ,(N/mm)

β = 1.45 ($t_{sheathing}/0.457$) for sheet steel (N/mm$^{1.5}$)

δ_υ = vertical deformation of hold-down (mm)

ρ = 0.075 ($t_{sheathing}/0.457$) for sheet steel

ω_1 = s/152.4 (mm)

ω_2 = $0.838/t_{stud}$

$$\omega_3 = \sqrt{\frac{\left({h}/{b}\right)}{2}}$$

$$\omega_4 = \sqrt{\frac{227.5}{F_y}}\ , where\ F_y = 350\ MPa\ for\ 54 mils\ nominal\ steel\ thickness\ and\ higher$$

Δ_{mx} = maximum inelastic deflection (mm)

Table 4.13 Determination of inelastic drift

Storey	Wall Location	Stud THK (mm)	Sheathing THK. (mm)	Spacing (mm)	b (mm)	A_c (mm^2)	v (N/mm)	ω_1	ω_2	ω_3	ω_4	ρ	β	Δ (mm)	Δ_{mx} (mm)	Drift (%)
2nd	A4:A6	1.372	0.762	100.00	2438	850	5.45	0.656	0.611	0.707	0.818	0.125	2.418	4.49	11.69	0.48
	A7:A8	1.372	0.762	100.00	3658	850	5.45	0.656	0.611	0.578	0.818	0.125	2.418	3.31	8.59	0.35
	B10:D10	1.372	0.762	100.00	3404	850	6.34	0.656	0.611	0.599	0.818	0.125	2.418	3.69	9.59	0.39
	F10:H10	1.372	0.762	100.00	1829	850	6.34	0.656	0.611	0.817	0.818	0.125	2.418	5.91	15.37	0.63
	H1:H2	1.372	0.762	100.00	1219	850	6.54	0.656	0.611	1.000	0.818	0.125	2.418	8.34	21.67	0.89
	H3:H5	1.372	0.762	100.00	1626	850	6.54	0.656	0.611	0.866	0.818	0.125	2.418	6.56	17.05	0.70
	H9:H10	1.372	0.762	100.00	2235	850	6.54	0.656	0.611	0.739	0.818	0.125	2.418	5.09	13.24	0.54
	C1:E1	1.372	0.762	100.00	3556	850	6.95	0.656	0.611	0.586	0.818	0.125	2.418	3.71	9.65	0.40
	G1:H1	1.372	0.762	100.00	1219	850	6.95	0.656	0.611	1.000	0.818	0.125	2.418	8.47	22.01	0.90
1st	A4:A6	1.727	0.762	75.00	2438	1183	10.33	0.492	0.485	0.707	0.818	0.125	2.418	4.69	12.20	0.50
	A7:A8	1.727	0.762	75.00	3658	1183	10.33	0.492	0.485	0.578	0.818	0.125	2.418	3.47	9.03	0.37
	B10:D10	1.727	0.762	75.00	3404	1183	12.04	0.492	0.485	0.599	0.818	0.125	2.418	3.89	10.11	0.41
	F10:H10	1.727	0.762	75.00	1829	1183	12.04	0.492	0.485	0.817	0.818	0.125	2.418	6.18	16.07	0.66
	H1:H2	1.727	0.762	75.00	1219	1183	12.40	0.492	0.485	1.000	0.818	0.125	2.418	8.68	22.58	0.93
	H3:H5	1.727	0.762	75.00	1626	1183	12.40	0.492	0.485	0.866	0.818	0.125	2.418	6.85	17.82	0.73
	H9:H10	1.727	0.762	75.00	2235	1183	12.40	0.492	0.485	0.739	0.818	0.125	2.418	5.34	13.89	0.57
	C1:E1	1.727	0.762	75.00	3556	1183	13.19	0.492	0.485	0.586	0.818	0.125	2.418	3.93	10.21	0.42
	G1:H1	1.727	0.762	75.00	1219	1183	13.19	0.492	0.485	1.000	0.818	0.125	2.418	8.84	22.98	0.94

[1] Refer to building floor plan (Figure 4.3) for shear wall locations

4.7 P-Δ Effects

The Structural Commentary J of the 2010 NBCC provides a procedure whereby second order P-delta effects can be estimated. The stability factor, θ_x,is the additional load due to second order effects and is calculated with Equation 4-15. If the stability factor at each storey was greater than 0.1 then P-delta effects must be included in the design whereby the seismic-induced forces and moments were multiplied by the amplification factor of (1 + θ_x). A live load reduction factor specified in Clause 4.1.5.9 of the 2010 NBCC was applied to load case (Equation 4-1) if the tributary area of the floor above was greater than 20 m^2 (Equation 4-16). The resulting stability factor for each storey was less than 0.1, thus P-delta effects were ignored (Table 4.14).

$$\theta_x = \frac{\sum_{i=1}^{n} W_i}{R_o \sum_{i=1}^{n} F_i} \frac{\Delta_{mx}}{h_s} \qquad (4\text{-}15)$$

where,

θ_x = Stability factor at storey x ,(rad)

W_i= Factored load at storey under consideration (Eq. 4-1), (kN)

Δ_{mx} = Maximum inelastic deflection, (mm)

R_o = Overstrength-related force modification factor, 1.3

F_i = Seismic force at storey under consideration, (kN)

h_s = interstorey height, (mm)

$$LLRF = 0.3 + \sqrt{\frac{9.8}{A}} \qquad (4\text{-}16)$$

where,

$LLRF$ = Live load reduction factor (< 1.0)

A= Cumulative tributary area of storey including storeys above, (m^2)

Table 4.14 Calculation of storey stability factor

Storey	δ_{max} (mm)	A (m^2)	LLRF	Gravity Load (kPa)	W_i (kN)	W_{iCum}	Θ_x
2nd/Roof	22.01	106.27	-	1.60	170	170	0.02
1st	22.98	212.54	0.51	3.49	371	541	0.03

4.8 Non-Linear Dynamic Analysis

This section describes the non-linear dynamic analysis that was carried out on the two-storey representative building designed in the previous section. The OpenSees software (*McKenna et al. 2006*) was utilized for modeling the representative building and performing non-linear time history dynamic analysis following the FEMA P695 methodology.

4.8.1 Description of Dynamic Model

The overall task of modeling the representative building was undertaken by the author's colleague, Shamim (*Shamim & Rogers, 2012*). The 3D model used was the product of extensive iterative numerical modeling. The results of past research programs on steel sheathed CFS shear walls, including shake table testing (*Shamim et al. 2010*) and displacement-based monotonic and reserved-cyclic testing (*Balh & Rogers 2010, Ong-Tone & Rogers 2009*) were used to calibrate the model elements, make appropriate assumptions, and improve the accuracy of the numerical model/models. A schematic of the east elevation of the building model used is shown in Figure 4.4.

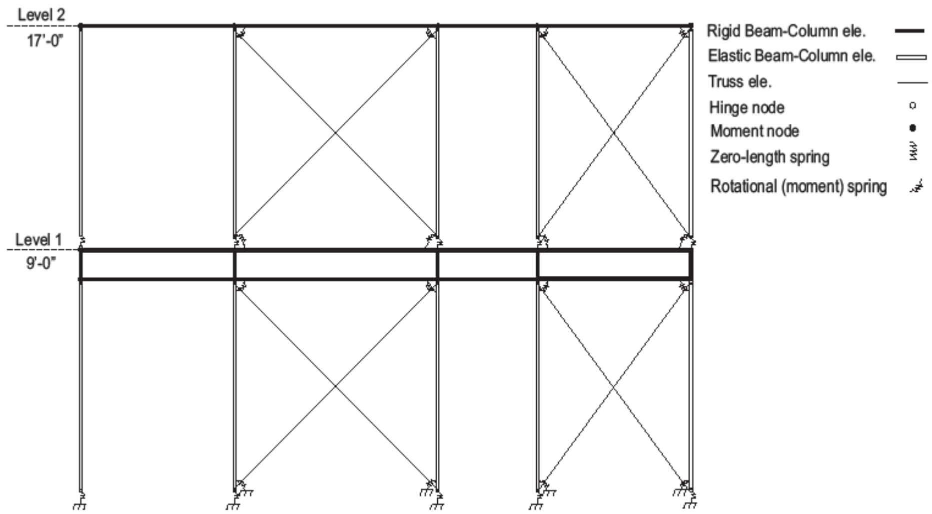

Figure 4.4 Schematic of east elevation of representative building model (*Shamim, 2011*)

The elements used to create the building model were representative of the properties and behaviour of the relevant structural components. Elastic beam-column elements with linear behaviour were used to represent stud columns. The roof and floor were considered rigid diaphragms with no out of plane flexibility and were modeled with rigid beam-column elements. Diagonal Truss elements with Pinching04 material (*Lowes et al. 2004*) were used to model the shear walls (steel sheathing and screw fastener connections). Pinching04 material, once calibrated, is able to represent the non-linear force-deformation hysteretic response of the shear wall (stiffness degradation, pinching, and strength degradation). Zero-length spring elements with linear elastic stiffness were used to model the hold-down anchor rods. Rotational (Moment) spring elements were used to represent the additional lateral stiffness of the bare CFS frame due to the blocking reinforcement.

The resulting stability factors calculated in accordance with the 2010 NBCC, allowed for the omission of P-delta effects (Section 4.7). Hence, the building model did not include considerations for integrating P-delta effects. The advantage of excluding P-delta effects was that data processing during the IDA procedure was less demanding. The disadvantage was that second order effects, which can have significant implications on the model building response (Section 4.8.3) and hence the concluding evaluation of the building performance (Section 4.8.6), were not accounted for. The final representative building models being used by Shamim (*Shamim & Rogers, 2012*) includes P-delta effects, thus the resulting building responses following IDA analyses are quite accurate. Detailed information regarding the numerical modeling of steel sheathing CFS framed shear walls is presented in the report by Shamim (*2012*).

4.8.2 Ground motion records

FEMA P695 lists ground motion records that are part of the Far-Field record set used specifically for the purpose of collapse evaluation of structures located away from active faults (*Table A-4A, FEMA P695 (2009)*). The record set consisted of forty-four horizontal ground motion records (22 horizontal component pairs) which were obtained from the PEER Ground Motion Database (*PEER, 2011*) for the purpose of Incremental Dynamic Analysis (IDA) (Table 4.15). Before the representative building was subjected to the ground motion records, the records needed to be scaled to UHS for Vancouver. The first stage of the scaling process was to find the median spectrum of the 44 record set (Figure 4.5). The median spectrum was then matched to the design response spectrum of Vancouver (Class C soil) at the fundamental period of the building by applying a scaling factor (Figure 4.6). The scale factor was then applied to all 44 ground motion records.

Table 4.15 Summary of far-field record used for FEMA P695

ID No.	Record Seq. No.	M	Name	Component 1	Component 2
1	953	6.7	Northridge	NORTHR/MUL009	NORTHR/MUL279
2	960	6.7	Northridge	NORTHR/LOS000	NORTHR/LOS270
3	1602	7.1	Duzce, Turkey	DUZCE/BOL000	DUZCE/BOL090
4	1787	7.1	Hector Mine	HECTOR/HEC000	HECTOR/HEC090
5	169	6.5	Imperial Valley	IMPVALL/H-DLT262	IMPVALL/H-DLT352
6	174	6.5	Imperial Valley	IMPVALL/H-E11140	IMPVALL/H-E11230
7	1111	6.9	Kobe, Japan	KOBE/NIS000	KOBE/NIS090
8	1116	6.9	Kobe, Japan	KOBE/SHI000	KOBE/SHI090
9	1158	7.5	Kocaeli, Turkey	KOCAELI/DZC180	KOCAELI/DZC270
10	1148	7.5	Kocaeli, Turkey	KOCAELI/ARC000	KOCAELI/ARC090
11	900	7.3	Landers	LANDERS/YER270	LANDERS/YER360
12	848	7.3	Landers	LANDERS/CLW-LN	LANDERS/CLW-TR
13	752	6.9	Loma Prieta	LOMAP/CAP000	LOMAP/CAP090
14	767	6.9	Loma Prieta	LOMAP/G03000	LOMAP/G03090
15	1633		Manjil, Iran	MANJIL/ABBAR-L	MANJIL/ABBAR-T
16	1633	6.5	Superstition Hills	SUPERST/B-ICC000	SUPERST/B-ICC090
17	721	6.5	Superstition Hills	SUPERST/B-POE270	SUPERST/B-POE360
18	725	7.0	Cape Mendocino	CAPEMEND/RIO270	CAPEMEND/RIO360
19	1244	7.6	Chi-Chi, Taiwan	CHICHI/HY101E	CHICHI/CHY101-N
20	1485		Chi-Chi, Taiwan	CHIHI/TCU045-E	CHIHI/TCU045-N
21	68	6.6	San Fernando	SFERN/PEL090	SFERN/PEL180
22	125	6.5	Friuli, Italy	FRIULI/A-TMZ000	FRIULI/A-TMZ270

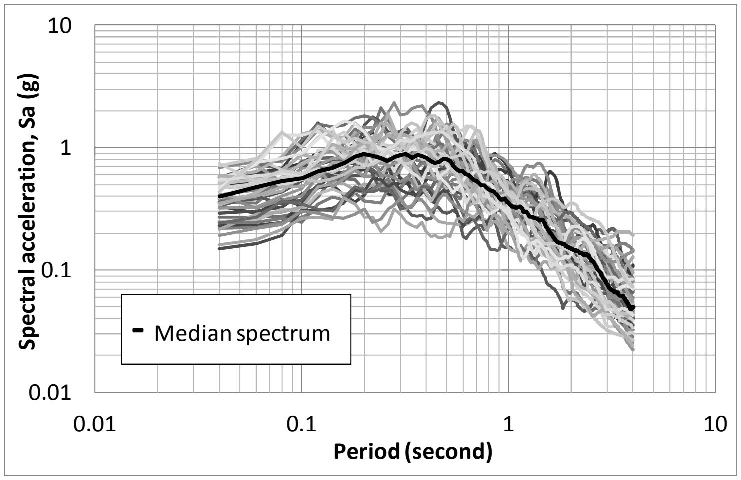

Figure 4.5 Response spectra and median spectrum of 44 normalized ground motion records

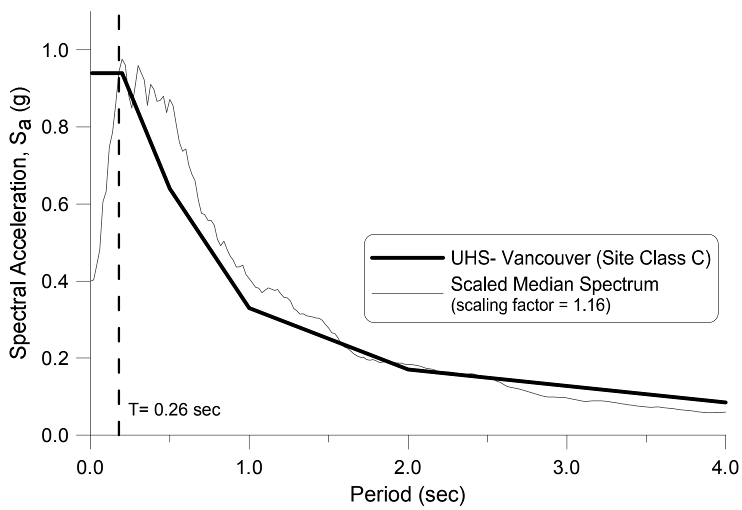

Figure 4.6 Median spectra scaled to design response spectrum (Vancouver) at building fundamental period (T=0.26s)

4.8.3 Incremental Dynamic Analysis

Once the representative building was designed for the location (Vancouver, Class C soil), the 3D model was subjected to the 44 ground motion records in each principal direction. Incremental dynamic analysis (IDA) was carried out whereby all the ground motion records that were previously scaled by the scale factor (1.16), were scaled from 0.2 to 3.0 and subjected to the building model at increasing intensities until failure (2% drift limit). The maximum inter-storey drifts at each scaling factor for a given ground motion was plotted and a suite of IDA curves where produced (Figure 4.7).

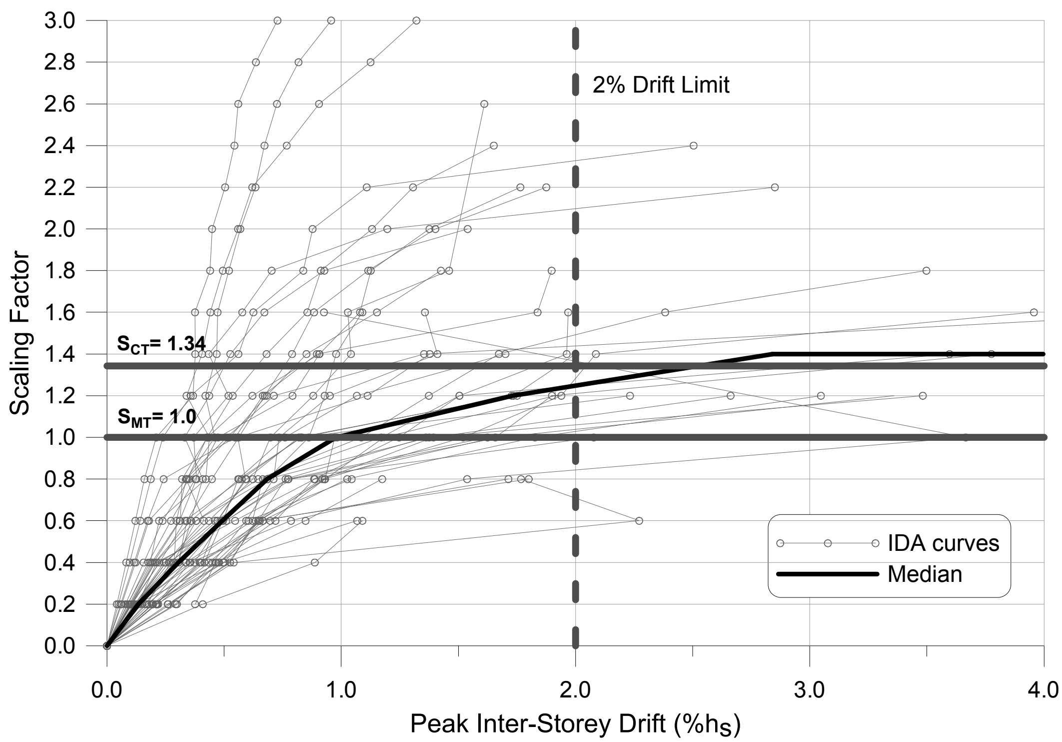

Figure 4.7 IDA curves for 44 ground motion records for the two-storey representative building

The FEMA P695 methodology requires that certain parameters be determined for the performance evaluation of the building. One of these parameters is the collapse margin ratio, *CMR*, which characterizes the collapse safety of a structure. The *CMR* was calculated with Equation 4-17. The median collapse capacity, S_{CT}, is defined as the intensity at which 50% of the ground motion records cause failure. The Maximum Considered Earthquake (*MCE*) ground motion intensity, S_{MT}, was equal to 1.0 since all the ground motion records were previously scaled to the design response spectrum of Vancouver (Class C soil). Hence, *CMR* was equal to S_{CT} and was interpreted as follows: at a scaling factor of 1.34, 50% of the ground motion records caused failure to the representative building model.

$$CMR = \frac{S_{CT}}{S_{MT}} \tag{4-17}$$

where,

CMR = Collapse margin ratio

S_{CT}= Median collapse capacity, 1.34

S_{MT}= Maximum Consider Earthquake ground motion intensity, 1.0

4.8.4 Pushover Analysis

The Spectral Shape Factor (*SSF*) is another parameters used in the performance evaluation of the building model. The *SSF* is dependent on the fundamental period and the period-based ductility of the building model obtained from a pushover analyse. Pushover analysis involved applying a unit force to the building model which was distributed at each storey based on the expected seismic force distribution listed in Table 4.5 (Figure 4.8). A ramp loading protocol was then applied to the structure to obtain force-displacement curve at the roof level which describes the pushover curve (Figure 4.9).

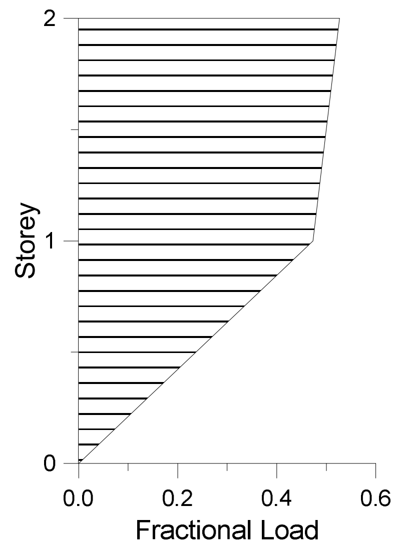

Figure 4.8 Unit force distribution for two-storey pushover analysis

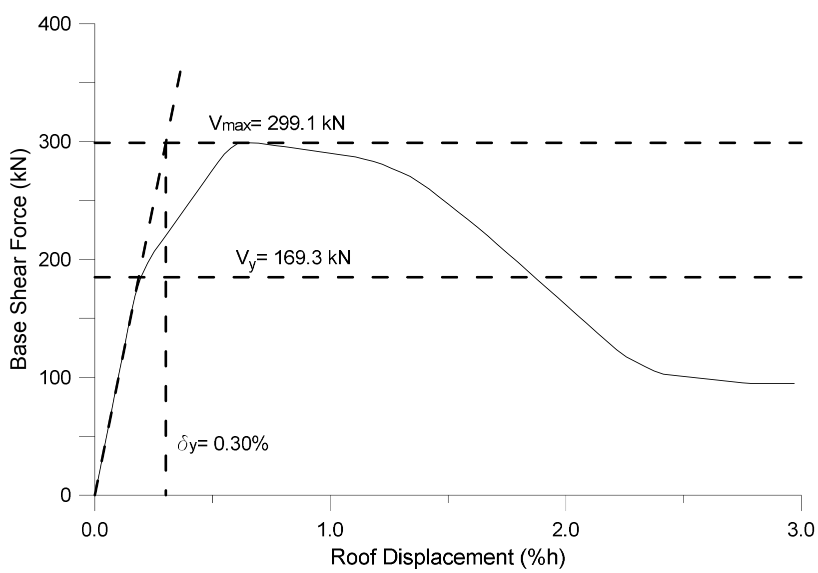

Figure 4.9 Pushover curve of two-storey building model

The pushover curve was then used to obtain the period-based ductility, μ_T, and the overstrength factor, Ω, of the building model (Equations 4-17 & 4-18).

$$\mu_T = \frac{\delta_u}{\delta_y} \tag{4-17}$$

$$\Omega = \frac{V_{max}}{V} \tag{4-18}$$

where,

μ_T = Period-based ductility of the structure

δ_u= Ultimate drift of structure, (rad)

δ_y = Yield drift of structure, (rad)

Ω= Overstrength factor of building model

V_{max} = Maximum shear strength from pushover curve, (kN)

V= Design base shear force, (kN)

The ultimate drift, δ_u, is defined as the drift at 2% drift limit. The yield drift, δ_y, corresponds to the drift where the elastic shear force portion of the pushover curve meet the maximum shear force, V_{max}. A value of 6.67 was determined for the period-based ductility. The overstrength factor is defined as the ratio of the maximum shear strength to the design/yield base shear force and is used to evaluate the reserve strength of a system. A value of 1.77 was calculated for the building overstrength which is greater than the overstrength value of Ω_o=1.4 recommended in Section 3.3.4. Though the FEMA P695 requirement was not met whereby the system overstrength factor, Ω_o, for use in design should not be less than the overstrength obtained from pushover analysis, only one archetype was involved in the author's study. A comprehensive study is being undertaken by Shamim (*Shamim & Rogers, 2012*) whereby many archetypes are involved.

4.8.5 Determination of Total Collapse Uncertainty

The total uncertainty associated with the FEMA P695 methodology is quantified by the total system collapse uncertainty, β_{TOT}, and is calculated using Equation 4-19.

$$\beta_{TOT} = \sqrt{\beta_{RTR}^2 + \beta_{DR}^2 + \beta_{TD}^2 + \beta_{MDL}^2} \tag{4-19}$$

where,

β_{TOT} = Total system collapse uncertainty

β_{RTR}= Record-to-record collapse uncertainty

β_{DR} = Design requirements related collapse uncertainty

β_{TD}= Test data-related collapse uncertainty

β_{MDL} = Modeling-related collapse uncertainty

The four components used in the calculation where uncertainties exist are: the uncertainty due the variability of the ground motion records, β_{RTR}, the uncertainty within the design requirements/procedure, β_{DR}, the uncertainty related to the test data, β_{TD}, and the uncertainty related to numerical modeling, β_{MDL}. FEMA P695 rates each uncertainty into four categories: superior (β=0.10), good (β=0.20), fair (β=0.35), or poor (β=0.50). FEMA P695 specifies β_{RTR}= 0.4 for systems with a period-based ductility, μ_T≥ 3.0.

The design requirements-related uncertainty was assigned an overall Good rating of value 0.20. The design procedure used was in accordance to the already established 2010 NBCC and AISI S213 standard which are used in practice and incorporates several design safety factors.

The test data-related uncertainty was assigned a rating of Good rating of value 0.20. Although the author's test program did not incorporate many configurations, the test data of the overall research program on steel sheathed shear walls was quite comprehensive (Balh (*2010*), El-Saloussy (*2010*), Ong-Tone (*2009*), Shamim (*2011*)). Also, gravity load effects which is one of general testing issues specified in Section 3.3.2 of FEMA P695 (*FEMA, 2009*) was considered in the test program described herein.

The building model provided by Shamim (*2011*), used for the non-linear time history analysis was robust with a high level of accuracy. The numerical modeling incorporated the past research (Balh (*2010*), El-Saloussy (*2010*), Ong-Tone (*2009*)), the author's research, and dynamic shake table testing (Shamim (*2010*) on steel sheathed shear walls. A Good rating of value 0.20 was assigned.

The total system collapse uncertainty of β_{TOT}=0.529 was calculated from the assigned ratings above. The resulting value of β_{TOT} was used as the standard deviation of the log-normal distribution of the collapse probabilities and takes into account the inherent uncertainties during the FEMA P695 methodology.

4.8.6 Evaluation of the Structure

The results from the IDA were used to determine the probability of collapse, which is defined as the percentage of the total ground motion records that cause structural collapse based on the 2% inter-storey drift failure criterion for a given scaling factor. A log-normal distribution was fitted to the probability data points to produce a fragility curve with β_{TOT} as the standard deviation (Figure 4.10). The spectral shape factor (*SSF*) determined from the pushover analysis was applied to the original scaling factors to increase the range whereby structure collapse takes place. The adjusted probability curve resulting from the preceding steps is shown in Figure 4.21.

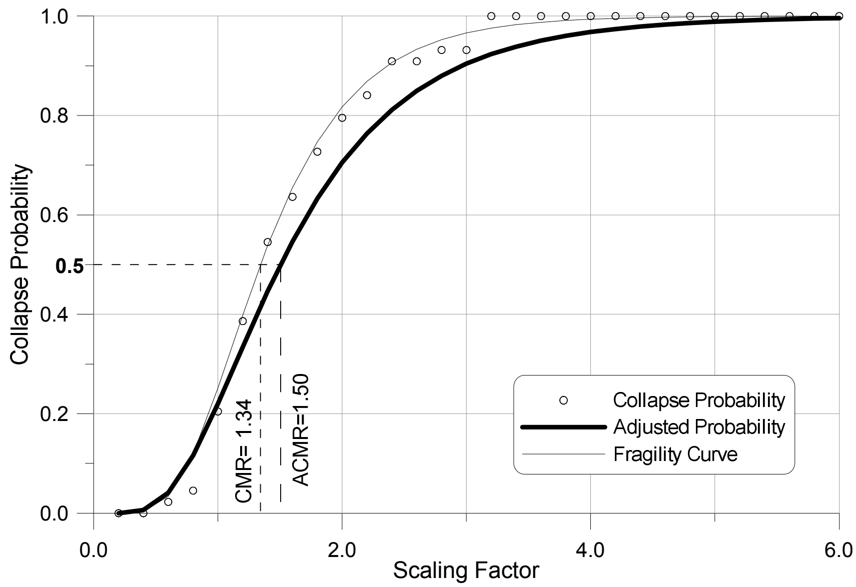

Figure 4.10 Fragility curve of two-storey building

An adjusted collapse margin ratio (*ACMR*) was identified from the adjusted probability curve and is defined as the collapse margin ratio (*CMR*) adjusted using the spectral shape factor (*SSF*) (Equation 4-20). The performance evaluation of a structure is based on the acceptable values of *ACMR* listed in Table 7-3 of FEMA P695 (*2009*) for the determined total system collapse uncertainty of that structure. To validate the test-based R-values, the *ACMR* must be greater than value of $ACMR_{20\%}$ listed (Equation 4-21). The *ACMR* obtained for the two storey building was 1.50 which slightly less than the allowable limit ($ACMR_{20\%}$=1.56) required by FEMA. All relevant parameters used in the performance evaluation of the structure are summarized in Table 4.16. Work is been carried out by Shamim & Rogers (*2012*) to improve resulting ACMR values of the full set of archetypes used to validate the proposed seismic force modification factors,R_d and R_o, and design procedure.

$$ACMR = SSF \times CMR \tag{4-20}$$

$$ACMR \geq ACMR_{20\%} \tag{4-21}$$

Table 4.16 Summary of performance evaluation results

S_{MT}	S_{CT}	CMR	μ_T	SSF	β_{TOT}	$ACMR$	$ACMR_{20\%}$	Ω
1.0	1.34	1.34	6.67	1.12	0.529	1.50	1.56	1.77

Chapter 5- Conclusions and Recommendations

5.1 Conclusions

In previous research a limited number of shear walls displayed unfavourable damage of the chord-studs due to twisting deformations and by local buckling. Also, the steel sheathed shear walls of these previous research programs were only lateral loaded (*Balh & Rogers 2010; Ong-Tone & Rogers 2009).* As such, the cold-formed steel framed/ steel sheathed shear wall research program at McGill University was expanded to address the above problems and add more comprehensive data to the existing database.

During the summer of 2010, a total of 14 single-storey steel sheathed shear walls (8 wall configurations) were tested under combined gravity and lateral loading. The configurations varied in framing thickness, sheathing thickness, and screw fastener spacings. The shear walls were constructed with blocked stud members with the intent of eliminating the occurrence of twisting deformations. The chord-studs of the test specimens were selected using capacity based design principles such that the sheathing screw fastener connections would act as the “fuse” element and dissipate energy through inelastic deformations; the other elements were to remain elastic and undamaged. In previous research only the probable/expected compression force was used to select the chord-stud. The author included moments due to eccentric loading into the chord-stud design; hence the chord-stud was designed as a beam-column using the interaction equations specified in the CSA-S136 Specification (*2007*).

The shear walls were subjected to monotonic and CUREE reversed-cyclic loading protocols. As required, the majority of the observed failures were to the sheathing-to-framing connections which consisted of sheathing bearing failures, screw fastener pull-out, screw fastener pull-through, and sheathing tear-out. Distortions of the flange-lip elements were observed in walls with smaller screw spacings, especially walls with 50 mm spacings, due to the high horizontal component of the sheathing tension field that developed at large displacements. These deformations did not compromise the loading carrying capacity of the chord-studs.

The test results were analysed using the Equivalent Energy Elastic Plastic (EEEP) method which provided an equivalent bi-linear elastic-plastic curve from which relevant values of shear resistances, displacements, elastic stiffness, ductility and energy dissipation were obtained for each shear wall.

The shear resistance of the walls was dependent on the wall configuration. As expected the shear resistance was higher for walls with smaller fastener spacing and thicker steel sheathing. A comparison of test results was made between the blocked walls tested by the author and of nominally identical conventional walls tested in previous research programs (*Balh & Rogers 2010; Ong-Tone & Rogers 2009*) to deduce the effects of the blocking reinforcement on the wall's behaviour and performance. The blocked walls achieved nominal design resistance values 1.37 to 1.80 times higher than their nominally identical counterparts. The blocked walls also achieved higher levels of energy dissipation. There was no conclusive pattern observed for the unit elastic stiffness; all the reversed cyclic tests resulted in increases of stiffness yet this was not the case for with the comparison of the monotonic test results. There was a general decrease in ductility and displacement at 80% post-peak of the blocked walls.

Nominal shear resistance values for each shear wall configuration were determined using thickness and tensile stress modification factors obtained from coupon tests. A resistance factor, $\phi = 0.7$, was determined for use in ultimate limit states design. Factors of safety of 1.91 and 2.68 were determined for limit states design (LSD) and allowable stress design (ASD) respectively. An overstrength factor of 1.4 was recommended for capacity based design. Finally, 'test-based' seismic force modification factors for ductility, $R_d = 2.0$, and for overstrength, $R_o = 1.3$, were recommended.

In order to validate the 'test-based' R-values, non-linear time-history dynamic analysis was carried out to evaluate the seismic performance of a two storey building following a methodology adopted from FEMA P695. The OpenSees software was utilized to model the representative building and to perform non-linear dynamic analysis. Thirty-eight ground motions were subjected to the building at different intensities/scale factors as part of the FEMA P695 incremental dynamic analysis (IDA) procedure. The resulting collapse probabilities from the IDA results and pushover analysis were used to produce the fragility curve of the building. The resulting adjusted collapse margin ratio (*ACMR*=1.50), needed to validate the 'test-based' R-values, was slightly less than the acceptable value ($ACMR_{20\%}$ =1.56) required by FEMA.

5.2 Recommendations for Future Study

To complete the validation process of the design procedure and *R*-values, dynamic shake table testing must be incorporated (*Shamim & Rogers, 2011*) and a wider range of archetypes which includes different seismic regions, building occupancy types, and building heights must be modeled and subjected to non-linear time history dynamic testing. At present, work is been carried out by Shamim & Rogers (*2012*) to improve resulting ACMR values and to finalise the validation process. The contribution from gypsum sheathing, which is used extensively in interior walls, can be introduced into the numerical model to improve the building performance under seismic loading.

The blocked shear walls tested by the author exhibited reduced ductile behaviour compared with their unblocked counterparts and unfavourable rates of strength degradation. It is recommended that a hybrid shear wall system be investigated whereby strapped braces can be incorporated into the steel sheathed shear wall system to improve the inelastic post peak behaviour, whereby increasing the ductility and decreasing the rate of strength degradation to more acceptable levels.

References

American Iron and Steel Institute (AISI). 2007. “AISI S213-07, North American Standard for Cold-Formed Steel Framing- Lateral Design”. Washington, DC, USA.

American Iron and Steel Institute (AISI). 2007. “AISI S230-07, North American Standard for Cold-Formed Steel Framing- Prescriptive Method for One and Two Family Dwelling 2007 Edition”. Washington, DC, USA.

American Society for Testing and Materials, A193. 2008. “Standard Specification for Alloy-Steel and Stainless Steel Bolting Materials for High Temperature or High Pressure Service and Other Special Purpose Applications”. West Conshohocken, PA, USA.

American Society for Testing and Materials, A370. 2009. “Standard test Methods and Definitions for Mechanical Testing of Steel Products”. West Conshohocken, PA, USA.

American Society for Testing and Materials, A653. 2008. “Standard Specification for Steel sheet, Zinc-Coated (Galvanized) or Zinc-Iron Alloy-Coated (Galvannealed by Hot-Dip Process”. West Conshohocken, PA, USA.

American Society for Testing and Materials, E2126. 2007. “Standard Test Methods for Cyclic (Reversed) Load Test for Shear Resistance of Vertical Elements of the Lateral Force Resisting Systems for Buildings”. ASTM International, West Conshohocken, PA, USA.

Balh, N. 2010. “Development of Canadian Seismic Design Provisions for Steel Sheathed Shear Walls”. M.Eng. thesis. Department of Civil Engineering and Applied Mechanics, McGill University. Montreal, QC.

Branston, A.E. 2004. “Development of a Design Methodology for Steel Frame/ Wood Panel Shear Walls". M.Eng. thesis. Department of Civil Engineering and Applied Mechanics, McGill University. Montreal, QC.

Boudreault, F.A. 2005. “Seismic Analysis of Steel Frame/ Wood Panel Shear Walls”. M.Eng. thesis, Department of Civil Engineering and Applied Mechanics, McGill University. Montreal, QC, Canada.

Carr, A.J. 2008. “RUAUMOKO- Inelastic Dynamic Analysis”, Dept. of Civil Eng., University of Canterbury, Christchurch, New Zealand.

Canadian Standards Association (CSA), S136. 2007. “North American Specification for the Design of Cold-Formed Steel Structural Members”. Mississauga, ON, Canada.

Canadian Wood Council (CWC), 2001. "Wood Design Manual 2001", Canadian Wood Council. Nepean, ON, Canada.

Canadian Wood Council (CWC), 2002. “Introduction to Wood Design: A learning guide to complement the Wood Design Manual”, Canadian Wood Council. Nepean, ON, Canada.

Consortium of Universities for Research in Earthquake Engineering (CUREE). 2004a. “Recommendations for Earthquake Resistance in Design and Construction of Woodframe Buildings- Part 1: Recommendations”. CUREE Publication No. W-30b, Richmond, CA, USA.

Comeau, G. 2008. “Inelastic Performance of Welded Cold-Formed Steel Strap Braced Walls”. M.Eng. thesis. Department of Civil Engineering and Applied Mechanics, McGill University. Montreal, QC.

El-Saloussy, K. 2010. “Additional Cold-Formed Steel Frame/Steel Sheathed Shear Wall Design Values for Canada”. Project Report, Department of Civil Engineering and Applied Mechanics, McGill University. Montreal, QC.

Federal Emergency Management Agency 2009. “Quantification of Building Seismic Performance Factors, FEMA-P695”. Redwood City, CA, USA.

Foliente, G.C. 1996. “Issues in Siesmic Performance Testing and Evaluation of Timber Structural Systems”. *Proc., International Wood Engineering Conference*. New Orleans, LA, USA, Vol. 1, 29-36.

Glauz, B. 2011. “CFS Version 6.0.4- RSG Software (2010)”, RSG Software, Inc., Lee's Summit, Missouri, USA.

Hikita. K. 2006. “Combined Gravity and Lateral Loading of Light Gauge Steel Frame/Wood Panel Shear Walls”. M.Eng. thesis. Department of Civil Engineering and Applied Mechanics, McGill University. Montreal, QC.

Krawinkler, H., Parisi, F., Ibarra, L., Ayoub, A., Medina, R. 2000. “Development of a Testing Protocol for Woodframe Structures”. *Report W-02 coving Task 1.3.2,* *CUREE/Caltech Woodframe Project*. Consortium of Universities for Research in Earthquake Engineering (CUREE). Richmond, CA, USA.

Madsen, R.L., Nakata, N., & Schafer, B.W. 2011. “CFS-NEES Building Structural Design Narrative”. CFS-NEES project R-CR: Enabling Performance-Based Seismic Design of Multi-Story Cold-Formed Steel Structures Project. Report No. RR01.

McKenna, F., Fenves, G.L., Filippou, F.C., & Mazzoni, S. (2006). “Open system for earthquake engineering simulation (OpenSees)”. Pacific Earthquake Engineering Research Center (PEER), University of California, Berkeley, CA.

Mitchell, D., Tremblay, R., Karacabeyli, E., Paultre, P., Saatcioglu, M., Anderson, D.L. 2003. “Seismic Force Modification Factors for the Proposed 2005 Edition of the National Building Code of Canada”. *Canadian Journal of Civil Engineering*, Vol. 30, No. 2, 308-327.

Morello, D. 2009. “Seismic Force Modification Factors for the Proposed 2005 Edition of the National Building Code of Canada”. M.Eng. thesis. Department of Civil Engineering and Applied Mechanics, McGill University. Montreal, QC.

National Research Council of Canada. 2005. “National Building Code of Canada 2005, 12th Edition”. Ottawa, ON, Canada.

National Research Council of Canada. 2010. “National Building Code of Canada 2010, 13th Edition”. Ottawa, ON, Canada.

Newmark, N.M., Hall, W.J., 1982. “Earthquake Spectra and Design”. *Engineering Monograph*, Earthquake engineering Research Institute. Berkeley, CA, USA.

Ong-Tone, C. 2009. “Tests and Evaluation of Cold-Formed Steel Framing/Steel Sheathed Shear Walls”. Project Report, Department of Civil Engineering and Applied Mechanics, McGill University. Montreal, QC.

Park, R. 1989. “Evaluation of Ductility of Structures and Structural Assemblages from Laboratory Testing”. *Bulletin of the New Zealand National Society for Earthquake Engineering*, Vol.22, No.3, 155-166.

Shamim, I. 2012. “Seismic Design of Lateral Resisting Cold-Formed Steel Framed (CFS) Structures”. Ph.D thesis. Department of Civil Engineering and Applied Mechanics, McGill University. Montreal, QC.

Stewart, W.G. 1987. “The Seismic Design of Plywood Sheathed Shear Walls”, PhD Thesis, University of Canterbury, New Zealand.

Steel Framing Alliance. 2005. “Management Report to the Steel Framing Alliance Board of Directors”. Washington, D.C., USA.

Velchev, K. 2008. “Inelastic Performance of Screw Connected Cold-Formed Steel Strap Braced Walls”. M.Eng. thesis. Department of Civil Engineering and Applied Mechanics, McGill University. Montreal, QC.

Yu, C., Vora, H., Dainard, T., Tucker, J., Veetvkuri, P. 2007. “Steel Sheet Sheathing Options for Cold-Formed Steel Framed Shear Wall Assemblies Providing Shear Resistance”. Report No. UNT-G76234, American Iron and Steel Institute, Department of Engineering Technology, University of North Texas, Denton, Texas, USA.

Yu, C., Chen, Y. 2009. “Steel Sheet Sheathing Options for Cold-Formed Steel Framed Shear Wall Assemblies Providing Shear Resistance- Phase 2”. Report No. UNT-G70752, American Iron and Steel Institute, Department of Engineering Technology, University of North Texas, Denton, Texas, USA.

APPENDIX A - RESULTS FROM CFS VERSION 6.0.4 SOFTWARE

(GLAUZ, 2011)

CFS Version 6.0.4

Section: Section 1.sct
Double Channel 92.1x41.3x12.7-1.37stud

Rev. Date: 1/19/2012 4:43:50 AM

Printed: 1/19/2012 5:24:55 AM

Full Section Properties

Area	517.71 mm^2	Wt.	0.039817 kN/m	Width	377.45 mm
Ix	690569 mm^4	rx	36.522 mm	Ixy	0 mm^4
Sx(t)	14996 mm^3	y(t)	46.050 mm	α	0.000 deg
Sx(b)	14996 mm^3	y(b)	46.050 mm		
		Height	92.100 mm		
Iy	217798 mm^4	ry	20.511 mm	Xo	0.000 mm
Sy(l)	5274 mm^3	x(l)	41.300 mm	Yo	0.000 mm
Sy(r)	5274 mm^3	x(r)	41.300 mm	jx	0.000 mm
		Width	82.600 mm	jy	0.000 mm
I1	690569 mm^4	r1	36.522 mm		
I2	217798 mm^4	r2	20.511 mm		
Ic	908368 mm^4	rc	41.888 mm	Cw	448209536 mm^6
Io	908368 mm^4	ro	41.888 mm	J	324.7 mm^4

Fully Braced Strength - 2007 North American Specification - Canada(LSD)

Material Type: A653 SS Grade 40, Fy=340 MPa

Compression		Positive Moment		Positive Moment	
ϕPno	112.65 kN	ϕMnxo	4.4536 kN-m	ϕMnyo	1.5351 kN-m
Ae	414.14 mm^2	Ixe	679286 mm^4	Iye	209228 mm^4
		Sxe(t)	14554 mm^3	Sye(l)	5117 mm^3
Tension		Sxe(b)	14953 mm^3	Sye(r)	5017 mm^3
ϕTn	147.24 kN				
		Negative Moment		Negative Moment	
		ϕMnxo	4.4536 kN-m	ϕMnyo	1.5351 kN-m
Shear		Ixe	679286 mm^4	Iye	209228 mm^4
ϕVny	34.71 kN	Sxe(t)	14953 mm^3	Sye(l)	5017 mm^3
ϕVnx	29.61 kN	Sxe(b)	14554 mm^3	Sye(r)	5117 mm^3

Member Check - 2007 North American Specification - Canada (LSD)

Material Type: A653 SS Grade 40, Fy=340 MPa
Design Parameters:

Lx	2.4400 m	Ly	0.6100 m	Lt	0.6100 m
Kx	1.0000	Ky	1.0000	Kt	1.0000
Cbx	1.0000	Cby	1.0000	ex	0.0000 mm
Cmx	0.8500	Cmy	0.8500	ey	0.0000 mm

Braced Flange: None   Red. Factor, R: 0   Stiffness, kϕ: 0 kN

Loads:	P (kN)	Mx (kN-m)	Vy (kN)	My (kN-m)	Vx (kN)

```
Entered      52.450     2.2100      0.000     0.0200      0.000
Applied      52.450     2.2100      0.000     0.0200      0.000
Strength     89.681     4.2815     34.706     1.5351     29.611

Effective section properties at applied loads:
Ae        517.71 mm^2   Ixe        690569 mm^4   Iye   217798 mm^4
                        Sxe(t)      14996 mm^3   Sye(l)  5274 mm^3
                        Sxe(b)      14996 mm^3   Sye(r)  5274 mm^3

Interaction Equations
NAS Eq. C5.2.2-1 (P, Mx, My) 0.585 + 0.566 + 0.012 = 1.162  > 1.0
NAS Eq. C5.2.2-2 (P, Mx, My) 0.466 + 0.516 + 0.013 = 0.995 <= 1.0
NAS Eq. C3.3.2-1     (Mx, Vy)   Sqrt(0.246 + 0.000)= 0.496 <= 1.0
NAS Eq. C3.3.2-1     (My, Vx)   Sqrt(0.000 + 0.000)= 0.013 <= 1.0
```

APPENDIX B - TABLES OF DESIGN OF DOUBLE CHORD STUDS

Table B.1 Design of double chord studs[1] with proposed S_y values

Test Label[1]	B1	B2	B3	B4	B5	B6	B7	B8
Measured Stud Thickness (mm)	1.37	1.12	1.12	1.12	1.12	1.12	1.37	1.37
Measured Yield Stress (MPa)	388	301	301	301	301	301	388	388
Measured Sheathing Thickness (mm)	0.79	0.45	0.79	0.79	0.45	0.45	0.79	0.45
Fastener Spacing (mm)	50	50	100	150	100	150	75	75
S_y, Nominal Yield Resistance[2] (kN/m)	23.31	13.52	14.33	11.69	9.68	7.37	19.88	11.60
Overstrength[2]	1.34	1.34	1.34	1.34	1.34	1.34	1.34	1.34
Gravity Load/per DCS (kN)	4.90	4.90	4.90	4.90	4.90	4.90	4.90	4.90
$\overline{\mathbf{P}}$, Probable Compression Force (kN)	81.06	49.08	51.72	43.10	36.53	28.98	69.86	42.80
$\overline{M_x}$ (kNm)	3.53	2.06	2.18	1.78	1.48	1.13	3.01	1.77
$\overline{M_y}$ (kNm)	0.02	0.02	0.02	0.02	0.02	0.02	0.02	0.02
Stability Interaction[3]								
$\emptyset_c P_n$ (kN)	120.70	81.03	81.03	81.03	81.03	81.03	120.70	120.70
$\emptyset_b M_{nx}$ (kNm)	5.21	3.40	3.40	3.40	3.40	3.40	5.21	5.21
$\emptyset_b M_{ny}$ (kNm)	1.84	1.22	1.22	1.22	1.22	1.22	1.84	1.84
Stability Interaction Eq. (C5.2.2-1)	**1.36**	**1.23**	**1.30**	**1.07**	**0.90**	**0.71**	**1.17**	**0.71**
Strength Interaction[3]								
$\emptyset_c P_{no}$ (kN)	153.09	95.28	95.28	95.28	95.28	95.28	153.09	153.09
$\emptyset_b M_{nx}$ (kNm)	5.52	3.55	3.55	3.55	3.55	3.55	5.52	5.52
$\emptyset_b M_{ny}$ (kNm)	1.84	1.22	1.22	1.22	1.22	1.22	1.84	1.84
Strength Interaction Eq. (C5.2.2-2)	**1.18**	**1.11**	**1.17**	**0.97**	**0.82**	**0.64**	**1.01**	**0.61**
Axial Ratio[3]								
$\overline{\mathbf{P}}/\emptyset_c P_n$	**0.67**	**0.61**	**0.64**	**0.53**	**0.45**	**0.36**	**0.58**	**0.35**

[1] Nominal dimensions of stud: 92.1mm (3-5/8") web, 41.3mm (1-5/8") flange, and 12.7mm (1/2") lip

[2] Proposed S_y values from author (Table 3.12)

[3] Calculations were according to CSA-S136 Standard (2007): resistance factors $\phi_c = \phi_b = 1.0$ end conditions $K_x = K_y = K_t = 1.0$ and buckling lengths $L_x = 2440$mm, $L_y = L_z = 610$mm

Table B.2 Design of double chord studs[1] with proposed S_y values & reduced M_x

Test Label[1]	B1	B2	B3	B4	B5	B6	B7	B8
Measured Stud Thickness (mm)	1.37	1.12	1.12	1.12	1.12	1.12	1.37	1.37
Measured Yield Stress (MPa)	388	301	301	301	301	301	388	388
Measured Sheathing Thickness (mm)	0.79	0.45	0.79	0.79	0.45	0.45	0.79	0.45
Fastener Spacing (mm)	50	50	100	150	100	150	75	75
S_y, Nominal Yield Resistance[2] (kN/m)	23.31	13.52	14.33	11.69	9.68	7.37	19.88	11.60
Overstrength[2]	1.34	1.34	1.34	1.34	1.34	1.34	1.34	1.34
Gravity Load/per DCS (kN)	4.90	4.90	4.90	4.90	4.90	4.90	4.90	4.90
$\overline{P}$, Probable Compression Force (kN)	81.06	49.08	51.72	43.10	36.53	28.98	69.86	42.80
$\overline{M_x}$ (kNm)	1.78	1.04	1.10	0.90	0.75	0.58	1.52	0.90
$\overline{M_y}$ (kNm)	0.02	0.02	0.02	0.02	0.02	0.02	0.02	0.02
Stability Interaction[3]								
$\phi_c P_n$ (kN)	120.70	81.03	81.03	81.03	81.03	81.03	120.70	120.70
$\phi_b M_{nx}$ (kNm)	5.21	3.40	3.40	3.40	3.40	3.40	5.21	5.21
$\phi_b M_{ny}$ (kNm)	1.84	1.22	1.22	1.22	1.22	1.22	1.84	1.84
Stability Interaction Eq. (C5.2.2-1)	**1.02**	**0.93**	**0.98**	**0.81**	**0.69**	**0.54**	**0.88**	**0.54**
Strength Interaction[3]								
$\phi_c P_{no}$ (kN)	153.09	95.28	95.28	95.28	95.28	95.28	153.09	153.09
$\phi_b M_{nx}$ (kNm)	5.52	3.55	3.55	3.55	3.55	3.55	5.52	5.52
$\phi_b M_{ny}$ (kNm)	1.84	1.22	1.22	1.22	1.22	1.22	1.84	1.84
Strength Interaction Eq. (C5.2.2-2)	**0.86**	**0.82**	**0.87**	**0.72**	**0.61**	**0.48**	**0.74**	**0.45**
Axial Ratio[3]								
$\overline{P}/\phi_c P_n$	**0.67**	**0.62**	**0.66**	**0.55**	**0.47**	**0.37**	**0.58**	**0.35**

[1] Nominal dimensions of stud: 92.1mm (3-5/8") web, 41.3mm (1-5/8") flange, and 12.7mm (1/2") lip

[2] Proposed S_y values from author (Table 3.12)

[3] Calculations were according to CSA-S136 Standard (2007): resistance factors $\phi_c = \phi_b = 1.0$ end conditions $K_x=K_y=K_t=1.0$ and buckling lengths L_x= 2440mm, $L_y=L_z$=610mm

APPENDIX C – TEST DATA SHEETS & OBSERVATION SHEETS

Cold Formed Steel Framed/Steel Sheathed Shear Walls
McGill University, Montreal

TEST: B1-M

RESEARCHER: Jamin DaBreo **ASSISTANTS:** Anthony Caruso, Nicholas DiTommaso

DATE: 24/08/2010 **TIME:** 2:19:54 PM

DIMENSIONS OF WALL: 1220 mm (W) 2440 mm (H) **PANEL ORIENTATION:** Vertical
Sheathing one side

SHEATHING:
[ ] 0.457 mm (0.018") Sheet Steel 230 MPa (33 ksi)
[X] 0.762 mm (0.030") Sheet Steel 230 MPa (33 ksi)

Connections:
Sheathing: [X] No.8 gauge 19 mm (0.75") self-drilling square drive pan head screws
Framing: [X] No.8 gauge 12.5 mm (0.5") self-drilling wafer head screws
Hold downs: [X] No.10 gauge 25.4 mm (1.0") self-drilling Hex head screws
Anchor Rods: [X] A193 Grade B7 22mm (7/8") diameter rods
Loading Beam: [X] A325 19.1 mm (3/4") bolts [X] 6 shear bolts + 2 anchor rods
Base: [X] A325 19.1 mm (3/4") bolts [X] 6 shear bolts + 2 anchor rods
Back-to-Back Chord Studs: [X] No.10 gauge 19.1 mm (0.075") self-drilling wafer head (2@300mm (12") O.C.)

SHEATHING FASTENER SCHEDULE: [X] 50 mm (2/12") [ ] 75 mm (3/12") [ ] 100 mm (4/12") [ ] 150 mm (6/12")

EDGE PANEL DISTANCE: [X] 3/8" [ ] 1/2" [ ] Other:

STUDS:
[ ] 92.1 W x 41.3 F x 12.7 mm Lip (3-5/8"x1-5/8"x1/2"); Thickness: 1.09 mm (0.043") 230 MPa (33ksi)
[X] 92.1 W x 41.3 F x 12.7 mm Lip (3-5/8"x1-5/8"x1/2"); Thickness: 1.37 mm (0.054") 345 MPa (50ksi)
[X] Double chord studs used
[ ] Other

STUD SPACING: [X] 600 mm (24") O.C.

TRACK:
Web: 92.1 mm (3-5/8") [ ] T= 1.09 mm (0.043") 230 Mpa (33ksi)
Flange: 31.8 mm (1-1/4") [X] T= 1.37 mm (0.054") 345 Mpa (50ksi)

HOLD DOWNS:
[X] Simpson Strong-Tie S/HD10S (# of screws): 33 per H.D.
[ ] Other

TEST PROTOCOL AND DESCRIPTION:
[X] Monotonic (Displacement control) rate of loading: 2.5 mm/min
[ ] Reserved Cyclic (Displacement control)

MEASUREMENT INSTRUMENTS:
[X] MTS Actuator LVDT [X] North Slip LVDT
[X] North Uplift LVDT [X] South Slip LVDT
[X] South Uplift LVDT [X] Load Cell North (Hold down)
[X] MTS Actuator Load Cell [X] Load Cell South (Hold down)
[X] String Potentiometer

DATA ACQ. RECORD RATE: 2 scan/sec **MONITOR RATE:** 10 scan/sec

COMMENTS:
– Gravity load of approximately 12.25 kN applied to wall top
– Hold down anchor rods pre-tensioned to 6580 N North & 9250 N South
– square plate washers 75 x 75 x 6 mm used on top and bottom shear bolt connections

Figure C.1 Test data sheet for test B1-M

Cold Formed Steel Framed/Steel Sheathed Shear Walls
McGill University, Montreal

TEST: B2-M

RESEARCHER: Jamin DaBreo **ASSISTANTS:** Anthony Caruso, Nicholas DiTommaso

DATE: 26/08/2010 **TIME:** 2:39:58 PM

DIMENSIONS OF WALL: 1220 mm (W) 2440 mm (H) **PANEL ORIENTATION:** Vertical
Sheathing one side

SHEATHING:
- [X] 0.457 mm (0.018") Sheet Steel 230 MPa (33 ksi)
- [ ] 0.762 mm (0.030") Sheet Steel 230 MPa (33 ksi)

Connections:
- Sheathing: [X] No.8 gauge 19 mm (0.75") self-drilling square drive pan head screws
- Framing: [X] No.8 gauge 12.5 mm (0.5") self-drilling wafer head screws
- Hold downs: [X] No.10 gauge 25.4 mm (1.0") self-drilling Hex head screws
- Anchor Rods: [X] A193 Grade B7 22mm (7/8") diameter rods
- Loading Beam: [X] A325 19.1 mm (3/4") bolts [X] 6 shear bolts + 2 anchor rods
- Base: [X] A325 19.1 mm (3/4") bolts [X] 6 shear bolts + 2 anchor rods
- Back-to-Back Chord Studs: [X] No.10 gauge 19.1 mm (0.075") self-drilling wafer head (2@300mm (12") O.C.)

SHEATHING FASTENER SCHEDULE: [X] 50 mm (2/12") [ ] 75 mm (3/12") [ ] 100 mm (4/12") [ ] 150 mm (6/12")

EDGE PANEL DISTANCE: [X] 3/8" [ ] 1/2" [ ] Other:

STUDS:
- [X] 92.1 W x 41.3 F x 12.7 mm Lip (3-5/8"x1-5/8"x1/2"); Thickness: 1.09 mm (0.043") 230 MPa (33ksi)
- [ ] 92.1 W x 41.3 F x 12.7 mm Lip (3-5/8"x1-5/8"x1/2"); Thickness: 1.37 mm (0.054") 345 MPa (50ksi)
- [X] Double chord studs used
- [ ] Other

STUD SPACING: [X] 600 mm (24") O.C.

TRACK:
- Web: 92.1 mm (3-5/8")
- Flange: 31.8 mm (1-1/4")
- [X] T= 1.09 mm (0.043") 230 Mpa (33ksi)
- [ ] T= 1.37 mm (0.054") 345 Mpa (50ksi)

HOLD DOWNS:
- [X] Simpson Strong-Tie S/HD10S (# of screws): 33 per H.D.
- [ ] Other

TEST PROTOCOL AND DESCRIPTION:
- [X] Monotonic (Displacement control) rate of loading: 2.5 mm/min
- [ ] Reserved Cyclic (Displacement control)

MEASUREMENT INSTRUMENTS:
- [X] MTS Actuator LVDT
- [X] North Uplift LVDT
- [X] South Uplift LVDT
- [X] MTS Actuator Load Cell
- [X] String Potentiometer
- [X] North Slip LVDT
- [X] South Slip LVDT
- [X] Load Cell North (Hold down)
- [X] Load Cell South (Hold down)

DATA ACQ. RECORD RATE: 2 scan/sec **MONITOR RATE:** 10 scan/sec

COMMENTS:
- Gravity load of approximately 12.25 kN applied to wall top
- Hold down anchor rods pre-tensioned to 6524 N North & 8860 N South
- square plate washers 75 x 75 x 6 mm used on top and bottom shear bolt connections

Figure C.2 Test data sheet for test B2-M

Cold Formed Steel Framed/Steel Sheathed Shear Walls
McGill University, Montreal

TEST: B3-M

RESEARCHER: Jamin DaBreo **ASSISTANTS:** Anthony Caruso, Nicholas DiTommaso

DATE: 25/08/2010 **TIME:** 11:07:26 AM

DIMENSIONS OF WALL: 1220 mm (W) 2440 mm (H) **PANEL ORIENTATION:** Vertical
Sheathing one side

SHEATHING:
[ ] 0.457 mm (0.018") Sheet Steel 230 MPa (33 ksi)
[X] 0.762 mm (0.030") Sheet Steel 230 MPa (33 ksi)

Connections:
Sheathing: [X] No.8 gauge 19 mm (0.75") self-drilling square drive pan head screws
Framing: [X] No.8 gauge 12.5 mm (0.5") self-drilling wafer head screws
Hold downs: [X] No.10 gauge 25.4 mm (1.0") self-drilling Hex head screws
Anchor Rods: [X] A193 Grade B7 22mm (7/8") diameter rods
Loading Beam: [X] A325 19.1 mm (3/4") bolts [X] 6 shear bolts + 2 anchor rods
Base: [X] A325 19.1 mm (3/4") bolts [X] 6 shear bolts + 2 anchor rods

Back-to-Back Chord Studs: [X] No.10 gauge 19.1 mm (0.075") self-drilling wafer head (2@300mm (12") O.C.)

SHEATHING FASTENER SCHEDULE: [ ] 50 mm (2/12") [ ] 75 mm (3/12") [X] 100 mm (4/12") [ ] 150 mm (6/12")

EDGE PANEL DISTANCE: [X] 3/8" [ ] 1/2" [ ] Other:

STUDS:
[X] 92.1 W x 41.3 F x 12.7 mm Lip (3-5/8"x1-5/8"x1/2"); Thickness: 1.09 mm (0.043") 230 MPa (33ksi)
[ ] 92.1 W x 41.3 F x 12.7 mm Lip (3-5/8"x1-5/8"x1/2"); Thickness: 1.37 mm (0.054") 345 MPa (50ksi)
[X] Double chord studs used
[ ] Other

STUD SPACING: [X] 600 mm (24") O.C.

TRACK:
Web: 92.1 mm (3-5/8") [X] T= 1.09 mm (0.043") 230 Mpa (33ksi)
Flange: 31.8 mm (1-1/4") [ ] T= 1.37 mm (0.054") 345 Mpa (50ksi)

HOLD DOWNS:
[X] Simpson Strong-Tie S/HD10S (# of screws): 33 per H.D.
[ ] Other

TEST PROTOCOL AND DESCRIPTION:
[X] Monotonic (Displacement control) rate of loading: 2.5 mm/min
[ ] Reserved Cyclic (Displacement control)

MEASUREMENT INSTRUMENTS:
[X] MTS Actuator LVDT [X] North Slip LVDT
[X] North Uplift LVDT [X] South Slip LVDT
[X] South Uplift LVDT [X] Load Cell North (Hold down)
[X] MTS Actuator Load Cell [X] Load Cell South (Hold down)
[X] String Potentiometer

DATA ACQ. RECORD RATE: 2 scan/sec **MONITOR RATE:** 10 scan/sec

COMMENTS:
– Gravity load of approximately 12.25 kN applied to wall top
– Hold down anchor rods pre-tensioned to 6301 N North & 9083 N South
– square plate washers 75 x 75 x 6 mm used on top and bottom shear bolt connections

Figure C.3 Test data sheet for test B3-M

Cold Formed Steel Framed/Steel Sheathed Shear Walls
McGill University, Montreal

TEST: B4-M

RESEARCHER: Jamin DaBreo **ASSISTANTS:** Anthony Caruso, Nicholas DiTommaso

DATE: 23/08/2010 **TIME:** 3:41:36 PM

DIMENSIONS OF WALL: 1220 mm (W) 2440 mm (H) **PANEL ORIENTATION:** Vertical
Sheathing one side

SHEATHING:
[ ] 0.457 mm (0.018") Sheet Steel 230 MPa (33 ksi)
[X] 0.762 mm (0.030") Sheet Steel 230 MPa (33 ksi)

Connections:
Sheathing: [X] No.8 gauge 19 mm (0.75") self-drilling square drive pan head screws
Framing: [X] No.8 gauge 12.5 mm (0.5") self-drilling wafer head screws
Hold downs: [X] No.10 gauge 25.4 mm (1.0") self-drilling Hex head screws
Anchor Rods: [X] A193 Grade B7 22mm (7/8") diameter rods
Loading Beam: [X] A325 19.1 mm (3/4") bolts [X] 6 shear bolts + 2 anchor rods
Base: [X] A325 19.1 mm (3/4") bolts [X] 6 shear bolts + 2 anchor rods

Back-to-Back Chord Studs: [X] No.10 gauge 19.1 mm (0.075") self-drilling wafer head (2@300mm (12") O.C.)

SHEATHING FASTENER SCHEDULE: [ ] 50 mm (2/12") [ ] 75 mm (3/12") [ ] 100 mm (4/12") [X] 150 mm (6/12")

EDGE PANEL DISTANCE: [X] 3/8" [ ] 1/2" [ ] Other:

STUDS:
[X] 92.1 W x 41.3 F x 12.7 mm Lip (3-5/8"x1-5/8"x1/2"); Thickness: 1.09 mm (0.043") 230 MPa (33ksi)
[ ] 92.1 W x 41.3 F x 12.7 mm Lip (3-5/8"x1-5/8"x1/2"); Thickness: 1.37 mm (0.054") 345 MPa (50ksi)
[X] Double chord studs used
[ ] Other

STUD SPACING: [X] 600 mm (24") O.C.

TRACK:
Web: 92.1 mm (3-5/8") [X] T= 1.09 mm (0.043") 230 Mpa (33ksi)
Flange: 31.8 mm (1-1/4") [ ] T= 1.37 mm (0.054") 345 Mpa (50ksi)

HOLD DOWNS:
[X] Simpson Strong-Tie S/HD10S (# of screws): 33 per H.D.
[ ] Other

TEST PROTOCOL AND DESCRIPTION:
[X] Monotonic (Displacement control) rate of loading: 2.5 mm/min
[ ] Reserved Cyclic (Displacement control)

MEASUREMENT INSTRUMENTS:
[X] MTS Actuator LVDT
[X] North Uplift LVDT
[X] South Uplift LVDT
[X] MTS Actuator Load Cell
[X] String Potentiometer
[X] North Slip LVDT
[X] South Slip LVDT
[X] Load Cell North (Hold down)
[X] Load Cell South (Hold down)

DATA ACQ. RECORD RATE: 2 scan/sec **MONITOR RATE:** 10 scan/sec

COMMENTS:
- Gravity load of approximately 12.25 kN applied to wall top
- Hold down anchor rods pre-tensioned to 6858 N North & 6550 N South
- square plate washers 75 x 75 x 6 mm used on top and bottom shear bolt connections

Figure C.4 Test data sheet for test B4-M

Cold Formed Steel Framed/Steel Sheathed Shear Walls
McGill University, Montreal

TEST: B5-M

RESEARCHER: Jamin DaBreo **ASSISTANTS:** Anthony Caruso, Nicholas DiTommaso

DATE: 26/08/2010 **TIME:** 10:53:00 AM

DIMENSIONS OF WALL: 1220 mm (W) 2440 mm (H) **PANEL ORIENTATION:** Vertical
Sheathing one side

SHEATHING:
- [X] 0.457 mm (0.018") Sheet Steel 230 MPa (33 ksi)
- [ ] 0.762 mm (0.030") Sheet Steel 230 MPa (33 ksi)

Connections:
- Sheathing: [X] No.8 gauge 19 mm (0.75") self-drilling square drive pan head screws
- Framing: [X] No.8 gauge 12.5 mm (0.5") self-drilling wafer head screws
- Hold downs: [X] No.10 gauge 25.4 mm (1.0") self-drilling Hex head screws
- Anchor Rods: [X] A193 Grade B7 22mm (7/8") diameter rods
- Loading Beam: [X] A325 19.1 mm (3/4") bolts [X] 6 shear bolts + 2 anchor rods
- Base: [X] A325 19.1 mm (3/4") bolts [X] 6 shear bolts + 2 anchor rods
- Back-to-Back Chord Studs: [X] No.10 gauge 19.1 mm (0.075") self-drilling wafer head (2@300mm (12") O.C.)

SHEATHING FASTENER SCHEDULE: [ ] 50 mm (2/12") [ ] 75 mm (3/12") [X] 100 mm (4/12") [ ] 150 mm (6/12")

EDGE PANEL DISTANCE: [X] 3/8" [ ] 1/2" [ ] Other:

STUDS:
- [X] 92.1 W x 41.3 F x 12.7 mm Lip (3-5/8"x1-5/8"x1/2"); Thickness: 1.09 mm (0.043") 230 MPa (33ksi)
- [ ] 92.1 W x 41.3 F x 12.7 mm Lip (3-5/8"x1-5/8"x1/2"); Thickness: 1.37 mm (0.054") 345 MPa (50ksi)
- [X] Double chord studs used
- [ ] Other

STUD SPACING: [X] 600 mm (24") O.C.

TRACK:
- Web: 92.1 mm (3-5/8")
- Flange: 31.8 mm (1-1/4")
- [X] T= 1.09 mm (0.043") 230 Mpa (33ksi)
- [ ] T= 1.37 mm (0.054") 345 Mpa (50ksi)

HOLD DOWNS:
- [X] Simpson Strong-Tie S/HD10S
- [ ] Other

(# of screws): 33 per H.D.

TEST PROTOCOL AND DESCRIPTION:
- [X] Monotonic (Displacement control) — rate of loading: 2.5 mm/min
- [ ] Reserved Cyclic (Displacement control)

MEASUREMENT INSTRUMENTS:
- [X] MTS Actuator LVDT
- [X] North Uplift LVDT
- [X] South Uplift LVDT
- [X] MTS Actuator Load Cell
- [X] String Potentiometer
- [X] North Slip LVDT
- [X] South Slip LVDT
- [X] Load Cell North (Hold down)
- [X] Load Cell South (Hold down)

DATA ACQ. RECORD RATE: 2 scan/sec **MONITOR RATE:** 10 scan/sec

COMMENTS:
- Gravity load of approximately 12.25 kN applied to wall top
- Hold down anchor rods pre-tensioned to 6663 N North & 9277 N South
- square plate washers 75 x 75 x 6 mm used on top and bottom shear bolt connections

Figure C.5 Test data sheet for test B5-M

Cold Formed Steel Framed/Steel Sheathed Shear Walls
McGill University, Montreal

TEST: B6-M

RESEARCHER: Jamin DaBreo **ASSISTANTS:** Anthony Caruso, Nicholas DiTommaso

DATE: 26/08/2010 **TIME:** 10:53:00 AM

DIMENSIONS OF WALL: 1220 mm (W) 2440 mm (H) **PANEL ORIENTATION:** Vertical; Sheathing one side

SHEATHING:
- [X] 0.457 mm (0.018") Sheet Steel 230 MPa (33 ksi)
- [ ] 0.762 mm (0.030") Sheet Steel 230 MPa (33 ksi)

Connections:

Sheathing:	X	No.8 gauge 19 mm (0.75") self-drilling square drive pan head screws
Framing:	X	No.8 gauge 12.5 mm (0.5") self-drilling wafer head screws
Hold downs:	X	No.10 gauge 25.4 mm (1.0") self-drilling Hex head screws
Anchor Rods:	X	A193 Grade B7 22mm (7/8") diameter rods
Loading Beam:	X	A325 19.1 mm (3/4") bolts; X 6 shear bolts + 2 anchor rods
Base:	X	A325 19.1 mm (3/4") bolts; X 6 shear bolts + 2 anchor rods
Back-to-Back Chord Studs:	X	No.10 gauge 19.1 mm (0.075") self-drilling wafer head (2@300mm (12") O.C.)

SHEATHING FASTENER SCHEDULE:
- [ ] 50 mm (2/12")
- [ ] 75 mm (3/12")
- [ ] 100 mm (4/12")
- [X] 150 mm (6/12")

EDGE PANEL DISTANCE:
- [X] 3/8"
- [ ] 1/2"
- [ ] Other:

STUDS:
- [X] 92.1 W x 41.3 F x 12.7 mm Lip (3-5/8"x1-5/8"x1/2"); Thickness: 1.09 mm (0.043") 230 MPa (33ksi)
- [ ] 92.1 W x 41.3 F x 12.7 mm Lip (3-5/8"x1-5/8"x1/2"); Thickness: 1.37 mm (0.054") 345 MPa (50ksi)
- [X] Double chord studs used
- [ ] Other

STUD SPACING:
- [X] 600 mm (24") O.C.

TRACK:
Web: 92.1 mm (3-5/8")
Flange: 31.8 mm (1-1/4")
- [X] T= 1.09 mm (0.043") 230 Mpa (33ksi)
- [ ] T= 1.37 mm (0.054") 345 Mpa (50ksi)

HOLD DOWNS:
- [X] Simpson Strong-Tie S/HD10S
- [ ] Other

(# of screws): 33 per H.D.

TEST PROTOCOL AND DESCRIPTION:
- [X] Monotonic (Displacement control)
- [ ] Reserved Cyclic (Displacement control)

rate of loading: 2.5 mm/min

MEASUREMENT INSTRUMENTS:
- [X] MTS Actuator LVDT
- [X] North Uplift LVDT
- [X] South Uplift LVDT
- [X] MTS Actuator Load Cell
- [X] String Potentiometer
- [X] North Slip LVDT
- [X] South Slip LVDT
- [X] Load Cell North (Hold down)
- [X] Load Cell South (Hold down)

DATA ACQ. RECORD RATE: 2 scan/sec **MONITOR RATE:** 10 scan/sec

COMMENTS:
- Gravity load of approximately 12.25 kN applied to wall top
- Hold down anchor rods pre-tensioned to 6635 N North & 8777 N South
- square plate washers 75 x 75 x 6 mm used on top and bottom shear bolt connections

Figure C.6 Test data sheet for test B6-M

Cold Formed Steel Framed/Steel Sheathed Shear Walls
McGill University, Montreal

TEST: B7-M

RESEARCHER: Jamin DaBreo **ASSISTANTS:** Anthony Caruso, Nicholas DiTommaso

DATE: 02/09/2010 **TIME:** 11:32:32 AM

DIMENSIONS OF WALL: 1220 mm (W) 2440 mm (H) **PANEL ORIENTATION:** Vertical
Sheathing one side

SHEATHING:
[ ] 0.457 mm (0.018") Sheet Steel 230 MPa (33 ksi)
[X] 0.762 mm (0.030") Sheet Steel 230 MPa (33 ksi)

Connections:
Sheathing: [X] No.8 gauge 19 mm (0.75") self-drilling square drive pan head screws
Framing: [X] No.8 gauge 12.5 mm (0.5") self-drilling wafer head screws
Hold downs: [X] No.10 gauge 25.4 mm (1.0") self-drilling Hex head screws
Anchor Rods: [X] A193 Grade B7 22mm (7/8") diameter rods
Loading Beam: [X] A325 19.1 mm (3/4") bolts [X] 6 shear bolts + 2 anchor rods
Base: [X] A325 19.1 mm (3/4") bolts [X] 6 shear bolts + 2 anchor rods

Back-to-Back Chord Studs: [X] No.10 gauge 19.1 mm (0.075") self-drilling wafer head (2@300mm (12") O.C.)

SHEATHING FASTENER SCHEDULE: [ ] 50 mm (2/12") [X] 75 mm (3/12") [ ] 100 mm (4/12") [ ] 150 mm (6/12")

EDGE PANEL DISTANCE: [X] 3/8" [ ] 1/2" [ ] Other:

STUDS:
[ ] 92.1 W x 41.3 F x 12.7 mm Lip (3-5/8"x1-5/8"x1/2"); Thickness: 1.09 mm (0.043") 230 MPa (33ksi)
[X] 92.1 W x 41.3 F x 12.7 mm Lip (3-5/8"x1-5/8"x1/2"); Thickness: 1.37 mm (0.054") 345 MPa (50ksi)
[X] Double chord studs used
[ ] Other

STUD SPACING: [X] 600 mm (24") O.C.

TRACK:
Web: 92.1 mm (3-5/8") [ ] T= 1.09 mm (0.043") 230 Mpa (33ksi)
Flange: 31.8 mm (1-1/4") [X] T= 1.37 mm (0.054") 345 Mpa (50ksi)

HOLD DOWNS:
[X] Simpson Strong-Tie S/HD10S (# of screws): 33 per H.D.
[ ] Other

TEST PROTOCOL AND DESCRIPTION:
[X] Monotonic (Displacement control) rate of loading: 2.5 mm/min
[ ] Reserved Cyclic (Displacement control)

MEASUREMENT INSTRUMENTS:
[X] MTS Actuator LVDT [X] North Slip LVDT
[X] North Uplift LVDT [X] South Slip LVDT
[X] South Uplift LVDT [X] Load Cell North (Hold down)
[X] MTS Actuator Load Cell [X] Load Cell South (Hold down)
[X] String Potentiometer

DATA ACQ. RECORD RATE: 2 scan/sec **MONITOR RATE:** 10 scan/sec

COMMENTS:
– Gravity load of approximately 12.25 kN applied to wall top
– Hold down anchor rods pre-tensioned to 6691 N North & 9222 N South
– square plate washers 75 x 75 x 6 mm used on top and bottom shear bolt connections

Figure C.7 Test data sheet for test B7-M

Cold Formed Steel Framed/Steel Sheathed Shear Walls
McGill University, Montreal

TEST: B8-M

RESEARCHER: Jamin DaBreo **ASSISTANTS:** Anthony Caruso, Nicholas DiTommaso

DATE: 02/09/2010 **TIME:** 3:40:10 PM

DIMENSIONS OF WALL: 1220 mm (W) 2440 mm (H) **PANEL ORIENTATION:** Vertical; Sheathing one side

SHEATHING:
[X] 0.457 mm (0.018") Sheet Steel 230 MPa (33 ksi)
[ ] 0.762 mm (0.030") Sheet Steel 230 MPa (33 ksi)

Connections:
Sheathing: [X] No.8 gauge 19 mm (0.75") self-drilling square drive pan head screws
Framing: [X] No.8 gauge 12.5 mm (0.5") self-drilling wafer head screws
Hold downs: [X] No.10 gauge 25.4 mm (1.0") self-drilling Hex head screws
Anchor Rods: [X] A193 Grade B7 22mm (7/8") diameter rods
Loading Beam: [X] A325 19.1 mm (3/4") bolts [X] 6 shear bolts + 2 anchor rods
Base: [X] A325 19.1 mm (3/4") bolts [X] 6 shear bolts + 2 anchor rods

Back-to-Back Chord Studs: [X] No.10 gauge 19.1 mm (0.075") self-drilling wafer head (2@300mm (12") O.C.)

SHEATHING FASTENER SCHEDULE: [ ] 50 mm (2/12") [X] 75 mm (3/12") [ ] 100 mm (4/12") [ ] 150 mm (6/12")

EDGE PANEL DISTANCE: [X] 3/8" [ ] 1/2" [ ] Other:

STUDS:
[ ] 92.1 W x 41.3 F x 12.7 mm Lip (3-5/8"x1-5/8"x1/2"); Thickness: 1.09 mm (0.043") 230 MPa (33ksi)
[X] 92.1 W x 41.3 F x 12.7 mm Lip (3-5/8"x1-5/8"x1/2"); Thickness: 1.37 mm (0.054") 345 MPa (50ksi)
[X] Double chord studs used
[ ] Other

STUD SPACING: [X] 600 mm (24") O.C.

TRACK:
Web: 92.1 mm (3-5/8") [ ] T= 1.09 mm (0.043") 230 Mpa (33ksi)
Flange: 31.8 mm (1-1/4") [X] T= 1.37 mm (0.054") 345 Mpa (50ksi)

HOLD DOWNS:
[X] Simpson Strong-Tie S/HD10S (# of screws): 33 per H.D.
[ ] Other

TEST PROTOCOL AND DESCRIPTION:
[X] Monotonic (Displacement control) rate of loading: 2.5 mm/min
[ ] Reserved Cyclic (Displacement control)

MEASUREMENT INSTRUMENTS:
[X] MTS Actuator LVDT [X] North Slip LVDT
[X] North Uplift LVDT [X] South Slip LVDT
[X] South Uplift LVDT [X] Load Cell North (Hold down)
[X] MTS Actuator Load Cell [X] Load Cell South (Hold down)
[X] String Potentiometer

DATA ACQ. RECORD RATE: 2 scan/sec **MONITOR RATE:** 10 scan/sec

COMMENTS:
– Gravity load of approximately 12.25 kN applied to wall top
– Hold down anchor rods pre-tensioned to 6746 N North & 8554 N South
– square plate washers 75 x 75 x 6 mm used on top and bottom shear bolt connections

Figure C.8 Test data sheet for test B8-M

Cold Formed Steel Framed/Steel Sheathed Shear Walls
McGill University, Montreal

TEST: B1-R

RESEARCHER: Jamin DaBreo **ASSISTANTS:** Anthony Caruso, Nicholas DiTommaso

DATE: 31/08/2010 **TIME:** 9:54:32 AM

DIMENSIONS OF WALL: 1220 mm (W) 2440 mm (H) **PANEL ORIENTATION:** Vertical; Sheathing one side

SHEATHING:
[ ] 0.457 mm (0.018") Sheet Steel 230 MPa (33 ksi)
[X] 0.762 mm (0.030") Sheet Steel 230 MPa (33 ksi)

Connections:
- Sheathing: [X] No.8 gauge 19 mm (0.75") self-drilling square drive pan head screws
- Framing: [X] No.8 gauge 12.5 mm (0.5") self-driling wafer head screws
- Hold downs: [X] No.10 gauge 25.4 mm (1.0") self-drilling Hex head screws
- Anchor Rods: [X] A193 Grade B7 22mm (7/8") diameter rods
- Loading Beam: [X] A325 19.1 mm (3/4") bolts [X] 6 shear bolts + 2 anchor rods
- Base: [X] A325 19.1 mm (3/4") bolts [X] 6 shear bolts + 2 anchor rods
- Back-to-Back Chord Studs: [X] No.10 gauge 19.1 mm (0.075") self-drilling wafer head (2@300mm (12") O.C.)

SHEATHING FASTENER SCHEDULE: [X] 50 mm (2/12") [ ] 75 mm (3/12") [ ] 100 mm (4/12") [ ] 150 mm (6/12")

EDGE PANEL DISTANCE: [X] 3/8" [ ] 1/2" [ ] Other:

STUDS:
[ ] 92.1 W x 41.3 F x 12.7 mm Lip (3-5/8"x1-5/8"x1/2"); Thickness: 1.09 mm (0.043") 230 MPa (33ksi)
[X] 92.1 W x 41.3 F x 12.7 mm Lip (3-5/8"x1-5/8"x1/2"); Thickness: 1.37 mm (0.054") 345 MPa (50ksi)
[X] Double chord studs used
[ ] Other

STUD SPACING: [X] 600 mm (24") O.C.

TRACK:
Web: 92.1 mm (3-5/8") [ ] T= 1.09 mm (0.043") 230 Mpa (33ksi)
Flange: 31.8 mm (1-1/4") [X] T= 1.37 mm (0.054") 345 Mpa (50ksi)

HOLD DOWNS: [X] Simpson Strong-Tie S/HD10S [ ] Other (# of screws): 33 per H.D.

TEST PROTOCOL AND DESCRIPTION:
[ ] Monotonic (Displacement control)
[X] Reserved Cyclic (Displacement control) CUREE cyclic protocol @ 0.1 Hz

MEASUREMENT INSTRUMENTS:
[X] MTS Actuator LVDT [X] North Slip LVDT
[X] North Uplift LVDT [X] South Slip LVDT
[X] South Uplift LVDT [X] Load Cell North (Hold down)
[X] MTS Actuator Load Cell [X] Load Cell South (Hold down)
[X] String Potentiometer

DATA ACQ. RECORD RATE: 50 scan/sec **MONITOR RATE:** 10 scan/sec

COMMENTS:
- Gravity load of approximately 12.25 kN applied to wall top
- Hold down anchor rods pre-tensioned to 7358 N North & 9055 N South
- square plate washers 75 x 75 x 6 mm used on top and bottom shear bolt connections

Figure C.9 Test data sheet for test B1-R

Cold Formed Steel Framed/Steel Sheathed Shear Walls
McGill University, Montreal

TEST: B2-R

RESEARCHER: Jamin DaBreo **ASSISTANTS:** Anthony Caruso, Nicholas DiTommaso

DATE: 31/08/2010 **TIME:** 3:34:19 PM

DIMENSIONS OF WALL: 1220 mm (W) 2440 mm (H) **PANEL ORIENTATION:** Vertical

Sheathing one side

SHEATHING:
- [X] 0.457 mm (0.018") Sheet Steel 230 MPa (33 ksi)
- [ ] 0.762 mm (0.030") Sheet Steel 230 MPa (33 ksi)

Connections:
- Sheathing: [X] No.8 gauge 19 mm (0.75") self-drilling square drive pan head screws
- Framing: [X] No.8 gauge 12.5 mm (0.5") self-drilling wafer head screws
- Hold downs: [X] No.10 gauge 25.4 mm (1.0") self-drilling Hex head screws
- Anchor Rods: [X] A193 Grade B7 22mm (7/8") diameter rods
- Loading Beam: [X] A325 19.1 mm (3/4") bolts [X] 6 shear bolts + 2 anchor rods
- Base: [X] A325 19.1 mm (3/4") bolts [X] 6 shear bolts + 2 anchor rods
- Back-to-Back Chord Studs: [X] No.10 gauge 19.1 mm (0.075") self-drilling wafer head (2@300mm (12") O.C.)

SHEATHING FASTENER SCHEDULE: [X] 50 mm (2/12") [ ] 75 mm (3/12") [ ] 100 mm (4/12") [ ] 150 mm (6/12")

EDGE PANEL DISTANCE: [X] 3/8" [ ] 1/2" [ ] Other:

STUDS:
- [X] 92.1 W x 41.3 F x 12.7 mm Lip (3-5/8"x1-5/8"x1/2"); Thickness: 1.09 mm (0.043") 230 MPa (33ksi)
- [ ] 92.1 W x 41.3 F x 12.7 mm Lip (3-5/8"x1-5/8"x1/2"); Thickness: 1.37 mm (0.054") 345 MPa (50ksi)
- [X] Double chord studs used
- [ ] Other

STUD SPACING: [X] 600 mm (24") O.C.

TRACK:
- Web: 92.1 mm (3-5/8") [X] T= 1.09 mm (0.043") 230 Mpa (33ksi)
- Flange: 31.8 mm (1-1/4") [ ] T= 1.37 mm (0.054") 345 Mpa (50ksi)

HOLD DOWNS:
- [X] Simpson Strong-Tie S/HD10S (# of screws): 33 per H.D.
- [ ] Other

TEST PROTOCOL AND DESCRIPTION:
- [ ] Monotonic (Displacement control)
- [X] Reserved Cyclic (Displacement control) CUREE cyclic protocol @ 0.1 Hz

MEASUREMENT INSTRUMENTS:
- [X] MTS Actuator LVDT
- [X] North Uplift LVDT
- [X] South Uplift LVDT
- [X] MTS Actuator Load Cell
- [X] String Potentiometer
- [X] North Slip LVDT
- [X] South Slip LVDT
- [X] Load Cell North (Hold down)
- [X] Load Cell South (Hold down)

DATA ACQ. RECORD RATE: 50 scan/sec **MONITOR RATE:** 10 scan/sec

COMMENTS:
- Gravity load of approximately 12.25 kN applied to wall top
- Hold down anchor rods pre-tensioned to 7442 N North & 9611 N South
- square plate washers 75 x 75 x 6 mm used on top and bottom shear bolt connections

Figure C.10 Test data sheet for test B2-R

Cold Formed Steel Framed/Steel Sheathed Shear Walls
McGill University, Montreal

TEST: B3-R

RESEARCHER: Jamin DaBreo **ASSISTANTS:** Anthony Caruso, Nicholas DiTommaso

DATE: 30/08/2010 **TIME:** 11:06:54 AM

DIMENSIONS OF WALL: 1220 mm (W) 2440 mm (H) **PANEL ORIENTATION:** Vertical
Sheathing one side

SHEATHING:
0.457 mm (0.018") Sheet Steel 230 MPa (33 ksi)
X 0.762 mm (0.030") Sheet Steel 230 MPa (33 ksi)

Connections:

Sheathing:	X	No.8 gauge 19 mm (0.75") self-drilling square drive pan head screws		
Framing:	X	No.8 gauge 12.5 mm (0.5") self-drilling wafer head screws		
Hold downs:	X	No.10 gauge 25.4 mm (1.0") self-drilling Hex head screws		
Anchor Rods:	X	A193 Grade B7 22mm (7/8") diameter rods		
Loading Beam:	X	A325 19.1 mm (3/4") bolts	X	6 shear bolts + 2 anchor rods
Base:	X	A325 19.1 mm (3/4") bolts	X	6 shear bolts + 2 anchor rods
Back-to-Back Chord Studs:	X	No.10 gauge 19.1 mm (0.075") self-drilling wafer head (2@300mm (12") O.C.)		

SHEATHING FASTENER SCHEDULE: [ ] 50 mm (2/12") [ ] 75 mm (3/12") [X] 100 mm (4/12") [ ] 150 mm (6/12")

EDGE PANEL DISTANCE: [X] 3/8" [ ] 1/2" [ ] Other:

STUDS:
[X] 92.1 W x 41.3 F x 12.7 mm Lip (3-5/8"x1-5/8"x1/2"); Thickness: 1.09 mm (0.043") 230 MPa (33ksi)
[ ] 92.1 W x 41.3 F x 12.7 mm Lip (3-5/8"x1-5/8"x1/2"); Thickness: 1.37 mm (0.054") 345 MPa (50ksi)
[X] Double chord studs used
[ ] Other

STUD SPACING: [X] 600 mm (24") O.C.

TRACK:
Web: 92.1 mm (3-5/8") [X] T= 1.09 mm (0.043") 230 Mpa (33ksi)
Flange: 31.8 mm (1-1/4") [ ] T= 1.37 mm (0.054") 345 Mpa (50ksi)

HOLD DOWNS:
[X] Simpson Strong-Tie S/HD10S (# of screws): 33 per H.D.
[ ] Other

TEST PROTOCOL AND DESCRIPTION:
[ ] Monotonic (Displacement control)
[X] Reserved Cyclic (Displacement control) CUREE cyclic protocol @ 0.1 Hz

MEASUREMENT INSTRUMENTS:

X	MTS Actuator LVDT	X	North Slip LVDT
X	North Uplift LVDT	X	South Slip LVDT
X	South Uplift LVDT	X	Load Cell North (Hold down)
X	MTS Actuator Load Cell	X	Load Cell South (Hold down)
X	String Potentiometer		

DATA ACQ. RECORD RATE: 50 scan/sec **MONITOR RATE:** 10 scan/sec

COMMENTS:
– Gravity load of approximately 12.25 kN applied to wall top
– Hold down anchor rods pre-tensioned to 6162 N North & 8888 N South
– square plate washers 75 x 75 x 6 mm used on top and bottom shear bolt connections

Figure C.11 Test data sheet for test B3-R

Cold Formed Steel Framed/Steel Sheathed Shear Walls
McGill University, Montreal

TEST:	B4-R		
RESEARCHER:	Jamin DaBreo	**ASSISTANTS:**	Anthony Caruso, Nicholas DiTommaso
DATE:	27/08/2010	**TIME:**	2:39:33 PM
DIMENSIONS OF WALL:	1220 mm (W) 2440 mm (H)	**PANEL ORIENTATION:**	Vertical Sheathing one side

SHEATHING:
- [ ] 0.457 mm (0.018") Sheet Steel 230 MPa (33 ksi)
- [X] 0.762 mm (0.030") Sheet Steel 230 MPa (33 ksi)

Connections:
- Sheathing: [X] No.8 gauge 19 mm (0.75") self-drilling square drive pan head screws
- Framing: [X] No.8 gauge 12.5 mm (0.5") self-drilling wafer head screws
- Hold downs: [X] No.10 gauge 25.4 mm (1.0") self-drilling Hex head screws
- Anchor Rods: [X] A193 Grade B7 22mm (7/8") diameter rods
- Loading Beam: [X] A325 19.1 mm (3/4") bolts [X] 6 shear bolts + 2 anchor rods
- Base: [X] A325 19.1 mm (3/4") bolts [X] 6 shear bolts + 2 anchor rods
- Back-to-Back Chord Studs: [X] No.10 gauge 19.1 mm (0.075") self-drilling wafer head (2@300mm (12") O.C.)

SHEATHING FASTENER SCHEDULE: [ ] 50 mm (2/12") [ ] 75 mm (3/12") [ ] 100 mm (4/12") [X] 150 mm (6/12")

EDGE PANEL DISTANCE: [X] 3/8" [ ] 1/2" [ ] Other:

STUDS:
- [X] 92.1 W x 41.3 F x 12.7 mm Lip (3-5/8"x1-5/8"x1/2"); Thickness: 1.09 mm (0.043") 230 MPa (33ksi)
- [ ] 92.1 W x 41.3 F x 12.7 mm Lip (3-5/8"x1-5/8"x1/2"); Thickness: 1.37 mm (0.054") 345 MPa (50ksi)
- [X] Double chord studs used
- [ ] Other

STUD SPACING: [X] 600 mm (24") O.C.

TRACK:
- Web: 92.1 mm (3-5/8")
- Flange: 31.8 mm (1-1/4")
- [X] T= 1.09 mm (0.043") 230 Mpa (33ksi)
- [ ] T= 1.37 mm (0.054") 345 Mpa (50ksi)

HOLD DOWNS:
- [X] Simpson Strong-Tie S/HD10S (# of screws): 33 per H.D.
- [ ] Other

TEST PROTOCOL AND DESCRIPTION:
- [ ] Monotonic (Displacement control)
- [X] Reserved Cyclic (Displacement control) CUREE cyclic protocol @ 0.1 Hz

MEASUREMENT INSTRUMENTS:
- [X] MTS Actuator LVDT
- [X] North Uplift LVDT
- [X] South Uplift LVDT
- [X] MTS Actuator Load Cell
- [X] String Potentiometer
- [X] North Slip LVDT
- [X] South Slip LVDT
- [X] Load Cell North (Hold down)
- [X] Load Cell South (Hold down)

DATA ACQ. RECORD RATE: 50 scan/sec **MONITOR RATE:** 10 scan/sec

COMMENTS:
- Gravity load of approximately 12.25 kN applied to wall top
- Hold down anchor rods pre-tensioned to 6413 N North & 8860 N South
- square plate washers 75 x 75 x 6 mm used on top and bottom shear bolt connections

Figure C.12 Test data sheet for test B4-R

Cold Formed Steel Framed/Steel Sheathed Shear Walls
McGill University, Montreal

TEST:	B5-R		
RESEARCHER:	Jamin DaBreo	**ASSISTANTS:**	Anthony Caruso, Nicholas DiTommaso
DATE:	31/08/2010	**TIME:**	12:39:43 PM
DIMENSIONS OF WALL:	1220 mm (W) 2440 mm (H)	**PANEL ORIENTATION:**	Vertical Sheathing one side

SHEATHING:
- [X] 0.457 mm (0.018") Sheet Steel 230 MPa (33 ksi)
- [ ] 0.762 mm (0.030") Sheet Steel 230 MPa (33 ksi)

Connections:
- Sheathing: [X] No.8 gauge 19 mm (0.75") self-drilling square drive pan head screws
- Framing: [X] No.8 gauge 12.5 mm (0.5") self-drilling wafer head screws
- Hold downs: [X] No.10 gauge 25.4 mm (1.0") self-drilling Hex head screws
- Anchor Rods: [X] A193 Grade B7 22mm (7/8") diameter rods
- Loading Beam: [X] A325 19.1 mm (3/4") bolts — [X] 6 shear bolts + 2 anchor rods
- Base: [X] A325 19.1 mm (3/4") bolts — [X] 6 shear bolts + 2 anchor rods
- Back-to-Back Chord Studs: [X] No.10 gauge 19.1 mm (0.075") self-drilling wafer head (2@300mm (12") O.C.)

SHEATHING FASTENER SCHEDULE: [ ] 50 mm (2/12") [ ] 75 mm (3/12") [X] 100 mm (4/12") [ ] 150 mm (6/12")

EDGE PANEL DISTANCE: [X] 3/8" [ ] 1/2" [ ] Other:

STUDS:
- [X] 92.1 W x 41.3 F x 12.7 mm Lip (3-5/8"x1-5/8"x1/2"); Thickness: 1.09 mm (0.043") 230 MPa (33ksi)
- [ ] 92.1 W x 41.3 F x 12.7 mm Lip (3-5/8"x1-5/8"x1/2"); Thickness: 1.37 mm (0.054") 345 MPa (50ksi)
- [X] Double chord studs used
- [ ] Other

STUD SPACING: [X] 600 mm (24") O.C.

TRACK:
- Web: 92.1 mm (3-5/8") — [X] T= 1.09 mm (0.043") 230 Mpa (33ksi)
- Flange: 31.8 mm (1-1/4") — [ ] T= 1.37 mm (0.054") 345 Mpa (50ksi)

HOLD DOWNS:
- [X] Simpson Strong-Tie S/HD10S — (# of screws): 33 per H.D.
- [ ] Other

TEST PROTOCOL AND DESCRIPTION:
- [ ] Monotonic (Displacement control)
- [X] Reserved Cyclic (Displacement control) — CUREE cyclic protocol @ 0.1 Hz

MEASUREMENT INSTRUMENTS:
- [X] MTS Actuator LVDT
- [X] North Uplift LVDT
- [X] South Uplift LVDT
- [X] MTS Actuator Load Cell
- [X] String Potentiometer
- [X] North Slip LVDT
- [X] South Slip LVDT
- [X] Load Cell North (Hold down)
- [X] Load Cell South (Hold down)

DATA ACQ. RECORD RATE: 50 scan/sec **MONITOR RATE:** 10 scan/sec

COMMENTS:
- Gravity load of approximately 12.25 kN applied to wall top
- Hold down anchor rods pre-tensioned to 6357 N North & 8804 N South
- square plate washers 75 x 75 x 6 mm used on top and bottom shear bolt connections

Figure C.13 Test data sheet for test B5-R

Cold Formed Steel Framed/Steel Sheathed Shear Walls
McGill University, Montreal

TEST:	B6-R		
RESEARCHER:	Jamin DaBreo	**ASSISTANTS:**	Anthony Caruso, Nicholas DiTommaso
DATE:	26/08/2010	**TIME:**	2:39:58 PM
DIMENSIONS OF WALL:	1220 mm (W) 2440 mm (H)	**PANEL ORIENTATION:**	Vertical Sheathing one side

SHEATHING:
- [X] 0.457 mm (0.018") Sheet Steel 230 MPa (33 ksi)
- [ ] 0.762 mm (0.030") Sheet Steel 230 MPa (33 ksi)

Connections:
- Sheathing: [X] No.8 gauge 19 mm (0.75") self-drilling square drive pan head screws
- Framing: [X] No.8 gauge 12.5 mm (0.5") self-drilling wafer head screws
- Hold downs: [X] No.10 gauge 25.4 mm (1.0") self-drilling Hex head screws
- Anchor Rods: [X] A193 Grade B7 22mm (7/8") diameter rods
- Loading Beam: [X] A325 19.1 mm (3/4") bolts — [X] 6 shear bolts + 2 anchor rods
- Base: [X] A325 19.1 mm (3/4") bolts — [X] 6 shear bolts + 2 anchor rods
- Back-to-Back Chord Studs: [X] No.10 gauge 19.1 mm (0.075") self-drilling wafer head (2@300mm (12") O.C.)

SHEATHING FASTENER SCHEDULE:
[ ] 50 mm (2/12") [ ] 75 mm (3/12") [ ] 100 mm (4/12") [X] 150 mm (6/12")

EDGE PANEL DISTANCE:
[X] 3/8" [ ] 1/2" [ ] Other:

STUDS:
- [X] 92.1 W x 41.3 F x 12.7 mm Lip (3-5/8"x1-5/8"x1/2"); Thickness: 1.09 mm (0.043") 230 MPa (33ksi)
- [ ] 92.1 W x 41.3 F x 12.7 mm Lip (3-5/8"x1-5/8"x1/2"); Thickness: 1.37 mm (0.054") 345 MPa (50ksi)
- [X] Double chord studs used
- [ ] Other

STUD SPACING:
[X] 600 mm (24") O.C.

TRACK:
- Web: 92.1 mm (3-5/8")
- Flange: 31.8 mm (1-1/4")
- [X] T= 1.09 mm (0.043") 230 Mpa (33ksi)
- [ ] T= 1.37 mm (0.054") 345 Mpa (50ksi)

HOLD DOWNS:
- [X] Simpson Strong-Tie S/HD10S
- [ ] Other

(# of screws): 33 per H.D.

TEST PROTOCOL AND DESCRIPTION:
- [ ] Monotonic (Displacement control)
- [X] Reserved Cyclic (Displacement control) — CUREE cyclic protocol @ 0.1 Hz

MEASUREMENT INSTRUMENTS:
- [X] MTS Actuator LVDT
- [X] North Uplift LVDT
- [X] South Uplift LVDT
- [X] MTS Actuator Load Cell
- [X] String Potentiometer
- [X] North Slip LVDT
- [X] South Slip LVDT
- [X] Load Cell North (Hold down)
- [X] Load Cell South (Hold down)

DATA ACQ. RECORD RATE: 50 scan/sec **MONITOR RATE:** 10 scan/sec

COMMENTS:
- Gravity load of approximately 12.25 kN applied to wall top
- Hold down anchor rods pre-tensioned to 6468 N North & 8665 N South
- square plate washers 75 x 75 x 6 mm used on top and bottom shear bolt connections

Figure C.14 Test data sheet for test B6-R

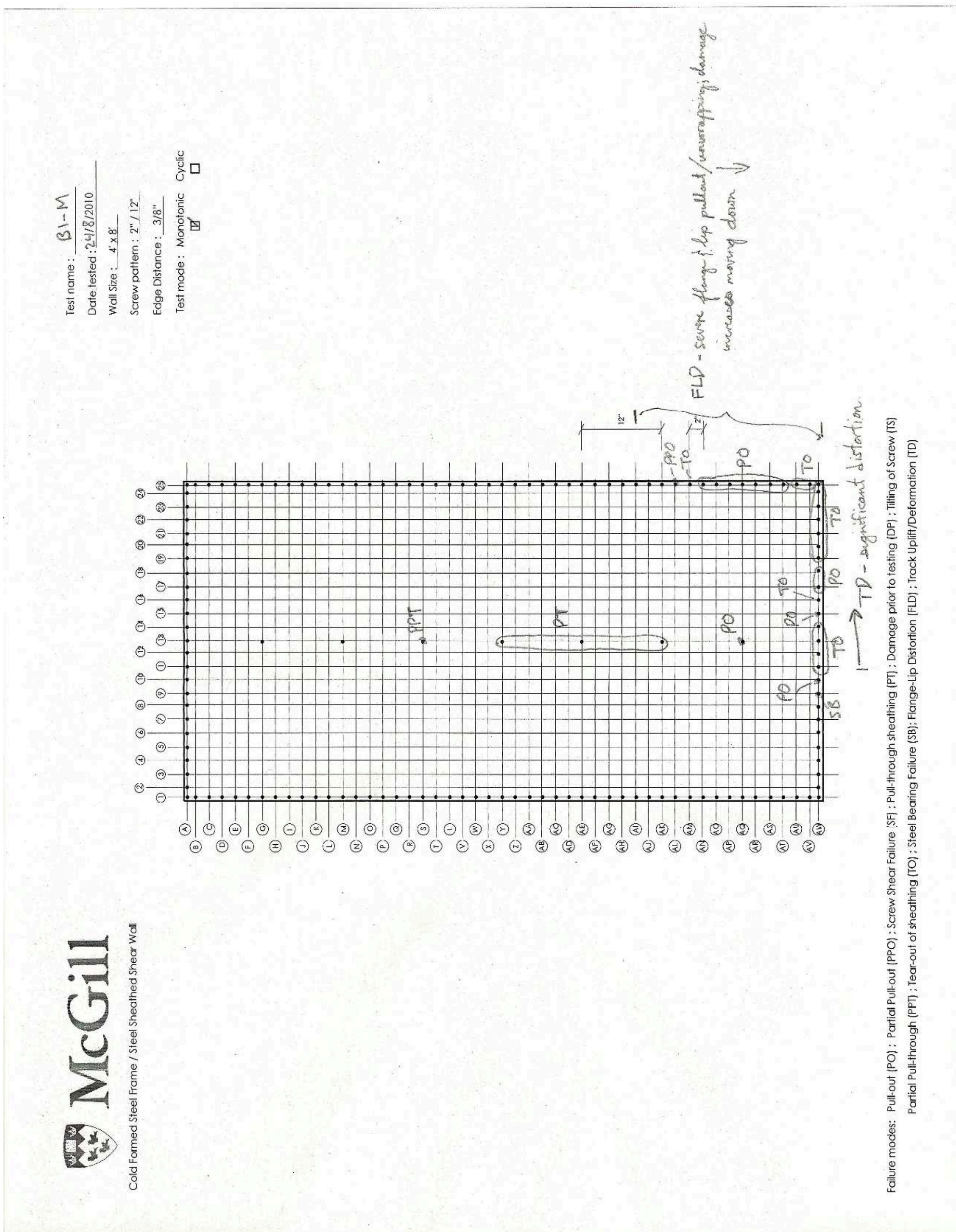

Figure C.15 Observation sheet for test B1-M

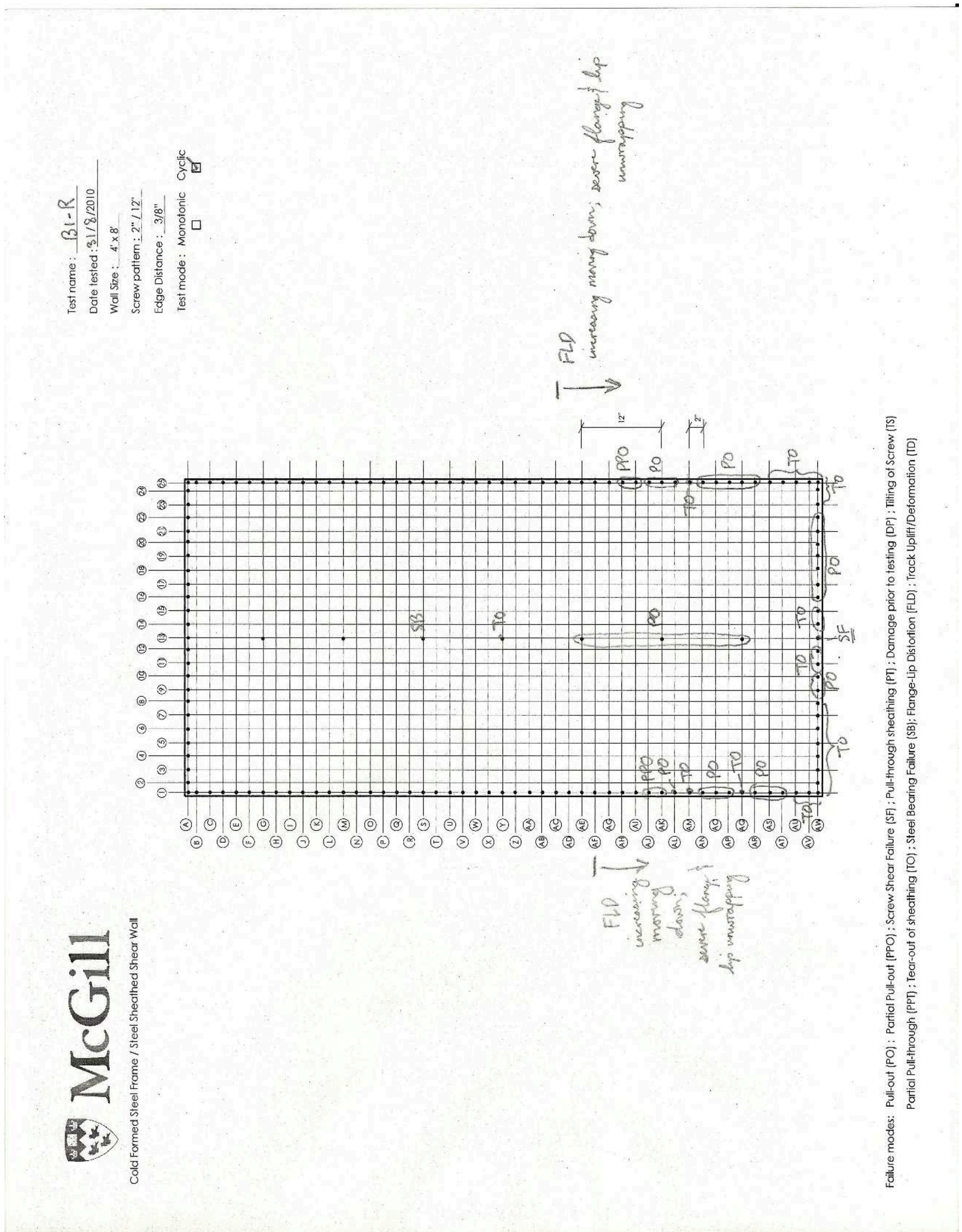

Figure C.16 Observation sheet for test B1-R

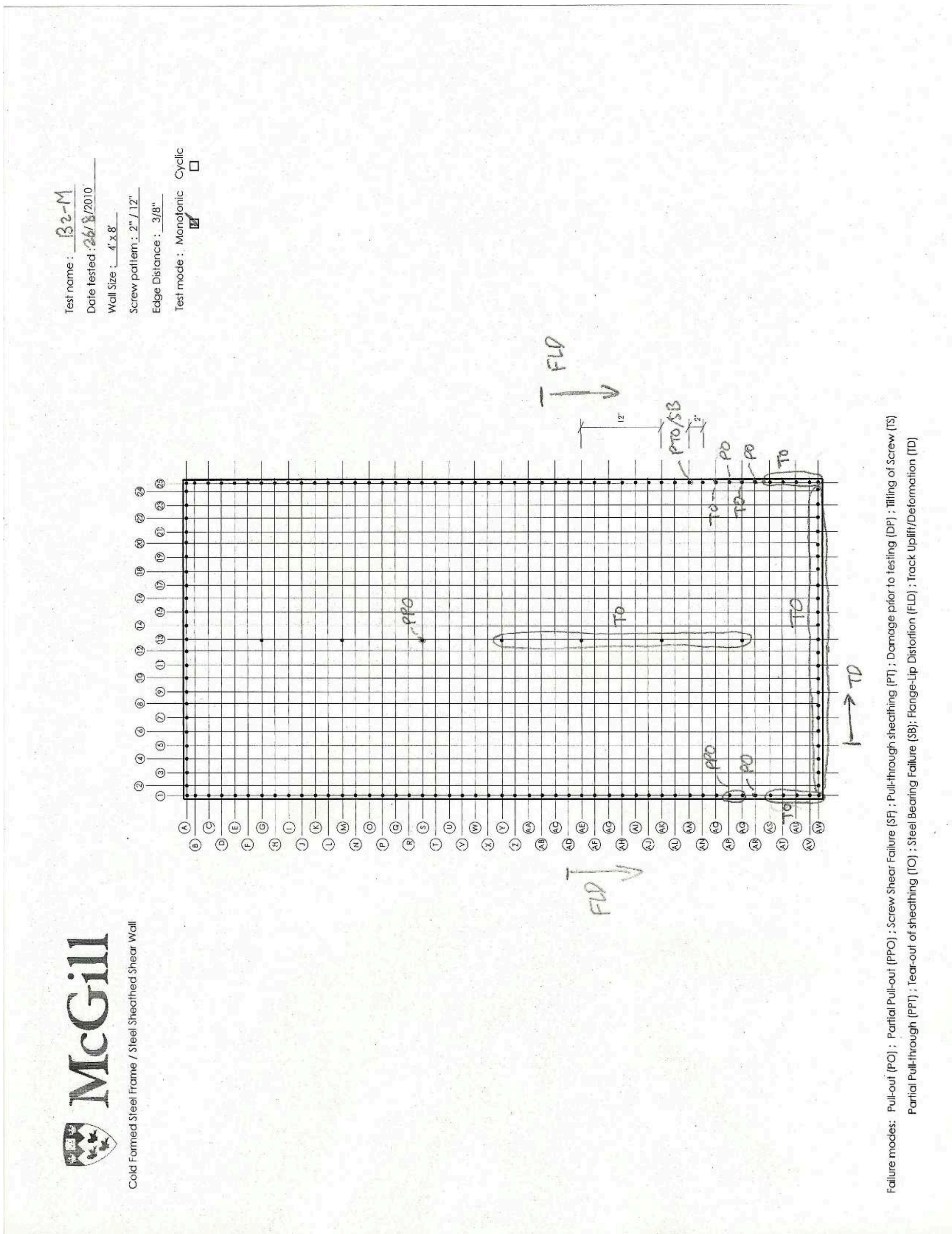

Figure C.17 Observation sheet for test B2-M

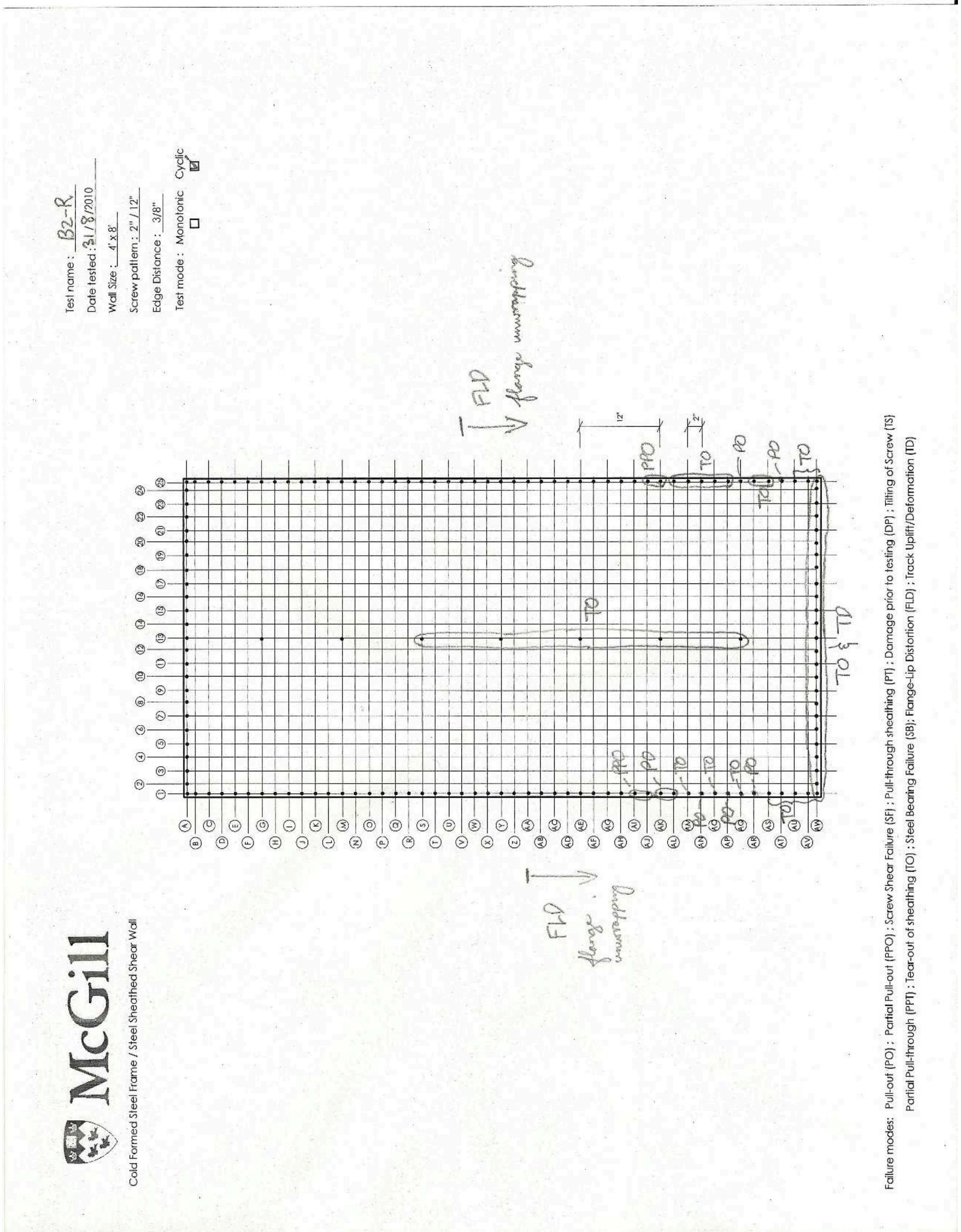

Figure C.18 Observation sheet for test B2-R

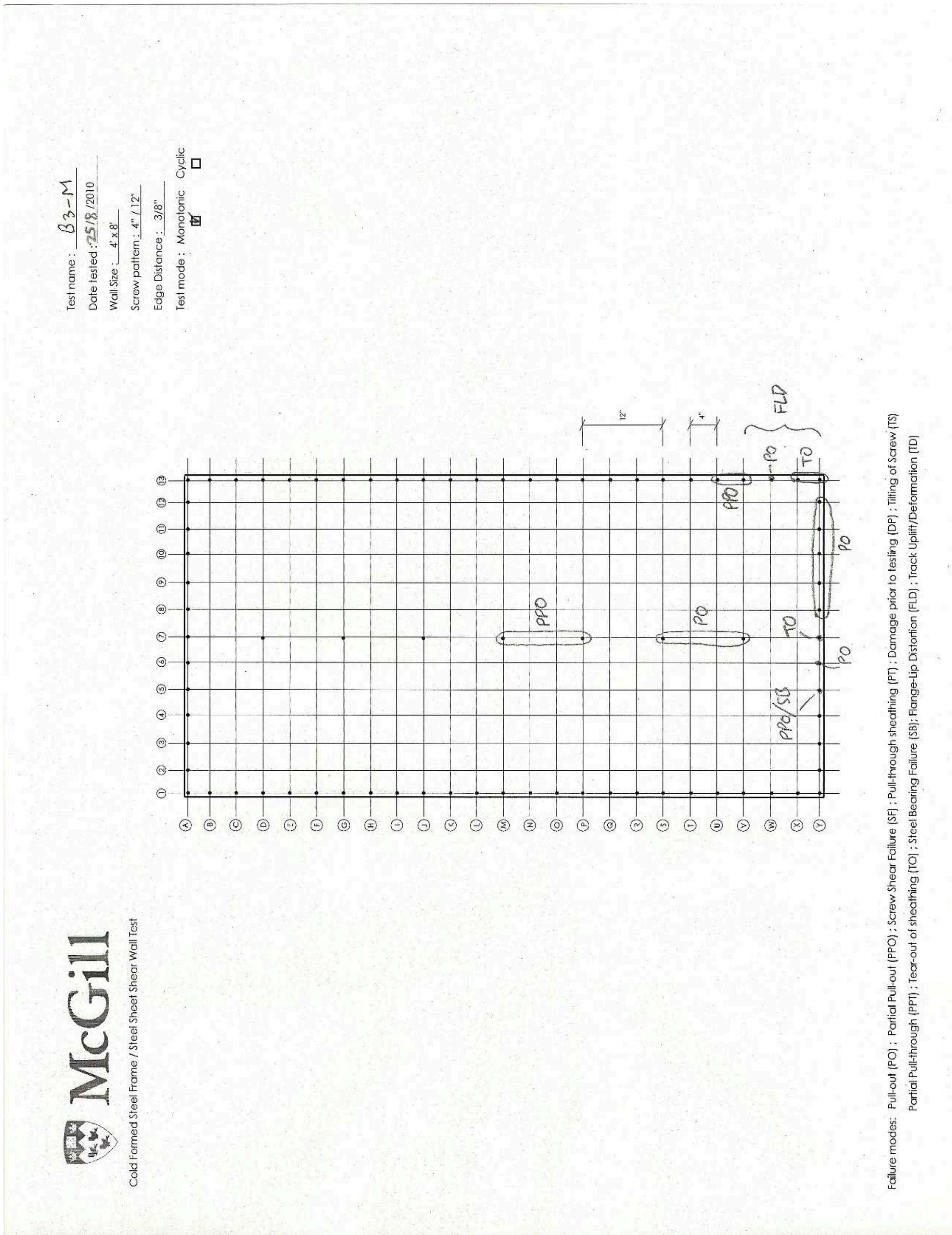

Figure C.19 Observation sheet for test B3-M

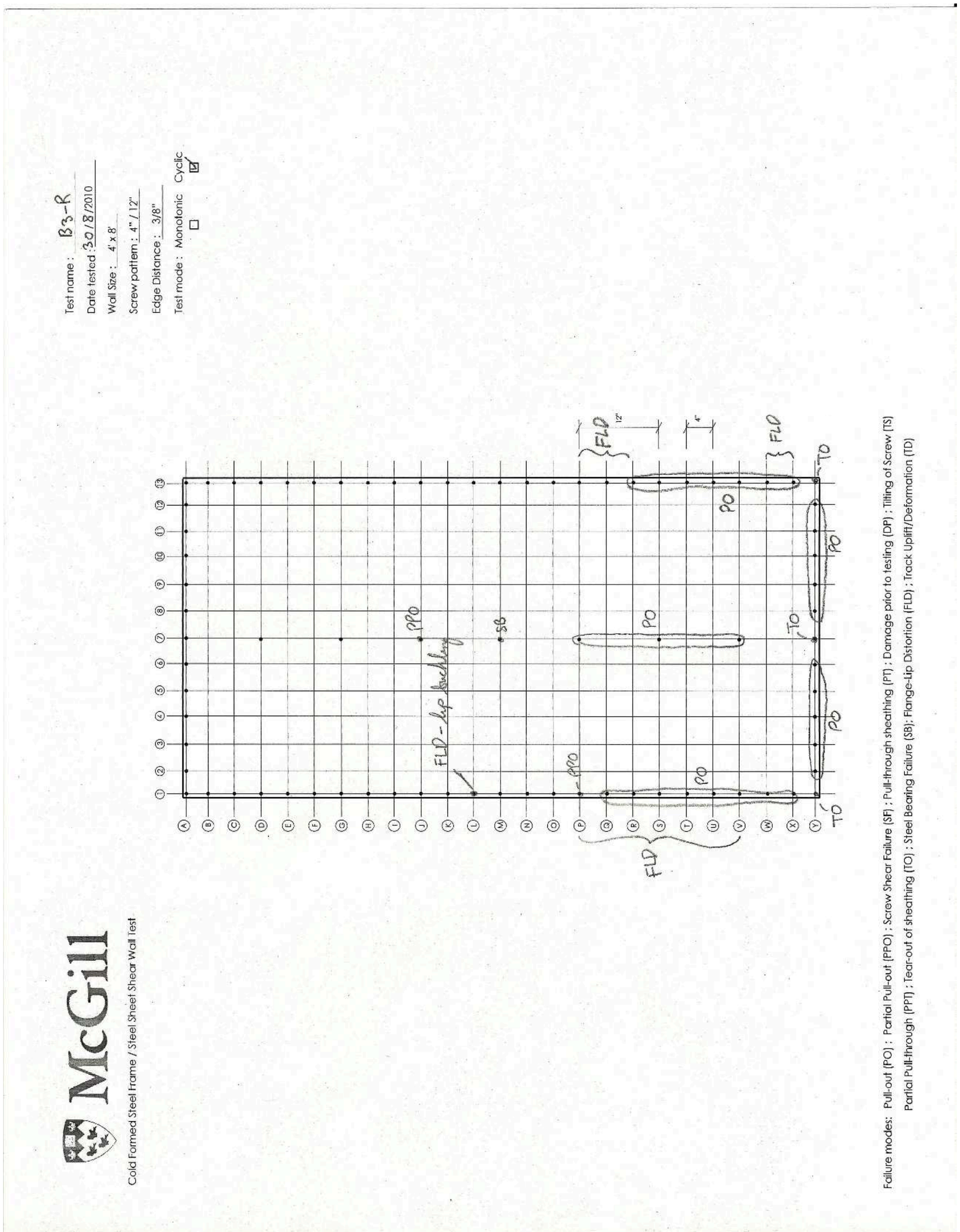

Figure C.20 Observation sheet for test B3-R

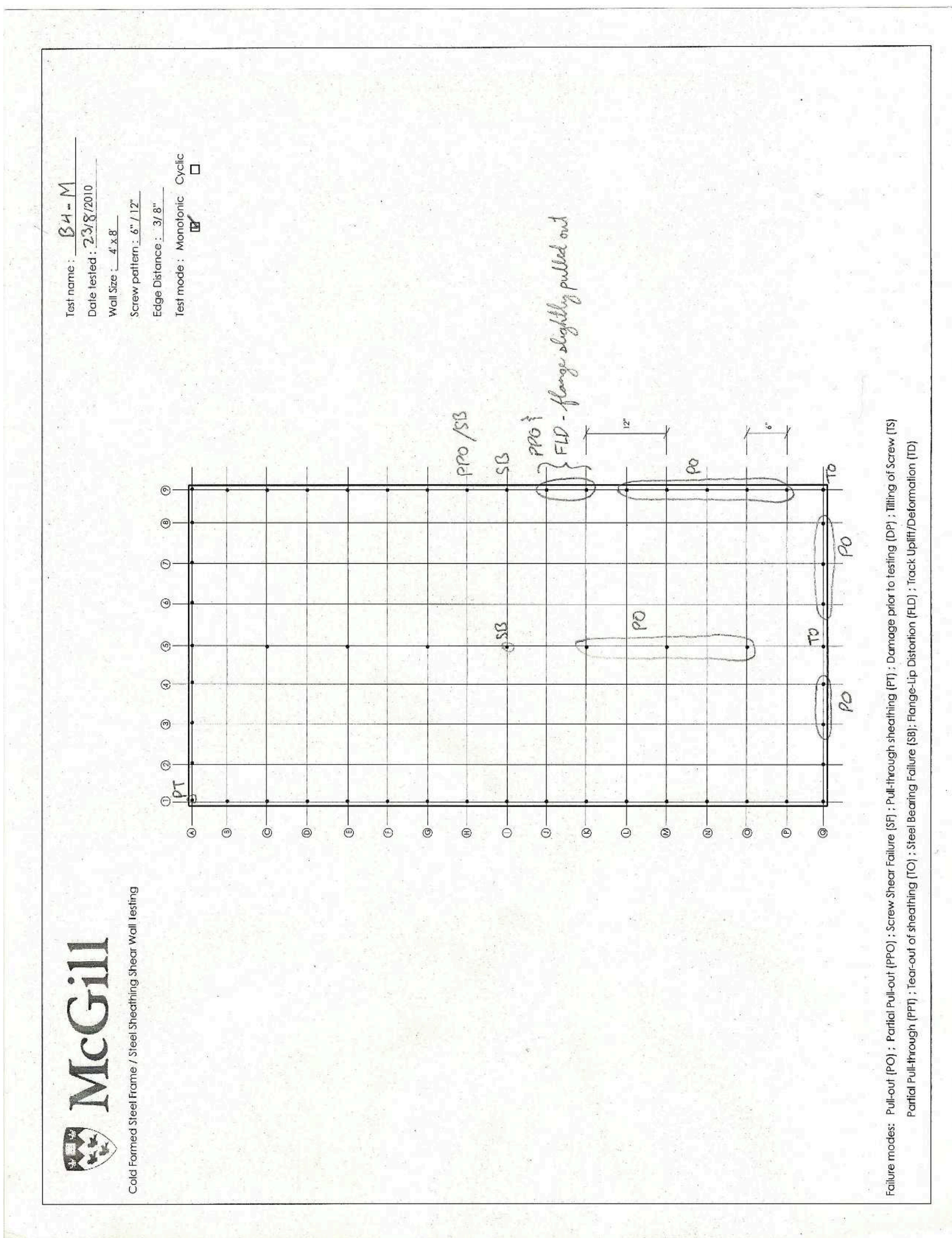

Figure C.21 Observation sheet for test B4-M

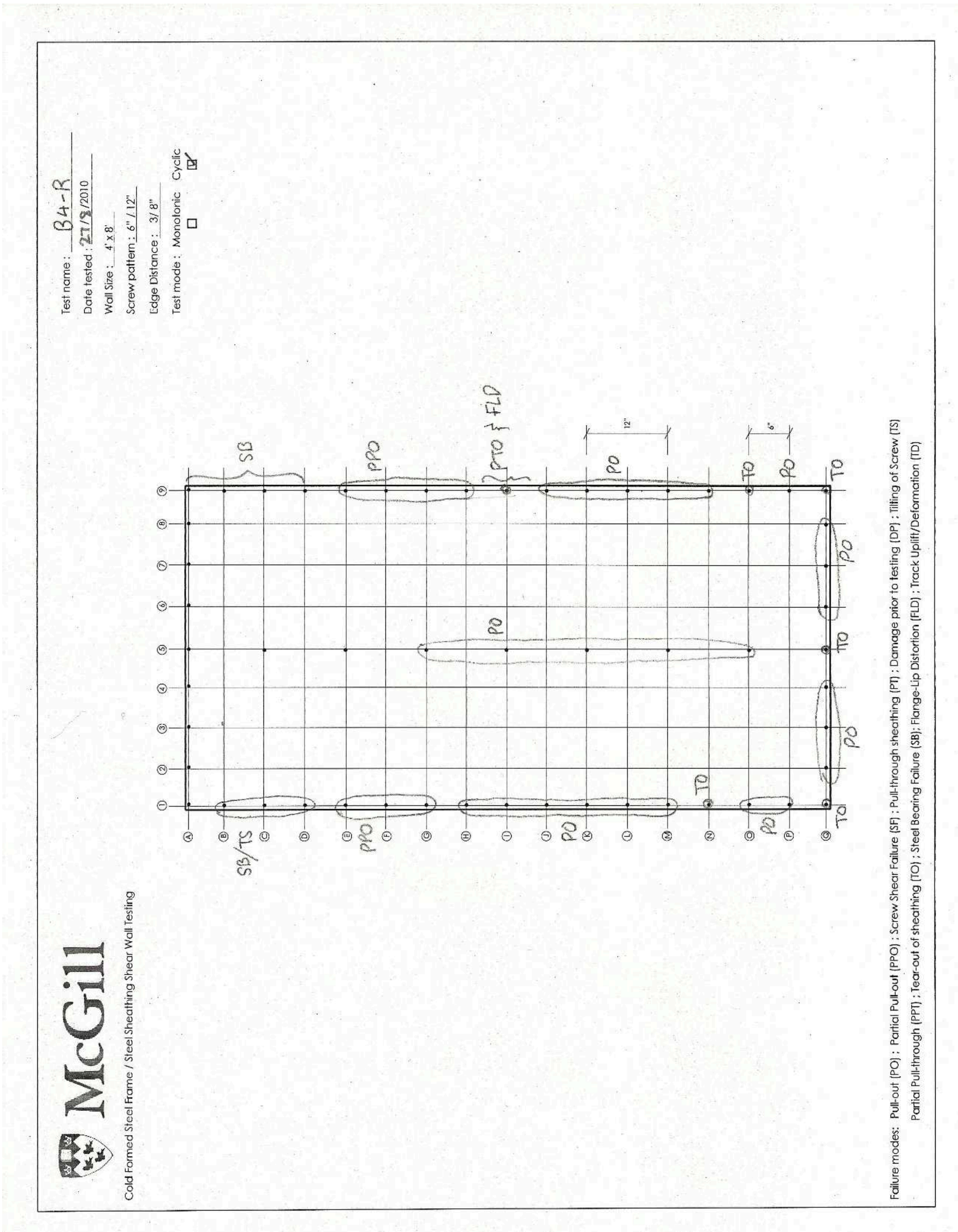

Figure C.22 Observation sheet for test B4-R

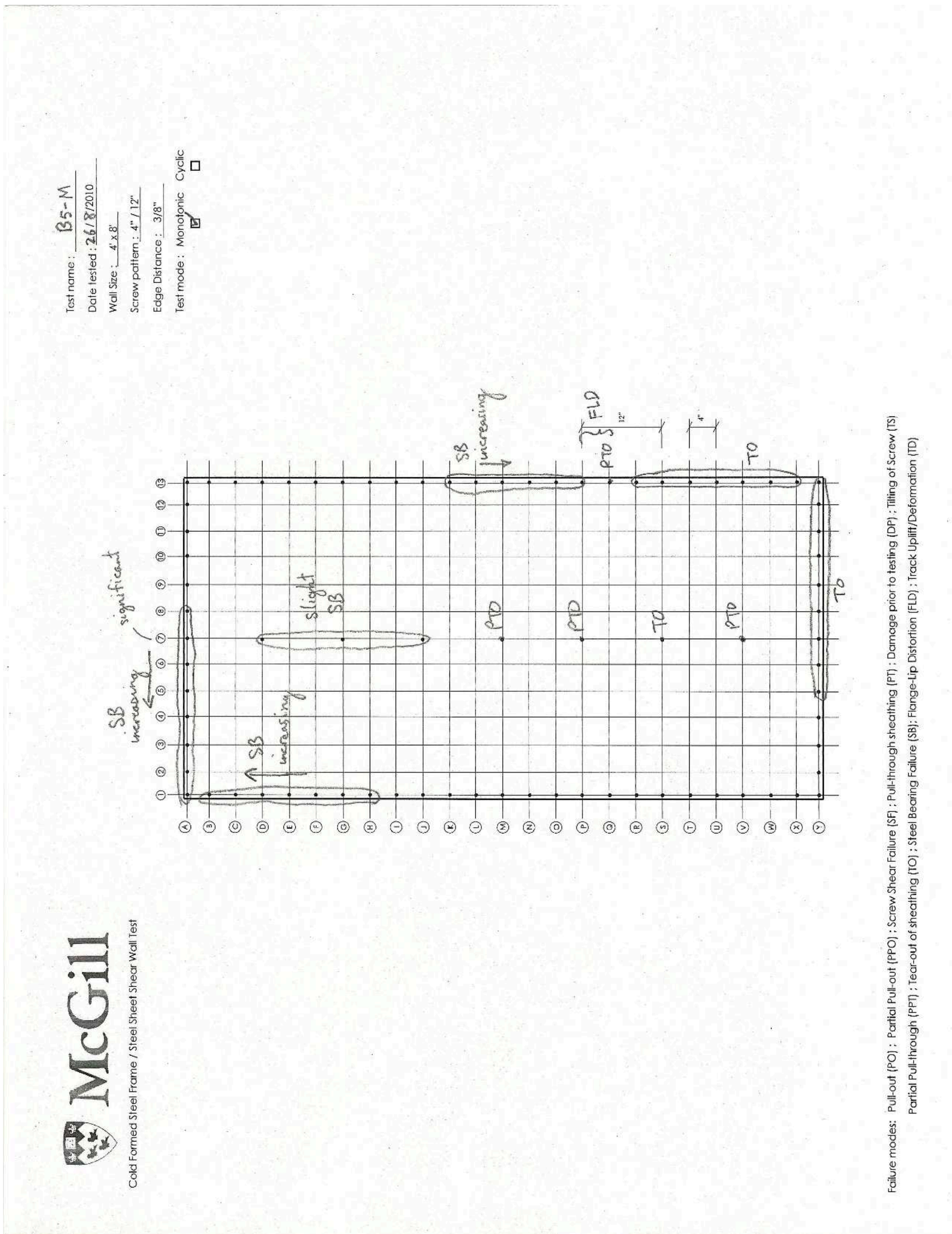

Figure C.23 Observation sheet for test B5-M

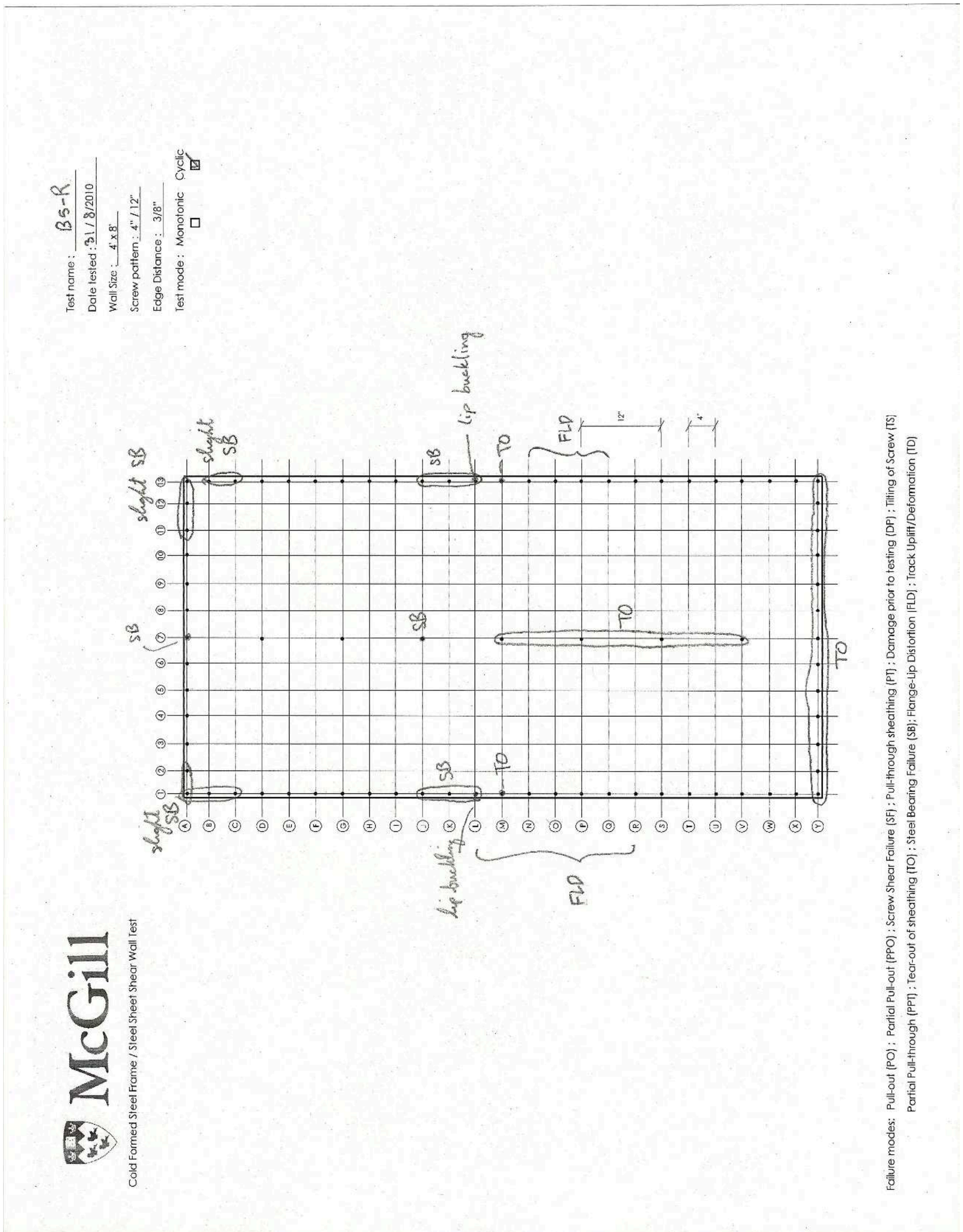

Figure C.24 Observation sheet for test B5-R

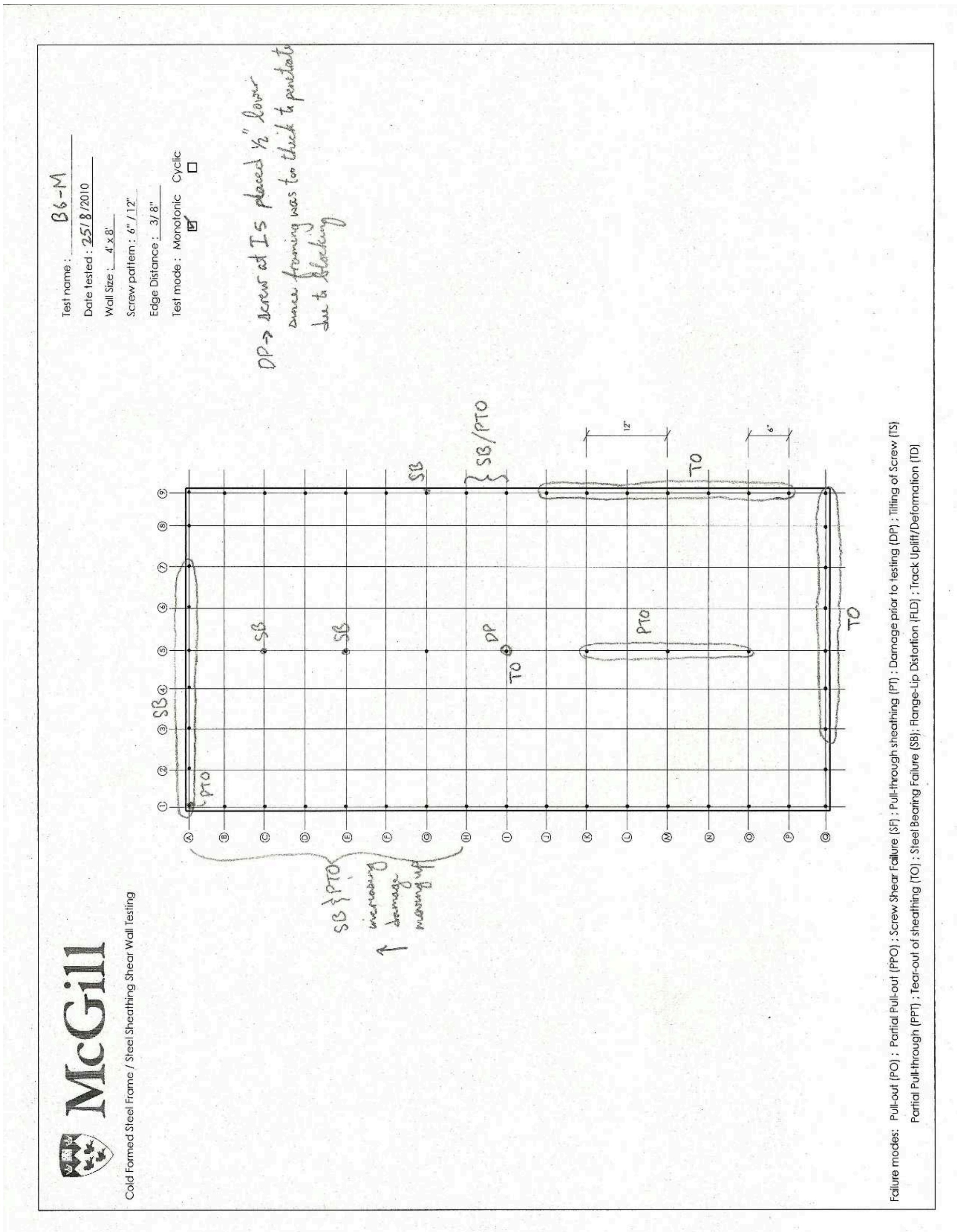

Figure C.25 Observation sheet for test B6-M

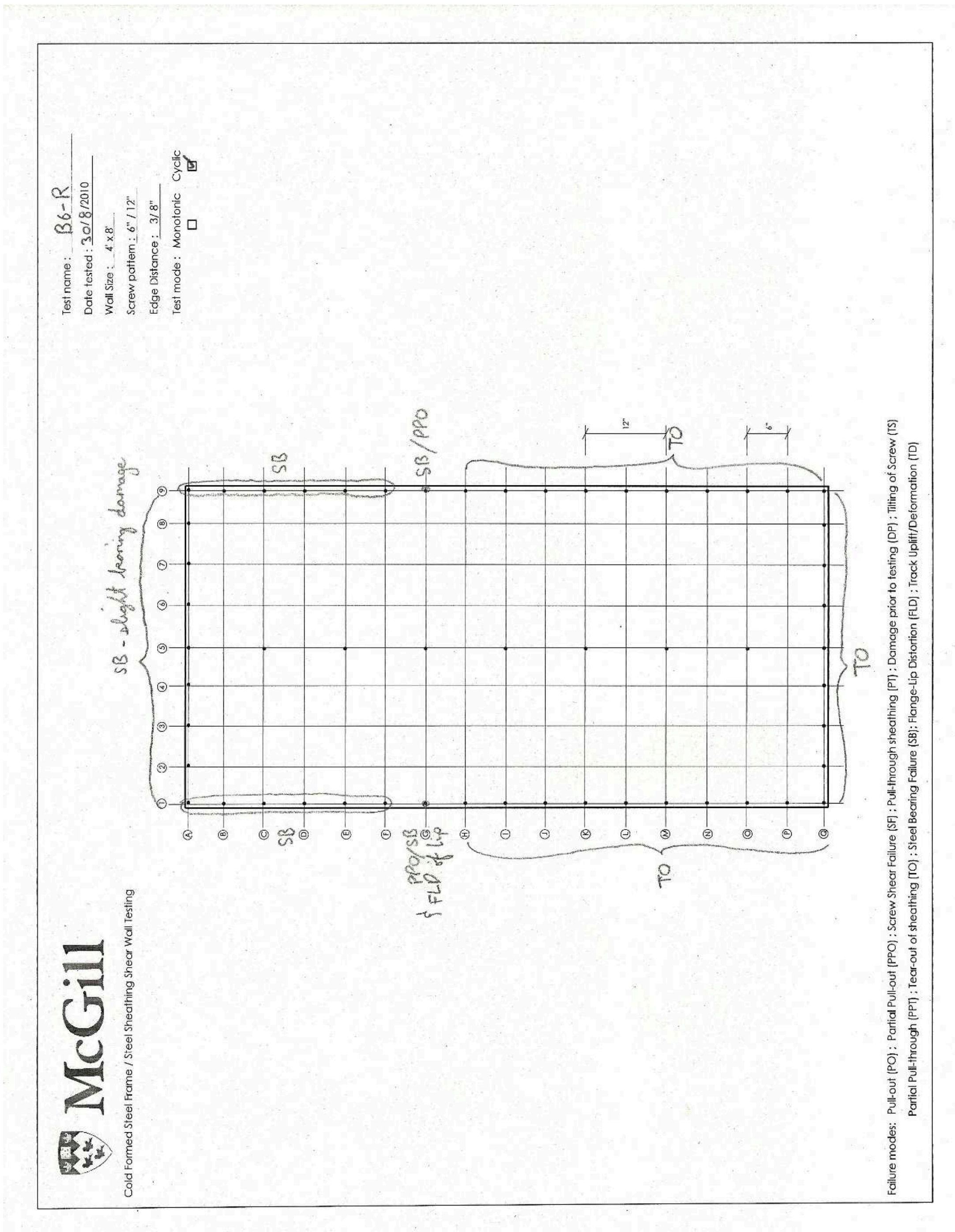

Figure C.26 Observation sheet for test B6-R

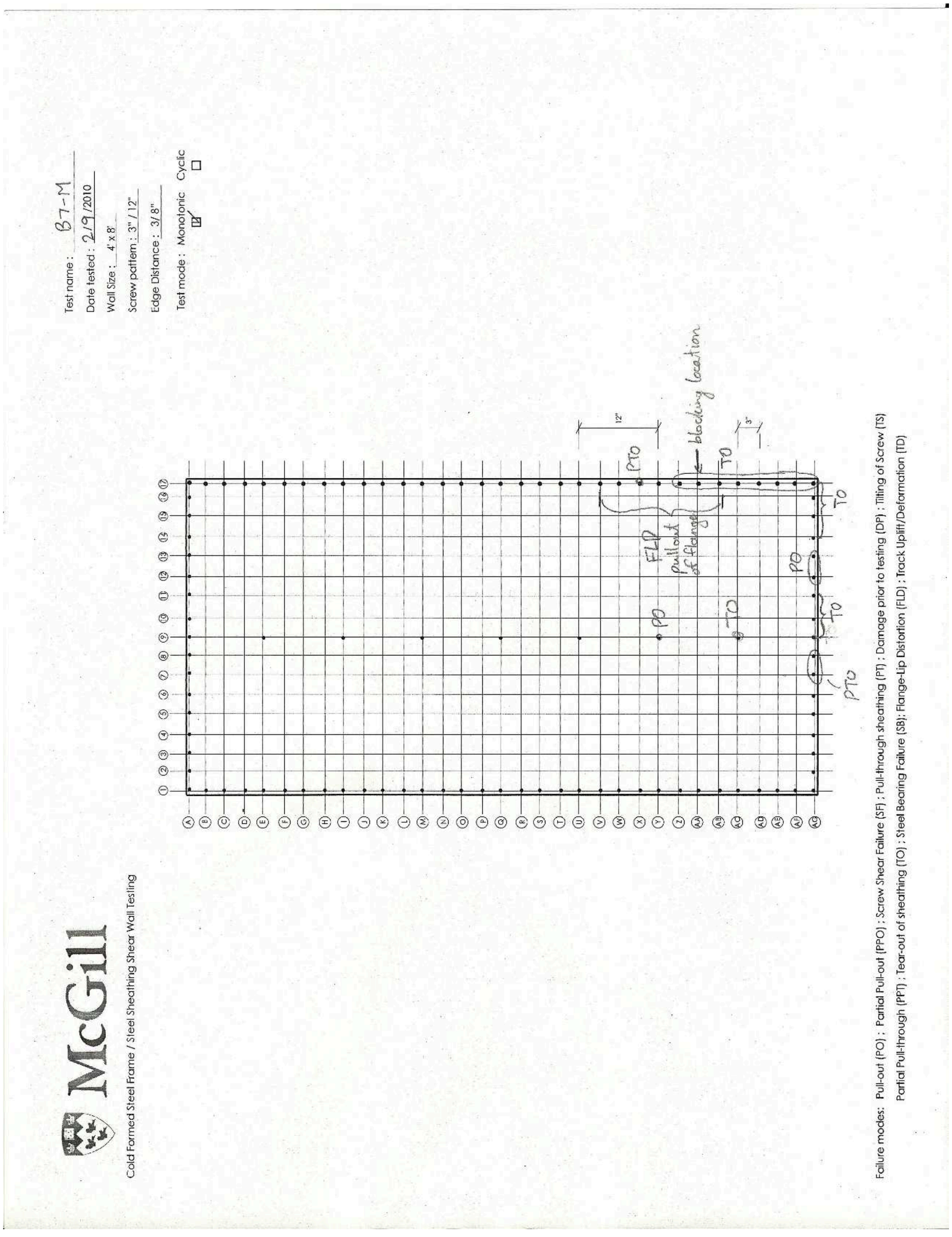

Figure C.27 Observation sheet for test B7-M

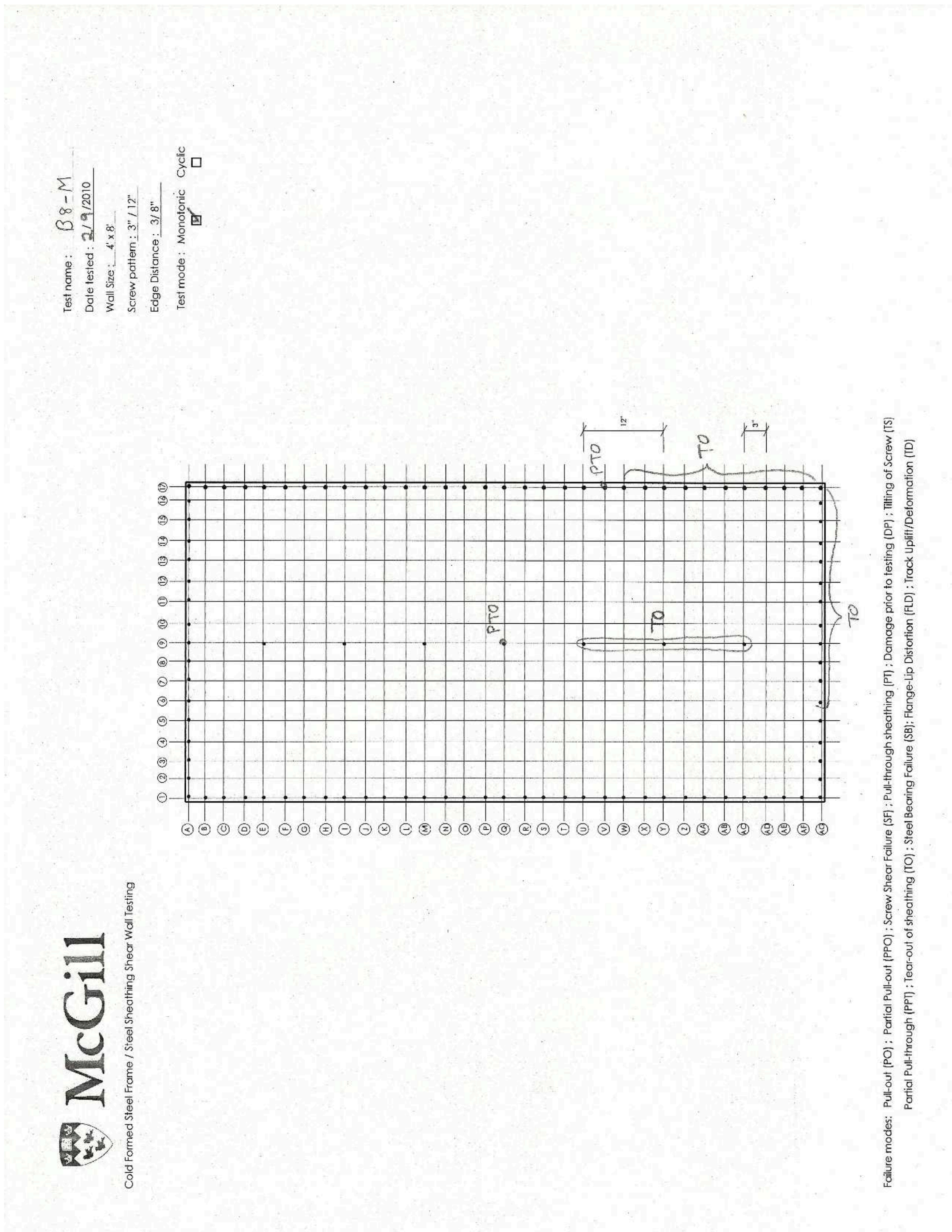

Figure C.28 Observation sheet for test B8-M

APPENDIX D – DISPLACEMENT TIME HISTORIES, RESPONSE CURVES FOR MONONTONIC TESTS& HYSTERESIS CURVES FOR REVERSED CYCLIC TESTS

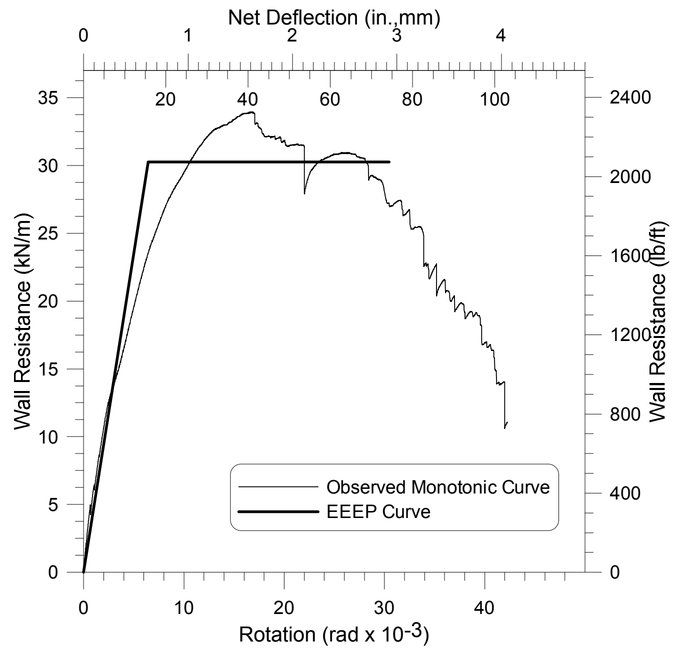

Figure D.1 Resulting EEEP curve for the observed reversed cyclic hysteretic curves (test B1-M)

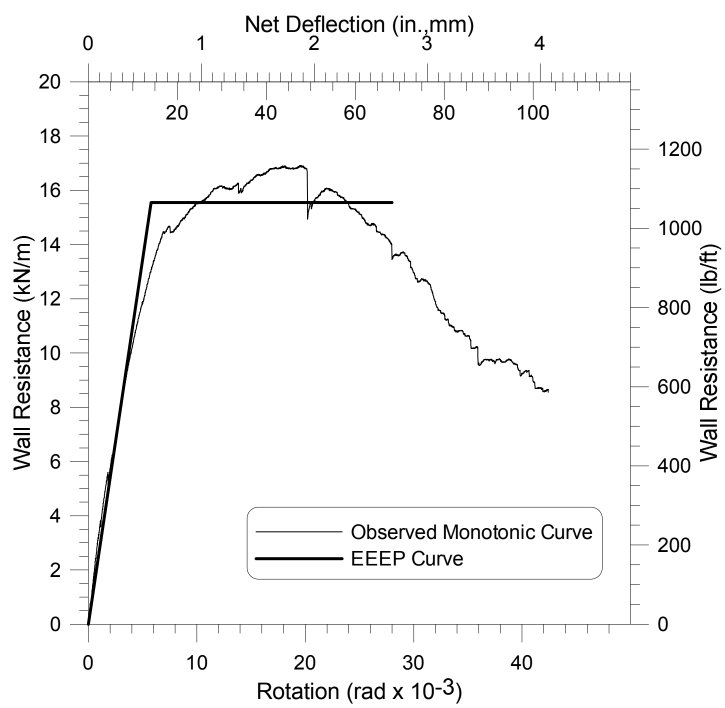

Figure D.2 Resulting EEEP curve for the observed reversed cyclic hysteretic curves (test B2-M)

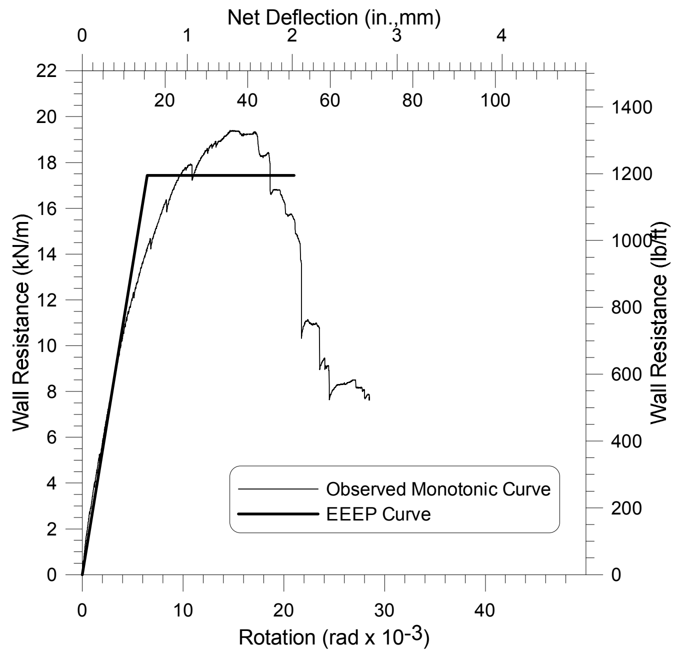

Figure D.3 Resulting EEEP curve for the observed reversed cyclic hysteretic curves (test B3-M)

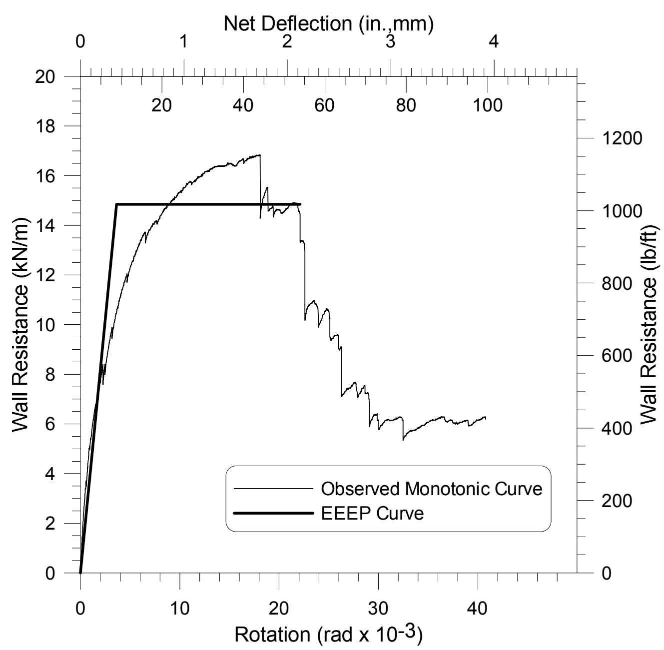

Figure D.4 Resulting EEEP curve for the observed reversed cyclic hysteretic curves (test B4-M)

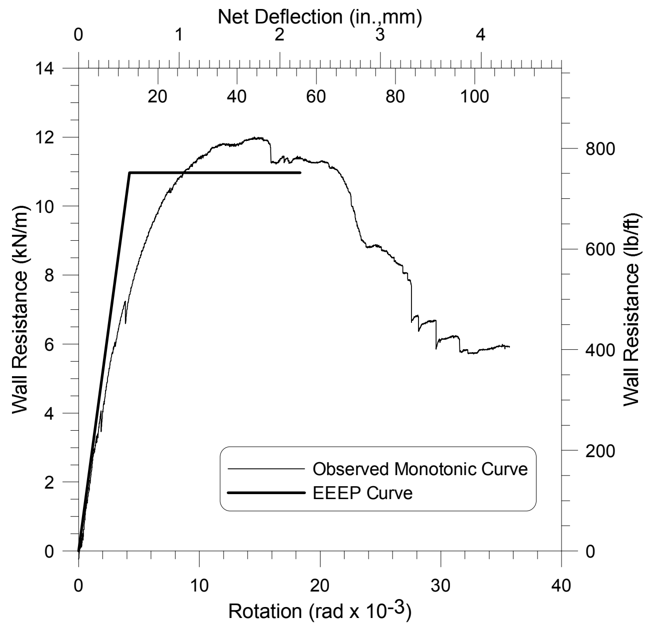

Figure D.5 Resulting EEEP curve for the observed reversed cyclic hysteretic curves (test B5-M)

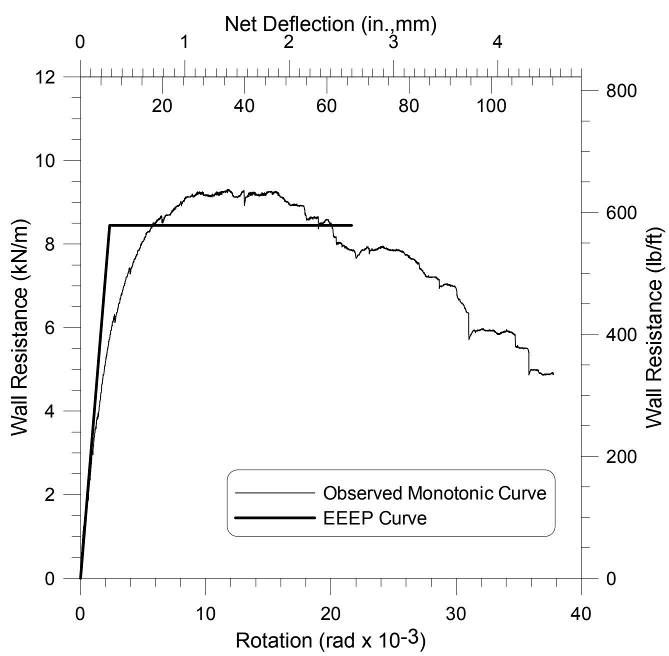

Figure D.6 Resulting EEEP curve for the observed reversed cyclic hysteretic curves (test B6-M)

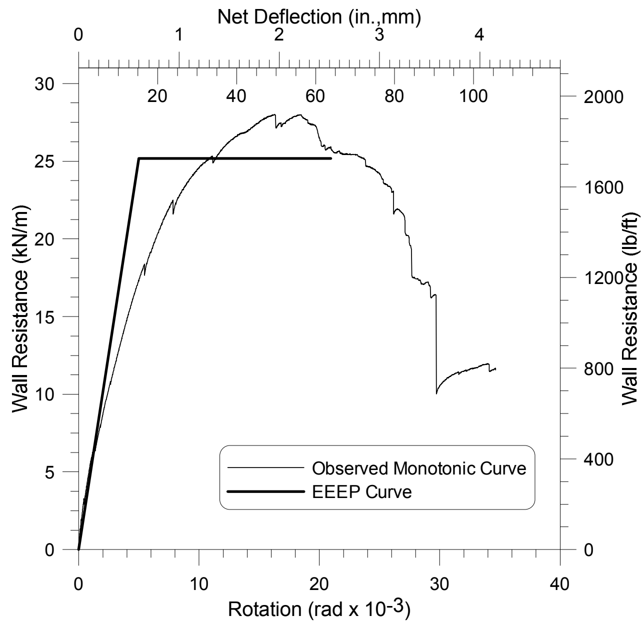

Figure D.7 Resulting EEEP curve for the observed reversed cyclic hysteretic curves (test B7-M)

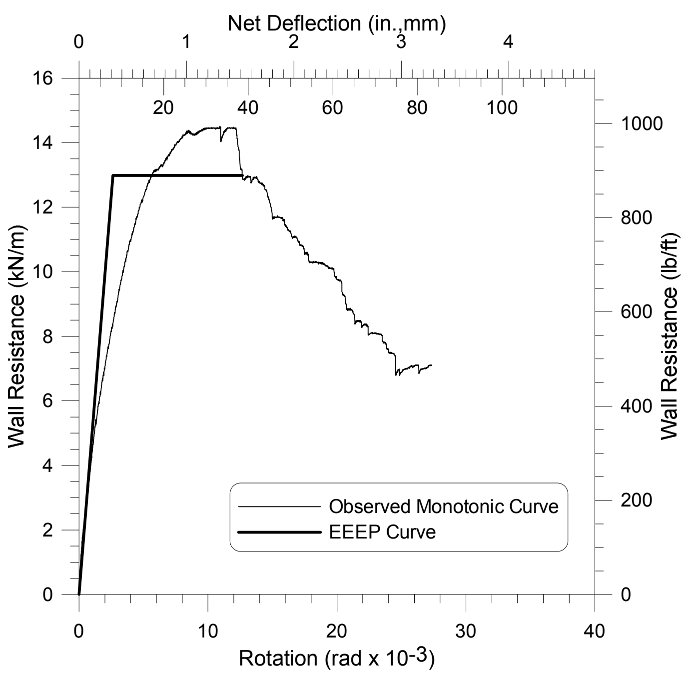

Figure D.8 Resulting EEEP curve for the observed reversed cyclic hysteretic curves (test B8-M)

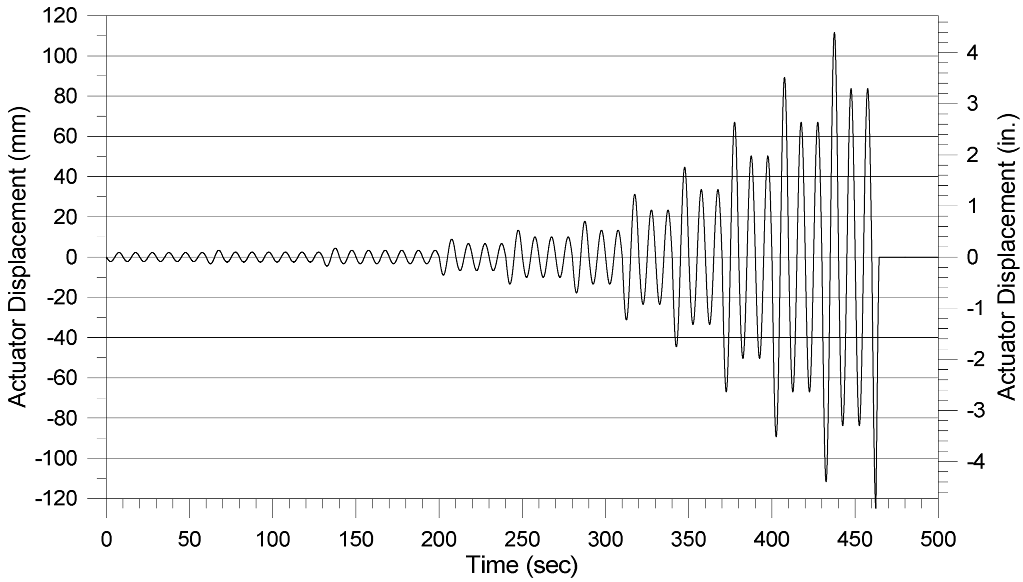

Figure D.9 Displacement time history for Test B1-R

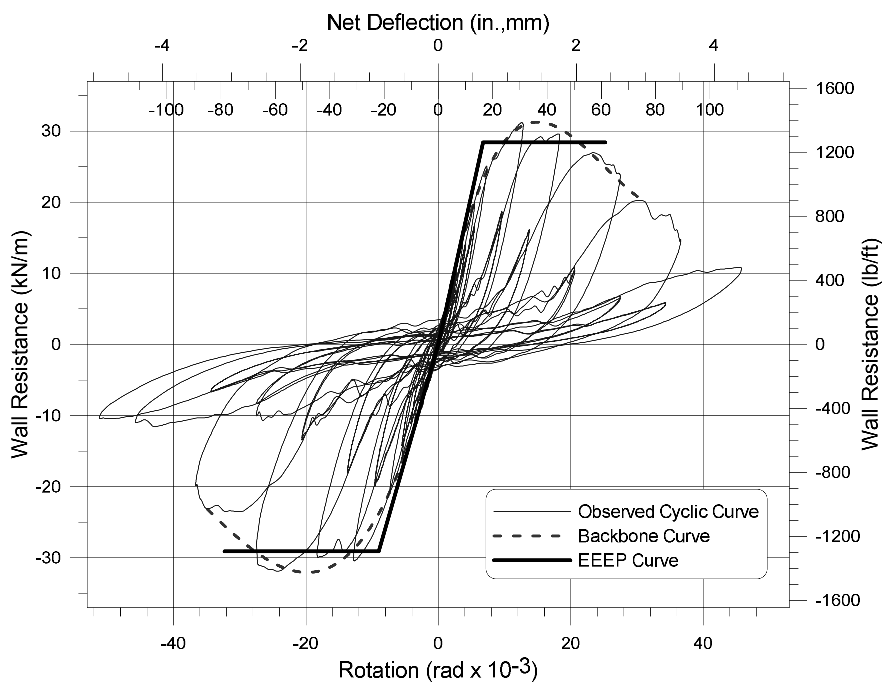

Figure D.10 Resulting EEEP curve for the observed reversed cyclic hysteretic curves (test B1-R)

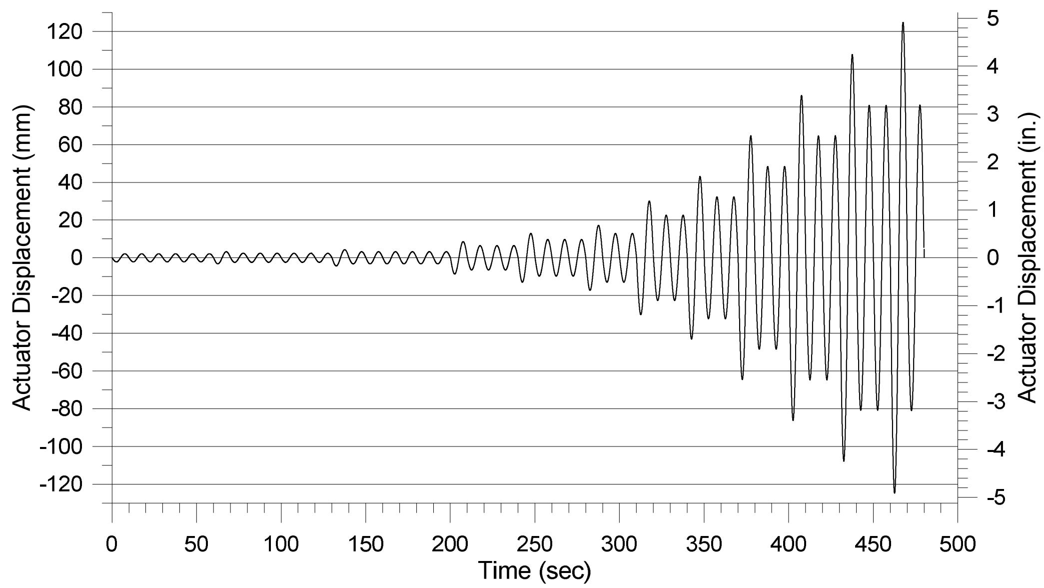

Figure D.11 Displacement time history for Test B2-R

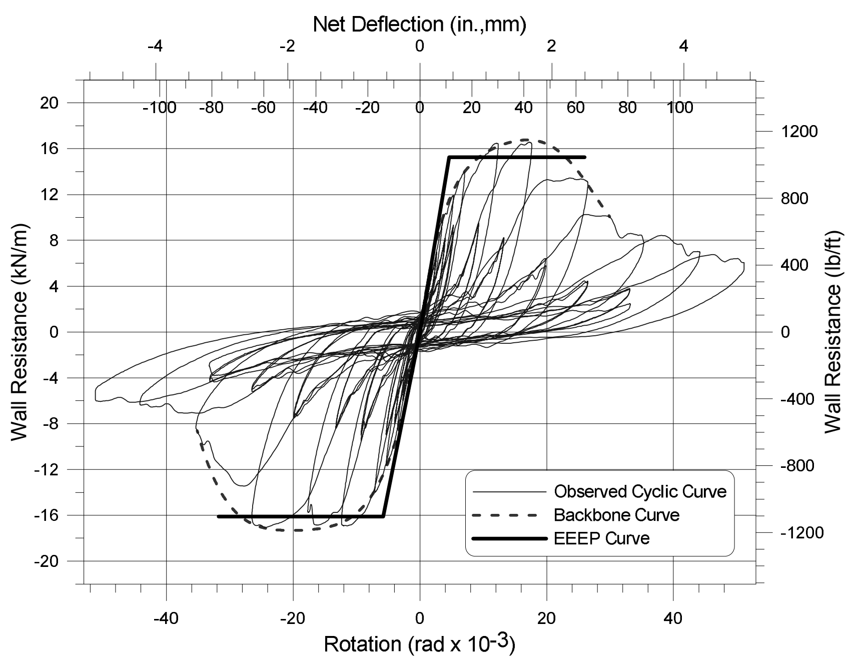

Figure D.12 Resulting EEEP curve for the observed reversed cyclic hysteretic curves (test B2-R)

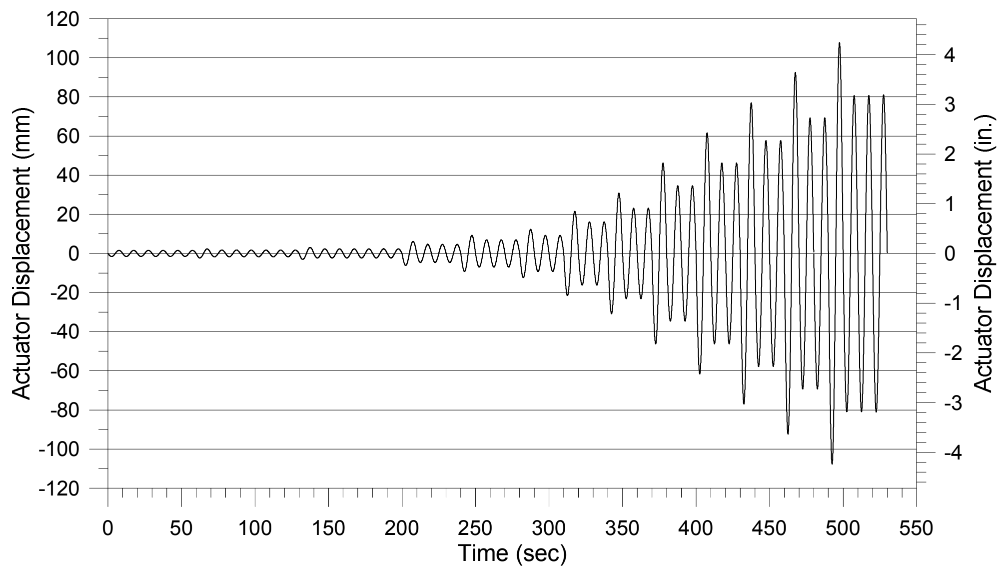

Figure D.13 Displacement time history for Test B3-R

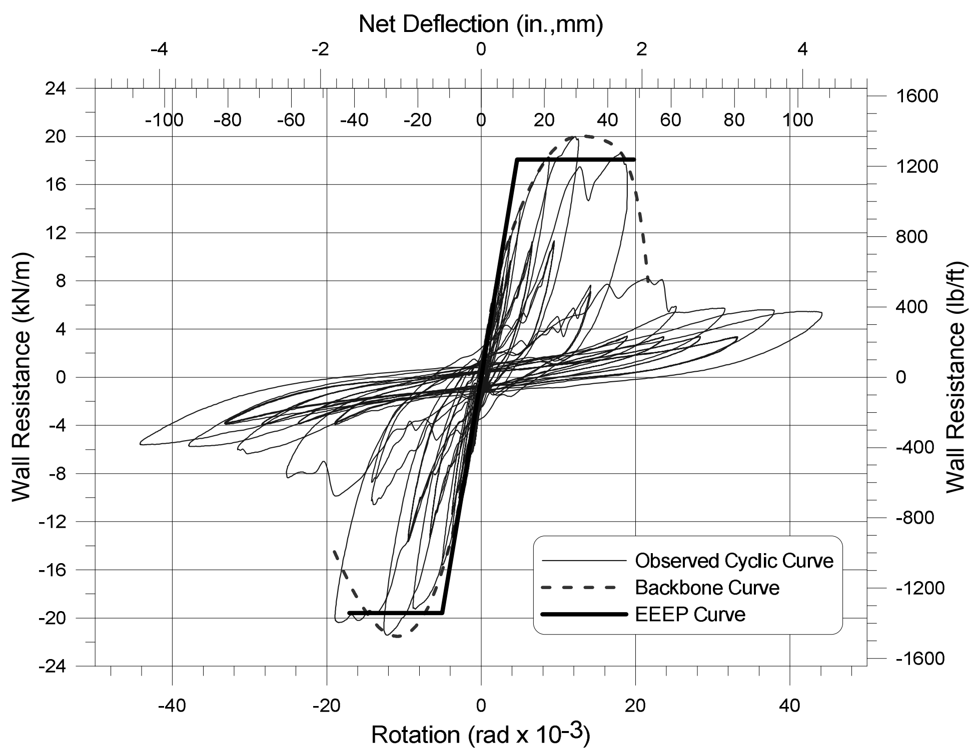

Figure D.14 Resulting EEEP curve for the observed reversed cyclic hysteretic curves (test B3-R)

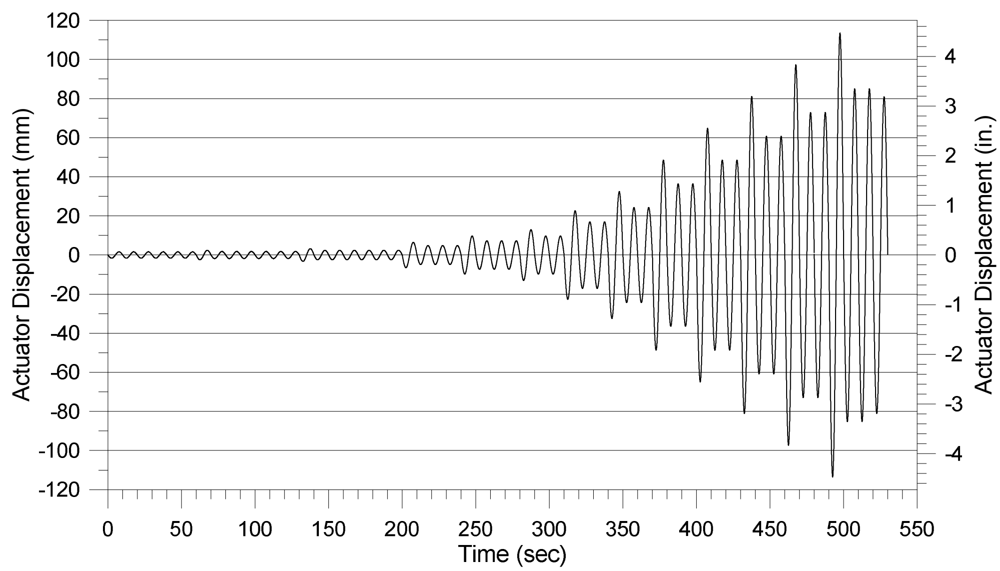

Figure D.15 Displacement time history for Test B4-R

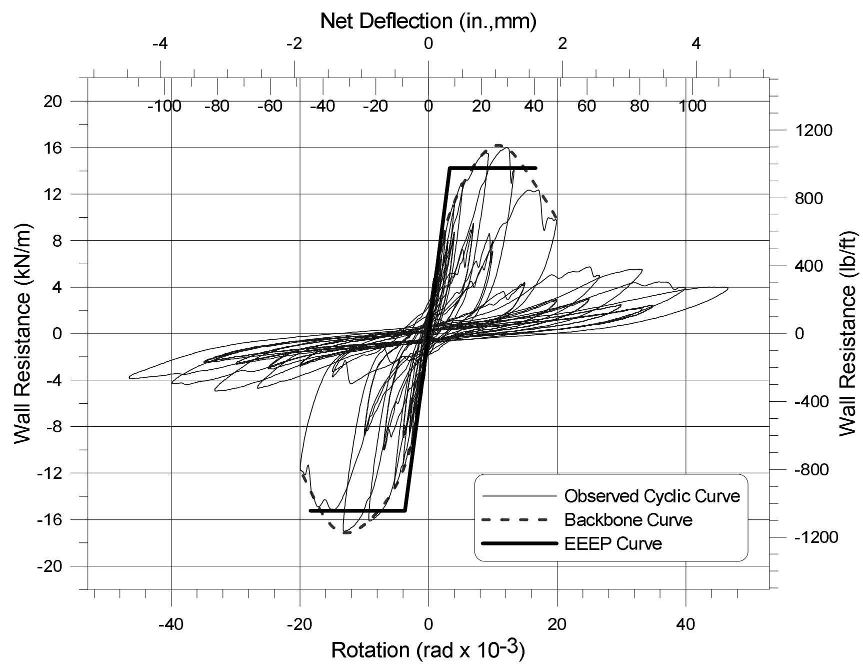

Figure D.16 Resulting EEEP curve for the observed reversed cyclic hysteretic curves (test B4-R)

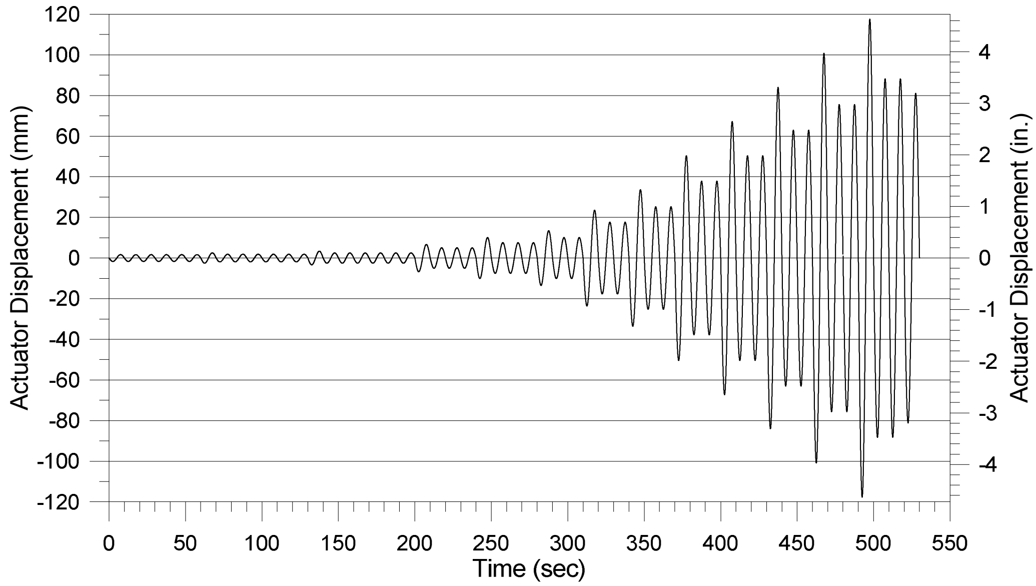

Figure D.17 Displacement time history for Test B5-R

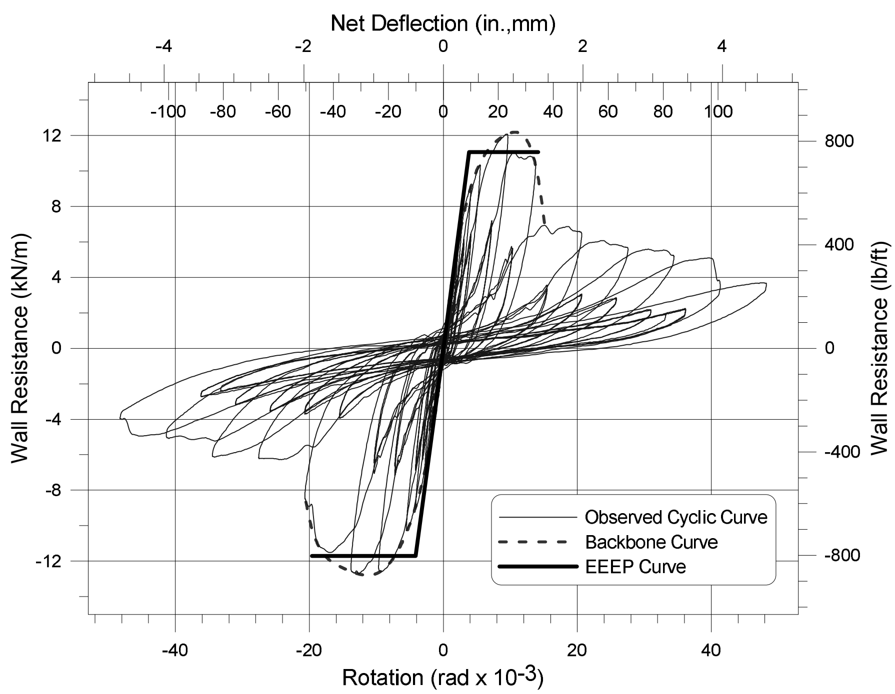

Figure D.18 Resulting EEEP curve for the observed reversed cyclic hysteretic curves (test B5-R)

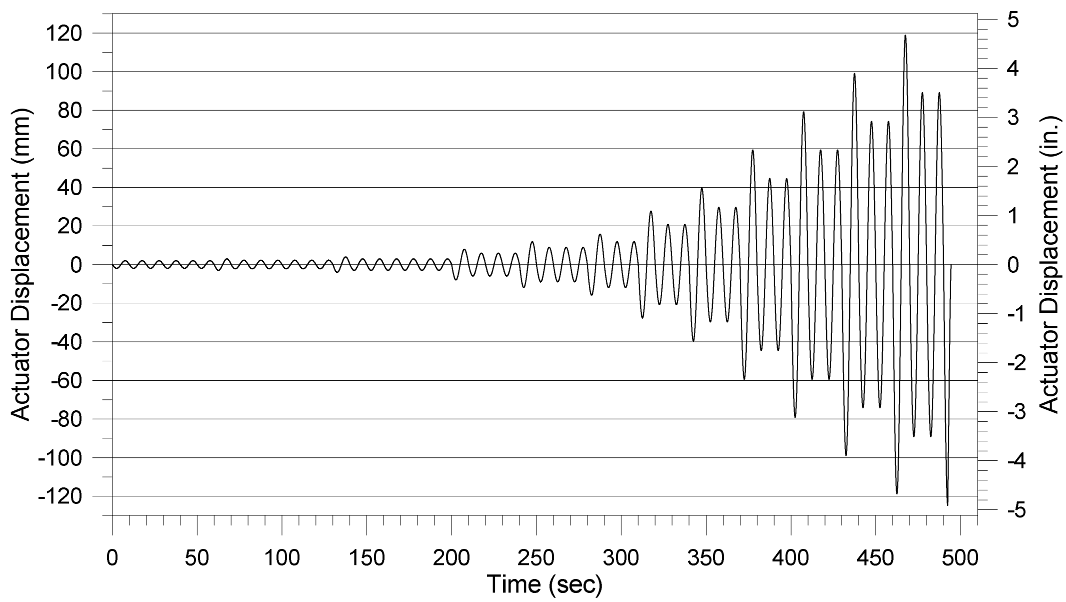

Figure D.19 Displacement time history for Test B6-R

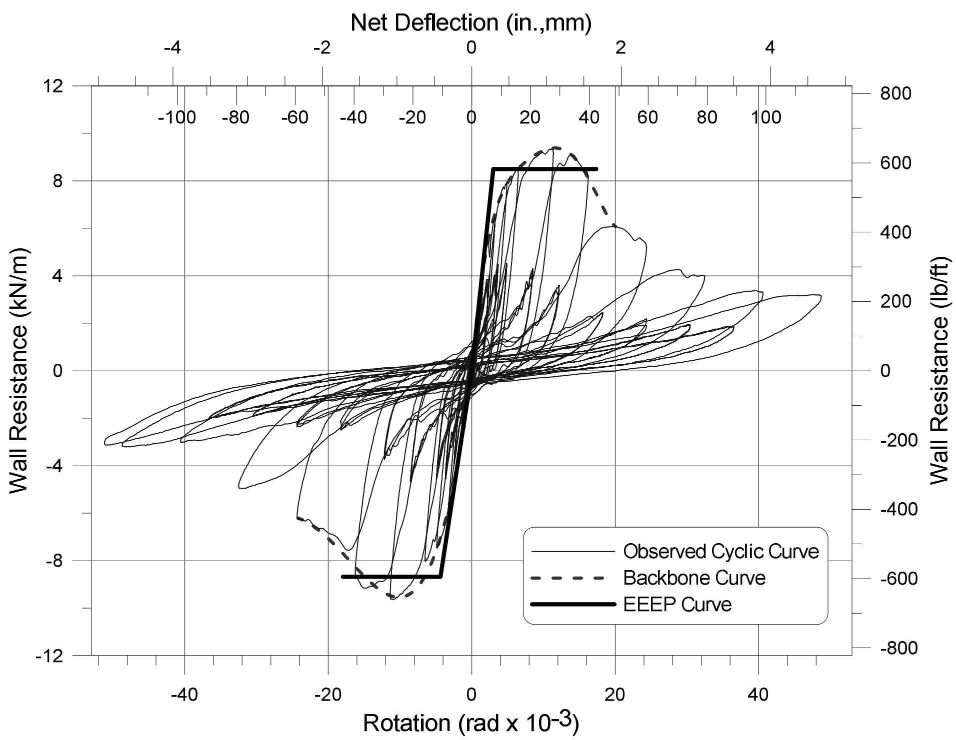

Figure D.20 Resulting EEEP curve for the observed reversed cyclic hysteretic curves (test B6-R)

APPENDIX E –BAR CHARTS COMPARING TEST & DESIGN VALUES OF BLOCKED SHEAR WALLS TO CONVENTIONAL (UNBLOCKED) SHEAR WALLS

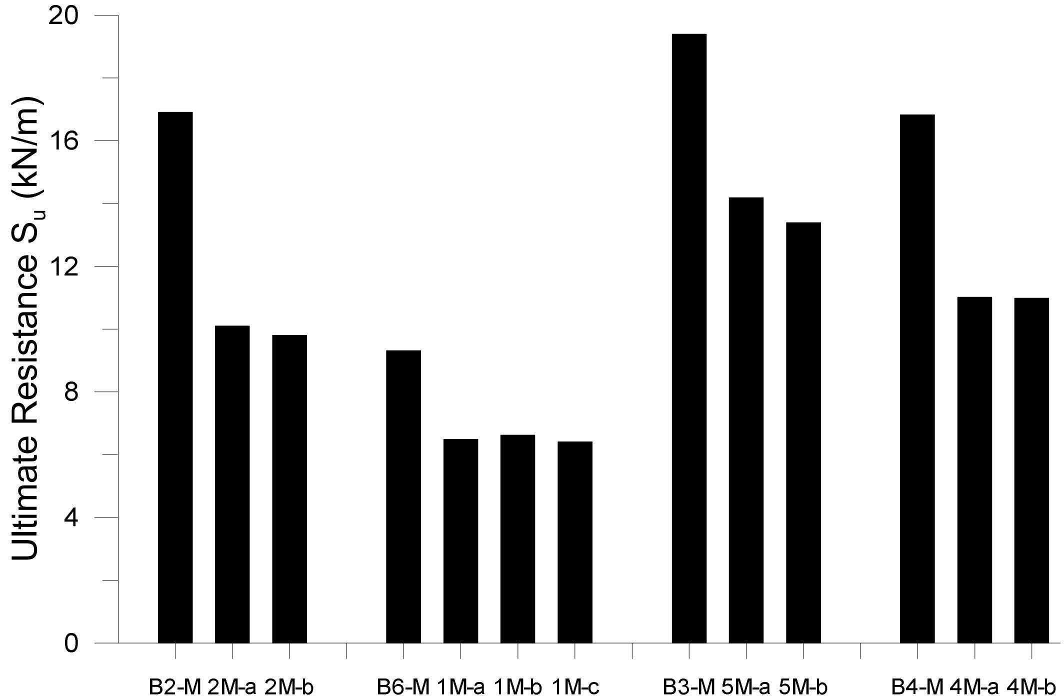

Figure E.1 Comparison of ultimate resistance for monotonic tests

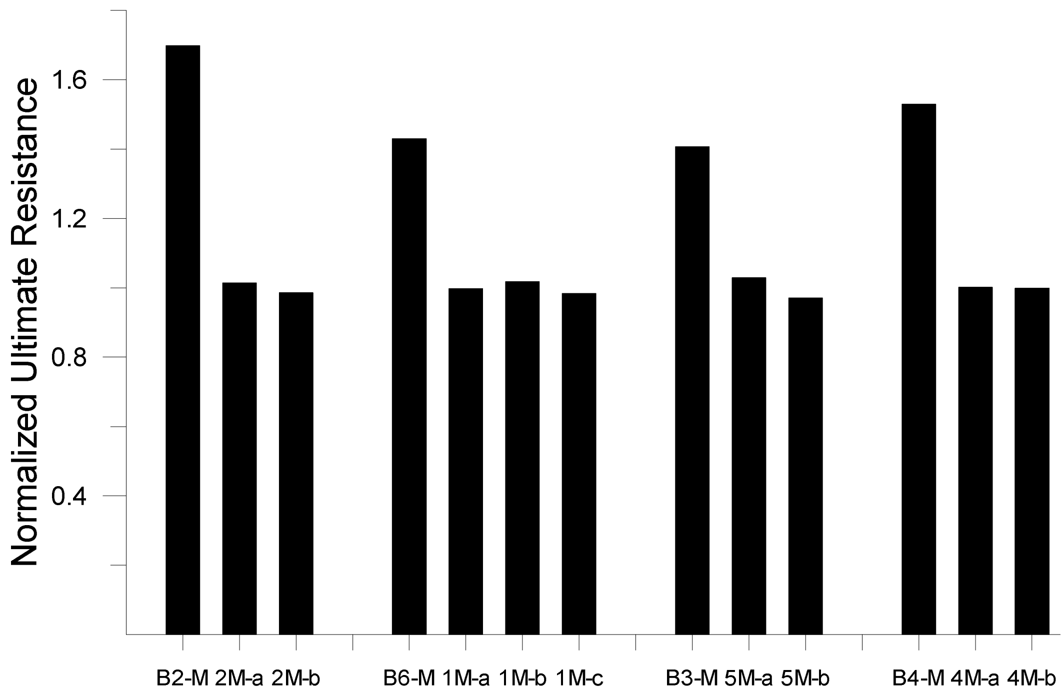

Figure E.2 Comparison of normalized ultimate resistance for monotonic tests

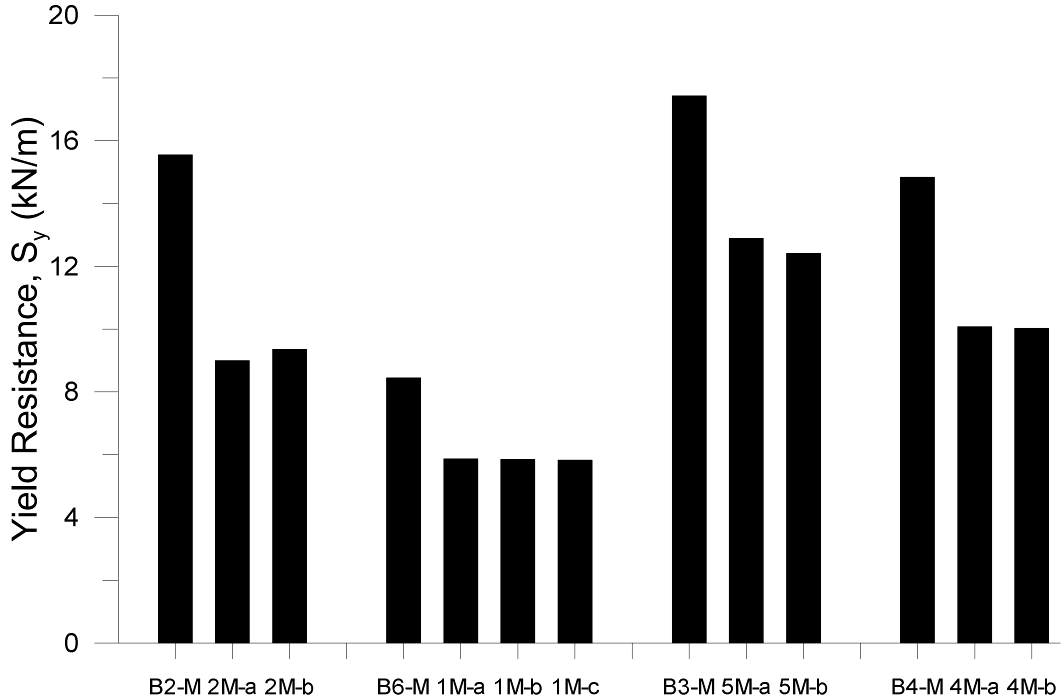

Figure E.3 Comparison of yield resistance for monotonic tests

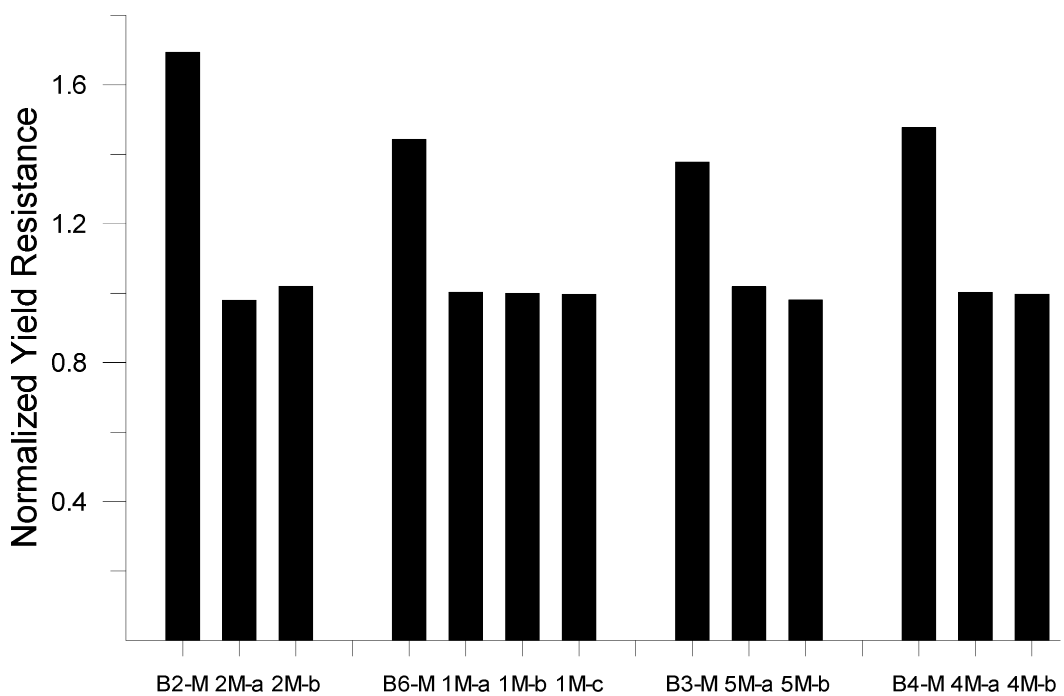

Figure E.4 Comparison of normalized yield resistance for monotonic tests

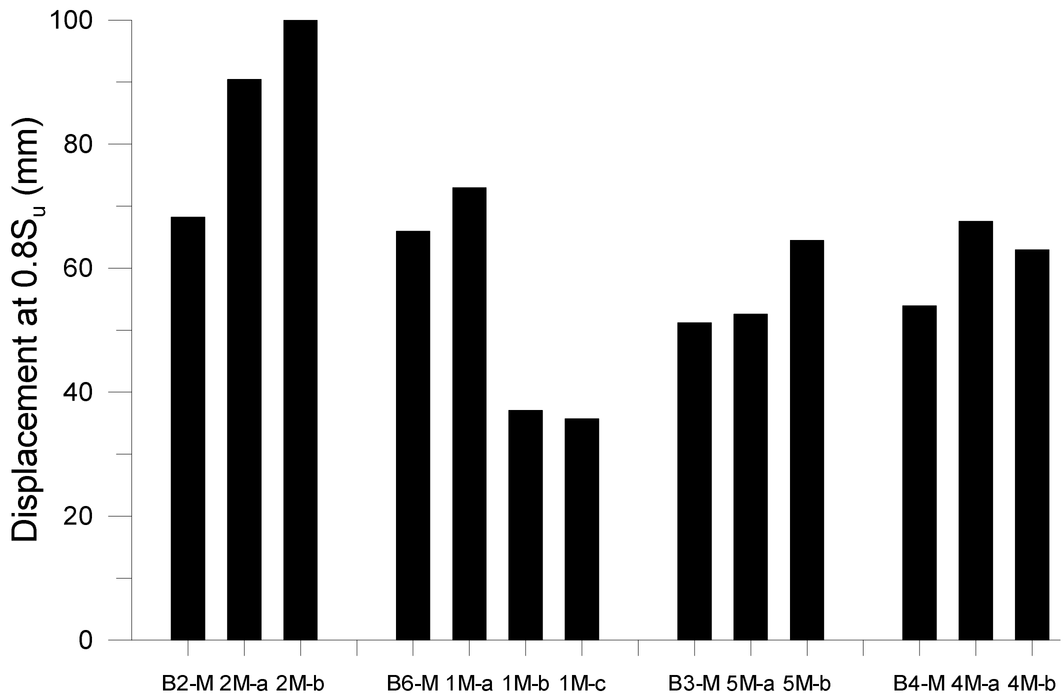

Figure E.5 Comparison of displacement at 0.8S$_u$ for monotonic tests

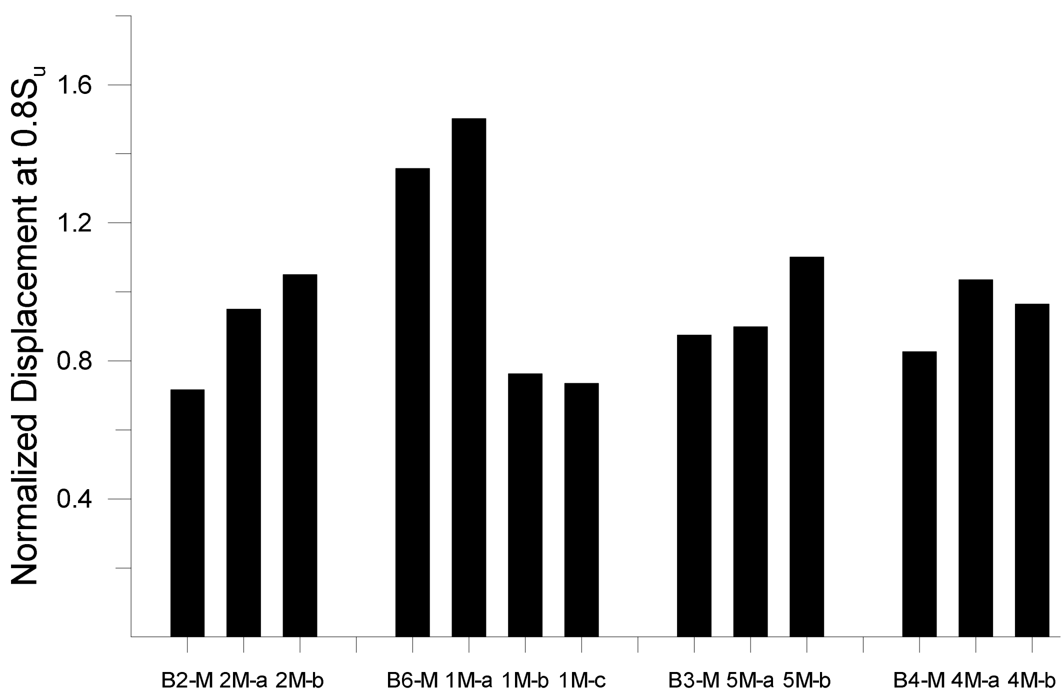

Figure E.6 Comparison of normalized displacement at 0.8S$_u$ for monotonic tests

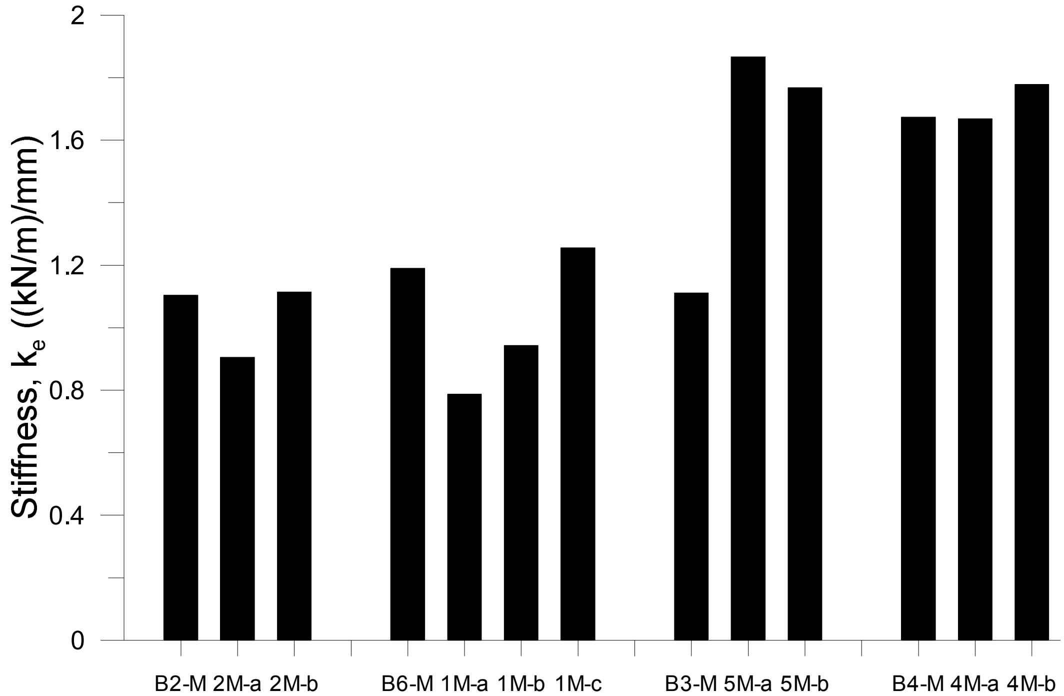

Figure E.7 Comparison of Unit Elastic Stiffness for Monotonic Tests

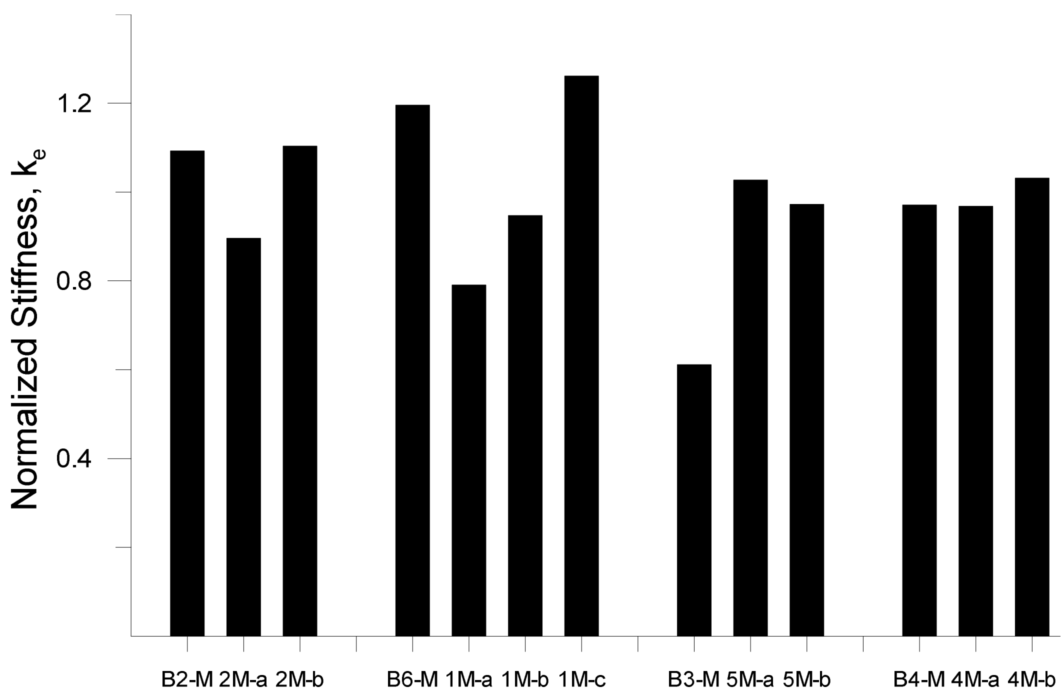

Figure E.8 Comparison of Normalized Unit Elastic Stiffness for Monotonic Tests

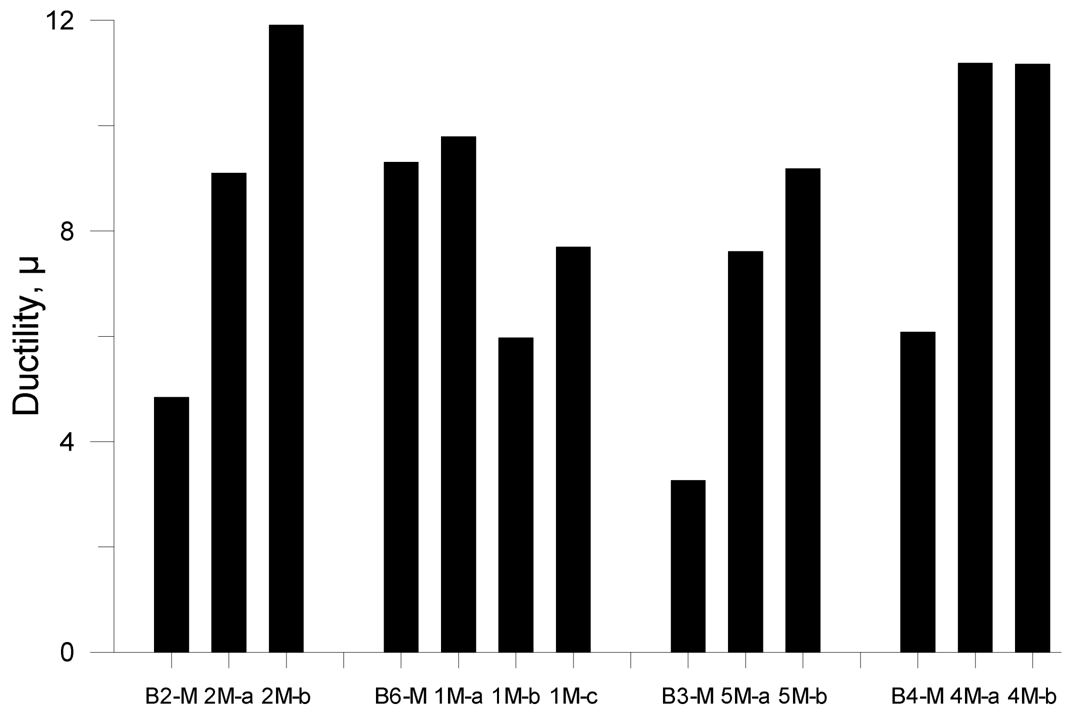

Figure E.9 Comparison of ductility for monotonic tests

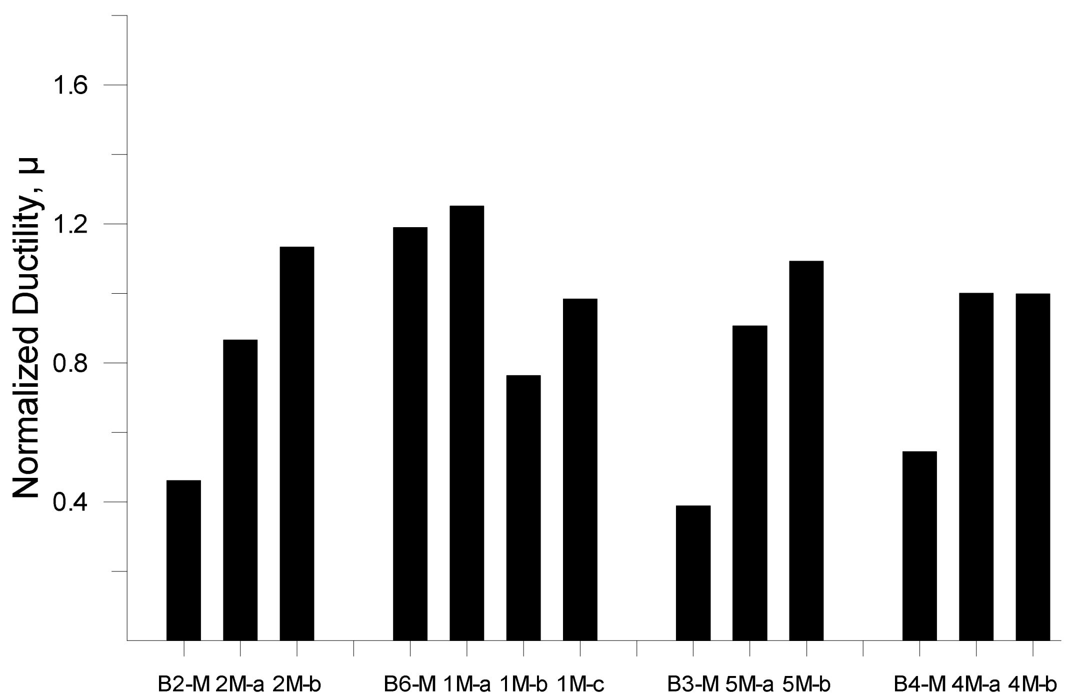

Figure E.10 Comparison of normalized ductility for monotonic tests

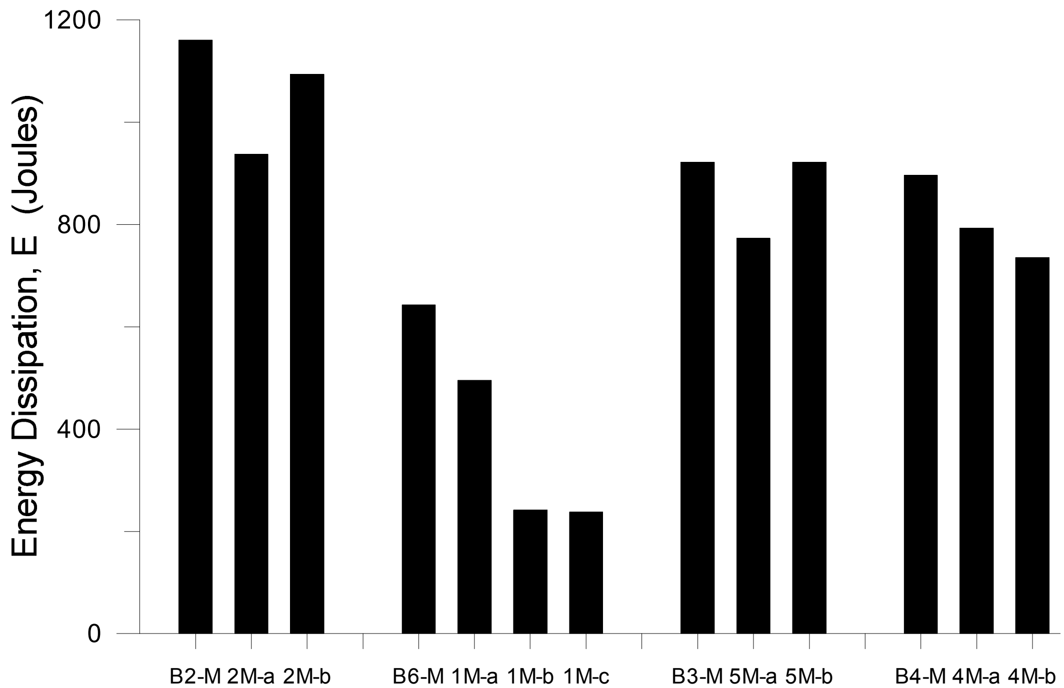

Figure E.11 Comparison of energy dissipated for monotonic tests

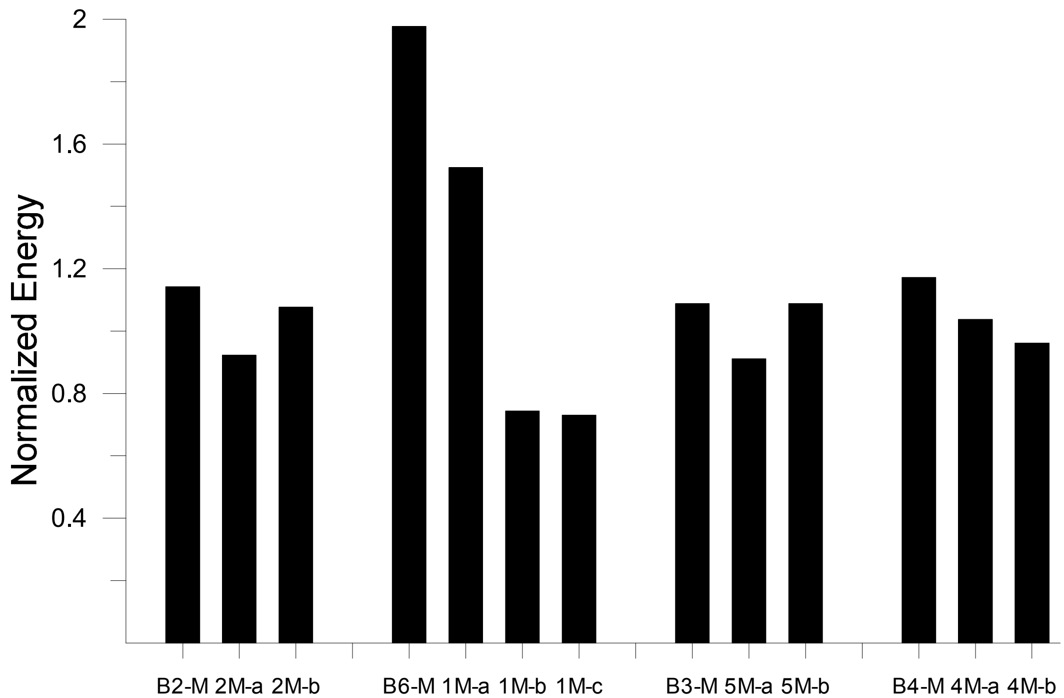

Figure E.12 Comparison of normalized energy dissipated for monotonic tests

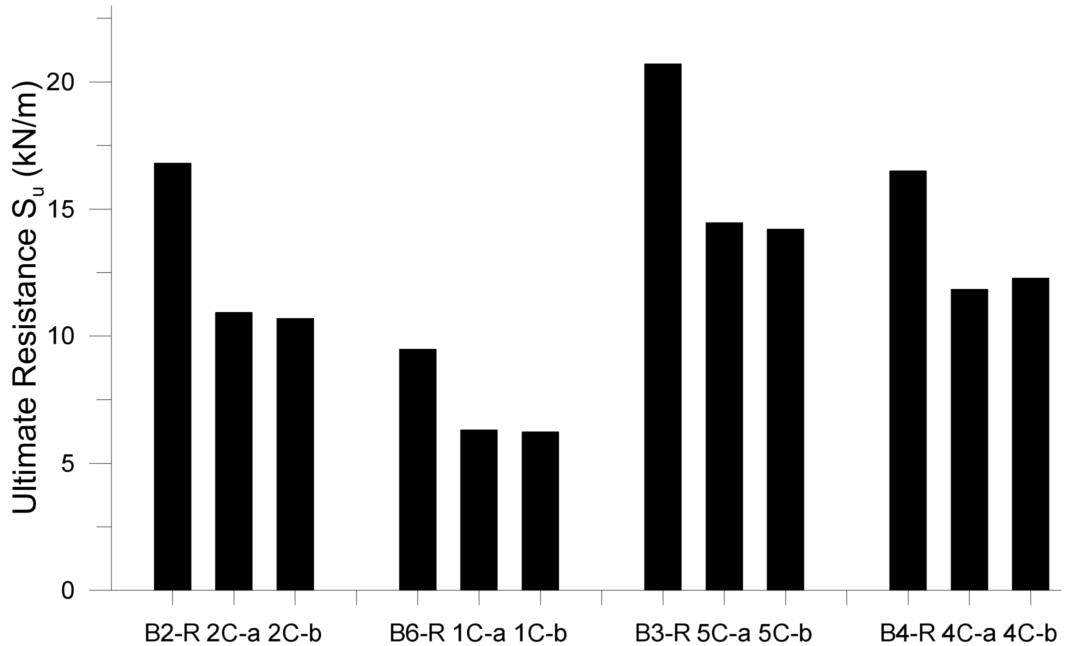

Figure E.13 Comparison of normalized ultimate resistance for reversed cyclic tests

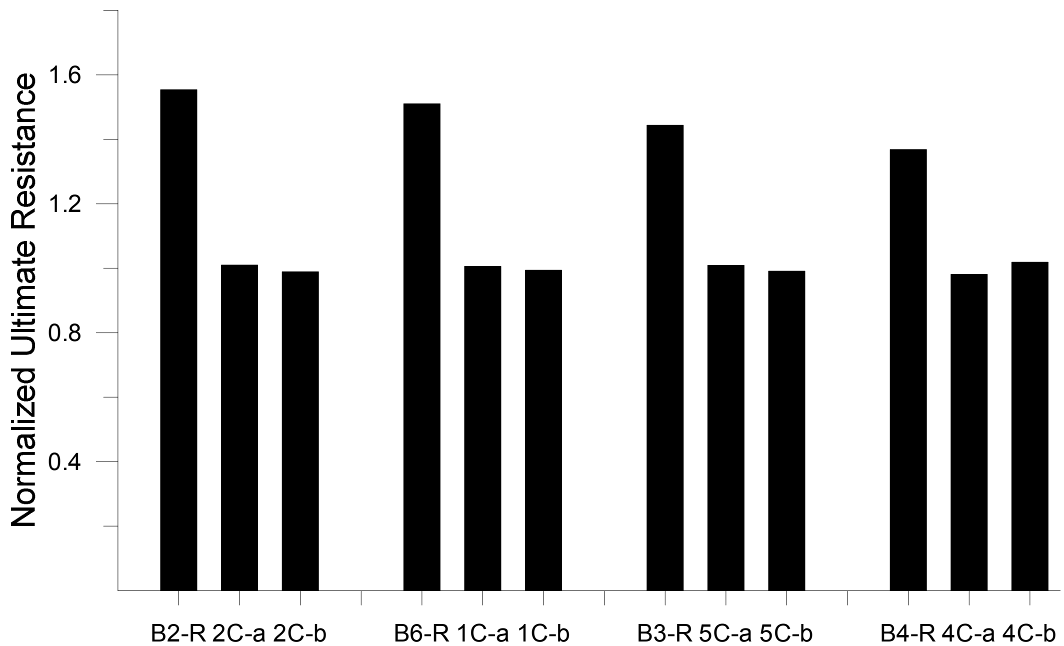

Figure E.14 Comparison of normalized ultimate resistance for reversed cyclic tests

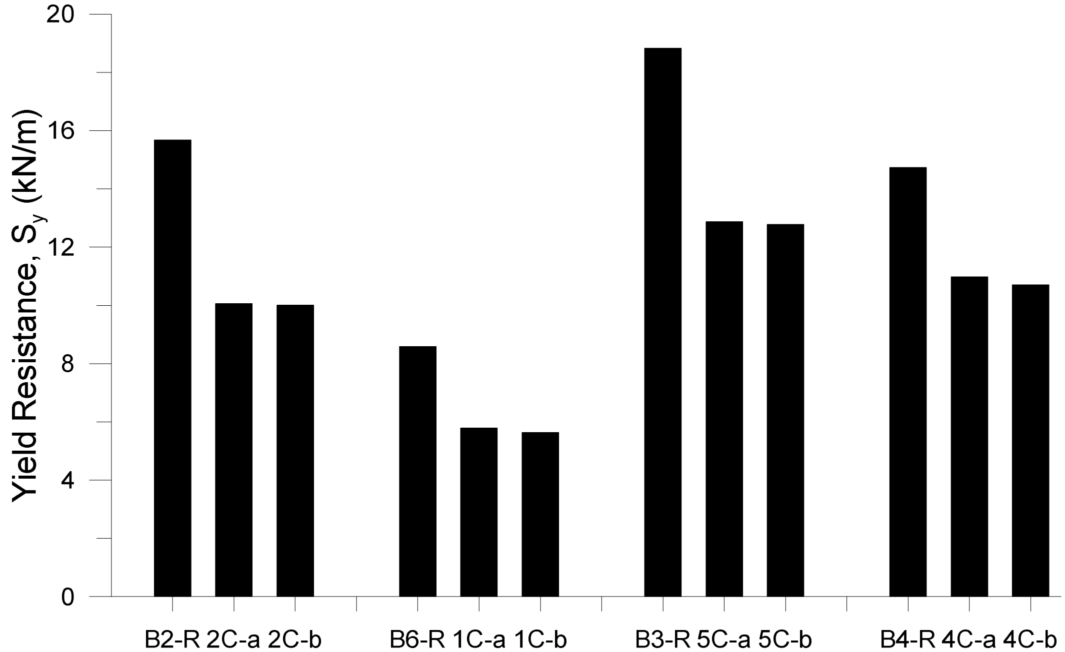

Figure E.15 Comparison of yield resistance for reversed cyclic tests

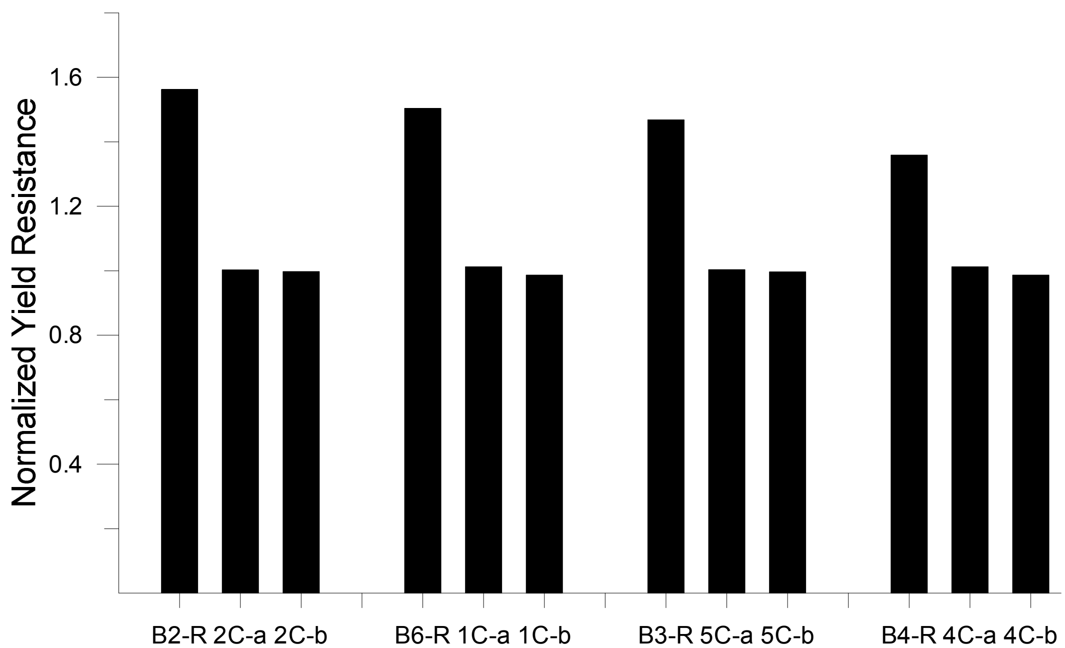

Figure E.16 Comparison of normalized yield resistance for reversed cyclic tests

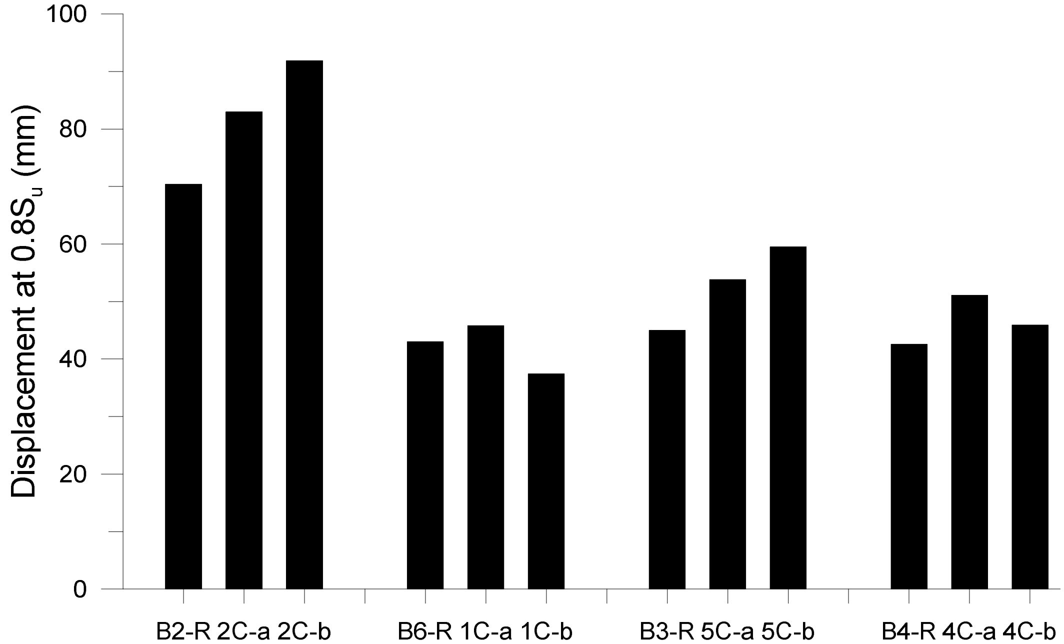

Figure E.17 Comparison of displacement at 0.8S_u for reversed cyclic tests

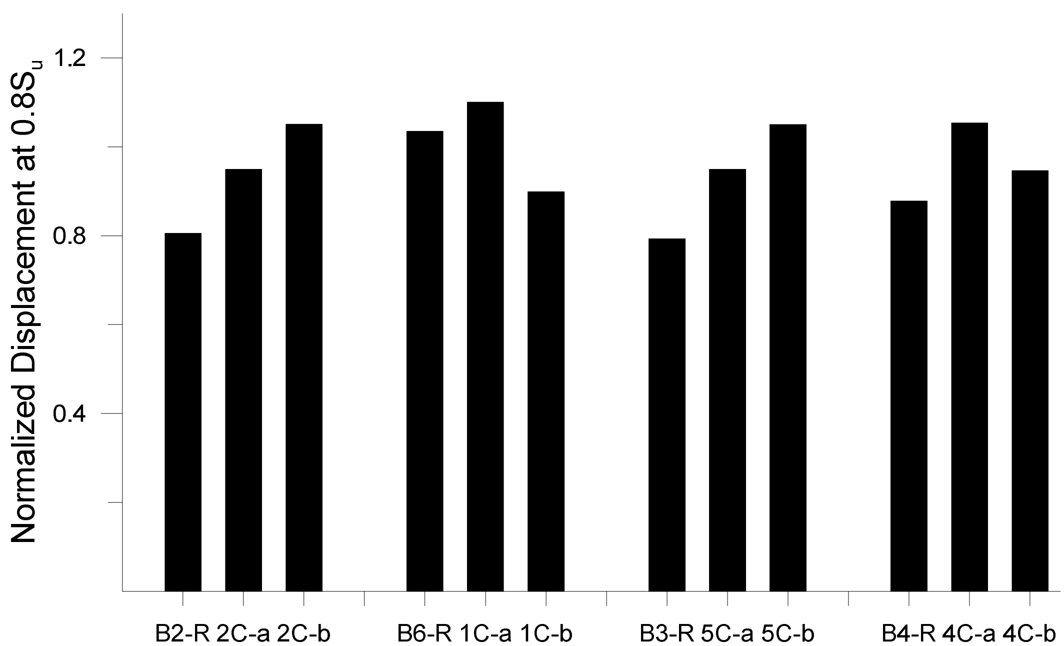

Figure E.18 Comparison of normalized displacement at 0.8S_u for reversed cyclic tests

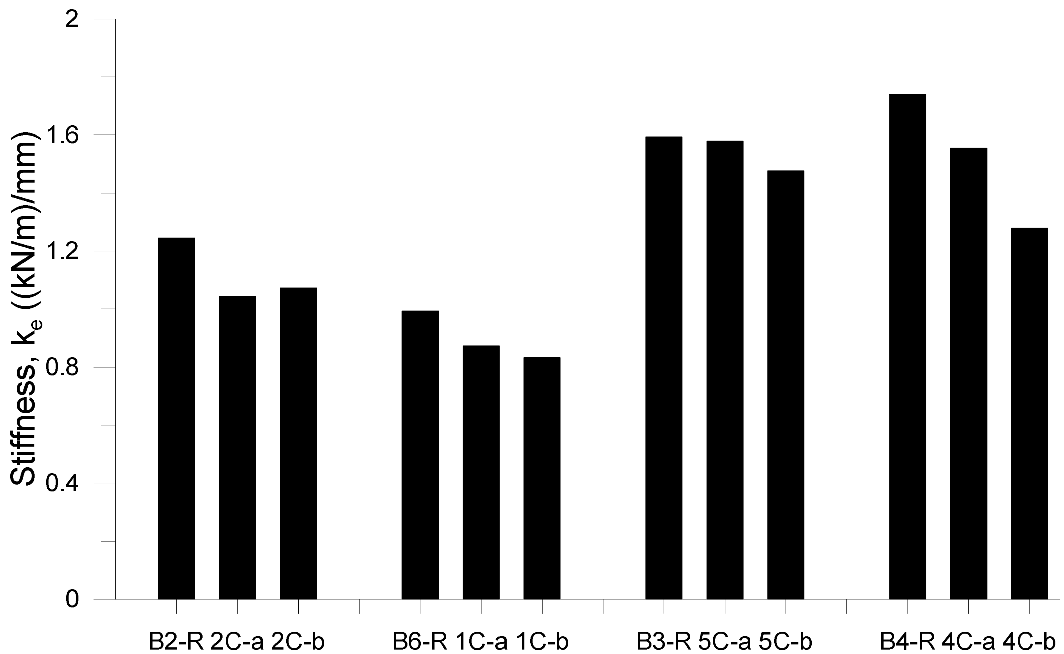

Figure E.19 Comparison of unit elastic stiffness for Reversed Cyclic Tests

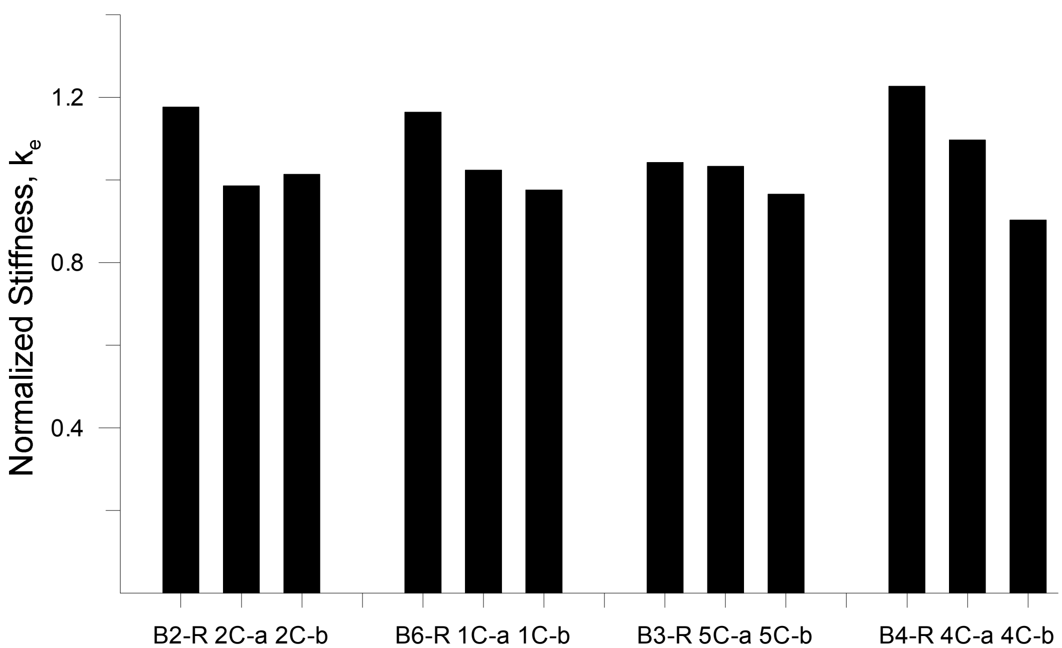

Figure E.20 Comparison of normalized unit elastic stiffness for Reversed Cyclic Tests

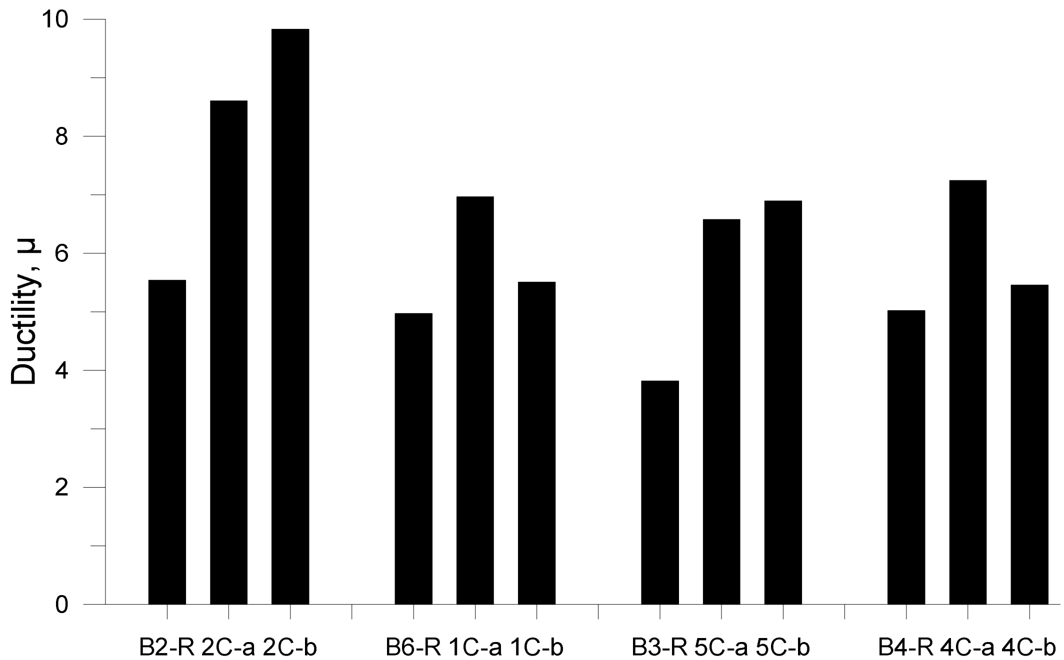

Figure E.21 Comparison of ductility for reversed cyclic tests

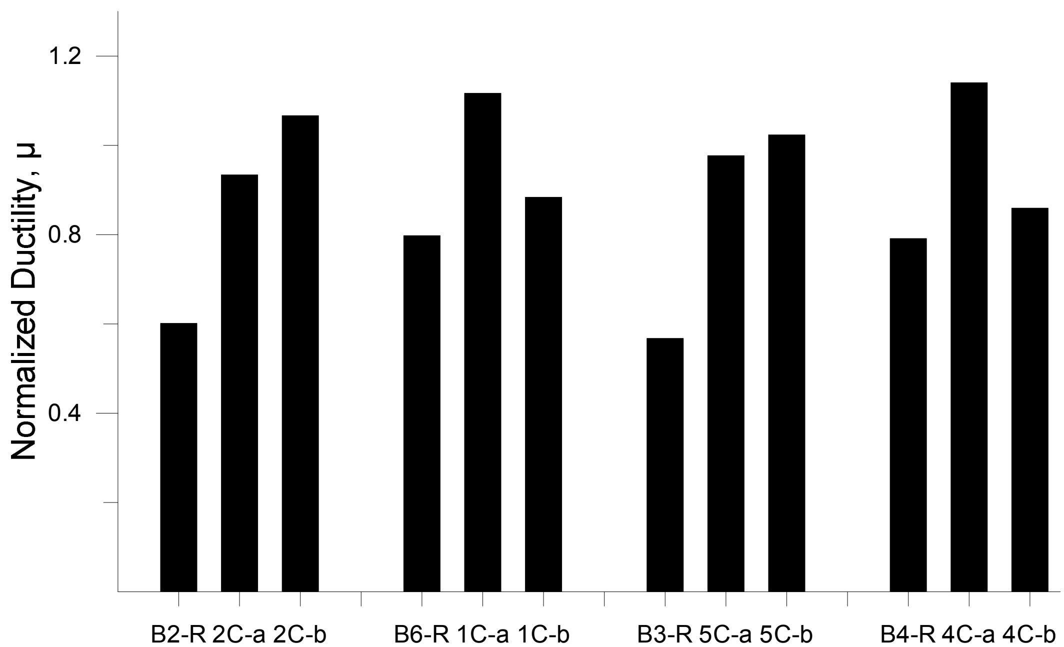

Figure E.22 Comparison of normalized ductility for reversed cyclic tests

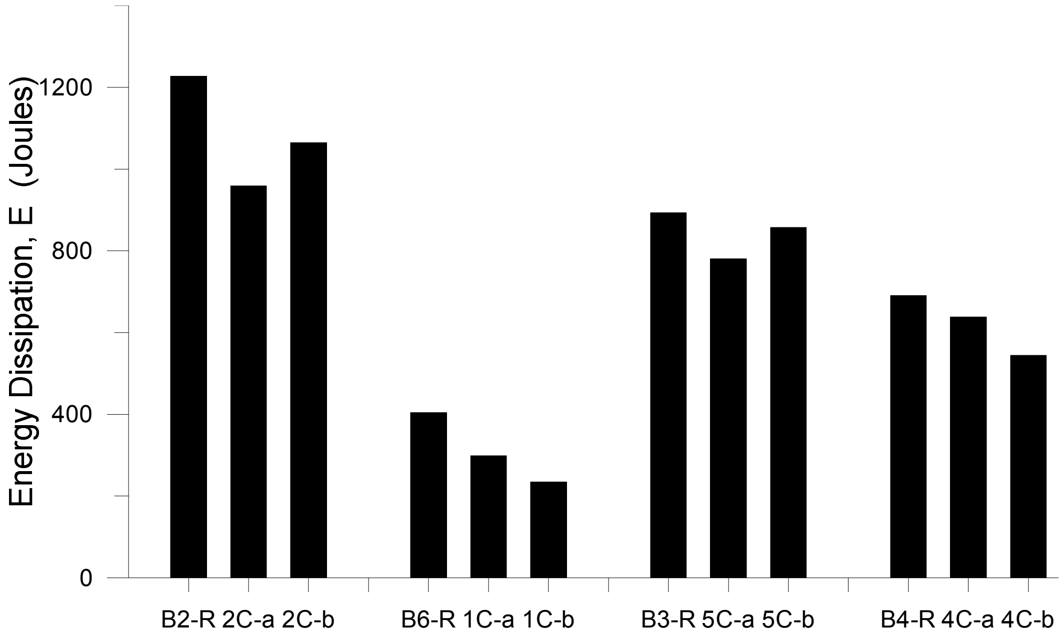

Figure E.23 Comparison of energy dissipated for reversed cyclic tests

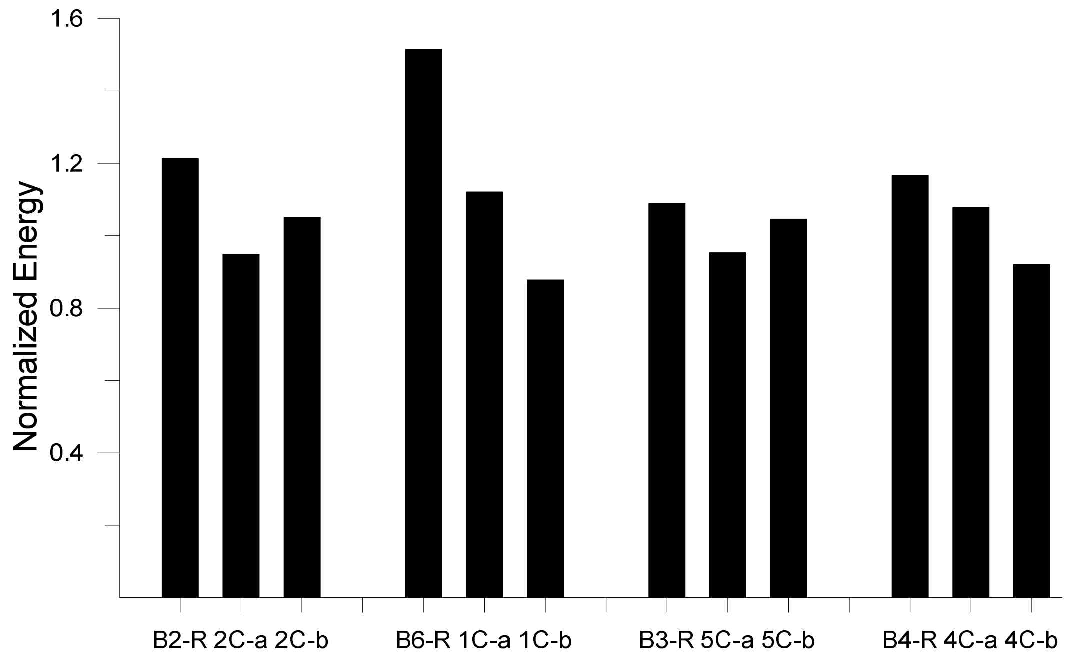

Figure E.24 Comparison of normalized energy dissipated for reversed cyclic tests